



**Michigan
Technological
University**

Michigan Technological University
Digital Commons @ Michigan Tech

Dissertations, Master's Theses and Master's Reports

2017

TECHNO-ECONOMIC AND LIFE CYCLE ASSESSMENTS OF BIOFUEL PRODUCTION FROM WOODY BIOMASS THROUGH TORREFACTION-FAST PYROLYSIS AND CATALYTIC UPGRADING


Olumide Winjobi
Michigan Technological University, owinjobi@mtu.edu

Copyright 2017 Olumide Winjobi

Recommended Citation

Winjobi, Olumide, "TECHNO-ECONOMIC AND LIFE CYCLE ASSESSMENTS OF BIOFUEL PRODUCTION FROM WOODY BIOMASS THROUGH TORREFACTION-FAST PYROLYSIS AND CATALYTIC UPGRADING", Open Access Dissertation, Michigan Technological University, 2017.
<https://digitalcommons.mtu.edu/etdr/476>

Follow this and additional works at: <https://digitalcommons.mtu.edu/etdr>

 Part of the [Chemical Engineering Commons](#)

TECHNO-ECONOMIC AND LIFE CYCLE ASSESSMENTS
OF BIOFUEL PRODUCTION FROM WOODY BIOMASS THROUGH
TORREFACTION-FAST PYROLYSIS AND CATALYTIC UPGRADING

By

Olumide A. Winjobi

A DISSERTATION

Submitted in partial fulfillment of the requirements for the degree of

DOCTOR OF PHILOSOPHY

In Chemical Engineering

MICHIGAN TECHNOLOGICAL UNIVERSITY

2017

© 2017 Olumide Winjobi

This dissertation has been approved in partial fulfillment of the requirements for the Degree of DOCTOR OF PHILOSOPHY in Chemical Engineering.

Department of Chemical Engineering

Dissertation Co-Advisor: *Dr. David Shonnard*

Dissertation Co-Advisor: *Dr. Wen Zhou*

Committee Member: *Dr. Audrey Mayer*

Committee Member: *Dr. Michael Mullins.*

Department Chair: *Dr. Pradeep K. Agrawal.*

Contents

Preface	6
Acknowledgments	10
Abstract	11
1. Introduction.....	13
1.1 Energy and the transport sector.....	13
2. Techno-economic Assessment of Bio-oil Production from pine	30
2.1 Abstract	30
2.2 Introduction.....	32
2.3 Material and Methods	35
2.3.1. Process Description.....	35
2.3.2 Design Objectives	39
2.3.3 Economics.....	41
2.3.4 Sensitivity Analysis	43
2.4 Results and discussion	44
2.4.1 Process modeling and simulation.....	44
2.4.2 Economic Assessment	46
2.4.3 Sensitivity Analysis	51
2.5 Conclusions.....	54
2.6 Acknowledgements.....	55
2.7 References.....	56
3. Life cycle greenhouse gas emissions of bio-oil from two-step torrefaction and fast pyrolysis of pine.....	61
3.1 Abstract.....	61
3.2 Introduction.....	62
3.3 Materials and methods	65
3.3.1 Definition of the case study	65
3.3.2 LCA framework, system definition, and modeling assumptions	67
3.3.3 Life Cycle Inventory	69
3.4 Results.....	78
3.5 Conclusions.....	87
3.6 Acknowledgements.....	88

3.7 References.....	89
4. Production of Hydrocarbon Fuel using Two-Step Torrefaction and Fast Pyrolysis of Pine.	
Part 1: Techno-economic Analysis.....	95
4.1. Abstract.....	95
4.2 Introduction.....	96
4.3 Materials and Methods.....	99
Process description.....	99
Definition of case studies.....	107
Techno-economic assessment of hydrocarbon fuel pathways.....	109
Heat Integration.....	112
4.4 Results.....	113
Sensitivity Analysis.....	125
4.5 Acknowledgments.....	131
4.6 References.....	132
5. Production of Hydrocarbon Fuel using Two-Step Torrefaction and Fast Pyrolysis of Pine.	
Part 2: Life Cycle Carbon Footprint.....	136
5.1. Abstract.....	136
5.2. Introduction.....	137
5.3. Material and Methods.....	140
Process description.....	140
Heat Integration.....	144
LCA framework, system definition, and modeling assumptions.....	144
Life Cycle Inventory.....	151
Sensitivity Analysis.....	159
5.4. Results.....	159
5.5. Acknowledgements.....	169
5.6. References.....	170
Chapter 6. TEA and LCA of hydrocarbon biofuel production via fast pyrolysis of poplar feedstock and catalytic upgrade.....	175
6.1. Introduction.....	175
6.2 Materials and methods.....	179
6.3 Results.....	184
6.4 Conclusions.....	193

6.5 References.....	194
Chapter 7. Conclusions and Recommendations for Future Work.....	198
Appendix A: Techno-economic assessment of the effect of torrefaction on fast pyrolysis of pine Supplementary Information	206
A.1. Supplementary material from Chapter 2	206
A.2. References.....	224
Appendix B: Life cycle assessment for greenhouse gas emissions of two-step torrefaction and fast pyrolysis of pine supplementary information	225
B.1 Supplementary material from Chapter 3	225
B.2 References	246
Appendix C: Production of Hydrocarbon Fuel using Two-Step Torrefaction and Fast Pyrolysis of Pine. Part 1: Techno-economic Analysis	248
C.1 Supplementary material from Chapter 4	248
C.2 References	281
Appendix D: Production of Hydrocarbon Fuel using Two-Step Torrefaction and Fast Pyrolysis of Pine. Part 2: Life Cycle Carbon Footprint	284
D.1 Supplementary material from Chapter 5	284
D.2 References.....	334
Appendix E: Copyright Clearance	337

Preface

This doctoral dissertation contains material previously reviewed and published in scientific journals along with material currently submitted to scientific journals. Full citation of these are as follows:

Chapter 2

Reprinted with permission from WINJOBI O, SHONNARD D. R, EZRA B, AND ZHOU W.2016. TECHNO-ECONOMIC ASSESSMENT OF THE EFFECT OF TORREFACTION ON FAST PYROLYSIS OF PINE. BIOFUELS, BIOPRODUCTS BIOREFINING 10(2): 117 – 128. Copyright 2016

DOI Link:

Author Contributions

Winjobi	Collection of data, analysis and interpretation of data, writing of the paper, responsible for submission and review of journal article
Shonnard	Analysis and interpretation of data, paper review and editing
Ezra	Review of the paper
Zhou	Analysis and interpretation of data, paper review and editing

Chapter 3:

Reprinted with permission from WINJOBI O, SHONNARD D. R, EZRA B, AND ZHOU W.2016. TECHNO-ECONOMIC ASSESSMENT OF THE EFFECT OF TORREFACTION ON FAST PYROLYSIS OF PINE. BIOFUELS, BIOPRODUCTS BIOREFINING 10(2): 117 – 128. Copyright 2016

DOI: 10.1002/bbb.1660

Author Contributions

Winjobi	Collection of data, analysis and interpretation of data, writing of the paper, responsible for submission and review of journal article
Shonnard	Analysis and interpretation of data, paper review and editing
Ezra	Review of the paper
Zhou	Analysis and interpretation of data, paper review and editing

Chapter 4:

Reprinted with permission from WINJOBİ, O, SHONNARD, D, ZHOU W.
PRODUCTION OF HYDROCARBON FUEL USING TWO-STEP TORREFACTION
AND FAST PYROLYSIS OF PINE. PART 1: TECHNO-ECONOMIC
ANALYSIS. COPYRIGHT (2017) AMERICAN CHEMICAL SOCIETY.

Author Contributions

Winjobi	Collection of data, analysis and interpretation of data, writing of the paper, responsible for submission and review of journal article
Shonnard	Analysis and interpretation of data, paper review and editing
Zhou	Analysis and interpretation of data, paper review and editing

Chapter 5:

Reprinted with permission from WINJOBİ, O, ZHOU W., KULAS, D., NOWICKI, J., AND SHONNARD D. PRODUCTION OF HYDROCARBON FUEL USING TWO-STEP TORREFACTION AND FAST PYROLYSIS OF PINE.PART 2: LIFE CYCLE CARBON FOOTPRINT. Copyright (2017) American Chemical Society

Author Contributions

Winjobi	Collection of data, analysis and interpretation of data, writing of the paper, responsible for submission and review of journal article
Zhou	Analysis and interpretation of data, paper review and editing
Kulas	Analysis and interpretation of data, paper review and editing
Nowicki	Analysis and interpretation of data, paper review and editing
Shonnard	Analysis and interpretation of data, paper review and editing

Acknowledgments

I would like to acknowledge the financial support I received from National Science Foundation's Sustainable Energy Pathway (MPS/CHE – ENG/ECCS –1230803) and the Richard and Bonnie Robbins Endowment.

I would also like to extend my utmost thanks to my advisors, Dr. David Shonnard and Dr. Wen Zhou for their constant help, suggestions and guidance throughout my program. Deep gratitude also goes to my committee members: Dr. Audrey Mayer and Dr. Michael Mullins for their help and guidance.

I would also like to thank various faculty and staff of the Chemical Engineering department for their unwavering assistance: Dr. Tony Rogers, Dr. Thomas Co, Dr. Faith Morrison, Dr. John Sandell, Alexis Snell, Taana Kalliainen, and Sue Niemi.

I would also like to thank my parents, Engr. And Mrs. Winjobi for their undying love and support as well as my siblings; Mayowa, Deola and Ife for everything.

Special thanks to goes to everyone in my research group, Dr. Bethany Klemetsrud, Ulises Garcia, Rui Shi, Suchada Ukaew, Sharath Kumar for always being there and the fun times all the way through San Francisco to Utah.

My deep thanks also go out to Dr. Renee Oats, all ASO members, and friends

And to my one and only 'ekuro', Simisola Arogundade thanks for always being there.

And most importantly, He that has always been my constant and dependable companion, the Author and Finisher of my faith.

Abstract

Biofuel production through fast pyrolysis of biomass is a promising conversion route in the production of biofuels compatible with existing technology. The bio-oil produced from fast pyrolysis is a versatile feedstock that can be used as a heating oil or upgraded to a transportation hydrocarbon biofuel. Comparative study of a one-step, fast pyrolysis only pathway and a two-step torrefaction-fast pyrolysis pathway was carried out to evaluate the effect of torrefaction on (i) the minimum selling price of biofuel and (ii) the potential life cycle GHG emissions of the biofuel production pathway.

To produce bio-oil which can serve as a substitute for heating oil from loblolly pine biomass feedstock, torrefaction at three different temperatures of 290, 310 and 330°C were investigated while fast pyrolysis occurred at 530°C. Three scenarios of producing process heat from natural gas, internal by-products biochar or torrefaction condensate were also investigated. Economic assessment showed more favorable economics for the two-step bio-oil production pathway relative to the one-step bio-oil production pathway. The lowest minimum selling price of \$1.04/gal was obtained for a two-step pathway with torrefaction taking place at 330°C. The environmental impact assessment also showed the two-step bio-oil production pathway to be more environmentally friendly. The lowest GWP of about -60g CO₂eq was observed for the two-step pathway at a torrefaction temperature of 330°C while GWP of about 36g CO₂eq was observed for the one-step pathway. Relative to heavy fuel oil, the one-step and two-step pathways are more environmentally friendly with lower GWP.

To produce hydrocarbon biofuel by the catalytic upgrade of bio-oil derived from fast pyrolysis of loblolly pine, three torrefaction temperatures of 290, 310 and 330°C were investigated with fast pyrolysis taking place at 530°C. Three scenarios of producing process heat from natural gas, internal by-products biochar or torrefaction condensate were investigated. The effect of heat integration was also examined. The economic assessment showed equal minimum selling price for the one-step hydrocarbon biofuel production pathway and a two-step pathway with torrefaction occurring at 290°C. A minimum selling price of \$4.82/gal was estimated while higher torrefaction temperatures showed less favorable economics. The environmental impact assessment however showed the two-step pathway to be more environmentally friendly when compared with the one-step pathway. GWP of about -66g CO₂eq was observed for the two-step pathway with torrefaction taking place at 330°C compared to a GWP of about 88g CO₂eq obtained for the one-step. Further reduction in minimum selling price and GWP were observed with heat integration. A minimum selling price of about \$4.01/gal was estimated for the one-step and two-step pathway with torrefaction taking place at 290°C while GWP of about -144 g CO₂eq was observed for the two-step hydrocarbon biofuel with torrefaction temperature of 330°C.

1.Introduction

1.1 Energy and the transport sector

Energy is one of the key factors required for social, economic and particularly industrial development.[1] With improved knowledge of the impact of fossil energy utilization on the global environment, more emphasis is now being placed on environmentally-sustainable sources of energy. According to the United Nations, for effective and sustainable industrial development, energy production and utilization must be planned with other factors such as technology, raw materials among other factors.[1] In 2016, the industrial sector was responsible for about a third of the primary energy consumption in the US as illustrated in Figure 1.1:

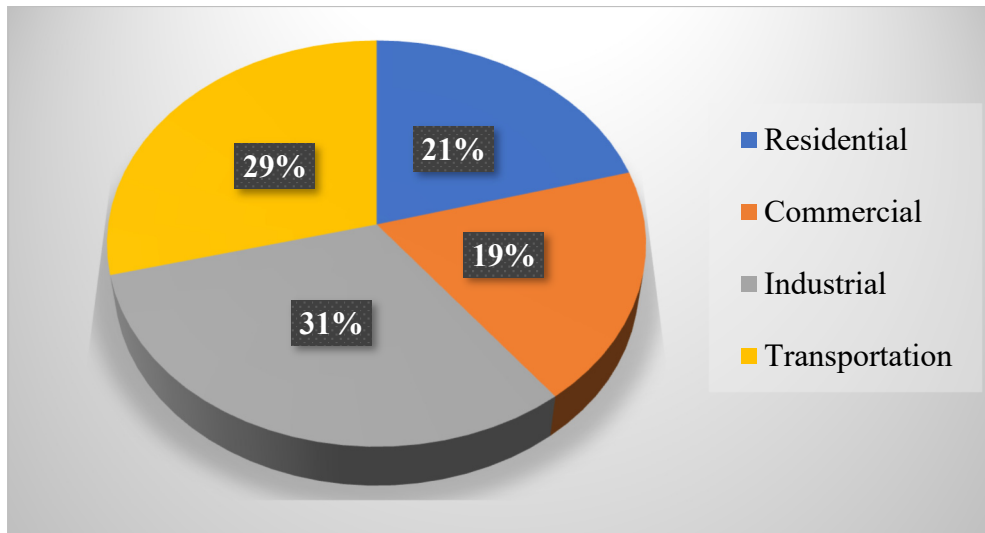


Figure 1.1. 2016 Primary energy consumption in the US by different sectors.[2]

Though the energy consumed by the transportation sector is slightly lower than that consumed by the industrial sector in 2016, an examination of the energy consumption over

the last five years shows an upward trend in energy consumption by the transportation sector while a downward trend is observed in the industrial sector, as presented in Figure 1.2

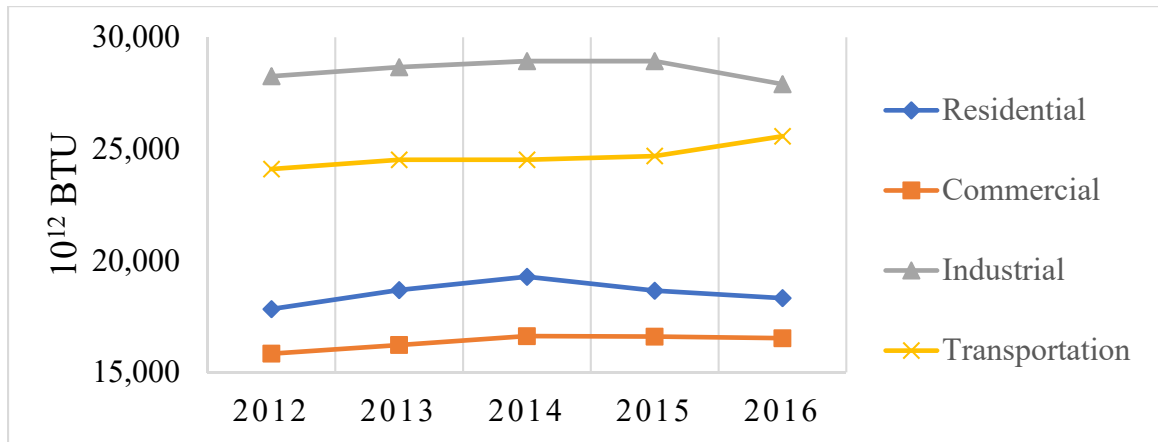


Figure 1.2. 5-year trend of primary energy consumption by different sectors in the United States.[2]

Opportunities for improvement in technology and better energy efficiency are being investigated to address the energy consumption of the transport sector. Aside from the high and increasing energy consumption in the transport sector, another concern is the source of energy, which for this sector is primarily fossil petroleum. Petroleum accounted for over 90% of the primary energy consumed by the transport sector in the United States in 2016 as illustrated in Figure 1.3.

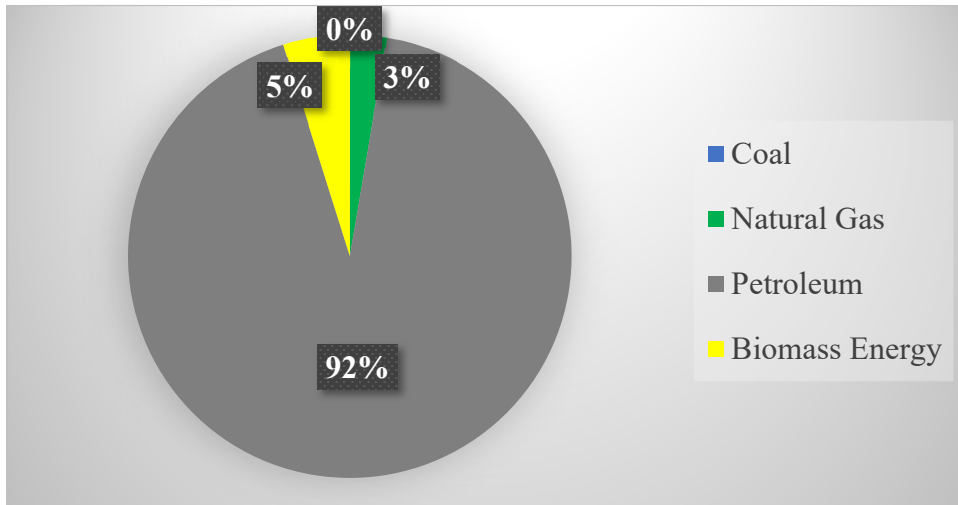


Figure 1.3. Source of primary energy consumed by the transportation sector in the United States in 2016[3].

As a result of the combination of fossil gasoline being the principal primary energy source and the high energy utilization of the transport sector, reducing the GHG emissions in the U.S. transportation sector requires both the use of highly efficient systems and low carbon fuels.[4] Approaches for reducing the carbon content of transportation fuels includes biofuels derived from biomass sources, hydrogen and electricity from low-carbon feedstocks.

Biomass is believed to be the most abundant, renewable unexplored energy and as a result has received considerable attention as a sustainable feedstock that can reduce the dependency on fossil fuels for the production of energy, in particular for the transportation sector.[5, 6] Biomass as a renewable energy feedstock also has the advantage of being converted directly into liquid fuels to meet transportation fuel needs, unlike some other renewable energy sources like solar and wind power. The 2016 Billion Ton Report, a study sponsored by the U.S. Department of Energy, concludes that the United States can potentially produce at least one billion dry tons of biomass resources on an annual basis to

produce enough biofuel, biopower, and bioproducts to displace about 30% of U.S. petroleum consumption without negatively affecting the production of food or other agricultural products and protecting soil quality.[7] The most common conversion processes for biomass are currently through biochemical and thermochemical approaches, while a photobiological conversion approach is being explored for energy production by algae.[8] Biochemical conversion of biomass utilizes enzymes, microorganisms, and bacteria to break down biomass into fuels using processes such as anaerobic digestion, fermentation, etc. Thermochemical conversion uses heat to break down biomass into fuels through processes such as fast pyrolysis, torrefaction, gasification, and liquefaction. This work focuses on the thermochemical conversion route because a wide range of fuels and value-added chemicals/materials can be produced from woody biomass feedstocks, the most common form in the future U.S. supply.[9]

Fast pyrolysis, as a thermochemical conversion process utilizes heat in the form of moderately high temperature of about 500°C at atmospheric pressure in the absence of oxygen, and a short residence time of about one second to break down biomass into non-condensable gases (mainly CO and CO₂), solid (char) and liquid (bio-oil). The short residence time of fast pyrolysis favors the formation of the desired liquid, bio-oil. Bio-oil produced from fast pyrolysis has a broad range of applications such as being combusted in boilers or furnaces for heating to replace heavy fuel oil, and it can also be co-fired with coal and natural gas at conventional power plants for commercial generation of electricity[10]. It can also be used to produce specialty chemicals[11] however most importantly to this study is the fact that the produced bio-oil can be upgraded to “drop-in” hydrocarbon transportation fuel.

The upgrade of the produced bio-oil is a necessary step in obtaining a 'drop-in' substitute to fossil gasoline because the produced bio-oil is highly oxygenated as well as acidic and therefore corrosive to conventional process equipment. Among the various thermochemical conversion approaches, fast pyrolysis is believed to be promising because it offers significant logistical and hence economic advantages because the liquid product, bio-oil can be stored until required or readily transported to where it can be most effectively utilized.[12] Another advantage of the fast pyrolysis approach is the similarity of the upgrade step which removes oxygen from pyrolysis bio-oil to the removal of sulfur from crude oil in petroleum refining to produce gasoline. It is believed that existing petroleum refining facilities can be used in the upgrade of bio-oil, thereby potentially reducing the capital intensity of a commercial biomass-to-biofuel facility. For example, blending of 2-5% wt. of pyrolysis bio-oil with vacuum gas oil in a fluid catalytic cracking unit has been demonstrated to be technically feasible.[13]

A couple of drawbacks however adversely impact the efficiency of hydrocarbon biofuel production via fast pyrolysis. These drawbacks are (i) the energy intensity of the process, and (ii) the quality of bio-oil. The energy intensity of the process looks at the energy required for converting wood chips to hydrocarbon biofuel. The input energy is needed to remove the moisture from the biomass and to reduce its size to about 2 mm particles before the fast pyrolysis step. Additional energy consuming steps include heating up the wood chips for pyrolysis and heating bio-oil for hydrotreatment. The quality of bio-oil relates to its corrosiveness due to the presence of acidic components in bio-oil. In addition to the corrosiveness, bio-oil typically has a low energy density due to its high oxygen content.[14,

15] To address these drawbacks, the inclusion of a torrefaction step before fast pyrolysis is being explored.

Torrefaction, like fast pyrolysis, is a thermochemical conversion process where biomass is partially degraded at relatively lower temperature of about 280°C to 330°C, at atmospheric pressure, in an absence of oxygen and for a residence time of about 20 to 40 minutes to produce a desired solid product (bio-coal/torrefied biomass), non-condensable gases (mainly CO and CO₂) and torrefaction condensed liquids. The addition of a torrefaction step before fast pyrolysis potentially improves the grindability of the bio-coal thereby reducing the energy intensity of the size reduction step required before fast pyrolysis and improving the quality of bio-oil from the pyrolysis of bio-coal.[16-21] The improvement in the quality of bio-oil is due to the reduction of the acidic components in bio-oil from the partial degradation caused by torrefaction. The bio-oil obtained from the torrefaction-fast pyrolysis step (two-step approach) is similarly like the bio-oil from raw wood and subsequently upgraded to a 'drop-in' hydrocarbon biofuel

Beyond establishing the feasibility of these alternative pathways for transportation fuel production, it is also of utmost importance that such pathways are sustainable. The United Nations defines sustainable development as that which meets the needs of the present without compromising the ability of future generations to meet their own needs.[22] It is, therefore, necessary to evaluate if this alternative fuel production pathway meets such requirements.

1.2 Process simulation software as a tool for sustainability assessment

To assess the sustainability of new process routes, there is a need for a comprehensive evaluation of the economic, environmental and social aspects of these new routes at an early design stage.[23] Process simulation provides a tool to carry out such sustainability assessment at an early design stage before commercialization by utilizing experimental, theoretical, or literature results to model the process routes. Mass and energy balances obtained from the design models subsequently serves as inputs in assessing the sustainability of the process routes. Various sustainability indicators can be used to evaluate the process once the mass and energy balances are obtained. Such indicators include but are not limited to feedstock renewability, energy intensity, life cycle carbon footprint of the process, the water footprint of the process, the minimum selling price of the product, chemicals safety, number of direct and indirect jobs, and waste generation. Figure 1.4 shows a typical methodology flowchart for using process simulation in sustainability assessment.

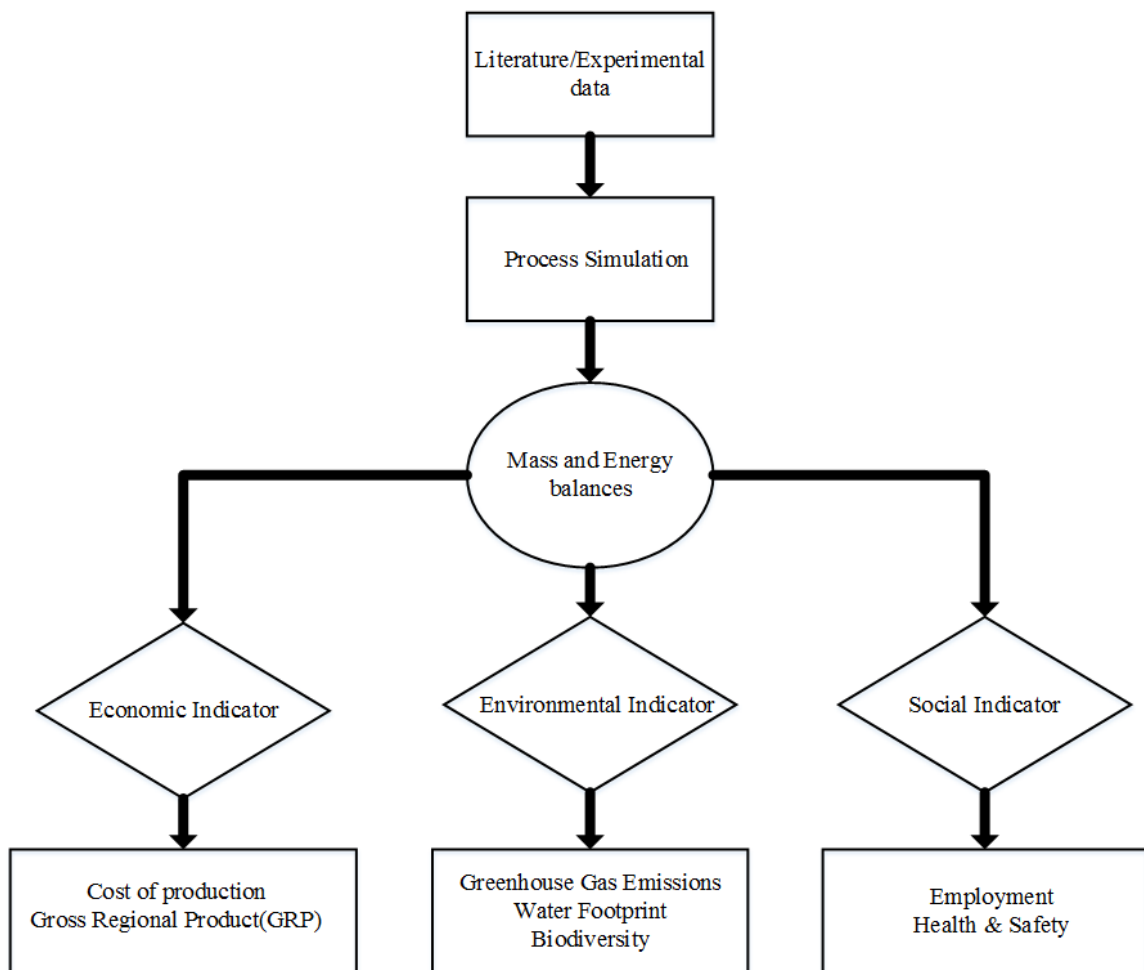


Figure 1.4. Flow chart for assessment methodology

The evaluation of the economic sustainability using the minimum selling price (MSP) of the product or the net present value (NPV) of the production route using process simulation is usually termed techno-economic assessment. The cost competitiveness of the production route is assessed using different indicators such as examining the return on investment (ROI), evaluating the discounted cash flow rate of return (DCFROR) among others. This involves estimating the MSP from the estimated capital expenditure (CAPEX) and operating expenditure (OPEX) of the process routes. CAPEX estimates of equipment

involved in the production pathway are obtained from vendors, process capital estimation software or existing literature while the OPEX estimates are evaluated using mass and energy balances obtained from the process simulation. The MSP serves as a measure of cost-competitiveness of different production routes. The workflow in estimating the minimum selling price of a product using the discounted cash flow economic model is illustrated in Figure 1.5.

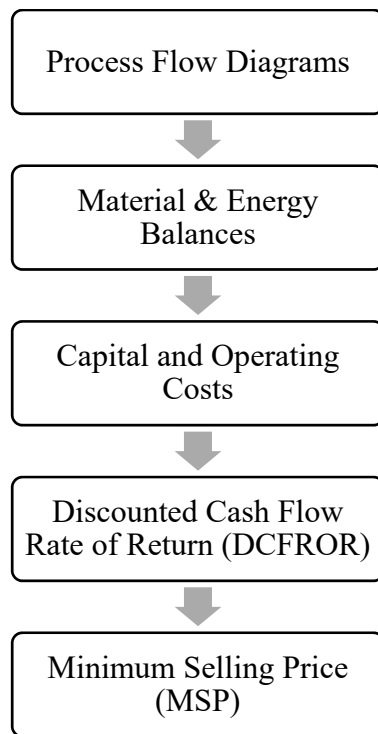


Figure 1.5. Minimum selling price assessment flow chart using the discounted rate of return (DCFROR) model. Adapted from Wooley et al.[24] Courtesy of Biotechnology Progress (See Appendix E for documentation of permission to republish the material)

The life cycle carbon footprint is one of the environmental indicators used in evaluating the potential greenhouse gas emissions from the production route. This involves estimating the predicted CO₂ equivalent emissions released to the atmosphere over the life cycle of the product which results in anthropogenic global warming. The assessment of the carbon

footprint of the production pathway over all the stages of a product's life is usually termed a "Life-cycle assessment (LCA)" Approach. The basic idea of LCA is that all environmental burdens connected with a product or service have to be comprehensively assessed, from cradle-to-grave.[25] Some studies in the literature have looked at the techno-economic assessment of hydrocarbon biofuel production via fast pyrolysis while some have used LCA methodology to evaluate the environmental impact of the fast pyrolysis production pathway.[10, 26-33]

In the literature TEA studies, Badger et al. estimated a price of \$0.94/gal for bio-oil produced from a 100 dry-ton/day transportable fast pyrolysis plant.[28] Wright et al. estimated a hydrocarbon biofuel price of \$3.09 and \$2.11 per gallon (2012 dollars) for hydrogen production and hydrogen purchase, respectively for a 2000 metric/ton day plant.[26] Jones et al. estimated a selling price of \$2.04/gal hydrocarbon fuel (2007 dollars) for a 2000 metric ton/day facility.[29] In a more recent study, Jones et al. estimated a minimum selling price of \$3.39/gallon gasoline equivalent (gge) (2011) for a 2000 dry metric ton dry biomass/day facility.[27] Brown et al. in their study estimated a selling price of \$2.57/gal (2012 dollars) for a 2000 metric/ton facility that produces hydrocarbon transportation biofuel and also supplies electricity to the electricity grid.[30]

In the LCA studies, Steele et al. estimated a 70% reduction in GHG emissions for bio-oil produced through fast pyrolysis relative to residual fuel oil.[31] Fan et al. reported GHG savings of about 77 – 99% for bio-oil combustion for power generation relative to fossil fuel based electricity.[10] Peters et al. reported GHG savings of about 54% for a fuel mix produced from poplar compared to conventional gasoline and diesel.[32] Dang et al.

reported a reduction in net GWP of about 69.1% for hydrocarbon biofuel derived from corn stover in contrast to conventional gasoline and diesel.[33] However, no reports or series of articles to my knowledge have evaluated how the inclusion of a torrefaction step before fast pyrolysis impacts the MSP of hydrocarbon fuel and the environment through C footprint and energy analyses. This dissertation research is part of Thrust 4 of the Sustainable Energy Pathways (SEP) Woods-to-Wheels: Forest-Based Biofuels project. This project investigated sustainable hydrocarbon transportation biofuel from woody biomass as shown in Figure 1.6. The project aims to develop new knowledge about complex coupled natural/industrial/societal systems by addressing potential issues that will span the entire value chain of biofuel production from biomass. The gained knowledge can then be used in carrying out a systems-level sustainability analyses to provide a holistic assessment of the Woods-to-Wheels project. To achieve this, the project aims to develop improved and sustainable bioenergy plantations to supply biomass feedstock that is converted to produce biofuel that is compatible with current technologies. This dissertation contributes to the examination of the sustainability of forest-based hydrocarbon “drop-in” biofuels.

Wood-to-Wheels: Forest-Based Biofuels

NSF Sustainable Energy Pathways, MPS/CHE - ENG/ECCS – 1230803

Research driven by the need to **understand** and **control** molecular identity

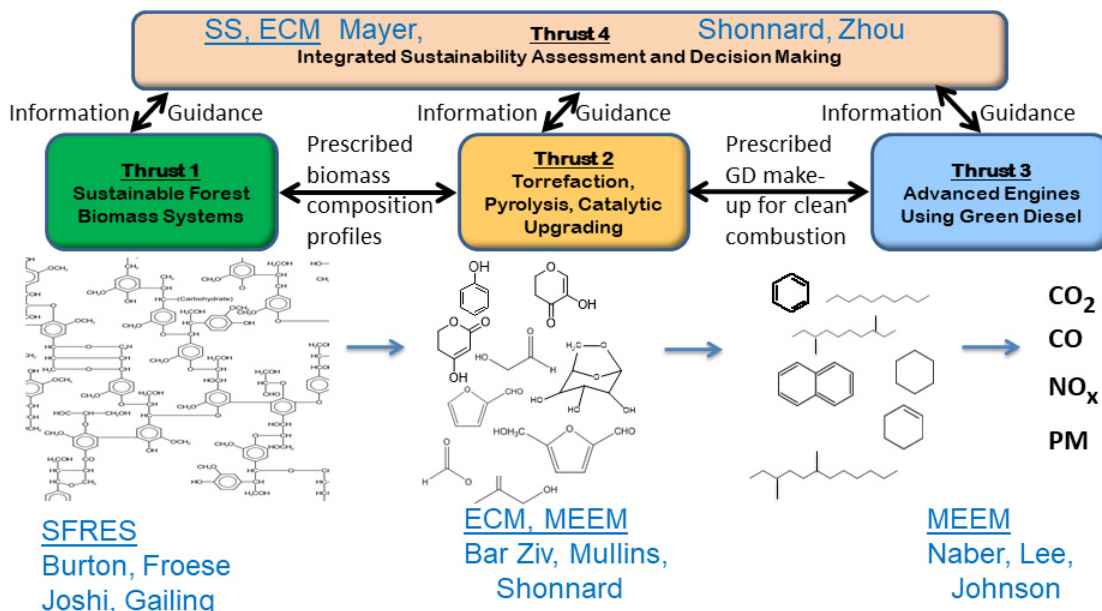


Figure 1.6. Relationship between thrusts in the SEP Woods-to-Wheels project

The research objectives for this dissertation are as follows

1. Understand and model the biomass to biofuel production pathway using a process simulation software, Aspen Plus
2. Evaluate the minimum selling price (MSP) of produced biofuel, both pyrolysis bio-oil and hydrocarbon biofuels, using simulation results
3. Evaluate the life cycle carbon footprint and energy balances of the biofuel production pathways.

4. Evaluate the effect of heat-integration on the minimum selling price and life cycle carbon footprint of the hydrocarbon biofuel production pathways.

This dissertation is divided into 5 parts. The first part focuses on the assessment of the cost of production of pyrolysis bio-oil produced from pine through one-step and two-step pathways (Chapter 2). The second part focuses on the life cycle carbon footprint and energy efficiency of producing pyrolysis bio-oil from pine through one-step and two-step pathways (Chapter 3). Chapter 4 investigates the MSP of hydrocarbon biofuel produced from pine through one-step and two-step pathways. Chapter 5 examines the life cycle carbon footprint of hydrocarbon biofuel produced from pine through one-step and two-step pathways. Chapter 6 examines the MSP and the life cycle carbon footprint of hydrocarbon biofuel produced from poplar through one-step and two-step pathways. Finally, Chapter 7 concludes with a summary the result from the studies and highlights the key conclusions of this dissertation.

References

1. United Nations Industrial Development, O., *Energy and industrialization*. OPEC Review, 1984. **8**(4): p. 409-433.
2. Administration, U.S.E.I. *Electric Power Monthly*. [cited 2013 01/25]; Available from:
https://www.eia.gov/electricity/monthly/epm_table_grapher.cfm?t=epmt_5_6_a.
3. Administration, U.S.E.I. *Energy consumption estimates by sector*. [cited 2017 03/13]; Available from: <https://www.eia.gov/consumption/>.
4. Andress, D., T.D. Nguyen, and S. Das, *Reducing GHG emissions in the United States' transportation sector*. Energy for Sustainable Development, 2011. **15**(2): p. 117-136.
5. Alonso, D.M., J.Q. Bond, and J.A. Dumesic, *Catalytic conversion of biomass to biofuels*. Green Chemistry, 2010. **12**(9): p. 1493-1513.
6. Singh, R. and S. Mishra, *Biofuels from Biomass*. 2005.
7. Langholtz, M., B. Stokes, and L. Eaton, *2016 Billion-ton report: Advancing domestic resources for a thriving bioeconomy, Volume 1: Economic availability of feedstock*. 2016.
8. Energy, U.S.D.o. *Biofuel Conversion Basics*. [cited 2017 03/13]; Available from: <https://energy.gov/eere/energybasics/articles/biofuel-conversion-basics>.
9. Mohan, D., C.U. Pittman, and P.H. Steele, *Pyrolysis of wood/biomass for bio-oil: a critical review*. Energy & fuels, 2006. **20**(3): p. 848-889.
10. Fan, J., et al., *Life cycle assessment of electricity generation using fast pyrolysis bio-oil*. Renewable Energy, 2011. **36**(2): p. 632-641.

11. Czernik, S. and A. Bridgwater, *Overview of applications of biomass fast pyrolysis oil*. Energy & Fuels, 2004. **18**(2): p. 590-598.
12. Bridgwater, A., D. Meier, and D. Radlein, *An overview of fast pyrolysis of biomass*. Organic Geochemistry, 1999. **30**(12): p. 1479-1493.
13. *Co-processing of biogenic feedstocks in petroleum refineries*. 2017.
14. Demirbas, A., *The influence of temperature on the yields of compounds existing in bio-oils obtained from biomass samples via pyrolysis*. Fuel Processing Technology, 2007. **88**(6): p. 591-597.
15. Zhang, Q., et al., *Review of biomass pyrolysis oil properties and upgrading research*. Energy conversion and management, 2007. **48**(1): p. 87-92.
16. Mani, S., L.G. Tabil, and S. Sokhansanj, *Grinding performance and physical properties of wheat and barley straws, corn stover and switchgrass*. Biomass and Bioenergy, 2004. **27**(4): p. 339-352.
17. Phanphanich, M. and S. Mani, *Impact of torrefaction on the grindability and fuel characteristics of forest biomass*. Bioresource technology, 2011. **102**(2): p. 1246-1253.
18. Van der Stelt, M., et al., *Biomass upgrading by torrefaction for the production of biofuels: A review*. Biomass and bioenergy, 2011. **35**(9): p. 3748-3762.
19. Uslu, A., A.P. Faaij, and P.C. Bergman, *Pre-treatment technologies, and their effect on international bioenergy supply chain logistics. Techno-economic evaluation of torrefaction, fast pyrolysis and pelletisation*. Energy, 2008. **33**(8): p. 1206-1223.

20. Zheng, A., et al., *Effect of torrefaction temperature on product distribution from two-staged pyrolysis of biomass*. Energy & Fuels, 2012. **26**(5): p. 2968-2974.
21. Meng, J., et al., *The effect of torrefaction on the chemistry of fast-pyrolysis bio-oil*. Bioresource technology, 2012. **111**: p. 439-446.
22. Brundtland, G.H. and M. Khalid, *Our common future*. New York, 1987.
23. Saavalainen, P., et al., *Sustainability assessment of chemical processes: Evaluation of three synthesis routes of DMC*. Journal of Chemistry, 2015. **2015**.
24. Wooley, R., et al., *Process design and costing of bioethanol technology: a tool for determining the status and direction of research and development*. Biotechnology Progress, 1999. **15**(5): p. 794-803.
25. Klöpffer, W., *Life cycle assessment*. Environmental Science and Pollution Research, 1997. **4**(4): p. 223-228.
26. Wright, M.M., et al., *Techno-economic analysis of biomass fast pyrolysis to transportation fuels*. Fuel, 2010. **89**: p. S2-S10.
27. Jones, S., et al., *Process design and economics for the conversion of lignocellulosic biomass to hydrocarbon fuels: fast pyrolysis and hydrotreating bio-oil pathway*. 2013, National Renewable Energy Laboratory (NREL), Golden, CO.
28. Badger, P., et al., *Techno-economic analysis: Preliminary assessment of pyrolysis oil production costs and material energy balance associated with a transportable fast pyrolysis system*. BioResources, 2010. **6**(1): p. 34-47.
29. Jones, S.B., et al., *Production of gasoline and diesel from biomass via fast pyrolysis, hydrotreating and hydrocracking: a design case*. Pacific Northwest National Laboratory: Richland, WA, 2009.

30. Brown, T.R., et al., *Techno-economic analysis of biomass to transportation fuels and electricity via fast pyrolysis and hydroprocessing*. Fuel, 2013. **106**: p. 463-469.
31. Steele, P., et al., *Life-cycle assessment of pyrolysis bio-oil production*. Forest Products Journal, 2012. **62**(4): p. 326-334.
32. Peters, J.F., D. Iribarren, and J. Dufour, *Simulation and life cycle assessment of biofuel production via fast pyrolysis and hydrouprgrading*. Fuel, 2015. **139**: p. 441-456.
33. Dang, Q., C. Yu, and Z. Luo, *Environmental life cycle assessment of bio-fuel production via fast pyrolysis of corn stover and hydroprocessing*. Fuel, 2014. **131**: p. 36-42.

2. Techno-economic Assessment of Bio-oil Production from pine*

2.1 Abstract

Techno-economic assessment of bio-oil production from fast pyrolysis of pine was explored through process simulation. In this work, bio-oil production via a one-step pyrolysis route and a two-step pyrolysis which included a torrefaction step before fast pyrolysis were modeled to process 1000 MT/day of dry feed through the pyrolyzer at a temperature of 530°C while two-step pyrolysis was investigated at 3 different torrefaction temperatures of 290, 310 and 330°C.

Different scenarios that included the use of fossil energy to produce process heat, as well as the use of renewable energy either through the combustion of char or portion of the condensates from torrefaction, were also investigated. Economic analysis indicates that a torrefaction step results in a reduction in the minimum selling price of bio-oil produced which reduced further with torrefaction temperature with the lowest bio-oil price of \$1.04/gal obtained for a two-step pyrolysis at torrefaction temperature of 330°C in comparison to \$1.32/gal for a one-step process. The minimum selling price of bio-oil on an energy basis, however, suggests a higher price of about \$22.19/GJ for a two-step in comparison to \$16.89/GJ for a one-step. There could be trade-offs between the higher

* Reprinted with permission from WINJOBI O, SHONNARD D. R, EZRA B, AND ZHOU W.2016. TECHNO-ECONOMIC ASSESSMENT OF THE EFFECT OF TORREFACTION ON FAST PYROLYSIS OF PINE. BIOFUELS, BIOPRODUCTS BIOREFINING 10(2): 117 – 128. Copyright 2016

quality and the higher selling price considering the downstream upgrade step to hydrocarbon fuel.

2.2 Introduction

Of all the energy consumed in the United States in 2013, renewable energy sources contributed about 12.87%, with energy from biomass sources contributing about half of the renewable energy consumed.⁽¹⁾ Biomass is considered to have the highest potential of all renewable energy sources to produce liquid transportation biofuels to partially offset consumption of imported petroleum.⁽²⁾

Biomass is typically converted to biofuels via either a biochemical or a thermochemical route.⁽³⁾ Biochemical conversions utilize enzymes to break down the biomass to monomer sugars, then microorganisms to ferment the sugars to produce liquid biofuels, typically oxygenated fuels such as ethanol or butanol. A thermochemical route utilizes high temperatures, in some cases high pressure, and catalysts to degrade biomass and upgrade intermediates to biofuel products, often hydrocarbon fuels. Examples of thermochemical conversion include pyrolysis, gasification, and liquefaction, which all have great potential for producing biofuels from sources, such as lignocellulosic biomass, which have lower potential to compete with food sources compared to crop-based biofuels such as corn ethanol.^(4,5) Fast pyrolysis of biomass is viewed as a very promising route to produce liquid fuels and as a result is now widely studied.⁽⁶⁻⁸⁾

Pyrolysis is normally carried out within a temperature range of 450 – 650°C at high heating rates in the absence of oxygen. Pyrolysis bio-oil is the main product in the pyrolysis of biomass in addition to the production of a solid co-product, char, and a non-condensable gas stream. Bio-oil has advantages over raw biomass as an energy carrier because it has a higher volumetric energy density and is more efficient to transport. A typical flow diagram

of a one-step pyrolysis process is shown in Figure 2.1, showing the main conversion steps and possible recycle of gaseous product to the reactor.

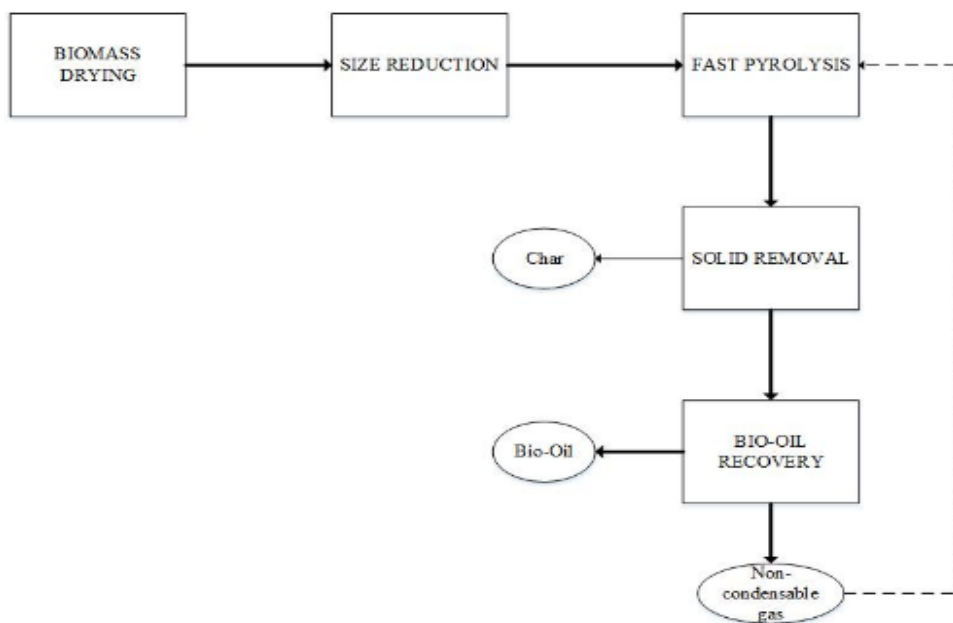


Figure 2.1. Typical process flow diagram for bio-oil production via a one-step fast pyrolysis pathway.

Bio-oil has disadvantages in that it contains water and oxygenated organic compounds which give it a relatively low heating value compared with fossil fuel, and is also acidic due to the presence of organic acids. A catalytic upgrade step (hydro-treatment) after pyrolysis is typically carried out to reduce the oxygen content and to produce a drop-in hydrocarbon biofuel.

To assess the economic viability of the conversion of biomass to bio-oil and eventual upgrade to a drop-in fuel, some researchers have conducted techno-economic assessments on the fast pyrolysis of biomass to produce bio-oil, while fewer researchers have conducted assessments for a fast pyrolysis step followed by an upgrade process to hydrocarbon fuel.^(5, 9-13) These techno-economic studies looked at different biomass feedstocks on different

scales of production with the feasibility of bio-oil production affirmed by currently existing and operational processes such as that of Envergent using a circulating fluidized bed as well as Biomass Technology Group (BTG) which utilizes a rotating cone reactor.

Results from these researches show that to be cost competitive, the energy intensity of the process needs to be reduced. The high energy requirement for fast pyrolysis stems from the fact that the optimal condition for the biomass feed entering the pyrolyzer should be of particle size of about 2mm with a moisture content of about 8%. Biomass however inherently contains high moisture content and this presents challenges for the conversion process as it reduces the efficiency of conversion.^(9, 14-16) Researchers have shown that the addition of a torrefaction step prior to the size reduction can considerably reduce the energy required for reducing the size of biomass prior to fast pyrolysis.^(17, 18) Torrefaction is a mild pyrolysis taking place at relatively lower temperatures of about 250 – 350°C over a residence time of about 30 - 40 minutes, degrading mostly the hemicellulose portion of the biomass.

During torrefaction, the degradation of chiefly the hemicellulose of the biomass is believed to give off oxygenated volatiles as well as moisture contained in the biomass to produce a torrefied biomass that is more hydrophobic than raw biomass and with a higher energy density. Subsequent pyrolysis of this torrefied biomass was found by some researchers to yield a better quality bio-oil (less corrosive, higher energy density) in comparison to that obtained from a one-step pyrolysis conversion.⁽¹⁹⁻²¹⁾ However, no studies have been carried out on the techno-economic assessment of the proposed two-step pyrolysis process to compare the cost of bio-oil production between a one-step and two-step pyrolysis

process, which is the goal of this study. Another goal of this research is to gain a better understanding of the relative importance of key unit operations on capital and operating costs. Finally, this study investigates the effects of process data uncertainty in the techno-economic assessment (TEA) results.

2.3 Material and Methods

2.3.1. Process Description

The bio-oil production process is assumed to convert 1000 dry metric tons of pine biomass entering the pyrolyzer unit per day in both the one-step and two-step routes. Process operations that were modeled in this study are drying, torrefaction (only for the two-step route), size reduction, fast pyrolysis, combustion step (to estimate process heat produced from combustion of char or condensed volatiles from torrefaction where applicable) as well as the conveyance of biomass. Model description for the torrefaction, size reduction and fast pyrolysis (the most important operations) are described below while the description of the drying operation, combustion and conveyance can be found in section A of the supplementary information.

Aspen Plus® (Aspen Technology Inc., Burlington, USA) was used for flowsheet simulation in this study. Yield reactors were used to model the torrefaction and fast pyrolysis steps in Aspen Plus®. Pine was modeled using its ultimate and proximate analysis as shown in Table 2.1.

Table 2.1. Ultimate and proximate analysis for raw pine chips.

Ultimate Analysis		Proximate Analysis	
Component	Wt %	Component	Wt %
Ash	0.6	Ash	0.60
Carbon	50.45	Moisture Content	25
Hydrogen	6.26	Volatile Matter	84.6
Chlorine	-	Fixed Carbon	14.8
Nitrogen	0.09		
Sulfur	-		
Oxygen	42.6		

Torrefaction

For the two-step fast pyrolysis route, a torrefaction step is included after the drying step but before size reduction. Torrefaction is carried out in an inert atmosphere in an auger reactor with a residence time of about 40 minutes as detailed in the literature and was modeled as a yield reactor.⁽²²⁾ Yield data used in the model was obtained from the work of Westerhoff et al. as shown in Table 2.2.⁽²³⁾ Torrefaction of biomass was investigated at different torrefaction temperatures of 290, 310 and 330°C. Representative components in the oil obtained from torrefaction were adapted from literature data as shown in Table A1 of Appendix A.^(22, 23) For modeling purpose, the non-condensable gaseous product from the torrefaction step was assumed in all cases to contain CO₂ and CO in an 80 to 20 ratio.

Table 2.2. Torrefaction yield data at different torrefaction temperatures.⁽²³⁾ Torrefaction temperatures are shown here

Material Yields (wt %)			
Torrefaction Temperature	290°C	310°C	330°C
Gas	6	8	11
Condensed Liquid	17	33	46
Torrefied Solid	78	56	43

This assumption is backed by the work of Tumuluru et al. which showed that though other components such as acetic acid and, furfural may be present, CO₂ and CO are essentially the main components.⁽¹⁵⁾ Changes in the structure of biomass from raw pine to torrefied pine at the different temperatures were accounted for by the changes to their ultimate and proximate analyses using data based on literature values as shown in Tables A2 and A3 in Appendix A.⁽²⁴⁾ We made slight adjustments to literature values to ensure that the values of proximate and ultimate analyses added up to 100% excluding the moisture content. Also, torrefied pine moisture content in all scenarios was adjusted to zero. The thermal heat required to be supplied for torrefaction is calculated by subtracting the heat of formation of the reactants from the heat of formation of the products. The standard heats of formation for pine and torrefied pine were calculated from their heats of combustion. The heat of combustion was estimated from ultimate analysis data using the Bioe correlation an established correlation used in coal analysis as shown in section A of Appendix A.

Size Reduction

A hammer mill is used to reduce the size of biomass particle from the delivered size of about 25mm to about 2mm, which has been established as an optimal size for efficient heat transfer for fast pyrolysis.^(9, 16) The energy requirement was estimated for raw pine for one step and torrefied pine/ bio-coal for two-step conversion using correlations established by Phanphanich et al.⁽¹⁷⁾ The size reduction step was modeled as a double pass through a hammer mill. Equations used in modeling the size reduction step can be found in section A of Appendix A.

Fast Pyrolysis

Fast pyrolysis of pine/ torrefied solid was carried out in a fluidized bed reactor at a temperature of 530°C and pressure of 1 bar in the absence of oxygen using nitrogen as the fluidizing agent, and this was modeled as a yield reactor. Yield data utilized for the model is based on literature data as shown in Table 2.3. The yields are based on the feed entering the pyrolyzer on a dry ash free basis.⁽²³⁾ For this study, a basis of 1000 dry metric tons per day of feed entering the pyrolyzer was modeled for both one-step and two-step routes. Bio-oil obtained from fast pyrolysis typically contains numerous products. This was modeled using representative components based on literature data as shown in Table A4 in Appendix A.⁽²²⁾

Table 2.3. Pyrolysis yield data at for one and two-step pyrolysis taking place at 530°C. (The yields are based on the feed entering the pyrolyzer on a dry ash free basis-one step is raw pine; two-step is torrefied pine)

Material yields (wt %)				
	One Step	Two Step (290°C)	Two Step (310°C)	Two Step (330°C)
Gas	28	24.4	26.8	23.3
Liquid	59	57.7	46.4	32.6
Solid/Char	10	12.8	23.2	39.5

The heat energy required to carry out pyrolysis was also estimated using the heat of formations of reactants and products. Gaseous products were also assumed to be essentially CO₂ and CO also in an 80 to 20 ratio. Char produced from pyrolysis was modeled in Aspen Plus® as an unconventional solid using its ultimate and proximate analysis shown in Table A5 in Appendix A.

2.3.2 Design Objectives

The economic viability of the conversion process of pine biomass to bio-oil was carried out under different scenarios as shown in Table 2.4. Scenario 1 assesses the economics of the conversion routes when fossil energy in the form of natural gas is combusted to supply the process heat required by the main unit operations. Bio-oil yield from two-step pyrolysis is also maximized by adding the condensed liquids from torrefaction to the condensed liquid from pyrolysis as shown in Figure 2.2. Char produced from the pyrolysis step was assumed to be sold as a substitute for coal in co-fired power plants.

Table 2.4. Design objectives for different analysis scenarios.

Scenarios	Objective 1	Objective 2
Scenario 1	Fossil energy inputs	Maximizing bio-oil yield
Scenario 2	Renewable energy inputs	Maximizing bio-oil yield
Scenario 3	Renewable energy inputs	Maximizing bio-oil quality

Scenario 2 assessed the economics of the conversion process by replacing fossil energy usage with renewable energy inputs to provide process heat. The objective here was to totally offset the use of natural gas by firstly combusting the char produced from pyrolysis to provide process heat energy. Combustion of a portion of the condensed liquid from torrefaction occurred only when the combustion of char did not sufficiently supply the process heat energy required. This scenario also aims to maximize bio-oil yield by adding torrefaction liquids not combusted to bio-oil obtained from pyrolysis as shown in Figure A2 of Appendix A.

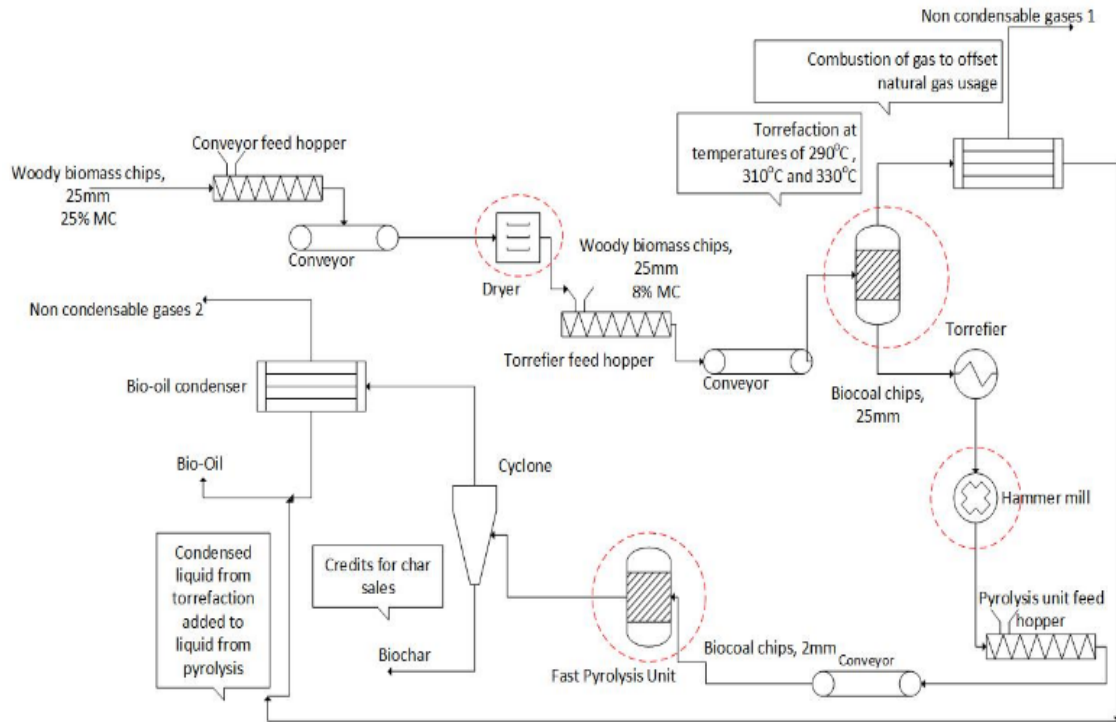


Figure 2.2. Schematic diagram for scenario 1 of a two-step conversion route

Scenario 3 also aims at offsetting natural gas inputs with renewable energy. This is however achieved by the combustion of the condensed liquid from torrefaction to provide process heat energy. The bio-oil quality is maximized as only the portion of torrefaction liquids not combusted is added to the liquid from pyrolysis. Combustion of char will be utilized to make up for process energy when the combustion of torrefaction liquids does not fulfill process heat energy requirements. Char not combusted was sold for revenue credit as shown in Figure A2 in Appendix A.

The same process was assumed in all cases with changes between scenarios and conversion routes being the size of the bio-oil storage units and size of the moving bed torrefier

respectively. The density of bio-oil in this study was assumed to be about 4.55kg/gal based on literature data.⁽¹²⁾

2.3.3 Economics

2.3.3.1 Minimum Selling Price of Bio-oil

This study employs literature and vendor quotes for its equipment costs and uses Peters and Timmerhaus installation factors based on the delivered equipment cost to estimate total project costs.⁽²⁵⁾ This approach is believed to be accurate within +/-30%. When sizes of equipment was of a different scale, cost of equipment was estimated using

$$C_1 = C_0 \times \left(\frac{S_1}{S_0}\right)^n \quad (1)$$

where S_0 is initial equipment capacity (tonnes/hr), S_1 is new equipment capacity (tonnes/hr), C_0 is equipment cost at capacity S_0 (\$), C_1 is equipment cost at capacity S_1 (\$) and n is the scaling factor which is 0.7.

The IRS Modified Accelerated Cost Recovery System (MARCS) was used to evaluate the federal tax with depreciation based on a Declining Balance (DB) method because it offered the shortest recovery period and largest tax deductions.⁽²⁶⁾ The plant depreciation was assumed to be 7 years and uses a 200% DB method. Cost from previous years was escalated to the base year of 2013 using the Chemical Engineering Plant Cost Index (CEPCI), which is provided monthly by the journal *Chemical Engineering*.⁽²⁷⁾

A Discounted Cash Flow Rate of Return (DCFROR) table prepared was used in estimating the minimum product value by setting the net present value (NPV) to zero as detailed in

the literature.⁽²⁸⁾ The cost of the fast pyrolysis unit was based on a quote given by Envergent for its Rapid Thermal Processing (RTP) unit which operates in a similar manner to a circulating fluidized bed modeled for this analysis and the method used by Jones et al. in estimating this cost was also employed in this study.⁽¹⁰⁾ The cost of the moving bed torrefier was estimated using a quote given by Batidzirai et al. with the cost of bio-oil storage based on the report by Ringer et al and, the cost of biomass feedstock handling are based on quotes given by Badger.^(12, 29-31) The costs for the dryer, hammer mills and after-cooler (comes after torrefaction for two-step processes) were obtained from vendors.

The hypothetical plant is situated in the state of Georgia, USA, and hence cost of electricity was based on delivered industrial electricity cost while the cost of natural gas was based on a 5-year average industrial delivered cost. Employee requirements were structured using the report by Ringer et al., while the wage rates were obtained from the Bureau of Labor and Statistics as shown in Table A6 in Appendix A.⁽¹²⁾ The increase in labor requirements for a two-step conversion pathway as a result of the addition of a torrefaction pre-treatment step was not factored into the assessment, but this should however not significantly affect our analysis since labor costs are a small factor having little impact on the overall economics.⁽³²⁾ Benefits and general overheads were taken to be about 90% of the total salaries while maintenance was about 3% of the total project investment. Table 2.5 shows some of the other process inputs and assumptions utilized for the economic assessment. The operating costs of the processes were estimated using the material and energy balances obtained from the process flowsheet model. Return on investment was calculated

Table 2.5. Some input values and assumption used for the economic assessment.

Parameter	Value
Pine chips cost (\$/ton) dry	60
Electricity price (cents/kW)	5.77
Cost of natural gas (\$/GJ)	5.04
Process Cooling water (\$/GJ)	0.16
Internal rate of return (%)	10
Project economic life (year)	20
Working capital (%)	5 % of total capital investment
Depreciation method	7-year MACRS
Tax rate (%)	30
Base year	2013

on a per gallon basis as well as on an energy basis, and the income tax was averaged over the plant life.

2.3.3.2 Energy Return on Energy Invested

The renewable energy return on fossil energy invested for all scenarios for one-step and two-step conversion of pine to bio-oil was carried out to look at the efficiency of the processes. Equations used in making estimates can be found in section A.5 of Appendix A.

2.3.4 Sensitivity Analysis

Some key model input variables were selected to look at how deviations from the inputs utilized in economic assessment impact the cost of bio-oil produced. Variables such as the fixed capital investment, the delivered cost of feedstock as well as cost of utilities such as electricity and natural gas were analyzed to see their impact on the final cost of production for a +/- 15% change in these variables.

2.4 Results and discussion

2.4.1 Process modeling and simulation

Simulation results from our model estimated the energy required in reducing the moisture content of pine chips from the delivered moisture content of about 25 % to the desired moisture content of about 8% in all scenarios to be about 3.35 MJ/kg of moisture removed. This value is a little lower than the value quoted by Wright et al; they stated that biomass drying requires about 50% more energy than the theoretical minimum of 2442 KJ/kg which translates to about 3663 KJ/kg of moisture removed.⁽³³⁾ Fagernas et al. also reported a higher value of 4.0MJ/kg of water removed as well as the Georgia Forestry Commission, which stated that energy required to dry wood chips falls within the range of 3486 KJ/kg – 3719 KJ/kg of moisture removed from the wood chips.⁽³⁴⁾

The energy required for torrefaction was estimated to be about 0.859MJ/kg of biomass going into the torrefier at a moisture content of 8% by calculating the heat of reaction from the heat of formations of products and reactants. Batidzirai et al. obtained a value of 1.04MJ/kg of biomass for eucalyptus (MC 40%) and 0.808MJ/kg of biomass for straw (MC 20%).⁽³⁰⁾

No literature values exist at the moment for the energy required in pyrolyzing torrefied biomass. Hence the simulation results obtained hinges on that obtained for a one step pyrolysis step. For a one step fast pyrolysis of pine, the heat of reaction estimated by our model found the reaction to be endothermic. The heat of reaction includes the sensible heat to raise the feed to the reaction temperature and the heat required for pyrolysis to take place at about 530°C. The energy required was estimated to be about 1.907 MJ/kg of feed

entering the pyrolysis unit, the heat solely for reaction was estimated based on the heat of formation of the reactants and the heat of formation of the products. This value lies within the range obtained from experimental results of Daugaard et al., where enthalpy for pyrolysis of several types of biomass was carried out.⁽³⁵⁾ They obtained values of about 1.04 MJ/kg (+/- 0.18) for oat hulls with a moisture content of 10.2%, 1.53 MJ/kg (+/- 0.26) for corn stover with a moisture content of 8.8% and 1.77 MJ/kg (+/- 0.31) for pine with a moisture content of about 7.5%, among other biomass. Yang et al. also estimated heat required for the pyrolysis of pine to be about 1.5MJ/kg pine on a dry, ash-free basis.⁽³⁶⁾ As a result of the good agreement between our simulation result and that from the literature, we believe the extension of our simulation approach to torrefied biomass is appropriate.

The reduction in size reduction energy due to torrefaction is an integral part of this economic assessment and is supported by other studies, such as reduction in grinding energy from about 850kWh/t for untreated beech to about 100kWh/t after torrefaction at 260°C over 40 minutes.⁽¹⁵⁾ Bergman and Kiel also found similar reductions from about 70 - 90% for biomass such as willow, woodcuttings using heavy-duty cutting mill as well as an increase of about 7.5 – 15% in mill capacity.⁽¹⁸⁾

The estimated energy from the combustion of condensates from torrefaction using the method earlier outlined estimated the lower heating value of the condensates at torrefaction temperatures of 290°C, 310°C and 330°C to be 11.4MJ/kg, 12.5MJ/kg and 13.1MJ/kg respectively, and these values are higher than the values of about 4.9MJ/kg for a torrefaction process at 250°C over 30 minutes and 10.7 MJ/kg at 300°C over 10 minutes found by Prins et al.⁽³⁷⁾ However this is expected because as torrefaction severity increases

the degradation of cellulose and lignin also becomes more pronounced, leading to more energy potentially being released from the combustion of the condensates from torrefaction.

2.4.2 Economic Assessment

2.4.2.1 Minimum Selling Price of Bio-oil

The bio-oil product value at zero net present value (NPV) for the one-step and two-step processes for the different scenarios are shown in Figures 2.9 and 2.10 on a \$/gal and \$/GJ basis respectively. On a per gallon basis, the minimum selling price of bio-oil ranged from about \$1.04/gal for scenario 2 of a two-step process at torrefaction temperature of 330°C, to about \$1.94/gal for scenario 3 of a two-step process at torrefaction temperature of about 290°C, as shown in Figure 2.9. It can be seen here that when bio-oil yield is maximized,

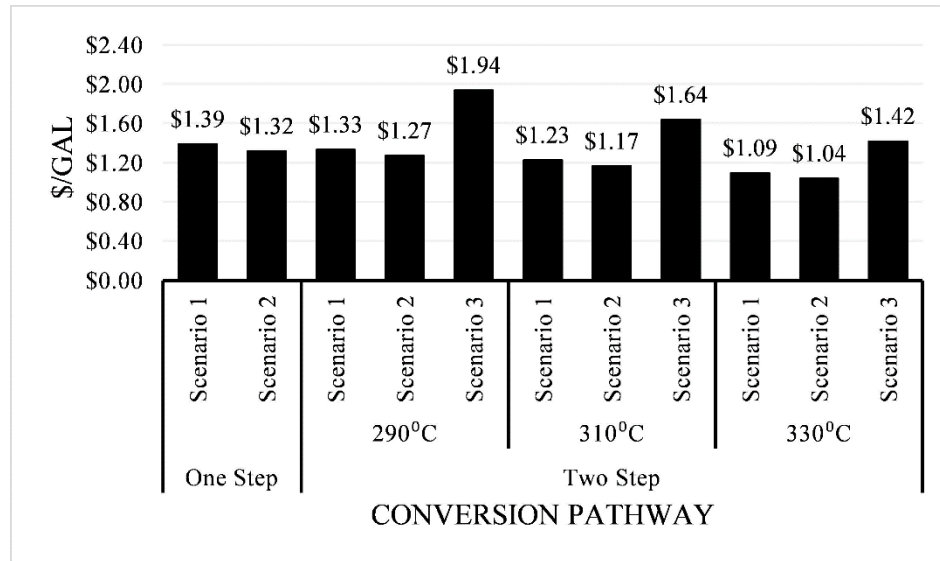


Figure 2.3. Product value of bio-oil on a gallon basis for one-step and two-step conversion processes. Torrefaction temperatures are shown for two-step pathways.

the use of renewable energy instead of fossil energy to fulfill process heating is a more viable production pathway, even though lower revenue credits were generated by char sales. Scenario 3 (maximize bio-oil quality while using renewable energy from torrefaction liquids) at all torrefaction temperatures for a two-step conversion gave the highest minimum selling price. This is because the yield of bio-oil produced is reduced. Though char was exported for revenue credits, it was not enough to make up for the reduction in bio-oil yield when bio-oil from torrefaction was used to offset natural gas. The minimum selling price was also assessed on a per energy basis using the estimated lower heating value (LHV) of the bio-oil produced. The lower heating value of the bio-oil, shown in Table 2.6, was estimated using the lower heating value of the representative components in the bio-oil and their relative mass yields in the bio-oil.

The LHV the bio-oil for a one-step conversion step was estimated to be about 17.14 MJ/kg which is in agreement with the value obtained by Oasma et al., for pine and is within typical range for bio-oil from different biomass sources for one-step conversion to bio-oil given by other literatures.^(7, 12, 38, 39)

Improved bio-oil quality was observed for the two-step conversion pathways in comparison with a one-step pathway. However, the addition of condensed liquid from torrefaction lowered the quality of the overall blended bio-oil produced. In scenario 3 of a two-step process with torrefaction taking place at 290°C, all the condensed vapors (liquid) from torrefaction was required to be combusted to fully offset use of natural gas to provide process heat. Hence, this scenario had the highest quality of bio-oil produced because no torrefaction condensed product was added to the pyrolysis bio-oil. Scenarios 3 in all two-

step processes showed that the bio-oil quality was maximized in comparison with scenarios 1 and 2 of each two-step process as seen in Table 2.6. Meng et al. showed an increase in the higher heating value (HHV) of bio-oil derived from fast pyrolysis of loblolly pine from about 21 MJ/kg for a one-step pyrolysis to about 23.5 MJ/kg for a two-step with torrefaction at 300°C, confirming our results.⁽⁴⁰⁾

Table 2.6. Estimated lower heating value (LHV) of bio-oil produced for different scenarios of the conversion pathway. Torrefaction temperatures for two-step shown here

LHV (MJ/kg)				
	One-Step	Two-Step		
Scenario		290°C	310°C	330°C
1	17.14	16.33	14.95	13.93
2	17.14	16.36	14.95	13.92
3		19.22	16.04	14.27

Using these estimated lower heating values of bio-oil, the minimum selling price of produced bio-oil on a per energy basis was estimated, and the results are as shown in Figure 2.4. Minimum selling price on an energy basis ranged from about \$16.89/GJ to about \$22.47/GJ. Though scenario 2 of a two-step processes at 310°C and 330°C showed prices comparable to a one-step process, the quality of bio-oil in these scenarios are lower than that obtained from a one-step. The minimum selling price of bio-oil produced from scenario 3 of a two-step process at 290°C though higher than that of one-step, the quality of bio-oil is better than that obtained from a one-step based on the energy content. The higher quality may be a good trade-off despite the slightly higher price.

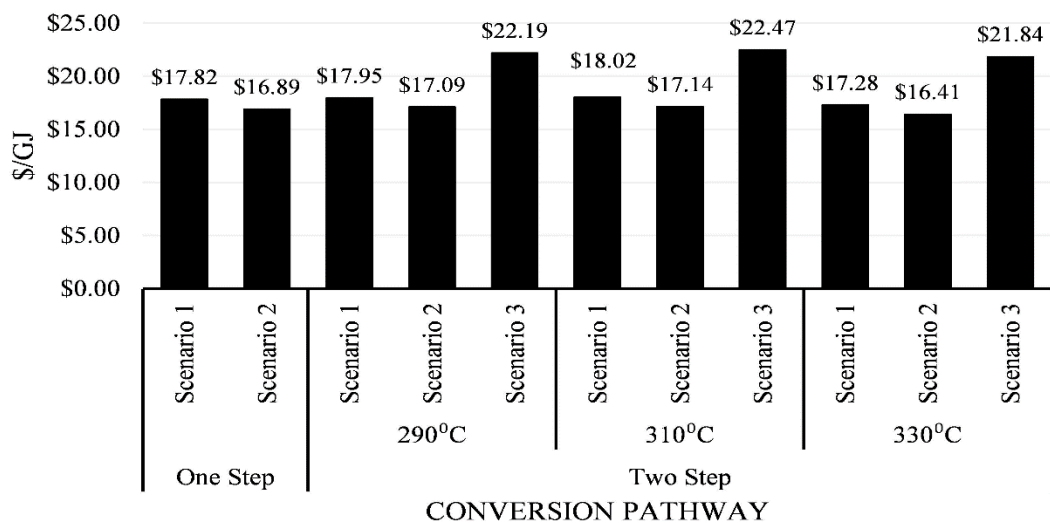


Figure 2.4. Product value of bio-oil on an energy basis for one-step and two-step conversion processes. Torrefaction temperatures are shown for two-step pathways.

Estimates for some of the operating costs obtained and used in the economic assessment are shown in Table 2.7.

Table 2.7. Some of the cost estimates for the one and two-step processes.

	One-Step		Two-Step								
			290°C			310°C			330°C		
Torrefaction temperature											
Scenarios	1	2	1	2	3	1	2	3	1	2	3
Feedstock (\$MM/year)	21.2	21.2	27.4	27.4	27.4	36.5	36.5	36.5	48.1	48.1	48.1
Electricity (\$MM/year)	9	9	1.4	1.4	1.4	0.8	0.8	0.8	0.4	0.4	0.4
Natural Gas (\$MM/year)	6.4	0.9	7.2	-	-	8.2	-	-	10.2	-	-
Char credit (\$MM/year)	1.8	-	2.4	-	2.2	4.2	1.4	4.2	7.1	3.7	7.1
Bio-oil (10 ⁸ kg/year)	2.3	2.3	3.2	3.2	2.1	4.2	4.2	2.9	5.6	5.6	3.9
Total Project Investment (\$MM)	132	132	238	238	236	278	278	276	327	327	325

Product value of bio-oil on a volume basis was compared to values obtained from some previous works, as shown in Table 2.8 with the cost in parenthesis being the adjustment made for inflation. Except for rice husks, bio-oil MSP from this study are higher than literature values after including effects of inflation on the literature values. It should also be noted that if a 50:50 ratio of CO₂ to CO in the non-condensable gases from fast pyrolysis was utilized in our models instead of 80:20 used in this study (based on our experimental result), the overall heat required for fast pyrolysis increased. This increase resulted in a negligible increase of about \$0.02 in the cost analysis carried out in this study.

Table 2. 8. Comparison of estimated bio-oil cost with previous works for one-step only.

Plant Size (MT/day)	Biomass Type	Feed cost (\$/dry ton)	Bio-oil cost (\$/gal)	Year	Source
24	Rice husk	22	1.73 (2.31)	2000	(46)
100	Pine wood chips	50	0.94 (1.00)	2010	(13)
1000	unspecified	44	0.41 (0.69)	1991	n/a
2000	Corn stover	83	0.83 (0.89)	2010	(9)
1000	Pine wood chips (one-step: scenario 1)	60	1.39		This study
1000	Pine wood chips (one-step: scenario 2)	60	1.32		This study

2.4.2.2 Energy Return on Energy Invested (EROEI)

EROEI analysis shows an increase from a one-step to a two-step conversion process. It also shows that higher returns on energy were achieved when renewable energy was used to provide process heat. Scenario 2, with the objective being maximum bio-oil yield while offsetting the use of natural gas and scenario 3, with the objective of maximum bio-oil yield while offsetting the use of natural gas as earlier discussed, showed almost equivalent

results. EROEI increased with the inclusion of a torrefaction step and also with an increase in torrefaction temperature as shown in Table 2.9.

Table 2.9. Energy Returns on Energy Invested analysis of the conversion pathways. Torrefaction temperatures are shown for the two-step.

Scenarios	One-Step	Two-Step		
		290°C	310°C	330°C
1	1.95	3.75	6.03	7.11
2	2.30	21.3	45.56	161.1
3		21.3	45.56	161.1

Scenario 1, where process heat was supplied by natural gas also showed an increase in energy returns for a two-step process compared to one-step. Energy returns also increased in this scenario with an increase in torrefaction temperature as shown in Table 2.9. For fair comparison, scenarios 1 of our pathways shows higher EROEI when compared to biodiesel which has an EROEI of 1.3, and corn-based ethanol with EROEI range of 0.8 to 1.6.⁽⁴¹⁻⁴³⁾ These EROEI values are however considerably lower than hydropower with EROEI over 100, coal (mine – mouth) with 80 and oil & gas with EROEI range of 11 to 18.^(41, 42, 44)

2.4.3 Sensitivity Analysis

Sensitivity analysis was conducted on the scenarios looked at for the impact of a +/- 15% deviation in some of the cost variables and TEA model inputs for the one-step and two-step conversion processes. Sensitivity analysis for scenario 1 for a one-step conversion of pine to bio-oil is shown in Figure 2.11. The cost of delivered feedstock, as well as estimated total project investment, are almost equal and the most important. The highest sensitivity, however, comes from the bio-oil yield; this is in line with the findings of Brown et al., that also identified biomass pyrolysis yield as an important factor in the cost competitiveness

of the process.⁽⁴⁵⁾ If the conversion technology is improved and the yield of oil obtained from the pyrolysis step is higher, then the economics can be improved. Based on the data used in this study, the high sensitivity of the price of bio-oil to the change in yield emphasizes the need for accurate yield data prior to commercialization of a pine-to-bio-oil facility. It should, however, be noted that unlike variables which are independent of other variables, change in the yield of bio-oil will have a resultant change in some variables such as the amount of natural gas that will be utilized as well as the credits obtainable from char, as changes in yield of bio-oil may translate to changes in amount of char produced. These potential associated changes as a result of changes to bio-oil yield were not considered when looking at how the change in bio-oil yield impacts cost of production. The minimum selling price is also sensitive to the rate of return; although a reduction in the rate of return will not be of benefit to potential investors, we still evaluated this variable, and the minimum selling price showed a strong sensitivity to changes in this variable as well.

Change to the estimated selling price of char shows the weakest impact on the cost of bio-oil produced. The cost of delivered electricity also show a mildly strong impact on the minimum selling price of bio-oil but points to the fact that even for areas where pine may be abundantly present, the minimum selling price may vary based on the cost of delivered electricity used in reducing the size of the pine as this varies across the different states in the United States. It should also be noted that the sensitivities of the yield of bio-oil and credits from char sales swings in directions different from other variables assessed. They vary

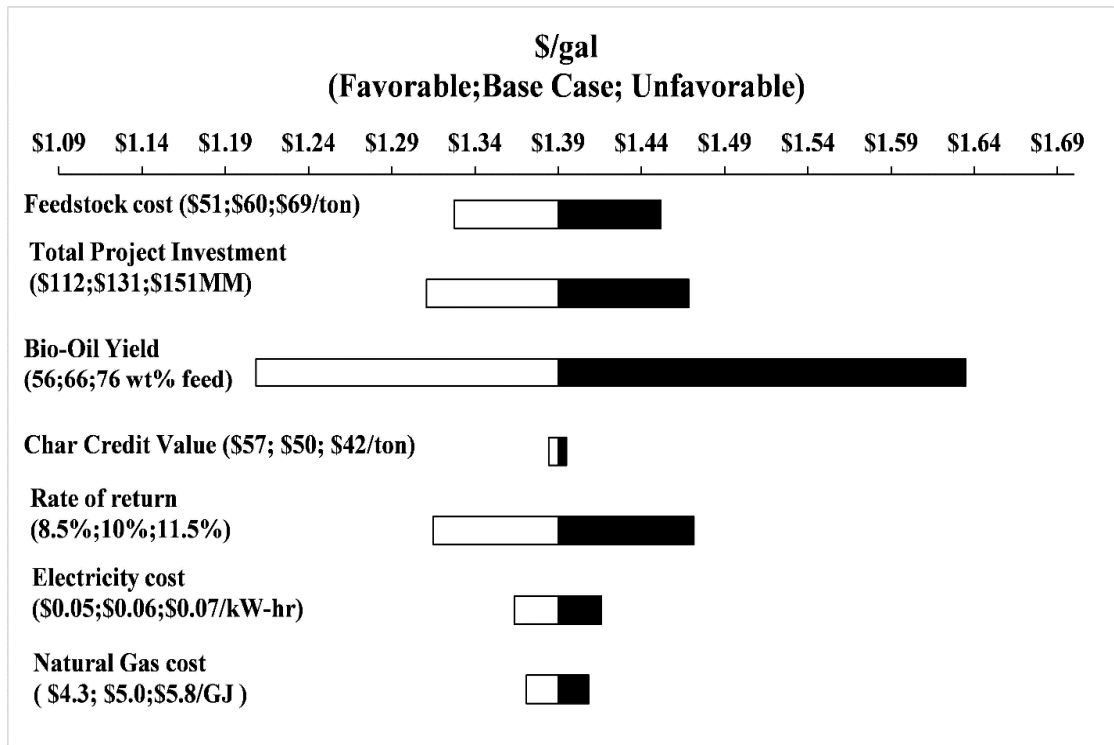


Figure 2.5. Sensitivity result for a one-step pyrolysis of pine scenario 1.

inversely with the change to the minimum selling price of bio-oil; i.e. increase in these two variables results in a decrease in estimated minimum selling price of bio-oil while increase or decrease in other variable is directly proportional to the changes in the minimum selling price of bio-oil produced. Some of the trends observed for this scenario for a one-step process are also found in other scenarios. Changes in the yield of bio-oil have the largest impact on the selling price of bio-oil and these results are shown as Figures A3 to A12 in Appendix A.

2.5 Conclusions

From the results of this study, a torrefaction step prior to fast pyrolysis of pine does not increase the cost of production of bio-oil when the NPV is zero compared to a one-step pyrolysis of raw pine. The use of char produced internally to provide process heat made a more positive impact on lowering the selling price of bio-oil produced than the sale of exported char to boost revenue credits. The addition of condensable volatiles from torrefaction for two-step processes increased the overall yield of bio-oil resulting in the lower selling price of bio-oil on a volume basis, with the lowest price of \$1.04/ gal for a two-step conversion with torrefaction taking places at 330°C. The addition of the condensable volatiles however negatively impacted the quality of bio-oil produced (LHV). The highest bio-oil quality of about 19.22 MJ/kg was obtained for a two-step process with torrefaction taking place at 290°C when the volatiles was completely used up to supply process heat. There could be a trade-off between the higher quality of bio-oil and higher selling price considering the downstream upgrade step to hydrocarbon fuel due to the possible reduction in the hydrogen required for upgrading. This consideration was beyond the scope of this work, and will be addressed in future research.

Energy return on energy invested also increased from a one-step conversion process to a two-step conversion step. This also increased with an increase in torrefaction temperature, with the highest energy returns obtained when char is combusted to internally produce the process heat required. From the sensitivity analysis, it can be seen that the yield of bio-oil is the most sensitive parameter.

It is worth mentioning that these results are based on loblolly pine as the biomass feedstock and the data utilized in this study, and may not be typical for other biomass feedstocks.

2.6 Acknowledgements

Financial support from the National Science Foundation MPS/CHE - ENG/ECCS – 1230803 Sustainable Energy Pathways (SEP) grant and the Richard and Bonnie Robbins Endowment.

2.7 References

1. EIA U. Annual energy outlook 2013 with projections to 2040. DOE/EIA-0383 April. 2013.
2. Perlack RD, Eaton LM, Turhollow Jr AF, Langholtz MH, Brandt CC, Downing ME, et al. US billion-ton update: biomass supply for a bioenergy and bioproducts industry. 2011.
3. Shonnard DR, Brodeur-Campbell MJ, Martin-Garcia AR, Kalnes TN. for Bioenergy Plants. Handbook of Bioenergy Crop Plants. 2012:133.
4. Naik S, Goud VV, Rout PK, Dalai AK. Production of first and second generation biofuels: a comprehensive review. Renewable and Sustainable Energy Reviews. 2010;14(2):578-97.
5. Shemfe MB, Gu S, Ranganathan P. Techno-economic performance analysis of biofuel production and miniature electric power generation from biomass fast pyrolysis and bio-oil upgrading. Fuel. 2015;143:361-72.
6. Bridgwater AV, Meier D, Radlein D. An overview of fast pyrolysis of biomass. Organic Geochemistry. 1999;30(12):1479-93.
7. Mohan D, Pittman CU, Steele PH. Pyrolysis of wood/biomass for bio-oil: a critical review. Energy & Fuels. 2006;20(3):848-89.
8. Lyu G, Wu S, Zhang H. Estimation and Comparison of Bio-Oil Components from Different Pyrolysis Conditions. Name: Frontiers in Energy Research. 2015;3:28.
9. Wright MM, Daugaard DE, Satrio JA, Brown RC. Techno-economic analysis of biomass fast pyrolysis to transportation fuels. Fuel. 2010;89, Supplement 1(0):S2-S10.

10. Jones S, Meyer P, Snowden-Swan L, Padmaperuma A, Tan E, Dutta A, et al. Process design and economics for the conversion of lignocellulosic biomass to hydrocarbon fuels: fast pyrolysis and hydrotreating bio-oil pathway. National Renewable Energy Laboratory (NREL), Golden, CO., 2013.
11. Jones SB, Valkenburg C, Walton CW, Elliott DC, Holladay JE, Stevens DJ, et al. Production of gasoline and diesel from biomass via fast pyrolysis, hydrotreating and hydrocracking: a design case: Pacific Northwest National Laboratory Richland, WA; 2009.
12. Ringer M, Putsche V, Scahill J. Large-Scale Pyrolysis Oil. Assessment. 2006.
13. Badger P, Badger S, Puettmann M, Steele P, Cooper J. Techno-economic analysis: Preliminary assessment of pyrolysis oil production costs and material energy balance associated with a transportable fast pyrolysis system. *BioResources*. 2010;6(1):34-47.
14. Renewables E. LLC. Biomass torrefaction as a preprocessing step for thermal conversion: Reducing costs in the biomass supply chain. 2009.
15. Shankar Tumuluru J, Sokhansanj S, Hess JR, Wright CT, Boardman RD. REVIEW: A review on biomass torrefaction process and product properties for energy applications. *Industrial Biotechnology*. 2011;7(5):384-401.
16. Bridgwater A, Toft A, Brammer J. A techno-economic comparison of power production by biomass fast pyrolysis with gasification and combustion. *Renewable and Sustainable Energy Reviews*. 2002;6(3):181-246.
17. Phanphanich M, Mani S. Impact of torrefaction on the grindability and fuel characteristics of forest biomass. *Bioresource technology*. 2011;102(2):1246-53.
18. Bergman PC, Kiel JH, editors. Torrefaction for biomass upgrading. Proc 14th European Biomass Conference, Paris, France; 2005.

19. Boateng A, Mullen C. Fast pyrolysis of biomass thermally pretreated by torrefaction. *Journal of Analytical and Applied Pyrolysis*. 2013;100:95-102.
20. Yang Z, Sarkar M, Kumar A, Tumuluru JS, Huhnke RL. Effects of torrefaction and densification on switchgrass pyrolysis products. *Bioresource technology*. 2014;174:266-73.
21. Neupane S, Adhikari S, Wang Z, Ragauskas A, Pu Y. Effect of torrefaction on biomass structure and hydrocarbon production from fast pyrolysis. *Green Chemistry*. 2015;17(4):2406-17.
22. Zheng A, Zhao Z, Chang S, Huang Z, He F, Li H. Effect of Torrefaction Temperature on Product Distribution from Two-Staged Pyrolysis of Biomass. *Energy & Fuels*. 2012;26(5):2968-74.
23. Westerhof RJ, Brilman DWF, Garcia-Perez M, Wang Z, Oudenhoven SR, Kersten SR. Stepwise fast pyrolysis of pine wood. *Energy & Fuels*. 2012;26(12):7263-73.
24. Park J, Meng J, Lim KH, Rojas OJ, Park S. Transformation of lignocellulosic biomass during torrefaction. *Journal of Analytical and Applied Pyrolysis*. 2013;100:199-206.
25. Peters M, Timmerhaus K, West R. *Plant design and economics for chemical engineers*: McGraw-Hill New York; 1968.
26. Aden A, Foust T. Technoeconomic analysis of the dilute sulfuric acid and enzymatic hydrolysis process for the conversion of corn stover to ethanol. *Cellulose*. 2009;16(4):535-45.
27. CEPCI. *Chemical Engineering Plant Cost Index*. *Chem Eng*. 2010:76.

28. Towler GP, Sinnott RK. Chemical Engineering Design: Principles, Practice, and Economics of Plant and Process Design: Access Online via Elsevier; 2012.
29. Boulard D, Morgan J. Ensyn. Personal Communication & Presentation. 2002.
30. Batidzirai B, Mignot A, Schakel W, Junginger H, Faaij A. Biomass torrefaction technology: Techno-economic status and future prospects. *Energy*. 2013;62:196-214.
31. Badger PC. Processing cost analysis for biomass feedstocks. DOE/EERE. 2002.
32. Turton R, Bailie RC, Whiting WB, Shaeiwitz JA. Analysis, synthesis and design of chemical processes: Pearson Education; 2008.
33. Wright MM, Dugaard DE, Satrio JA, Brown RC. Techno-economic analysis of biomass fast pyrolysis to transportation fuels. *Fuel*. 2010;89:S2-S10.
34. Fagernäs L, Brammer J, Wilén C, Lauer M, Verhoeff F. Drying of biomass for second generation synfuel production. *Biomass and Bioenergy*. 2010;34(9):1267-77.
35. Dugaard DE, Brown RC. Enthalpy for Pyrolysis for Several Types of Biomass. *Energy & Fuels*. 2003;17(4):934-9.
36. Yang H, Kudo S, Kuo H-P, Norinaga K, Mori A, Mašek Oe, et al. Estimation of enthalpy of bio-oil vapor and heat required for pyrolysis of biomass. *Energy & Fuels*. 2013;27(5):2675-86.
37. Prins MJ, Ptasiński KJ, Janssen FJJG. More efficient biomass gasification via torrefaction. *Energy*. 2006;31(15):3458-70.
38. Czernik S, Bridgwater A. Overview of applications of biomass fast pyrolysis oil. *Energy & Fuels*. 2004;18(2):590-8.
39. Oasmaa A, Czernik S. Fuel oil quality of biomass pyrolysis oils state of the art for the end users. *Energy & Fuels*. 1999;13(4):914-21.

40. Meng J, Park J, Tilotta D, Park S. The effect of torrefaction on the chemistry of fast-pyrolysis bio-oil. *Bioresource technology*. 2012;111:439-46.
41. Murphy DJ, Hall CA. Year in review—EROI or energy return on (energy) invested. *Annals of the New York Academy of Sciences*. 2010;1185(1):102-18.
42. Hall C. Reports published on The Oil Drum. 2008.
43. Farrell AE, Plevin RJ, Turner BT, Jones AD, O'hare M, Kammen DM. Ethanol can contribute to energy and environmental goals. *Science*. 2006;311(5760):506-8.
44. Cleveland CJ. Net energy from oil and gas extraction in the United States, 1954-1997. *Energy*. 2005;30:769-82.
45. Brown TR, Zhang Y, Hu G, Brown RC. Techno-economic analysis of biobased chemicals production via integrated catalytic processing. *Biofuels, Bioproducts and Biorefining*. 2012;6(1):73-87.
46. Islam M, Ani F. Techno-economics of rice husk pyrolysis, conversion with catalytic treatment to produce liquid fuel. *Bioresource technology*. 2000;73(1):67-75.

3. Life cycle greenhouse gas emissions of bio-oil from two-step torrefaction and fast pyrolysis of pine[†]

3.1 Abstract

Life cycle assessment of bio-oil from woody biomass through two pathways was carried out: a one-step pathway that utilizes fast pyrolysis of pine and a two-step pathway that incorporates a torrefaction step prior to fast pyrolysis. A two-step pathway with torrefaction at a temperature of 330°C and pyrolysis at 530°C had a global warming potential of about 6g CO₂ equivalent per MJ of bio-oil compared to about 39g CO₂ equivalent per MJ of bio-oil for a one-step pathway using an energy allocation-based analysis. For a one-step pathway, the size reduction step made the highest contribution of over 50% of the overall global warming potential. Greenhouse gas (GHG) savings of up to 80% compared to heavy fuel oil (HFO) were achieved for a two-step pathway in comparison to a one-step pathway due to savings in size reduction energy. The use of renewable energy sources produced internally to provide process heat either by first burning char, and then condensables from torrefaction (oil) or vice versa resulted in similar global warming potential reduction in comparison to use of natural gas to provide process heat. The bio-oil production pathways were found to be more sustainable in comparison to HFO due to relying chiefly on renewable biomass rather than fossil energy.

[†] Reprinted with permission from WINJOBI O, SHONNARD D. R, EZRA B, AND ZHOU W.2016. TECHNO-ECONOMIC ASSESSMENT OF THE EFFECT OF TORREFACTION ON FAST PYROLYSIS OF PINE. BIOFUELS, BIOPRODUCTS BIOREFINING 10(2): 117 – 128. Copyright 2016

3.2 Introduction

Being a carbon carrier capable of storage and on-demand usage, biomass is deemed unique, making it an attractive renewable energy source.⁽¹⁾ The 'Billion Ton Study,' released initially in 2005 and updated in 2011 by the United States Department of Energy, looked at potentially producing at least one billion dry tons of biomass annually, in a sustainable manner, enough to displace about 30% of the current petroleum consumption in the United States.⁽²⁾ Fuels from biomass can be produced either through a biochemical pathway, where biomass is degraded using enzymes and microbes, or a thermochemical pathway, where biomass is thermally degraded. Fast pyrolysis, one of the thermochemical routes, is believed to be one of the more promising options for producing liquid biofuels from lignocellulosic biomass.⁽³⁻⁹⁾ Thermal degradation via fast pyrolysis is achieved by subjecting biomass to high temperature, typically between 450 – 600°C, at atmospheric pressure in the absence of oxygen and a short residence time of about one second. The products from the fast pyrolysis include char (mostly carbon), bio-oil and gas (mostly CO and CO₂).⁽¹⁰⁾ The desired product from this process is the bio-oil, a liquid of moderate heating value usable as fuel in boilers, but can be further upgraded via a hydroprocessing step to hydrocarbon transportation fuel.

Required size reduction and drying of biomass feedstock prior to fast pyrolysis makes the production of bio-oil an energy intensive process.^(11, 12) One recently proposed method to address the energy intensity of pyrolysis is the introduction of a torrefaction step prior to the size reduction step. Torrefaction is achieved at lower temperatures between 200 – 350°C in an inert environment over a residence time of about 30 minutes. The main product is torrefied solid bio-coal, which is of higher energy density compared to raw

biomass. The introduction of torrefaction prior to fast pyrolysis is believed to improve the quality of the bio-oil produced from fast pyrolysis as well as reduce the energy consumption associated with the size reduction of biomass to optimal pyrolysis size of about 2mm.⁽¹³⁻¹⁷⁾ Besides energy independence, biofuels can also help mitigate greenhouse gas emissions by having a production and usage pathway that places a lower burden on the environment when compared to fossil fuels. One way of assessing the environmental impacts of the production and use of biofuels is by conducting a cradle-to-grave life cycle assessment (LCA).

LCA is a standardized methodology used to study the potential environmental impacts throughout a product's or system's life cycle from raw material acquisition through production, use, and disposal.^(18, 19) It provides information on energy and material inputs as well as waste and emission outputs of a product or system and their associated environmental impacts.⁽²⁰⁾ In developing new process and retrofitting existing technologies, LCA provides information that highlights processes that place negative burdens on the environment. Such processes can be targeted for improvement or where possible alternative processes utilized.

LCA has been used by several investigators to look at the environmental burdens of bioenergy processes. Focusing on fast pyrolysis bioenergy pathways, Steele et al. in their LCA study of bio-oil production via fast pyrolysis, reported a 70 percent reduction in greenhouse gas emissions over residual fuel oil.⁽²¹⁾ For power generation from biomass, Zhong et al. used an LCA study to show that power generation through flash pyrolysis of wood waste is environmentally friendly.⁽²²⁾ Fan et al. showed GHG savings of 77 – 99%

for power generation from pyrolysis oil combustion relative to fossil fuels combustion using LCA. ^(22, 23) Other LCA studies have also investigated transportation hydrocarbon fuel production pathways via fast pyrolysis of biomass with the subsequent upgrade of bio-oil.^(3, 24-26) Though different biomass, reactor configurations, and functional units were utilized in these studies, they all reported lower GHG emissions compared to gasoline. This study will investigate the environmental impact of bio-oil production and use by utilizing a two-step production pathway employing torrefaction as a pretreatment step prior to fast pyrolysis using LCA.

The advantages and limitations of the two-step approach will be explored in this LCA using chemical process simulation guided by experiments on product yields and compositions. The effects of the type of renewable energy utilized i.e. either energy from solid or liquid co-products from pyrolysis and torrefaction, respectively, to replace fossil inputs for process heat will also be investigated.

3.3 Materials and methods

3.3.1 Definition of the case study

This study is a comparative cradle-to-grave life cycle assessment of the production and use of bio-oil from loblolly pine wood chips via one-step and two-step pyrolysis pathways. The main operations in the biomass conversion pathway are shown in Figure 3.1. The drying of biomass to reduce the moisture content is modeled here through an indirect contact dryer with steam acting as the drying medium. The torrefaction of dried biomass occurs within an auger reactor over a residence time of about 30 minutes. The torrefied solid (bio-coal) then passes through hammer mills after cooling to room temperature to reduce size from approximately 25 mm to the desired 2mm dimension. The fast pyrolysis step is modeled as a “yield” reactor in the process simulator. Loblolly pine was selected for this study as the biomass type because of its importance as a bioenergy feedstock, the availability of torrefaction and pyrolysis data from the literature on yields and compositions of the gas, liquid, and solid products, and also the availability of data on size reduction for pine with and without torrefaction.^(13, 27, 28) The basis of the study is a 1000 metric tons of feed (dry basis) into the pyrolysis unit; for the one-step process, the feed is raw loblolly pine wood chips, while for two-step process the feed is torrefied loblolly pine wood chips. The processes analyzed are based on design cases modeled in Aspen Plus using data from the literature.⁽²⁷⁻²⁹⁾

This study carried out the life cycle assessment by investigating 3 different scenarios as shown in Table 3.1. Objectives of scenario 1 referred to as FMBY, were met by utilizing fossil energy inputs (i.e. natural gas) to meet the process heat requirements; and

Table 3.1. Design objectives for different scenarios

Scenarios	Design Objective 1	Design Objective 2
Scenario 1 – FMBY Fossil, Maximize Bio-oil Yield	Fossil energy inputs	Maximizing bio-oil yield
Scenario 2 – RMBY Renewable, Maximize Bio-oil Yield	Renewable energy inputs	Maximizing bio-oil yield
Scenario 3 – RMBQ Renewable, Maximize Bio-oil Quality	Renewable energy inputs	Maximizing bio-oil quality

maximizing bio-oil yield by condensing the vapor portion from torrefaction and adding it to the liquid yield from fast pyrolysis, as shown in Figure 3.1. The co-product char produced from the pyrolysis step is carbon-rich and has a high energy content. For FMBY, the char produced was assumed to be collected and sold to co-fire in power plants to displace coal.

Scenario 2 referred to as RMBY, maximizes bio-oil yield while using renewable energy. This scenario totally offsets fossil energy usage for process heat by first combusting the char produced, then the condensed liquid from torrefaction if necessary. The objective of maximizing bio-oil yield is met by the addition of the remaining condensed liquid from torrefaction to the liquid yield from fast pyrolysis. Scenario 3 referred to as RMBQ also investigates totally offsetting fossil fuel usage with the use of renewable energy. This was however achieved by initially utilizing the condensed liquid from torrefaction, which is normally of lower quality due to corrosivity and lowers heating value for process heat, then char if necessary. Pyrolysis bio-oil from torrefied biomass is usually of higher quality (less acidity, greater heating value), which is one key objective of RMBQ. Schematic

diagrams for RMBY and RMBQ can be found as Figures B1 and B2 respectively in Appendix B.

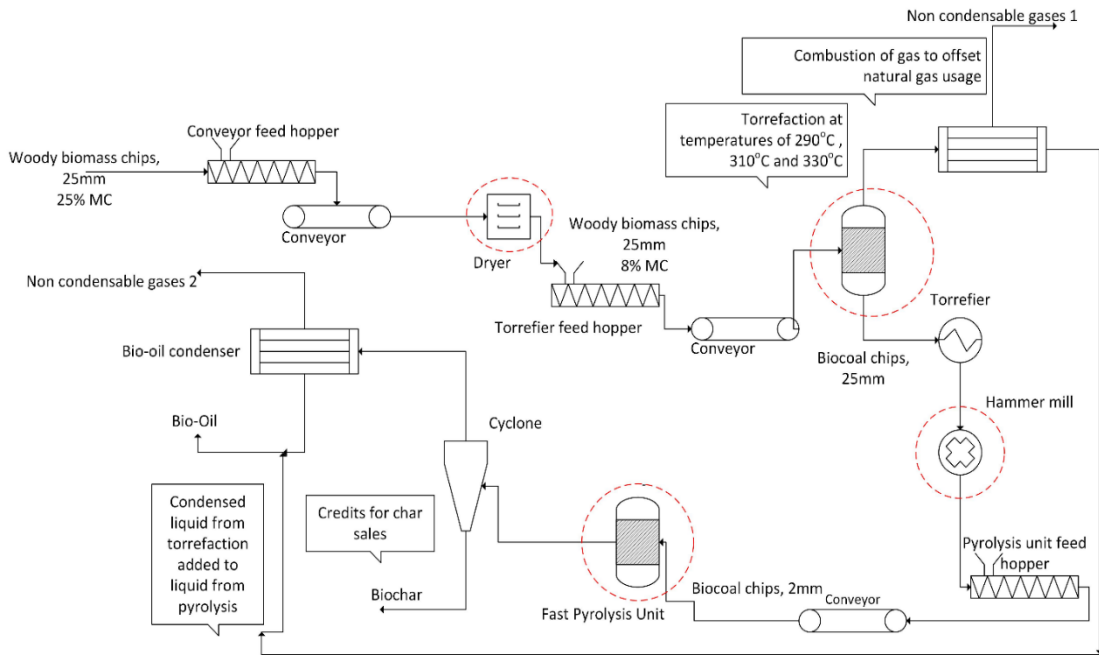


Figure 3.1. Schematic diagram for scenario 1 (FMBY) of a two-step conversion pathway.²⁹ Courtesy of Biofuels, Bioproducts and Biorefining (See Appendix E for documentation of permission to republish the material)

3.3.2 LCA framework, system definition, and modeling assumptions

The cradle-to-grave system boundary of this LCA study is shown in Figure 3.2 in which the pyrolysis bio-oil pathway encompasses biomass supply logistics through biomass conversion and the final combustion of produced bio-oil. Biomass logistics includes the collection of biomass, coarse chipping of biomass in the forest, loading operations and transport of chipped biomass to the conversion site. Due to the assumption that the biomass

being converted is wood waste and logging residues, direct and indirect land use change emissions of CO₂ will not be considered in our assessment. Emission factors for biomass logistics were based on values obtained from the Greenhouse Gases, Regulated Emissions, and Energy Use in Transportation (GREET) model.⁽³⁰⁾ Input data for the pyrolysis conversion step were based on an Aspen Plus model of the biomass conversion processes. Emissions from the final combustion of pyrolysis bio-oil would not be included in our carbon accounting as these emissions are biogenic and are assumed to occur rapidly if the residue were to remain on the forest floor instead. Therefore, only fossil carbon is included in the CO₂ accounting.

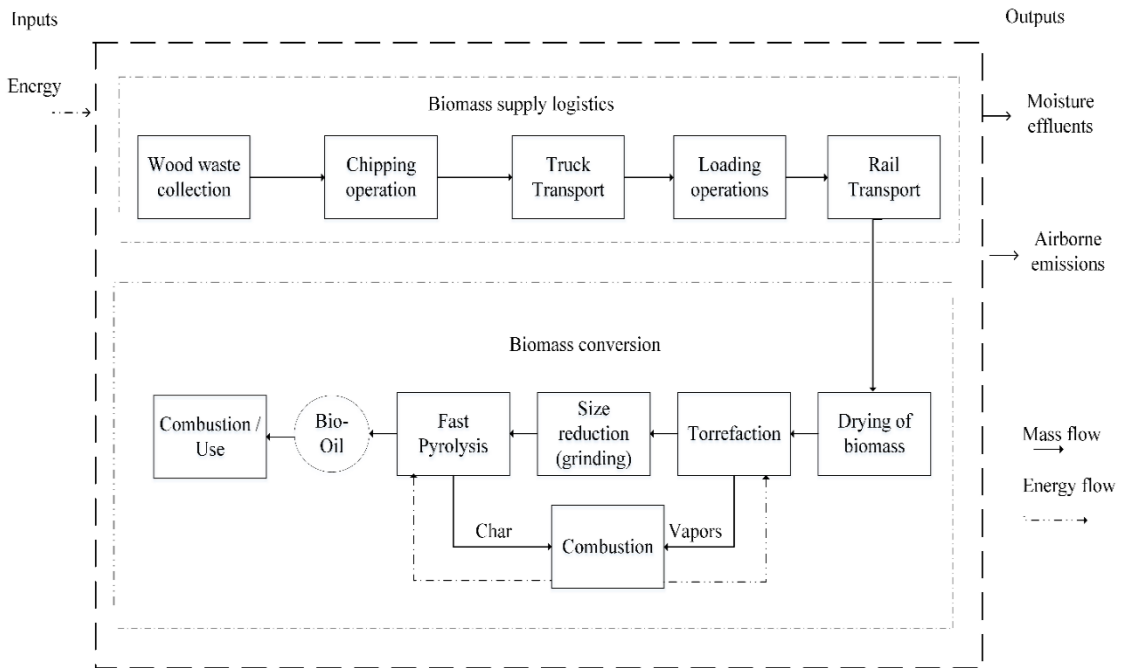


Figure 3.2. Cradle-to-grave system boundary for two-step production of bio-oil.

The functional unit (FU) defines the function of the product and further determines the equivalence between products or processes being compared. For this study, the functional unit was set to 1 MJ of energy content of the bio-oil produced and was used to compare to fossil heavy fuel oil (HFO).

SimaPro® 8.0 is the LCA software used in this study. SimaPro® provides accessible databases of environmental inventory data including the U.S. Life Cycle Inventory (US LCI), the European Life cycle database (ELCD), ecoinvent™, etc. These databases were used to define the inputs and outputs of the process.

3.3.3 Life Cycle Inventory

The life cycle inventory includes all material and energy inputs to each stage in the life cycle as well as the cradle-to-gate inventory of greenhouse gas emissions and energy demand for those inputs.⁽²⁰⁾ The main processes that were inventoried for the LCA under biomass supply logistics and biomass conversion are further described as follows, with details provided in Appendix B.

3.3.3.1 Biomass supply logistics

Wood collection

The inventory of greenhouse gas emissions for wood residue collection was obtained from the GREET 2014 model spreadsheet on the basis of 1 dry metric ton of biomass. The greenhouse gases per dry ton of biomass collected include CO, CH₄, N₂O and CO₂. Because the basis of 1,000 metric dry ton/day of feed into pyrolysis unit was used in this study, the wood collected varied based on the yield of torrefied solids obtained from the

torrefaction step. See Table B1 of Appendix B for the details on fuel use and emission factors for this step.

Coarse chipping of biomass

Wood residue chipping for this study was assumed to occur onsite in the forest where the residue was collected using a stationary reciprocating diesel-powered chipper machine. It was assumed that 0.5 kg of diesel was combusted per dry ton of biomass chipped based on the LCA by Maleche et al.⁽³¹⁾ The inventory of greenhouse gas emissions was obtained from the GREET 2014 model for the production and combustion of diesel for the chipping step. See Table B2 of Appendix B for the details on fuels use and emission factors of this step.

Transport of wood residue chips

This study assumed two transport processes for the residue chips from the harvest site to the plant location. A 90-mile transport of the coarse chips by trucks as well as a 490-mile rail transport were assumed based on the GREET 2014 model. These distances are considered representative of a logging residue collection scenario using multi-modal transport. Emissions for the transportation step were obtained from the GREET 2014 model per dry ton of wood residue transported. When diesel was utilized such as in the transport by rail, emissions for both production and combustion of diesel were included. See Table B3 of Appendix B for the details on fuels use and emission factors of this step.

Loading operations

Three loading operations were considered in the biomass supply chain. The first is the loading of coarse chips in the forest onto trucks for transport to the rail landing, followed by a second loading of chips from trucks onto rail cars. The final loading operation would take place at the conversion plant location. A previous study by Handler et al. determined that 0.5 kg diesel/dry short ton of forest woody biomass would be required for each loading step, resulting in a total of about 1.5 kg diesel/dry short ton for the harvest site to plant site supply chain.⁽³²⁾ Emissions relating to the production and combustion of diesel were also factored into this step and were also obtained from the GREET 2014 model using diesel upstream and combustion emission factors. See Table B5 in Appendix B for the details on fuel use and emission factors of this step.

3.3.3.2 Biomass conversion

Drying of biomass

Chipped pine delivered to the conversion plant is assumed to contain about 25% moisture (dry basis). A previous study showed that optimal moisture content of pine chips fed into the pyrolyzer should have a maximum feed moisture of 10%, with a moisture content of 7% preferred (dry basis).⁽³³⁾ The amount of process heat required to achieve the drying step was estimated using the sensible and latent heat model developed in Aspen Plus®. This was estimated to be about 3.35 MJ/kg of moisture removed. Previous studies have put the quantity of energy required for reducing moisture content in biomass to range from about 2.9 to 4.0 MJ/kg of water removed ⁽³⁴⁻³⁷⁾. For scenario 1, the drying energy was provided by natural gas while other scenarios looked to partially or fully offset natural gas by

internally utilizing renewable energy in the form of char or condensable vapors from torrefaction.

Size reduction

Initial forest coarse chipping found in biomass logistics was assumed to reduce collected pine wood residue to chips with a particle size of about 25mm. The preferred particle size of feed entering the pyrolyzer has been found to be about 2mm.⁽³³⁾ Energy required for reducing the sizes of both the dried pine wood chips and torrefied chips were obtained from the study by Phanphanich et al. using the correlation⁽¹³⁾

$$E_g = -0.756T + 260.0 \quad (1)$$

where E_g is the specific energy consumption for grinding in kW-hr/metric ton, and T is torrefaction temperature in °C. Grinding energy for wood chips for one-step conversion was estimated using equation 1 to be about 240 kW-hr/ton of wood chips while for two-step conversion it was estimated as 40.8, 25.6, and 10.5 kW-hr/ton of torrefied chips at torrefaction temperatures of 290, 310 and 330°C, respectively. The reduction in energy required is in line with other studies such as a reduction from about 850 kW-hr/ton for untreated beech to about 100 kW-hr/ton after torrefaction at 260°C over 40 minutes observed by Tumuluru et al.⁽¹⁵⁾ Bergman and Kiel also found reductions of about 70 – 90% for biomass such as willow and woodcuttings while an estimate of about 77 kW-hr/ton was given by Batidzirai et al. for Scots pine torrefied at 250°C.^(14, 16) A double pass through the hammer mill was assumed in this study. The hammer mill is assumed to be driven by electricity delivered to the plant using the US grid electricity mix.⁽³⁸⁾

Torrefaction

Torrefaction is explored for the pretreatment of loblolly pine chips to expel the moisture and some of the volatile substances mostly associated with thermal degradation of hemicellulose. Torrefaction of loblolly pine chips was modeled in Aspen Plus at temperatures of 290, 310 and 330°C.⁽²⁹⁾ In the absence of oxygen at these torrefaction temperatures and a residence time of about 30 minutes, a charcoal-like solid (bio-coal) is produced. The bio-coal produced serves as feed for the fast pyrolysis unit in the two-step pathways in this study. Mass and energy balances obtained from the model served as input parameters for the LCA. This step was modeled as a yield reactor with the calculated process heat energy required based on the heats of formation of the reactants and products, as well as the sensible heat to raise the biomass temperature from room temperature to torrefaction temperature. Yields of non-condensable gases, condensed liquid and torrefied solid at different torrefaction temperatures, and the yield distribution of the oil and gas for torrefaction obtained from literature are shown in Tables B6 and B7 respectively in Appendix B.^(27, 28) Change in the structure of torrefied solid, i.e. the ultimate and proximate analysis after torrefaction at the different temperatures, were based on data from Park et al. as shown in Tables B8 and B9, respectively in Appendix B.⁽³⁹⁾ FMBY of the two-step pathway satisfied the energy requirement for this step by using natural gas while RMBY and RMBQ offset the natural gas by internally utilizing energy from co-products. The energy required was estimated using the model developed in Aspen Plus® as shown in section B of Appendix B.

Fast pyrolysis

Fast pyrolysis of loblolly pine chips and torrefied pine chips for this study were modeled in Aspen Plus using a yield reactor at 530°C and 1 bar with recycled inert gas to eliminate oxygen from the reactor.⁽²⁹⁾ Yields of gas, liquid, and char for the pyrolysis step and the component distribution of organics in the bio-oil for one and two-step pathways were obtained from literature are shown in Tables B10 and B11, respectively, in Appendix B.^{(27,}
²⁸⁾ A quick vapor quenching step after fast pyrolysis produces a liquid bio-oil, non-condensable gases, and char. The energy required for fast pyrolysis was supplied by natural gas for FMBY for all the cases while other scenarios utilized internally-generated renewable energy to offset natural gas. The energy required was estimated using the model developed in Aspen Plus® as shown in section B of Appendix B assuming adiabatic operation.

Combustion of char and torrefaction condensable fraction

RMBY and RMBQ utilized internally-generated renewable energy to provide the process heat. This was achieved either through the combustion of char, or the combustion of condensable vapors from torrefaction or in some cases combustion of both to fully offset natural gas. This study estimated energy from char based on its lower heating value (LHV) using an established correlation as shown in section B of Appendix B. Energy from condensable vapors from torrefaction was estimated based on the LHVs of the representative compounds found in the condensables and their mass fraction in the condensables. LHVs of the representative compounds were obtained from literature or estimated as shown in section B of Appendix B.^(40, 41) A sample calculation is also shown

in section E of Appendix B. An efficiency of 80% was assumed for all combustion steps including when natural gas is utilized to supply process heat.

Emissions from the combustion step for char and torrefaction condensables were not included in the GHG and CO₂ accounting as they are biogenic. Based on the unit operation for the conversion step described, an inventory table for the conversion step for FMBY of a one-step bio-oil production pathway is shown in Table 3.2. Conversion inventory data for other scenarios can be found in section D of Appendix B.

Table 3.2. Inventory inputs for scenario 1 of a one-step bio-oil production from fast pyrolysis of pine wood chips.

<i>Products</i>		
Bio-oil	1	MJ
Char (displaces coal)	0.009	kg
<i>Material Inputs</i>		
Pine (8 % moisture content)	0.095	kg
Water, completely softened, at plant ^a	9.4	kg
<i>Process Inputs or Displaced Products (negative values)</i>		
Electricity, medium voltage US (size reduction) ^a	0.039	kWh
Natural gas, burned in industrial furnace low-NO _x > 100kW ^a (biomass drying)	0.072	MJ
Natural gas, burned in industrial furnace low-NO _x > 100kW ^a (pyrolysis)	0.182	MJ
Bituminous coal, combusted in industrial boiler NREL/US ^a	-0.008	kg

3.3.3.3 Allocation

Allocation arises when a process produces more than one valuable output.⁽⁴²⁾ The conversion pathways studied here produce a valuable co-product, char, in addition to the pyrolysis bio-oil. In carrying out an LCA for such systems, inventory data and associated environmental burdens must be allocated to each co-product.⁽⁴³⁾ This study looked at

allocation using two approaches: (1) a system expansion approach and (2) an energy allocation approach. The system expansion approach (also referred to as a displacement allocation) gives credits to the main pathway product (bio-oil) the avoided life cycle impacts required to produce and use material that is displaced by the co-product.^(44, 45) This approach is the U.S. EPA's preferred allocation method for life cycle energy and GHG analyses for the Renewable Fuel Standard Program. The energy allocation method is an appropriate choice for a system in which all the primary products and co-products can be quantified on the basis of their energy content. Using the determined energy content, a calculated allocation factor will be used to reflect the individual contribution of each product and co-product.

3.4. Life Cycle Impact Assessment

An impact assessment converts the inventory of emissions and wastes into impacts to the environment through a consideration of environmental damage mechanisms. This study looked at the life cycle impact assessment using the global warming potential and the cumulative energy demand.

3.4.1 Global Warming Potential (GWP)

The Global Warming Potential is an indicator of how much radiative heat a greenhouse gas traps compared to an equivalent amount of carbon dioxide within a certain period of time. This study analyzed the GWP over a period of 100 years using the guidelines of the Intergovernmental Panel for Climate Change of the United Nations (IPCC).⁽⁴⁶⁾ The GWP IPCC 100a 2013 method in SimaPro was selected, in which the GWP for CO₂ is 1, for CH₄

is 28, and for N₂O is 265. GWP values for other greenhouse gases are included in this method for refrigerants and solvents emitted due to certain inputs to the bio-oil pathway.

3.4.2 Cumulative Energy Demand (CED)

CED represents the direct and indirect energy use throughout the life cycle of the product, i.e. the energy utilized during extraction, manufacturing, and disposal of the raw and auxiliary materials.⁽⁴⁷⁻⁴⁹⁾ It has been widely used as an indicator of energy resource consumption.^(50, 51) CED includes the energy embodied in the material and energy inputs to the bio-oil pathway as well as energy embodied in the forest biomass feedstock. The CED method distinguishes between different primary energy types, such as fossil and renewable energy.

3.5. Sensitivity Analysis

Using results from the baseline FMBY analysis, important LCA inputs were identified as parameters for the sensitivity analysis. This study looked at the effects of +/- 20% changes in selected parameters on LCA results. A 20% variation is an appropriate uncertainty metric for a preliminary LCA that is based on laboratory experiments and process simulation rather than commercial process data.

3.4 Results

3.4 Global warming potential (GWP)

System Expansion Allocation: Global warming potential (GWP) results for the analysis of fast pyrolysis of pine via one-step and two-step pathways for all scenarios are shown in Figure 3.3 for system expansion allocation. The results highlight contributions from major pathway stages where emissions are dominated by size reduction in the one-step pathway and by char credits in the two-step pathway. It can be seen from the results that the two-step pathway scenarios show a significant decrease in GWP compared to one-step, mostly due to significantly lower size reduction impacts and char credits. Relative to FMBY of a one-step conversion pathway, reduction in GHG emissions by 78%, 116%, and 155% was observed for FMBY of two-step conversion pathways at torrefaction temperatures of 290,

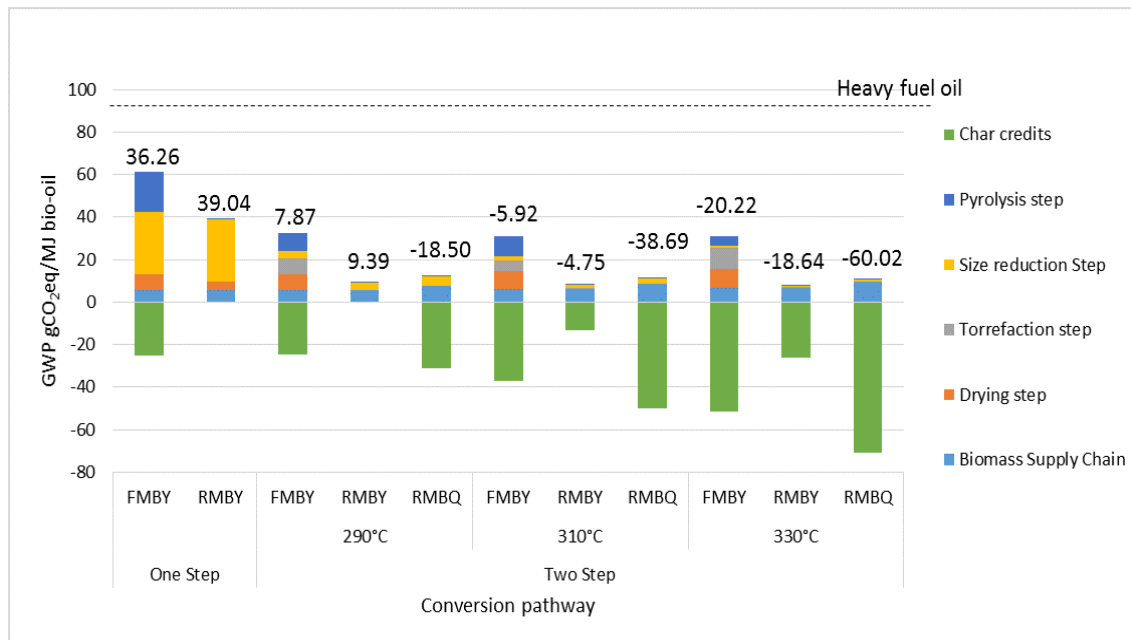


Figure 3.3. Global warming potential impacts for pine conversion to bio-oil via one-step and two-step pathways (system expansion).

310 and 330°C respectively. GHG emissions in all scenarios for one-step and two-step pathways were lower in comparison with heavy fuel oil. Percent reduction in comparison with heavy fuel oil ranged from about 55% for RMBY of a one-step conversion to about 168% for RMBQ of a two-step conversion with torrefaction taking place at 330°C. Size reduction of untreated pine to the optimal operating size of about 2mm is the largest contributor to the net emissions observed for a one-step pathway. Overall, as torrefaction temperature increases in each scenario, the net global warming potential reduces as shown in Figure 3.3. This trend is caused by the export of increasing amounts of co-product char (based on the functional unit of 1 MJ of energy content of the bio-oil produced) from the

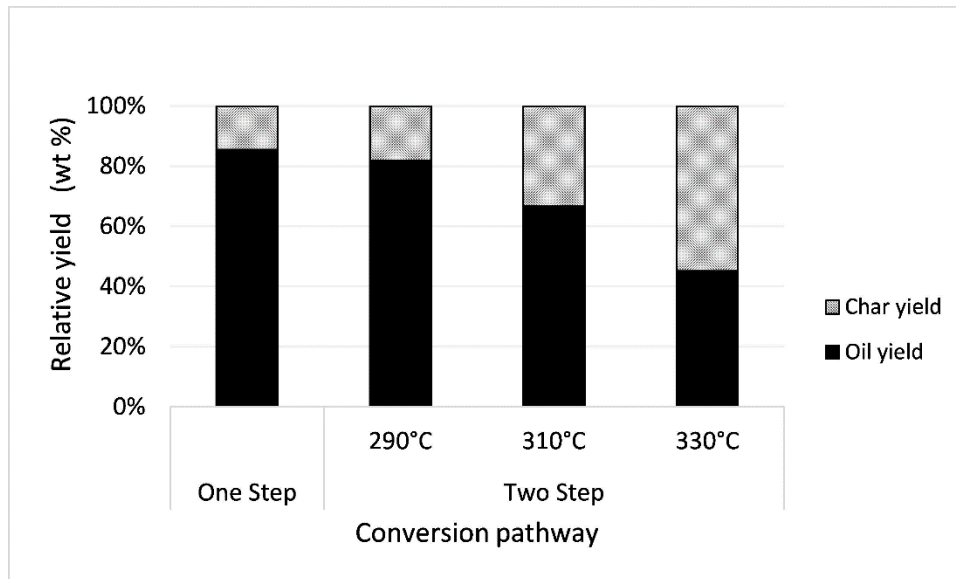


Figure 3.4. Relative yield of oil to char for the fast pyrolysis step only⁽²⁷⁾

bio-oil pathway to displace coal emissions (cradle-to-grave) as torrefaction temperature increases. From the data which was used for our analysis shown in Figure 3.4, an increase in torrefaction temperature resulted in an increase in the ratio of the yield of char to the

yield of oil. In addition, for each torrefaction temperature, the lowest emissions were observed for RMBQ. An interesting and unexpected result is that emissions are slightly higher for the use of renewable energy (RMBY) rather than fossil energy (FMBY) for two-step conversion pathway. This is due to the use of a comparative clean energy source (natural gas) and the avoiding of a highly impactful energy source (coal) in FMBY. The net negative emissions observed for some of the scenarios implies that bio-oil and char production will have the net effect of removing CO₂ from the atmosphere compared to the current reliance on coal for much of society's energy needs. It must also be acknowledged that this consequential effect of coal displacement is uncertain and depends on market forces and policy actions.

Energy Allocation: The system expansion allocation method used above places all the environmental burden on the bio-oil, the desired product. However, energy allocation distributes the pathway environmental impacts among all co-products according to their energy flows. Allocation factors were calculated based on the lower heating values of the bio-oil and char using the following equation:

$$Allocation\ factor = \frac{(LHV_{bio-oil} * \dot{m}_{bio-oil})}{(LHV_{bio-oil} * \dot{m}_{bio-oil}) + (LHV_{char} * \dot{m}_{char})}$$

where LHV_{bio-oil} is the lower heating value of the bio-oil, LHV_{char} is the lower heating value of char and $\dot{m}_{bio-oil}$ and \dot{m}_{char} are the mass flowrates of bio-oil produced and char obtained from the process simulation model. The LHV of char was estimated using an established correlation while the LHV of bio-oil was calculated based on the LHV of the individual components in the bio-oil and their mass fraction in the bio-oil. LHV of the components were obtained from literature and in cases where these values were not found

in literature, they were estimated. Estimation methods used for char and bio-oil can be found in section B of Appendix B. Calculated energy allocation factors and a sample calculation for the LHV of bio-oil are also shown in section E of Appendix B.

Figure 3.5 shows the GWP results obtained using energy allocation. Net emissions are shown above each bar with the energy allocation factors in parentheses for each scenario. Like Figure 3.3, two-step conversion pathways show significantly lower emissions in comparison to one-step conversion. One-step pyrolysis exhibits the largest emissions from the size reduction step, while in the two-step pathway for FMBY size reduction is only a minor contribution. Emissions of fossil CO₂ disappear for drying, torrefaction, and pyrolysis in RMBY and RMBQ compared to FMBY for all two-step conversion pathways due to substituting biomass-derived energy in place of imported natural gas. Relative to FMBY of a one-step conversion pathway, reduction in GHG emissions by 47%, 54%, and 59% was observed for FMBY of two-step conversion pathways at torrefaction temperatures of 290, 310 and 330°C respectively, for the size reduction step alone.

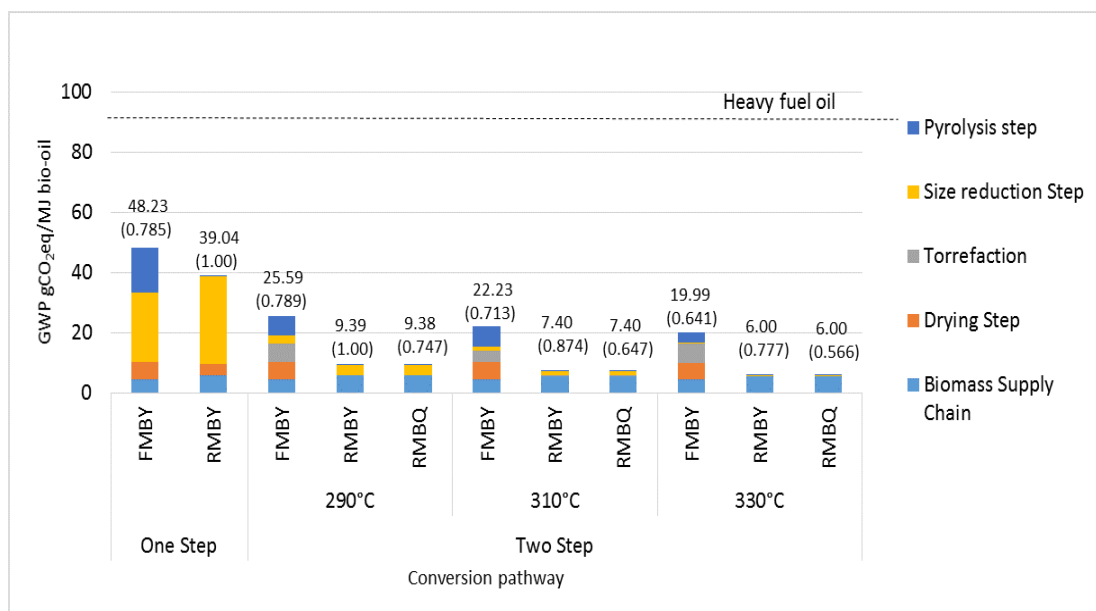


Figure 3.5. Global warming potential impact for pine conversion to bio-oil via one-step and two-step pathways based on energy allocation. Energy allocation factors are shown in parentheses.

As observed for system expansion (Fig. 3.3), all scenarios for one-step and two-step pathways were lower in comparison with heavy fuel oil. Percent reduction here ranged from about 45% for FMBY of a one-step pathway to about 93% for RMBY and RMBQ of the two-step pathway with torrefaction taking place at a temperature of 330°C.

3.5 Cumulative Energy Demand

Figure 3.6 shows results for cumulative energy demand for one-step and two-step scenarios using system expansion. Two-step conversion pathways exhibit lower net cumulative energy results compared to one-step pathways due to the effect of decreased energy demand for size reduction. In the two-step scenarios, RMBQ consumes more biomass energy than FMBY and RMBY because the torrefaction condensable fraction is utilized for energy process demands, thus reducing overall bio-oil yield in RMBQ but improving bio-oil quality. Though a decrease in the net energy of about 22%, 20%, and 21% was

observed for FMBY of two-step pathways at torrefaction temperature of 290, 310 and 330°C, respectively, compared to FMBY of a one-step pathway, the two-step pathways show higher biomass energy demand.

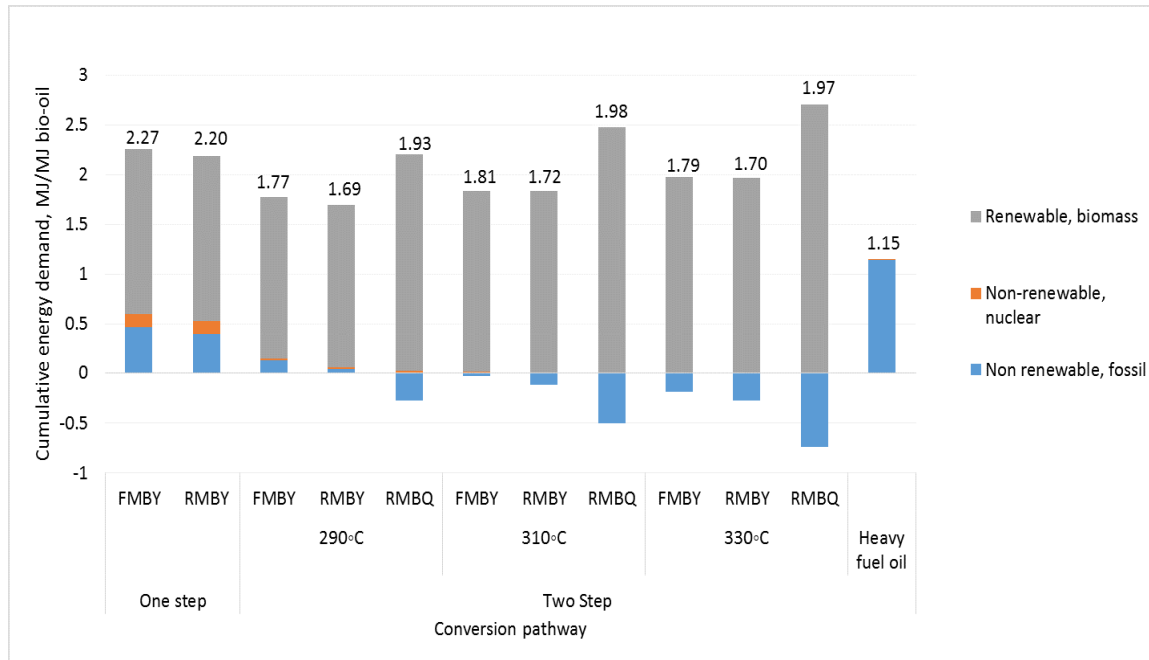


Figure 3.6. Cumulative energy demand for pine conversion to bio-oil via one-step and two-step pathways based on system expansion allocation

This is because higher feed throughput is required by the two-step pathways to make up for the loss of mass, because of the torrefaction step to ensure the basis of a 1,000-metric ton/day of feed going into the pyrolysis unit. The production of bio-oil through both pathways is, however, less efficient when compared to the cumulative energy demand obtained for heavy fuel oil production (i.e. only 1.15 MJ energy demand per MJ heavy fuel oil produced). Though less energy efficient, the major energy utilized by the bio-oil conversion pathway is renewable biomass in comparison to heavy fuel oil that utilizes mostly non-renewable fossil energy. It can, therefore, be inferred that the bio-oil production

pathway is a more sustainable production pathway when compared with the production of heavy fuel oil because it does not consume as much non-renewable energy. The results also point out the need to improve bio-oil pathway energy efficiency by increasing product yields and by waste energy recovery and use in the process (for example, no heat integration was employed in the process simulations for this study).

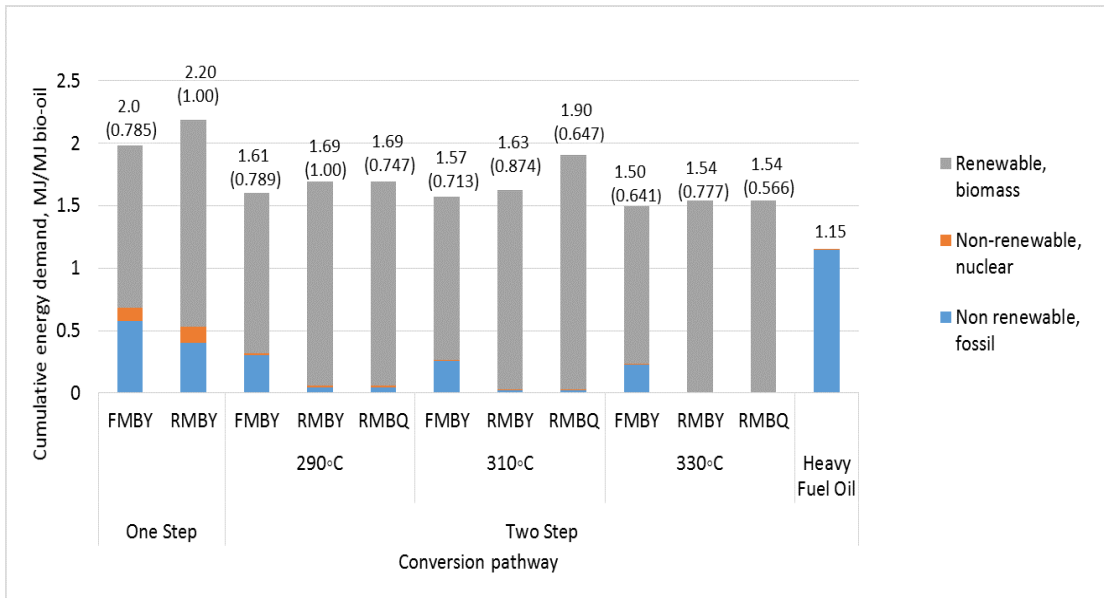


Figure 3.7. Cumulative energy demand for pine conversion to bio-oil via one-step and two-step pathways based using energy allocation. Energy allocation factors are shown in parenthesis

Figure 3.7 shows the cumulative energy demand using energy allocation. The trend is like that obtained using system expansion. However, the net cumulative energy demand results are slightly lower. The net energy demand reduced by 19.5%, 21.5% and 25% for FMBY of two-step pathways at torrefaction temperatures of 290, 310 and 330°C, respectively, relative to FMBY of a one-step conversion pathway. The values are also higher than that obtained for heavy fuel oil.

4.3. Sensitivity Analysis - system expansion allocation case.

A sensitivity analysis was carried out to analyze how uncertainty in some of the LCA input data affects GWP results. For the sensitivity analysis, some of the LCA model input parameters were changed one at a time by a factor of +/- 20%. The sensitivity analysis was carried out for the system expansion allocation only. This study also shows results for only two scenarios; RMBY of a one-step conversion pathway and RMBQ of a two-step conversion pathway with torrefaction taking place at 310°C. These scenarios are interesting because they utilize renewable energy for internal process energy demands and then are differentiated by bio-oil quality, which is higher for a two-step pathway, RMBQ.

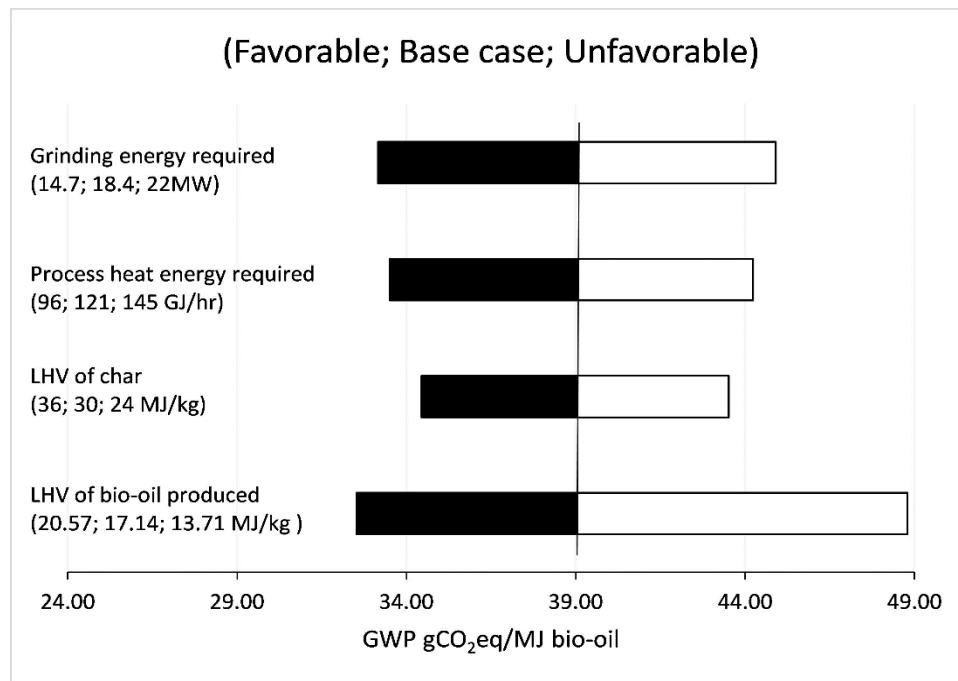


Figure 3.8. Sensitivity analysis for bio-oil production from pine for scenario two for a FMBY conversion pathway for +/- 20% change in some input parameters (displacement allocation-system expansion). About 88.5 gCO₂eq/MJ for heavy fuel oil.

From Figure 3.8, for RMBY of a one-step conversion pathway, large changes in GHG emissions of between 10-20% of base case values occurs for changes of 20% to input

values. All the parameters are important, but LHV of bio-oil shows the greatest change and is thus the most sensitive parameter. Uncertainties in the process heat energy required can arise due to factors such as uncertainties in the calculated heat of formations of products and reactants and uncertainties in the specific heat capacities calculated for biomass and char. The upper limits of the uncertainties for the lower heating values of bio-oil and char produced, though not physically feasible in all cases, were also included to understand parameter sensitivities.

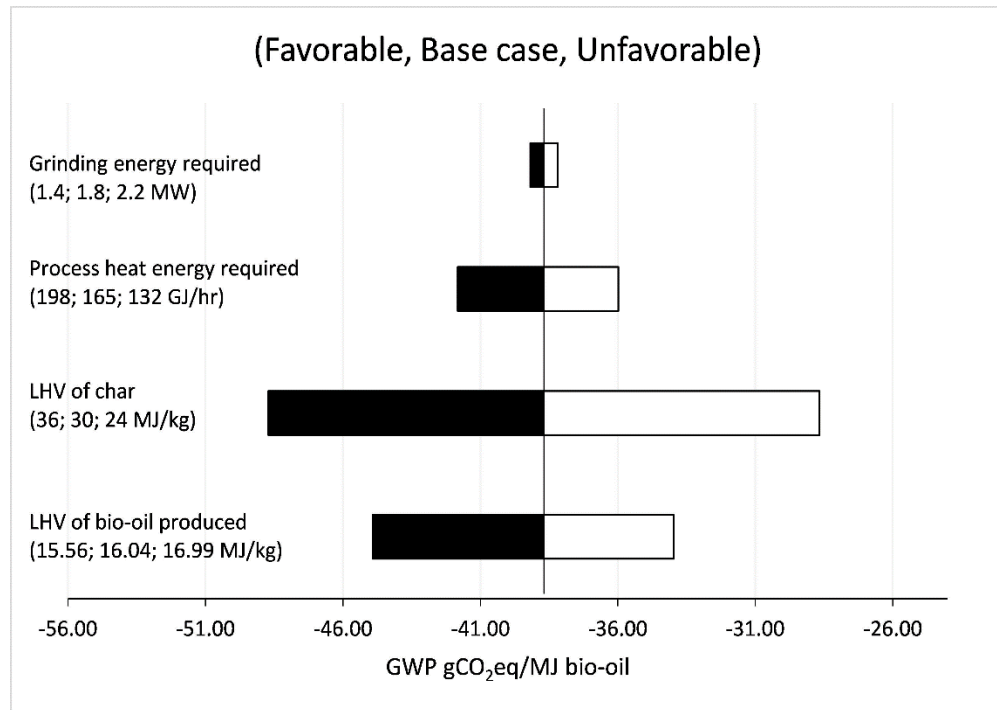


Figure 3.9. Sensitivity analysis for bio-oil production from pine for RMBQ of a two-step conversion pathway at torrefaction temperature of 310°C for +/- 20% change in some input parameters (displacement allocation - system expansion). About 88.5 gCO₂eq/MJ for heavy fuel oil.

For RMBQ of a two-step conversion pathway with torrefaction taking place at a temperature of 310°C, the sensitivity analysis results are shown in Figure 3.9. From the figure, it can be observed that the impact of uncertainty in the energy required for size

reduction is very low. This is due to the significant reduction in energy required because of the torrefaction step. The LCA model parameters with the largest effect on GHG emissions are the LHV of char and bio-oil.

3.5 Conclusions.

Our results show that the inclusion of a torrefaction step prior to the fast pyrolysis of pine is expected to reduce environmental impacts from the production of bio-oil via fast pyrolysis by reducing energy demand for size reduction. The environmental burdens assessed in terms of the global warming potential were further reduced with an increase in torrefaction temperature prior to fast pyrolysis. The effect of allocation method choice on scenario results was important. For energy allocation, the use of renewable energy either through the burning of char or the lower quality liquid fuel from torrefaction to fully satisfy process heat energy requirements lowered greenhouse gas emissions compared to the use of natural gas for process heat. For system expansion, emissions actually increased slightly when burning char for internal process energy compared to using natural gas, due to avoiding the beneficial coal displacement credit. The LCA results also show that use of torrefaction condensables for process heat will yield a higher quality bio-oil product while reducing GHG emissions, but it will consume more renewable energy resources. Based on these LCA results, it is recommended to process woody biomass using a two-step torrefaction and pyrolysis conversion pathway in order to produce bio-oil with minimal environmental impacts compared to a one-step pyrolysis or fossil heavy fuel oil.

3.6 Acknowledgements

The authors of this article acknowledge the financial support provided by a National Science Foundation MPS/CHE - ENG/ECCS – 1230803 Sustainable Energy Pathways (SEP) grant and the Richard and Bonnie Robbins Endowment at Michigan Technological University.

3.7 References

1. Lamers P, Junginger M, Hamelinck C, Faaij A. Developments in international solid biofuel trade—An analysis of volumes, policies, and market factors. *Renewable and Sustainable Energy Reviews*. 2012;16(5):3176-99.
2. Perlack RD, Wright LL, Turhollow AF, Graham RL, Stokes BJ, Erbach DC. Biomass as feedstock for a bioenergy and bioproducts industry: the technical feasibility of a billion-ton annual supply. DTIC Document, 2005.
3. Peters JF, Iribarren D, Dufour J. Simulation and life cycle assessment of biofuel production via fast pyrolysis and hydrougrading. *Fuel*. 2015;139:441-56.
4. Bridgwater A, Peacocke G. Fast pyrolysis processes for biomass. *Renewable and sustainable energy reviews*. 2000;4(1):1-73.
5. Bridgewater AV. Biomass fast pyrolysis. *Thermal Science*. 2004;8(2):21-50.
6. Czernik S, Bridgwater A. Overview of applications of biomass fast pyrolysis oil. *Energy & Fuels*. 2004;18(2):590-8.
7. Pollex A, Ortwein A, Kaltschmitt M. Thermo-chemical conversion of solid biofuels. *Biomass Conversion and Biorefinery*. 2012;2(1):21-39.
8. Peters JF, Petrakopoulou F, Dufour J. Exergetic analysis of a fast pyrolysis process for bio-oil production. *Fuel Processing Technology*. 2014;119:245-55.
9. Shemfe MB, Gu S, Ranganathan P. Techno-economic performance analysis of biofuel production and miniature electric power generation from biomass fast pyrolysis and bio-oil upgrading. *Fuel*. 2015;143:361-72.
10. Sheu Y-HE, Anthony RG, Soltes EJ. Kinetic studies of upgrading pine pyrolytic oil by hydrotreatment. *Fuel processing technology*. 1988;19(1):31-50.

11. Wright MM, Daugaard DE, Satrio JA, Brown RC. Techno-economic analysis of biomass fast pyrolysis to transportation fuels. *Fuel*. 2010;89:S2-S10.
12. Onarheim K, Lehto J, Solantausta Y. Technoeconomic Assessment of a Fast Pyrolysis Bio-oil Production Process Integrated to a Fluidized Bed Boiler. *Energy & Fuels*. 2015;29(9):5885-93.
13. Phanphanich M, Mani S. Impact of torrefaction on the grindability and fuel characteristics of forest biomass. *Bioresource technology*. 2011;102(2):1246-53.
14. Bergman PC, Kiel JH, editors. Torrefaction for biomass upgrading. Proc 14th European Biomass Conference, Paris, France; 2005.
15. Shankar Tumuluru J, Sokhansanj S, Hess JR, Wright CT, Boardman RD. REVIEW: A review on biomass torrefaction process and product properties for energy applications. *Industrial Biotechnology*. 2011;7(5):384-401.
16. Batidzirai B, Mignot A, Schakel W, Junginger H, Faaij A. Biomass torrefaction technology: Techno-economic status and future prospects. *Energy*. 2013;62:196-214.
17. Boateng A, Mullen C. Fast pyrolysis of biomass thermally pretreated by torrefaction. *Journal of Analytical and Applied Pyrolysis*. 2013;100:95-102.
18. Standardization IO. Environmental Management: Life Cycle Assessment: Principles and Framework: ISO; 1997.
19. ISO I. 14044: environmental management—life cycle assessment—requirements and guidelines. International Organization for Standardization. 2006.
20. Owens J. Life cycle assessment. *J of Industrial Ecology*. 1997;1(1):37-49.
21. Steele P, Puettmann ME, Kanthi Penmetsa V, Cooper JE. Life-cycle assessment of pyrolysis bio-oil production. *Forest Products Journal*. 2012;62(4):326.

22. Zhong Z, Song B, Zaki M. Life-cycle assessment of flash pyrolysis of wood waste. *Journal of Cleaner Production*. 2010;18(12):1177-83.
23. Fan J, Kalnes TN, Alward M, Klinger J, Sadehvandi A, Shonnard DR. Life cycle assessment of electricity generation using fast pyrolysis bio-oil. *Renewable Energy*. 2011;36(2):632-41.
24. Iribarren D, Peters JF, Dufour J. Life cycle assessment of transportation fuels from biomass pyrolysis. *Fuel*. 2012;97:812-21.
25. Han J, Elgowainy A, Dunn JB, Wang MQ. Life cycle analysis of fuel production from fast pyrolysis of biomass. *Bioresource technology*. 2013;133:421-8.
26. Hsu DD. Life cycle assessment of gasoline and diesel produced via fast pyrolysis and hydroprocessing. *Biomass and Bioenergy*. 2012;45:41-7.
27. Westerhof RJ, Brilman DWF, Garcia-Perez M, Wang Z, Oudenhoven SR, Kersten SR. Stepwise fast pyrolysis of pine wood. *Energy & Fuels*. 2012;26(12):7263-73.
28. Zheng A, Zhao Z, Chang S, Huang Z, He F, Li H. Effect of Torrefaction Temperature on Product Distribution from Two-Stage Pyrolysis of Biomass. *Energy & Fuels*. 2012;26(5):2968-74.
29. Winjobi O, Shonnard DR, Bar-Ziv E, Zhou W. Techno-economic assessment of the effect of torrefaction on fast pyrolysis of pine. *Biofuels, Bioproducts and Biorefining*. 2016.
30. Wang M. The Greenhouse Gases, Regulated Emissions, and Energy Use in Transportation (GREET) Model: Version 1.5. Center for Transportation Research, Argonne National Laboratory. 2008.

31. Maleche E. Life cycle assessment of biofuels produced by the new integrated hydrolysis-hydroconversion (IH 2) process. 2012.
32. Handler RM, Shonnard DR, Lautala P, Abbas D, Srivastava A. Environmental impacts of roundwood supply chain options in Michigan: Life-cycle assessment of harvest and transport stages. *Journal of Cleaner Production*. 2014;76:64-73.
33. Bridgwater A, Toft A, Brammer J. A techno-economic comparison of power production by biomass fast pyrolysis with gasification and combustion. *Renewable and Sustainable Energy Reviews*. 2002;6(3):181-246.
34. Koppejan J, Sokhansanj S, Melin S, Madrali S, editors. Status overview of torrefaction technologies. IEA bioenergy task; 2012.
35. Wright MM, Daugaard DE, Satrio JA, Brown RC. Techno-economic analysis of biomass fast pyrolysis to transportation fuels. *Fuel*. 2010;89, Supplement 1(0):S2-S10.
36. Fagernäs L, Brammer J, Wilén C, Lauer M, Verhoeff F. Drying of biomass for second generation synfuel production. *Biomass and Bioenergy*. 2010;34(9):1267-77.
37. Adams P, Shirley J, McManus M. Comparative cradle-to-gate life cycle assessment of wood pellet production with torrefaction. *Applied Energy*. 2015;138:367-80.
38. Consultants P. SimaPro 7 Life-cycle assessment software package, version 7. Amersfoort The Netherlands; 2012.
39. Park J, Meng J, Lim KH, Rojas OJ, Park S. Transformation of lignocellulosic biomass during torrefaction. *Journal of Analytical and Applied Pyrolysis*. 2013;100:199-206.
40. Perry RH, Green DW, Maloney JO, Abbott MM, Ambler CM, Amero RC. Perry's chemical engineers' handbook: McGraw-hill New York; 1997.

41. Domalski ES. Selected Values of Heats of Combustion and Heats of Formation of Organic Compounds Containing the Elements C, H, N, O, P, and S. *Journal of Physical and Chemical Reference Data*. 1972;1(2):221-77.
42. Cherubini F, Strømman AH, Ulgiati S. Influence of allocation methods on the environmental performance of biorefinery products—A case study. *Resources, Conservation and Recycling*. 2011;55(11):1070-7.
43. Ayer NW, Tyedmers PH, Pelletier NL, Sonesson U, Scholz A. Co-product allocation in life cycle assessments of seafood production systems: review of problems and strategies. *The International Journal of Life Cycle Assessment*. 2007;12(7):480-7.
44. Edwards K, Anex R, editors. Co-product allocation in life cycle assessment: a case study. *Extended Abstract*; 2009.
45. Guinée JB. Handbook on life cycle assessment operational guide to the ISO standards. *The international journal of life cycle assessment*. 2002;7(5):311-3.
46. Change IPOC. 2006 IPCC guidelines for national greenhouse gas inventories. 2006.
47. Huijbregts MA, Hellweg S, Frischknecht R, Hendriks HW, Hungerbühler K, Hendriks AJ. Cumulative energy demand as predictor for the environmental burden of commodity production. *Environmental science & technology*. 2010;44(6):2189-96.
48. Hirst E. Food-related energy requirements. *Science*. 1974;184(4133):134-8.
49. Frischknecht R, Heijungs R, Hofstetter P. Einstein's sons for energy accounting in LCA. *The International Journal of Life Cycle Assessment*. 1998;3(5):266-72.
50. Frischknecht R, Jungbluth N, Althaus H, Bauer C, Doka G, Dones R, et al. Implementation of life cycle impact assessment methods. *Ecoinvent report*. 2007.

51. Vollrath F, Carter R, Rajesh G, Thalwitz G, Astudillo MF, editors. Life cycle analysis of cumulative energy demand on sericulture in Karnataka, India. 6th BACSA international conference: building value chains in sericulture (BISERICA 2013), Padua, Italy; 2013.

4. Production of Hydrocarbon Fuel using Two-Step Torrefaction and Fast Pyrolysis of Pine. Part 1: Techno-economic Analysis.[‡]

4.1. Abstract

As part I of two companion papers, the present paper evaluates the economic feasibility of hydrocarbon biofuel production via two pathways: a one-step production pathway through fast pyrolysis of biomass followed by the catalytic upgrade of bio-oil to a liquid hydrocarbon biofuel, and a novel two-step pathway that includes a torrefaction pretreatment step prior to fast pyrolysis and then the catalytic upgrade. These two pathways were modeled using Aspen Plus® to process 1000 dry metric tons/day of feed through the fast pyrolysis unit operating at 530°C while torrefaction for the two-step pathway was investigated at three different torrefaction temperatures of 290, 310 and 330°C. Three scenarios of producing process heat from natural gas, internal by-products biochar or torrefaction condensate were investigated, with additional heat integration considered. Minimum selling price ranged from \$4.01/gal to \$4.78/gal for the heat-integrated processes while the price ranged from \$4.70/gal to \$6.84/gal without heat integration. Analysis indicated that a one-step pathway and a two-step pathway with torrefaction taking place at 290°C yielded comparable least minimum selling price and it increased with increasing torrefaction temperature. Sensitivity analysis showed that the

[‡] Reprinted with permission from ACS SUSTAINBLE CHEMISTRY AND ENGINEERING WINJOBI, O, SHONNARD, D, ZHOU W. PRODUCTION OF HYDROCARBON FUEL USING TWO-STEP TORREFACTION AND FAST PYROLYSIS OF PINE. PART 1: TECHNO-ECONOMIC ANALYSIS. Copyright (2017) American Chemical Society

yield of hydrocarbon biofuel, total project investment and internal rate of return have the greatest impact.

4.2 Introduction

An increasing global population constitutes a dual challenge of meeting rising energy demands while also reducing environmental impacts associated with the production and consumption of energy. The total world consumption of energy is projected to increase by 48% from 2012 to 2040, with petroleum remaining the largest source of energy despite having a declining share of the total energy market.¹ Though advancements in technology has improved energy efficiency, alternative and renewable energy sources are still needed to address this dual challenge. In this regard, policies such as the Energy Independence and Security Act of 2007 enacted by the U.S. government to increase biofuel production from 4.7 billion gallons per year in 2007 to 36 billion gallons per year by 2022, are geared towards reducing fossil fuel consumption and greenhouse gas emissions while meeting energy demand through increased production of clean renewable fuels.² To meet the biofuel production target, there is a preference for production from lignocellulosic biomass feedstock because they do not compete with food.

Fast pyrolysis of woody biomass has gained attention as a promising pathway for the thermochemical conversion of biomass.³ The development of a fast pyrolysis pathway is believed to have advantages over conventional pyrolysis, flash pyrolysis and gasification with respect to liquid product yield, quality, and flexibility.⁴ The products from the fast pyrolysis of biomass include a solid product often referred to as biochar, a gaseous product often termed non-condensable gas comprised mainly of CO and CO₂, and the desired liquid

product, bio-oil which is a more energy-dense liquid product compared to raw wood chips.⁵ However, due to the properties of the bio-oil such as its high oxygen and water content, corrosivity, and low heating value, bio-oil cannot be used as a drop-in hydrocarbon transportation fuel. Upgrading of bio-oil to hydrocarbon transportation fuel can be achieved via hydrotreatment, including hydrodeoxygenation (HDO). HDO of bio-oil to totally or partially remove the oxygen content is analogous to hydrodesulfurization (HDS) carried out in petroleum refineries to remove sulfur from crude oil and refined products. The possibility of utilizing existing infrastructure for the HDO step due to its similarity to HDS thereby potentially minimizing capital cost, is another factor that makes the biofuel production pathway via fast pyrolysis attractive.

As an alternative transportation hydrocarbon fuel source to partially offset the use of fossil fuel, biofuel needs to be cost competitive with fossil transportation fuel. Aside from being cost competitive, it is also desired that the biofuel production pathway place a lower burden on the environment compared with fossil fuel. These requirements of cost-competitiveness and potential lower environmental impacts can be evaluated by carrying out techno-economic and environmental life cycle assessments, respectively. Some previous works have investigated the costs of production of biofuel via fast pyrolysis of biomass and upgrading while some considered just the environmental impacts of the biofuel production pathway.

From previous works, the minimum selling price of hydrocarbon fuel produced via fast pyrolysis and upgrading ranged from \$2.04/gal (2007) to \$3.39/gal (2011).⁶⁻⁹ Jones et al. estimated a selling price of \$2.04/gal (2007) for a 2000 metric ton/day facility that produces

biofuel by processing hybrid poplar chips.⁶ Wright et al. estimated a minimum selling price of \$3.09 (2012) and \$2.11/gal (2012) for a 2000 metric ton/day facility that produces transportation fuels from corn stover for hydrogen producing and purchasing scenarios, respectively.⁷ Brown et al. estimated a selling price of \$2.57/gal (2012) for a 2000 metric ton/day facility that produces transportation fuel and also supplies electricity to the electricity grid.⁸ Jones et al. recently reported a minimum selling price of \$3.39/gge (2011) for a 2000 dry metric ton dry biomass /day facility.⁹ Winjobi et al. investigated the effect of torrefaction on the cost of pyrolysis bio-oil for a 1000 dry metric ton/day facility.¹⁰ They reported a decreasing trend in price with an increase in torrefaction temperature, the selling price of bio-oil decreased from about \$1.32/gal (2013) for a one-step bio-oil production pathway without torrefaction to about \$1.04/gal (2013) for a two-step bio-oil production pathway with torrefaction taking place at a temperature of 330°C.¹⁰

To our knowledge, no work has looked at the inclusion of torrefaction before fast pyrolysis to investigate the trade-offs, cost implications, and uncertainty effects, both economically and environmentally on the produced hydrocarbon biofuel. We address this challenge by two companion papers. The present paper focuses entirely on the effect of torrefaction on the minimum selling price of hydrocarbon biofuel. This study aims to investigate how the benefits (improved pyrolysis oil quality and increase biomass grindability) and drawbacks (reduction in biofuel yield and increased capital cost) from the inclusion of a torrefaction step impact the economic assessments of the hydrocarbon biofuel production pathway. In a companion article, we will present the effect of torrefaction on the greenhouse gas emission from the hydrocarbon biofuel production pathway.¹¹

4.3 Materials and Methods

Process description

The biofuel production process is assumed to convert 1000 dry metric tons of biomass feedstock entering the pyrolyzer unit per day for both the one-step and two-step processes. Loblolly pine is fed to the pyrolyzer for the one-step while bio-coal/torrefied biomass obtained from the torrefaction of loblolly pine is fed to the pyrolyzer for the two-step routes. Figure 4.1 shows a schematic diagram of the plant flowsheet for a two-step route.

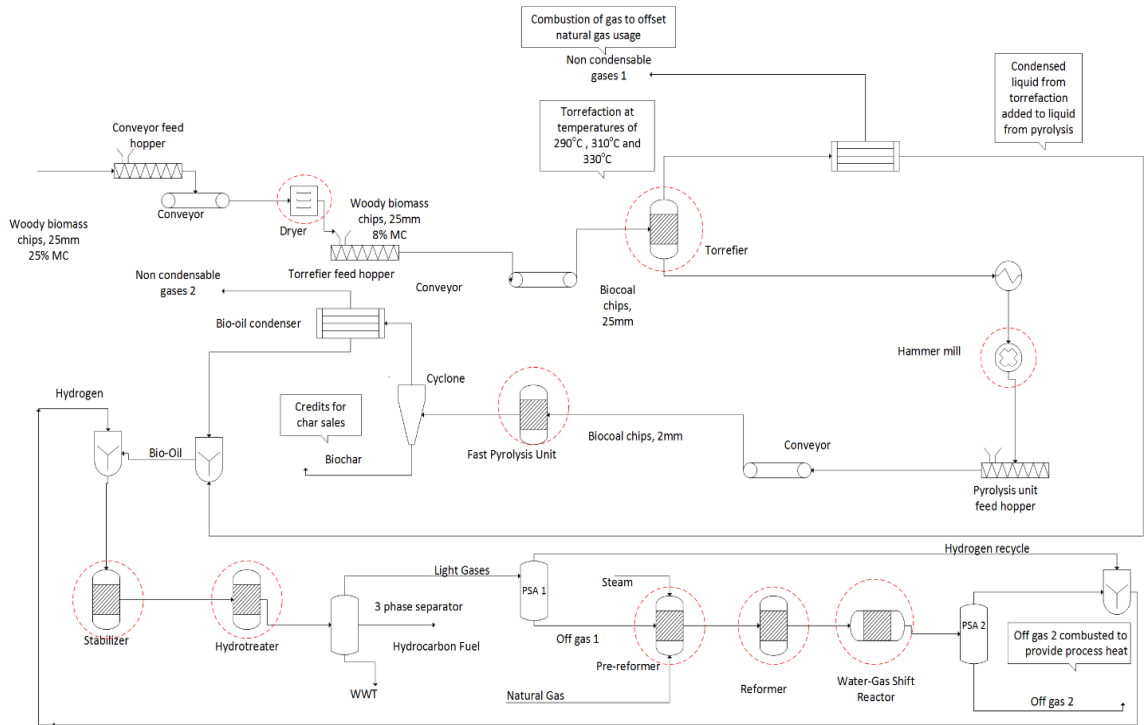


Figure 4.1. Schematic diagram for two-step hydrocarbon fuel production from pine biomass

Process operations that were modeled in this study include drying, torrefaction (only for the two-step route), size reduction, fast pyrolysis, upgrade of pyrolysis bio-oil, on-site hydrogen production, combustion of internal by-products for process heat (when

applicable), heat exchangers as well as the conveyance of biomass. Model description for the torrefaction, size reduction, fast pyrolysis, upgrade of bio-oil and hydrogen production (the most important operations) are described below while the description of the drying operation, combustion and conveyance can be found in section A of Appendix C. The loblolly pine chips were assumed to be delivered at particle size of about 25mm and moisture content of 25%. Aspen Plus® (Aspen Technology Inc., Burlington, USA) was used for flowsheet simulation in this study.

Size reduction of dried wood chips

A further size reduction of delivered loblolly pine chips to the desired size of about 2mm is required before fast pyrolysis. Due to the relatively small biomass size required, this size reduction step is energy intensive. Besides potential improvement in the quality of pyrolysis bio-oil, studies have established that torrefaction improves biomass grindability.¹²⁻¹⁵ The inclusion of torrefaction before size reduction, as a result, has the potential to reduce the energy intensity of the size reduction step. This study modeled the effect of torrefaction on the energy required for grinding using correlations developed by Mani et al. shown in section A of Appendix C.¹² Hammer mill was modeled in Aspen Plus® to carry out the size reduction step.

Fast Pyrolysis

For both one-step and two-step cases, fast pyrolysis was modeled to take place at one atmospheric pressure in a fluidized bed reactor with an inert environment at 530°C and with a residence time of 1 second. The pyrolysis reactor was modeled as a yield reactor

with the yield factors for the bio-oil, char and non-condensable products obtained from literature as shown in Table 4.1.^{16,17}

Table 4.1. Pyrolysis yield data at for one and two-step pyrolysis taking place at 530°C. (The yields are based on the feed entering the pyrolyzer on a dry ash free basis - raw pine for one-step; torrefied pine for two-step)

Material yields (wt %)				
	One Step	Two Step (290°C)	Two Step (310°C)	Two Step (330°C)
Gas	28	24.4	26.8	23.3
Liquid	59	57.7	46.4	32.6
Solid/Char	10	12.8	23.2	39.5

Component product distribution of the bio-oil product was also based on literature data as shown in Table C1 in Appendix C. An inert environment was modeled by using nitrogen as a fluidizing agent in the reactor. The non-condensable gas generated from fast pyrolysis in this study was diluted by the fluidizing gas (nitrogen) resulting in a low calorific value of the overall gas.¹⁸ As a result, overall gas from the pyrolysis reaction was recirculated to serve as the fluidizing media in the reactor. The loblolly pine and char product were modeled using their ultimate and proximate analyses respectively as shown in Tables C2, C3, and C5 in section B of Appendix C. This study assumed that in all cases there would be negligible difference in the properties of char as shown in Table C5 of Appendix C. Chen et al. found no significant differences in the properties and energy content of char

produced with and without torrefaction pretreatment prior to catalytic pyrolysis in their work.¹⁹

Torrefaction

Torrefaction is carried out in an inert environment at lower temperatures and with a longer residence time than fast pyrolysis. It predominantly degrades the hemicellulose portion of the biomass to yield mainly a solid termed torrefied biomass, often called bio-coal because it is a replacement for fossil coal. Studies have investigated and observed the yield of better quality bio-oil because of a torrefaction pretreatment of biomass prior to fast pyrolysis.²⁰ Thermal degradation of hemicellulose is believed to yield mainly CO₂, water, and organic acids; these products typically result in low energy content and acidity of pyrolysis bio-oil. Subsequent fast pyrolysis of the torrefied biomass thus potentially produces higher quality pyrolysis bio-oil with lower water content and lower acidic components.

The torrefaction step is assumed to be carried out in an auger reactor at atmospheric condition, in an inert environment and with a residence time of about 40 minutes and was modeled using a yield reactor in Aspen Plus®. The effect of torrefaction temperature was investigated at 290, 310 and 330°C. The yield factors for the torrefied pine biomass, condensed liquid and non-condensable gases based on literature are shown in Table 4.2. Component product distribution of the condensable organics from torrefaction were also based on literature data as shown in Table C4 in section b of Appendix C.^{16,17}

Table 4.2. Torrefaction yield data at different torrefaction temperatures for pine.¹⁶

Material Yields (wt %)			
Torrefaction Temperature	290°C	310°C	330°C
Gas	6	8	11
Condensed Liquid	17	33	46
Torrefied Solid	78	56	43

Changes in the structure of the torrefied biomass at the different torrefaction temperatures were modeled for energy content using their ultimate and proximate analyses obtained from literature as shown in Tables C2 and C3 in section B of Appendix C.²¹

Catalytic upgrading of bio-oil

The upgrading of pyrolysis bio-oil to hydrocarbon transportation fuel was achieved by the hydrodeoxygenation of the model compounds contained in the bio-oil. Reaction pathways for the different model compounds were obtained from the literature.²²⁻²⁵ In a process analogous to hydrodesulfurization used in removing sulfur in the refining of crude oil, the oxygen in the pyrolysis bio-oil is removed via catalytic hydrodeoxygenation under high-pressure hydrogen. A two-stage upgrade step consisting of a mild hydrotreatment step, usually called a stabilization step, at lower temperatures followed by a more severe hydrotreatment at a higher temperature as described in the literature was utilized.^{22,24} Initial conversion of acids, aldehydes to alcohols was modeled to occur during stabilization.²⁶ Conversion of unreacted bio-oil components and the intermediate products from the stabilization step then took place in the second hydrotreating step. The major reaction

pathway for hydrocarbon fuel production in this study was assumed to be via hydrodeoxygenation. Several other types of reactions such as hydrolysis, decarboxylation, decarbonylation and dehydration were also assumed to take place to produce intermediates that were subsequently converted via hydrodeoxygenation. Sugars such as levoglucosan and cellobiose were first hydrolysed to glucose followed by the hydrogenation of glucose to sorbitol. Sorbitol was subsequently converted to hexane as described by Huber et al.²⁷ The reaction pathways for each representative bio-oil compound can be found in Figure 4.2. Operating pressures and temperatures of 1200 psia, 140°C and 2000 psia, 410°C were used in the stabilization and second hydrotreating steps respectively in our model.⁹ The reactors were modeled as yield reactors in Aspen Plus® and the hydrogen required was estimated based on the amount required to convert the representative compounds in the bio-oil to hydrocarbons. Reaction pathways for the remaining bio-oil representative compounds modeled are shown in section F of Appendix C. Deoxygenated aromatic hydrocarbon shown in Figure 4.2 were produced in a 0.55 to 0.45 ratio, for example, 55% vinylbenzene and 45% ethylcyclohexane. This ratio is based on the overall ratio of aliphatics to aromatics contained in the biofuel from the study of Jones et al.⁹ Yield factors obtained using this approach were used to model the stabilization and hydrotreatment steps in Aspen Plus®. The yield factors for the one-step and two-step hydrocarbon biofuel production are shown in Tables C7 to C13 in section B of Appendix C.

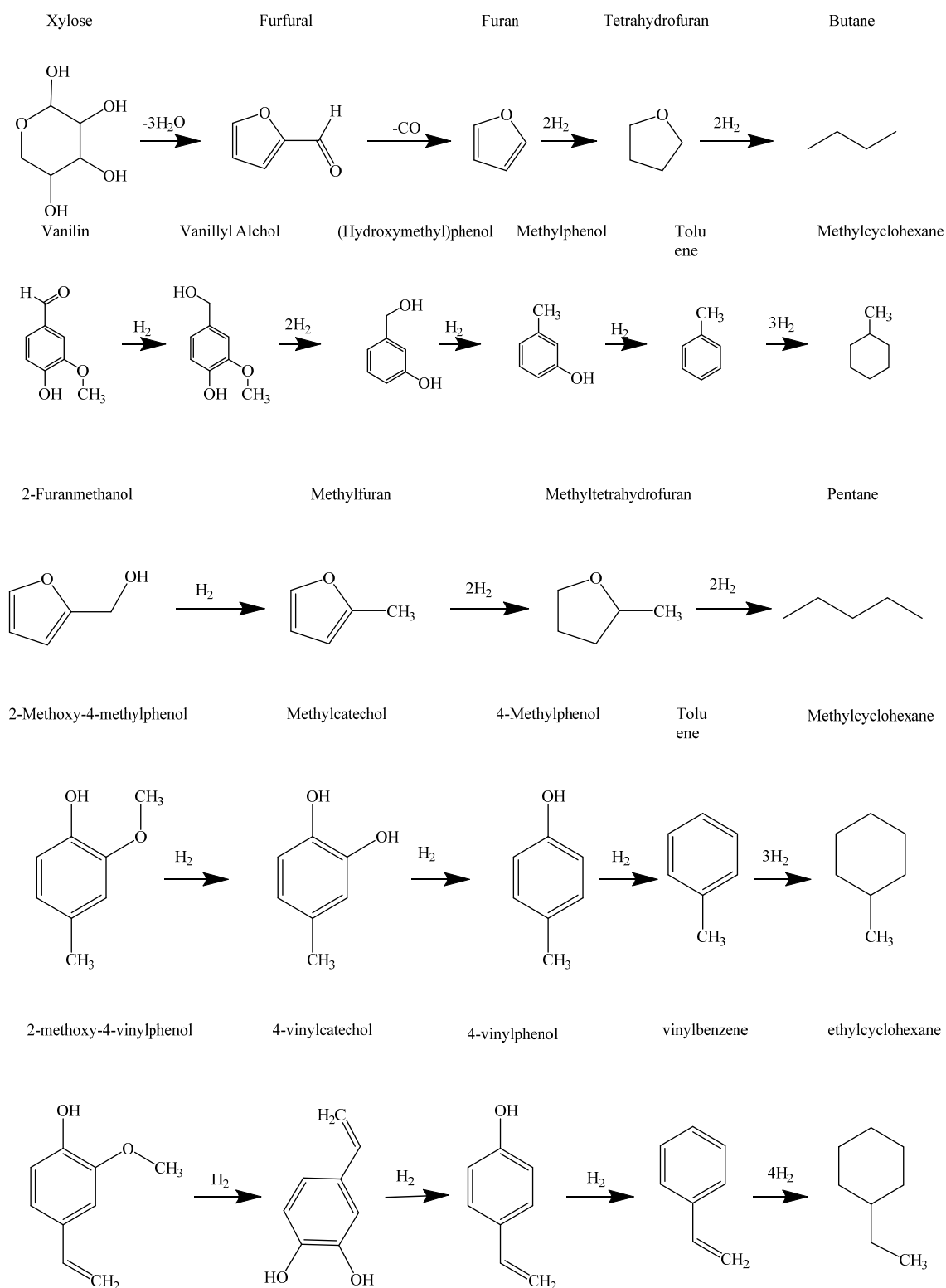


Figure 4.2. Reaction pathway for representative components in pyrolysis bio-oil.

Hydrogen production via steam methane reforming

Hydrogen required for the hydrodeoxygenation reactions in the stabilizer and second hydrotreater was obtained through steam reforming of the hydrocarbon gases produced from the upgrade steps. Natural gas was used to complement the hydrogen demand not met by the reforming of light hydrocarbons from the hydrotreatment stage. Onsite hydrogen production instead of purchase was included in this study as it is considered to be more economical due to the large amount of hydrogen required for the catalytic upgrade step.²⁸ Steam methane reforming of the combined hydrocarbon gases and natural gas was achieved through pre-reforming, reforming, and high-temperature water-gas shift (HTS) reactions using operating conditions from the literature.^{9,29} Typically steam to carbon (S/C) ratio of about 2.5 to 4 are utilized to limit coke formation from unwanted reactions.^{30,31} This study used an S/C ratio of 3. Conversion of C₂+ components into methane was modeled to occur in the pre-reformer while the conversion of methane to hydrogen took place in the reformer. The pre-reformer, reformer and HTS reactors were modeled as equilibrium reactors in Aspen Plus. Operating conditions for these reactors are shown in Table 4.3 while the composition of the make-up natural gas is shown in Table C14 in section B of Appendix C.

Table 4.3. Design operating basis for hydrogen production.⁹

Pre-reformer	
Temperature	593°C
Pressure	24 bar
Steam-to-carbon ratio	3
Steam pressure	46.5 bar
Methane Reformer	
Temperature	850°C
Pressure	22 bar
HTS	
Temperature	358°C
Pressure	21 bar
PSA	
Hydrogen delivery pressure	19.5 bar
Hydrogen recovery	85%

Definition of case studies

The economic assessment for the hydrocarbon biofuel production was investigated under different scenarios as shown in Table 4.4. Scenario 1 objectives include using fossil inputs for process energy and maximizing biofuel yields by combining torrefaction and fast pyrolysis bio-oil. As shown in Figure 4.1, for a two-step conversion pathway the non-condensable gas from the torrefaction step (contains predominantly CO and CO₂) as well

as the off gas obtained from hydrogen production that contains H₂ (about 2.5 wt. %), CO (about 8.5 wt.%) and unreacted CH₄ (about 12 wt.%) are combusted to provide process heat. The unsatisfied process heat requirement is then met by combusting natural gas. Objective 2 of maximizing bio-oil yield in this scenario was achieved as lower quality torrefaction condensed liquid was blended with the pyrolysis bio-oil and then upgraded to maximize the yield of produced hydrocarbon biofuel. The char produced here was used in generating revenue by selling to coal-fired power plants.

Table 4.4. Design objectives for different analysis scenarios.

Scenarios	Objective 1	Objective 2
Scenario 1	Fossil energy inputs	Maximizing bio-oil yield
Scenario 2	Minimize fossil energy inputs	Maximizing bio-oil yield
Scenario 3	Renewable energy inputs	Maximizing bio-oil quality

Scenario 2 aims to minimize or totally offset fossil energy inputs by utilizing the char to provide process heat instead of generating revenue through sales. As a result, process heat in this scenario was provided through the combustion of non-condensable gas from torrefaction, off gas from hydrogen production, and biochar. Any unmet heat requirements will then be satisfied by utilizing natural gas, hence minimizing the fossil energy inputs. Unused char leftover after process heat requirements is fully satisfied without utilizing fossil energy inputs was sold to generate revenue. Torrefaction condensed liquid was blended with pyrolysis bio-oil in this scenario, thus maximizing the yield of bio-oil that is upgraded as shown in Figure c1 in section C of Appendix C.

Scenario 3 aims to totally offset fossil energy inputs by combusting the non-condensable gas from torrefaction, the off gas from hydrogen production, and either totally or partially combust the torrefaction condensed liquid to satisfy process heat requirements. When necessary, produced char is also combusted to ensure natural gas is not required to provide process heat. Partial or total utilization of torrefaction condensed liquid for process heat instead of blending with pyrolysis bio-oil results in a higher quality oil that is subsequently upgraded to biofuel. However, upgrade of high-quality oil will result in a lower yield of hydrocarbon fuel. Furthermore, this scenario may potentially have a benefit of requiring less hydrogen for upgrade because of lower oxygen content, and may positively affect the economic assessment. Revenue is also generated from unused biochar as shown in Figure c2 in section C of Appendix C.

Techno-economic assessment of hydrocarbon fuel pathways

This analysis employed literature and vendor quotes for most of the equipment costs. Purchase costs of major equipment are shown in Table C15 in section F of Appendix C. The cost of heat exchangers was estimated using correlations from literature as shown in section E of Appendix C. Total capital investment was then estimated from the total equipment purchase cost using the capital cost methodology developed by Peters et al³² as shown in Table 4.5.

Table 4.5. Inputs for capital cost estimation.

Total Purchased Equipment Cost (TPEC)	100%	
Purchased Equipment Installation	39%	Percent of TPEC
Instrumentation and Controls	26%	Percent of TPEC
Piping	31%	Percent of TPEC
Electrical Systems	10%	Percent of TPEC
Buildings (including services)	29%	Percent of TPEC
Yard Improvements	12%	Percent of TPEC
Service Facilities	55%	Percent of TPEC
Total Installed Cost (TIC)	3.02	
Indirect Costs		
Engineering	32%	Percent of TPEC
Construction	34%	Percent of TPEC
Legal and Contractors Fees	23%	Percent of TPEC
Project Contingency	34.0%	Percent of TPEC
Total Indirect		
Land	6.00%	Percent of TPEC
Working capital (WC)		5% of (TIC + TI)
Total Project Investment (TPI)		TIC + TI + WC + Land

For equipment sizes and costs obtained from literature, when sizes of equipment were of a different scale than required in our design, cost of equipment was estimated using equation 1,

$$C_1 = C_0 \times \left(\frac{S_1}{S_0}\right)^n \quad (1)$$

where S_0 is initial equipment capacity (tonnes/hr), S_1 is new equipment capacity (tonnes/hr), C_0 is equipment cost at capacity S_0 (\$), C_1 is equipment cost at capacity S_1 (\$) and n is the scaling factor which is 0.7. Setting 2015 as the base year, equipment cost from previous years were escalated using the Chemical Engineering Plant Cost Index (CEPCI), which is provided monthly by the journal *Chemical Engineering*.³³

A discounted cash flow rate of return (DCFROR) analysis spreadsheet is used in calculating the minimum selling price of produced liquid hydrocarbon fuel. Major economic assumptions used in the DCFROR analysis are shown in Table 4.6.

Table 4.6. Some input values and assumption used for the economic assessment.

Parameter	Value
Pine chips cost (\$/ton) dry ¹⁰	60
Electricity price (cents/kWh) ³⁴	5.77
Cost of natural gas (\$/GJ) ³⁵	5.04
Process Cooling water (\$/GJ) ³⁶	0.16
Refrigerant cost (\$/GJ) ³²	20
Price of residual fuel oil (\$/tonne) ³⁷	600
Price of coal (\$/lb) ³⁸	0.03

Internal rate of return (%)	10
Project economic life (year)	20
Working capital (%)	5 % of total capital investment
Depreciation method	7-year MACRS
Tax rate (%)	35
Base year	2015

Heat Integration

This study looked at how energy recovery through heat integration affects the cost of hydrocarbon fuel for the one- and two-step production pathways. The software Super Target® was used in carrying out the heat integration process with inputs of source and target stream temperatures, and heat exchanger duties. Overall heat-transfer coefficient values between process streams and the utility streams for the shell and tube exchangers were estimated as the average of the specified range suggested in literature were input into the software, and are shown in Table C17 in section D of Appendix C.³⁹ Hot utility fluid was assumed as Dowtherm going from 1000°C to 900°C while the cold utility was assumed to be cold water going from 20 to 30°C. With these parameters and a heat exchanger minimum approach temperature (ΔT_{min}) constraint of 10°C, stream matches were made by Super Target®. We selected one out of the different possible matches made by the software for each scenario in carrying out the economic assessment for our scenarios with heat integration. With the selected ΔT_{min} of 10°C, about 80% of the theoretical process heat requirements was met with heat integration. Purchased cost of heat exchangers for the scenarios was estimated using correlations from the literature as shown in section E of Appendix C.³⁶

4.4 Results

Table 4.7 shows the biomass feedstock inputs and the major outputs from our simulations for the cases without heat integration. Because of the basis of 1,000 tons into the pyrolysis unit, more biomass feedstock is required as torrefaction temperature increases. The yield of hydrocarbon fuel reduces with increase in torrefaction temperature due to the decrease in the yield of pyrolysis bio-oil that is subsequently upgraded and an increase in the yield of char. As observed by Boateng et al., the torrefaction step in the two-step processes predisposed the biomass for the conversion to biochar instead of liquid pyrolysis bio-oil.²⁰ For scenario 3 of each two-step conversion pathway, maximizing the pyrolysis bio-oil quality by either not blending in the torrefaction condensed liquid (torrefaction temperature of 290⁰C), or partially blending in the torrefaction condensed liquid (torrefaction temperatures of 310 and 330⁰C) with the pyrolysis bio-oil prior to upgrading, resulted in the lowest yield of hydrocarbon fuel for each two-step process. In addition to the torrefaction condensed liquid combusted internally for thermal heat for two-step pathway with 290⁰C torrefaction, some of the produced biochar was also combusted to fully offset natural gas requirements for process heat. Process heat requirements for scenario 3 at torrefaction temperatures of 310⁰C and 330⁰C were fully satisfied with portions of the torrefaction condensed liquid. Hence all the produced biochar was used to generate revenue from sales to coal-fired power plants.

Table 4.7. Feedstock input and some of the outputs from the biofuel production pathway for one-step and two-step processes without heat integration.

	One-step		Two-step								
Torrefaction temperature			290°C			310°C			330°C		
	Sc 1	Sc 2	Sc 1	Sc 2	Sc 3	Sc 1	Sc 2	Sc 3	Sc 1	Sc 2	Sc 3
Input of Biomass											
Biomass feedstock , 10 ⁶ kg/yr (dry basis)	352.8	352.8	457.1	457.1	457.1	609	609	609	801.8	801.8	801.8
Output of Biofuels											
Hydrocarbon biofuel , 10 ⁶ kg/yr (10 ⁶ gal/yr)	89.7 (31.8)	89.7 (31.8)	116.8 (41.4)	116.8 (41.4)	97.1 (34.5)	125 (44.3)	125 (44.3)	84.4 (29.9)	149.5 (53.0)	149.5 (53.0)	89.2 (31.7)
Hydrocarbon biofuel yield (% wt/wt feed dry basis)	25.4	25.4	25.5	25.5	21.2	20.5	20.5	13.9	18.6	18.6	11.1
Bio-char , 10 ⁶ kg/yr	36.4	-	47.3	-	16.1	84	-	84	144.8	-	144.8
Bio-char yield	10.3	-	10.3	-	3.5	13.8	-	13.8	18.1	-	18.1

(% wt./wt. feed drybasis)											
Torrefaction condensed liquid , 10 ⁶ kg/yr	-	-	-	-	-	-	-	-	-	-	-
Process Heat Inputs											
Combustion energy, 10 ⁶ GJ/yr	2.95	2.95	3.89	3.89	2.90	4.88	4.88	3.13	6.43	6.43	4.16
Combusted material											
Natural Gas, 10 ⁶ m3/yr	2265	1211	2889	1521	-	3569	1140	-	4792	605	-
Off-gas, 10 ⁶ kg/yr	136.2	136.2	184.8	184.8	123.1	241.6	241.6	121.4	313.9	313.9	158
Char, 10 ⁶ kg/yr	-	36.4	-	47.3	31.2	-	84.0	-	-	144.8	-
Torr. condensed liquid,10 ⁶ kg/yr	-	-	-	-	119.3	-	-	205.6	-	-	270.4

Table 4.8 shows inputs and outputs for the cases with heat integration. Here, the objective to offset natural gas requirements while maximizing bio-oil yield (i.e. scenario 1) was met without the need to combust biochar, thus scenarios 1 and 2 are equivalent. The amount of biochar or torrefaction condensed liquid required to be internally combusted to offset natural gas for process heat decreased significantly. In Scenario 3, torrefaction condensed liquid not combusted internally was not further blended in with the pyrolysis bio-oil but was used to generate revenue from sales to displace heavy fuel oil. The net amounts of torrefaction condensed liquid and biochar produced with heat integration are shown in Table 4.8.

Table 4.8. Feedstock input and some of the outputs from the biofuel production pathway for one-step and two-step processes with heat integration.

	One-step	Two-step					
		290°C		310°C		330°C	
	Sc 1	Sc 1	Sc 3	Sc 1	Sc 3	Sc 1	Sc 3
Input of Biomass							
Biomass feedstock, 10 ⁶ kg/yr (dry basis.)	352.8	457.1	457.1	609	609	801.8	801.8
Output of Biofuels							
Hydrocarbon biofuel , 10 ⁶ kg/yr (10 ⁶ gal/yr)	89.7 (31.8)	116.8 (41.4)	97.1 (34.5)	125 (44.3)	84.4 (29.9)	149.5 (53.0)	89.2 (31.7)
Hydrocarbon biofuel yield	25.4	25.5	21.2	20.5	13.9	18.6	11.1

(% wt/wt feed dry basis.)							
Bio-char , 10 ⁶ kg/yr	36.4	47.3	47.3	84	84	144.8	144.8
Bio-char yield (% wt./wt. feed, dry basis)	10.3	10.3	10.3	13.8	13.8	18.1	18.1
Torrefaction condensed liquid , 10 ⁶ kg/yr	-	-	52.5	-	153.0	-	194.6
(% wt./wt. feed, dry basis)			11.5		25.1		24.3
Process Heat Inputs							
Combustion Energy, 10 ⁶ GJ/yr	0.51	0.87	0.65	0.88	0.62	1.39	0.77
Combusted Material							
Natural Gas, 10 ⁶ m3/yr	-	-	-	-	-	-	-
Off-gas, 10 ⁶ kg/yr	64.8	105.4	-	103.8	-	238.3	-
Char, 10 ⁶ kg/yr	-	-	-	-	-	-	-
Torr. condensed liquid,10 ⁶ kg/yr	-	-	66.8	-	52.6	-	75.8

Hydrogen Consumption

Table 4.9 shows hydrogen consumption for different scenarios. The amount of hydrogen required for the hydrotreatment of the bio-oil produced from fast pyrolysis was estimated to be about 6.38% wt. per pyrolysis bio-oil for a one-step production pathway. This is comparable to the experimental value of 5.8% wt. per pyrolysis oil obtained by Jones et

al.⁹ The results show a decrease in hydrogen consumption between one-step and two-step conversion and a decrease with increasing severity of torrefaction. This trend occurs because as torrefaction severity increases, the water content of the condensed liquid from torrefaction increased. The higher water content does not consume hydrogen during the upgrade step. Another interesting trend is the increase in hydrogen consumption for scenario 3 of the two-step pathway with torrefaction at 290°C compared to scenarios 1 and 2 while a decrease in hydrogen consumption was observed for the two-step pathway at higher torrefaction temperatures of 310 and 330°C for scenario 3 compared to 1 and 2. This is because, at the lowest torrefaction temperature of 290°C, it is believed that the hemicellulose portion of the wood is mainly degraded producing chiefly water, acetic acid, and some furans. Maximizing the bio-oil quality at this temperature resulted in bio-oil of lower yield due to the loss of compounds from hemicellulose but the relative higher composition of sugars and phenolics in the bio-oil increased. Hydrogen consumption of the sugars and phenolics are relatively higher than that of the acids, resulting in higher relative hydrogen consumption for scenario 3. At higher torrefaction temperatures of 310 and 330°C, there is an increasing degradation of the cellulose and lignin portions of the wood. As a result, maximizing the bio-oil quality at these temperatures also leads to loss of some of the sugars and phenolics in addition to the water and acids from hemicellulose degradation. This resulted in a decrease in relative hydrogen consumption for scenarios 3 at these temperatures. It should be noted that the hydrogen consumption for each scenario does not change with or without heat integration.

Table 4.9. Amount of hydrogen required for the upgrade of bio-oil to hydrocarbon fuel.

Hydrogen consumption (% wt. per upgraded bio-oil)				
	One-step	Two-step		
Scenario		290°C	310°C	330°C
1	6.38	6.17	5.91	5.05
2	6.38	6.17	5.91	5.05
3		6.66	5.84	4.86

Scenario 3 of a two-step production pathway with torrefaction taking place at 290°C showed the highest hydrogen consumption per amount of bio-oil upgraded. This scenario also showed the best quality of bio-oil based on the LHV of the bio-oil produced in the different scenarios. The LHV of bio-oil for the scenario 3 of the two-step production pathway at 290°C was estimated to be about 19.22 MJ/kg while LHV of about 17.4 MJ/kg was estimated for the one-step pathway as shown in Table C16 in section D of Appendix C. This is due to complete combustion of the condensed liquid from torrefaction for process heat; thus, the lower quality torrefaction condensed liquid was not blended in with pyrolysis bio-oil for further upgrading process. However, overall hydrogen consumed in scenarios 1 and 2 for the two-step pathway at 290°C is higher due to much higher bio-oil yield. At higher torrefaction temperatures of 310 and 330°C, the torrefaction condensed liquid was not completely combusted for process heat, and the unused condensed liquid was blended in with pyrolysis bio-oil lowering the LHV of the blended bio-oil. Estimation of the LHV of the bio-oil was carried out using the LHV of the components found in the bio-oil as shown in section D of Appendix C.

Minimum Selling Price

The estimated minimum selling price (MSP) of the hydrocarbon fuel for all scenarios of the one-step and two-step processes without heat integration are shown in Figure 4.3. The MSP of the hydrocarbon biofuel produced via a two-step conversion pathway with 290°C torrefaction is almost the same as the MSP estimated for the one-step pathway. The highest price in both cases (one-step and two-step at 290°C) ranged from about \$4.82/gal to about \$4.70/gal. The lowest MSP in both cases was obtained for scenario 2, which had the objective of minimizing fossil energy inputs for process heat, by combusting biochar for process energy while maximizing hydrocarbon fuel yield. In general, for all scenario 1, the effect of torrefaction as a pretreatment step prior to pyrolysis has the effect of increasing MSP of hydrocarbon fuels, and this is amplified with increased severity of torrefaction compared to a one-step pathway. It is also observed that a small decrease in MSP occurs for the use of renewable energy for process heat in Scenario 2 compared to 1.

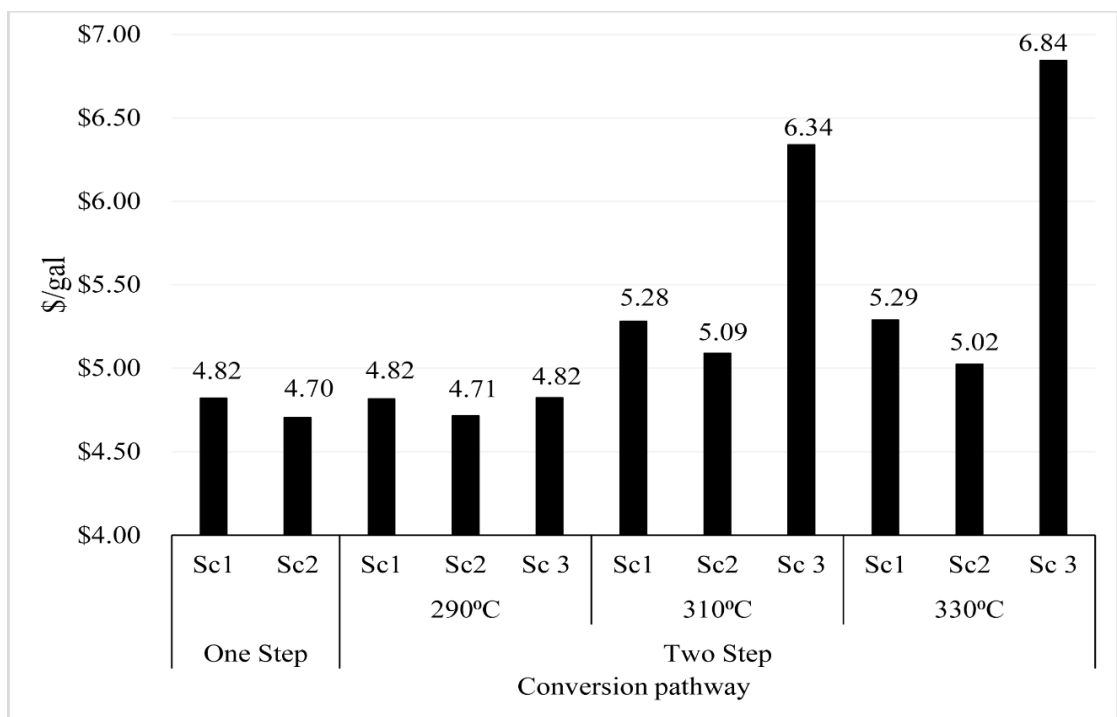


Figure 4.3. Minimum selling price of liquid hydrocarbon fuel for one-step and two-step pathways without heat integration. Torrefaction temperatures are shown for two-step pathways.

The prices varied from about \$4.70/gal for scenario 2 of the one-step production pathway to about \$6.84/gal for scenario 3 of the two-step pathway with 330°C. High MSP was estimated for scenario 3 at higher torrefaction temperatures of 310 and 330°C in comparison with other scenarios. This is because maximizing bio-oil quality at these temperatures led to a relatively low yield of hydrocarbon fuel as earlier shown in Table 4.7. In contrast, a recent result in the literature shows favorable economics for two-step pathways at higher torrefaction temperature when bio-oil is the final product instead of the upgraded biofuel.¹⁰ This is because bio-oil contains water and low molecular weight compounds which during the upgrading process were converted to gases such as ethane. Thus they do not contribute to the yield of hydrocarbon biofuel.

The effect of heat integration on the minimum selling price of biofuel can be seen in Figure 4.4. In all scenarios, the heat-integrated process has lower MSP of hydrocarbon biofuels

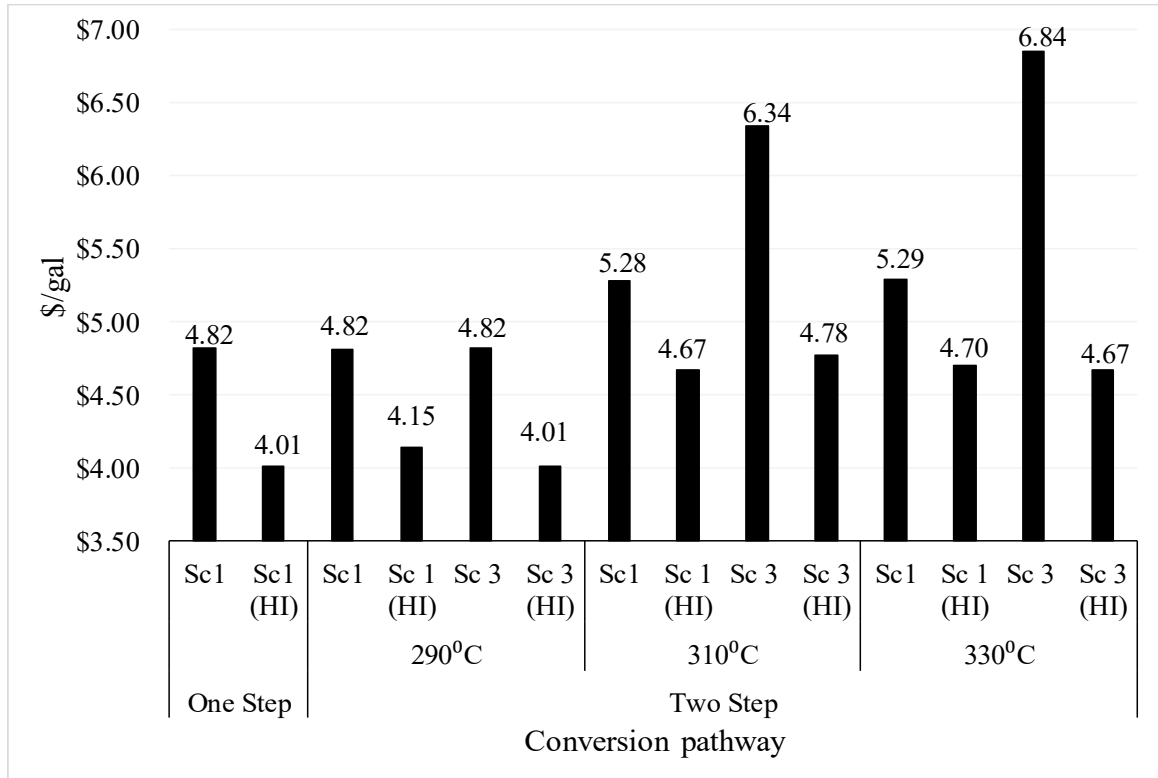


Figure 4.4. Minimum selling price of liquid hydrocarbon fuel for one-step and two-step pathways with and without heat integration. Torrefaction temperatures are shown for two-step pathways. *HI shows results with heat integration. Note that Sc2 is equivalent to Sc1 for all heat-integrated pathways

when compared to the scenarios without heat integration. The percentage reduction in minimum selling price for the heat integrated scenarios increased as torrefaction severity increased from about 14% at 290°C torrefaction to about 30% at 330°C torrefaction. With heat integration, the MSP of hydrocarbon biofuel ranged from about \$4.01/gal for scenario 1 of the one-step and scenario 3 of the two-step pathway with torrefaction taking place at 290°C to about \$4.78/gal for scenario 3 of the two-step pathway at 310°C torrefaction.

Reduced MSP of hydrocarbon biofuel with heat-integrated processes was due to the reduction in utility costs as well as an increase in revenue generated from sales of unused by-products biochar and torrefaction condensed liquid. Revenue was also generated from the off gas obtained from hydrogen separation after the hydrogen production through SMR. For all scenario 1 cases of the one-step and two-step pathways, we observed that heating requirements not met with heat integration were totally satisfied with the combustion of the off-gas from hydrogen separation. Because of fully offsetting natural gas for process heat through heat integration without the need to combust biochar, scenario 2 with heat integration would give rise to the same results as that of scenario 1 for all torrefaction temperatures. Revenue was generated from the sale of surplus off-gas based on the cost of natural gas on an energy basis, which we assumed to be displaced in this study.

Contributions of various costs and revenues to the minimum selling price of hydrocarbon fuel for the one-step and two-step pathway 290°C torrefaction with almost the same prices were investigated as shown in Figure 4.5. In general, the total project investment was the greatest contributor, followed by the cost of biomass feedstock while depreciation cost was the largest credit received. With heat integration, there was a trade-off between reduction in utility costs and an increase in the total project investment cost. The benefit of reduced utility cost outweighed the increase in the incurred total project investment resulting in lower MSP for the heat-integrated process.

The amount of refrigerant required for the quick quench of hot vapor after pyrolysis and torrefaction to a temperature of about 20°C was eliminated, resulting in a cost reduction of \$.50/gal. The cooling water utilized in this study is assumed to come in at 20°C and return

at 30°C. With heat exchanger approach temperature of 10°C, it was required to utilize a refrigerant to cool the cooling water required to quench the vapors to about 10°C.

Comparing the price of \$4.01/gal calculated for the one-step pathway and scenario 3 of the two-step pathway with torrefaction occurring at 290°C, there is a reduction in the cost of electricity for the two-step pathway because of the torrefaction step prior to fast pyrolysis. Though an increase in the total project investment is observed due to the torrefaction step, its effect is offset by the revenue generated from the sales of the torrefaction condensed liquid and the reduction in electricity requirements for size reduction. In comparison with other studies, Wright et al. estimated MSP of \$3.09 (2007) for hydrocarbon biofuel produced via the fast pyrolysis of corn stover while Jones et al. estimated MSP of \$3.39 (2011) for hydrocarbon biofuel from woody biomass.^{7,9} These prices are also based on a hydrogen production scenario, however, both studies processed 2000 metric tons of biomass per day in their assessments, which may account for some of the difference with our study which was based on 1000 metric tons input to the pyrolysis unit (difference in scale).

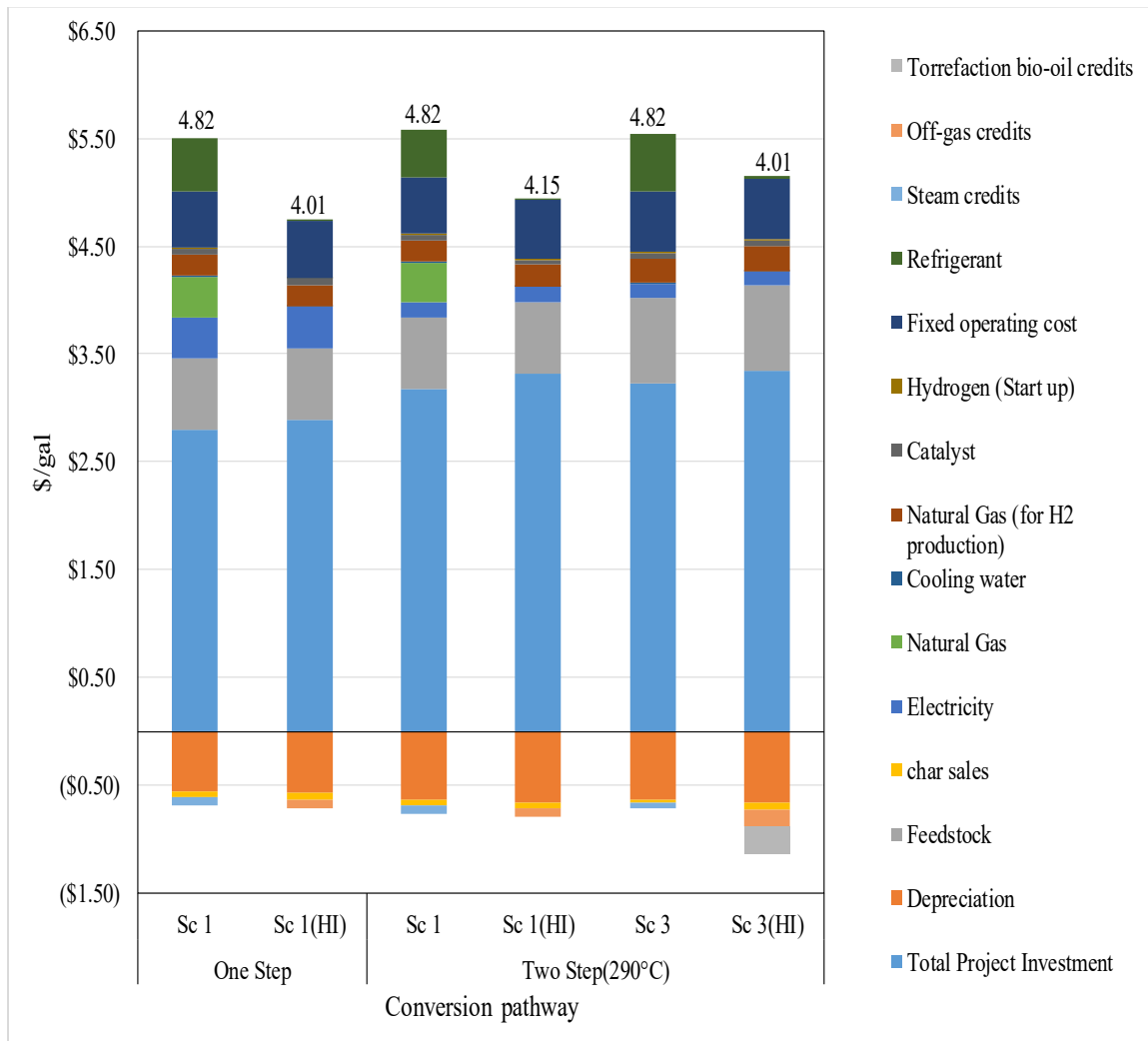


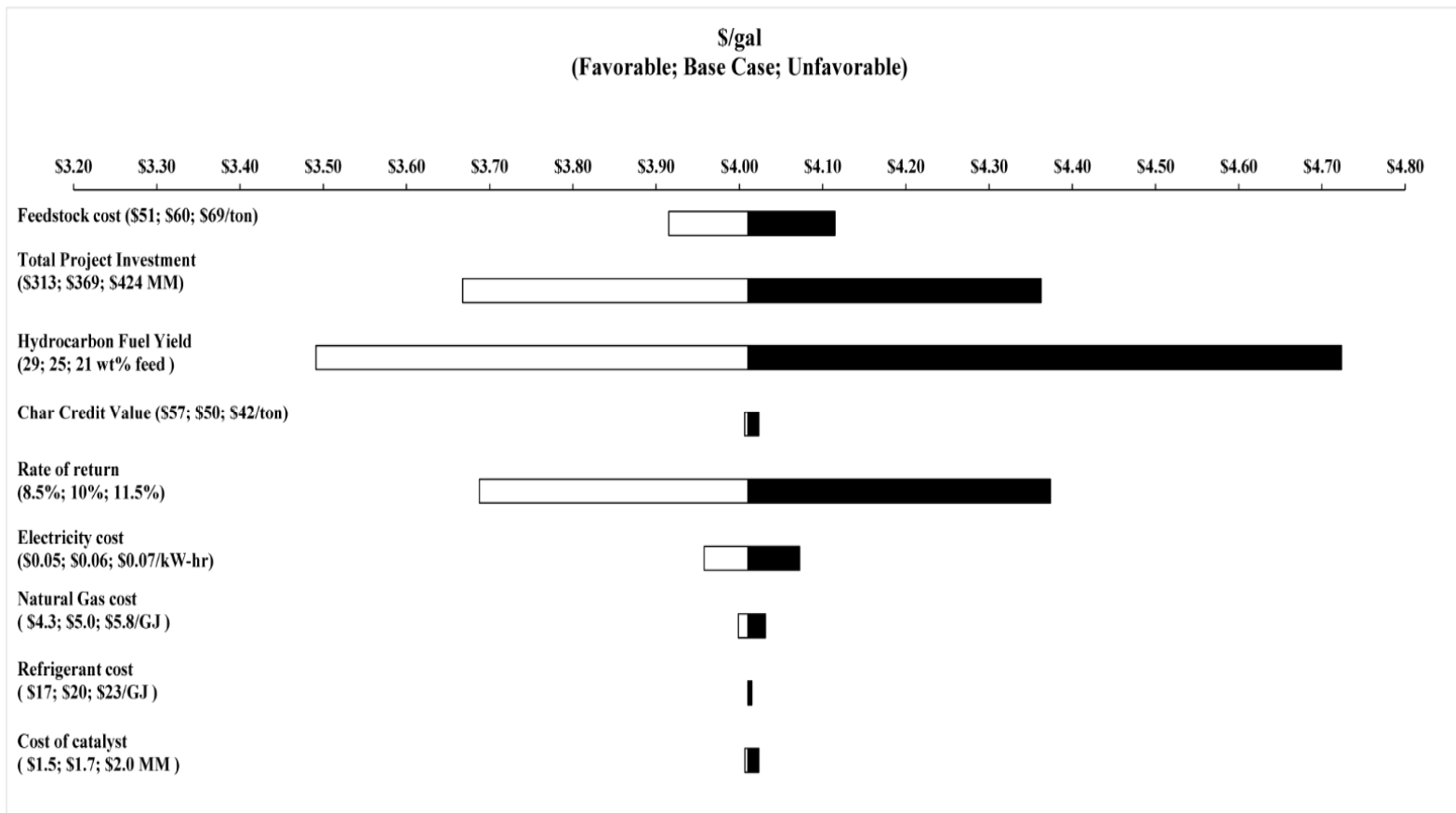
Figure 4.5. Contribution of various operating costs and equipment cost to the minimum selling price of liquid hydrocarbon fuel.

Sensitivity Analysis

The impact of a change of +/- 15% in some of the cost variables was investigated for the heat-integrated processes. As shown in Figures 4.6, 4.7 and 4.8, the MSP is more sensitive to variables such as the yield of hydrocarbon biofuel, total project investment cost, the

assumed internal rate of return, and the cost of feedstock, in that order. Though natural gas requirements for process heat was totally offset in these scenarios, sensitivity results are due to the cost of natural gas for hydrogen production and revenue credits from the sale of torrefaction condensed liquid.

The high sensitivity of the yield of hydrocarbon biofuel and the total project investment costs emphasizes the need for accurate yield data and equipment cost quotes prior to commercialization. It should also be noted that changes in the yield of hydrocarbon fuel will typically have a chain effect on other variables such as the amount of process heat requirements. These potential changes were not considered when investigating how changes in the yield of hydrocarbon biofuel impact the calculated MSP. For the heat-integrated one-step pathway, using a tax rate of 15% instead of 35% utilized in this study resulted in a 7% reduction in the MSP of hydrocarbon biofuel to about \$3.72/gal from \$4.01/gal.



127

Figure 4.6. Sensitivity of the minimum selling price to some of the economic parameters. One-step conversion pathway scenario 1 with heat integration.

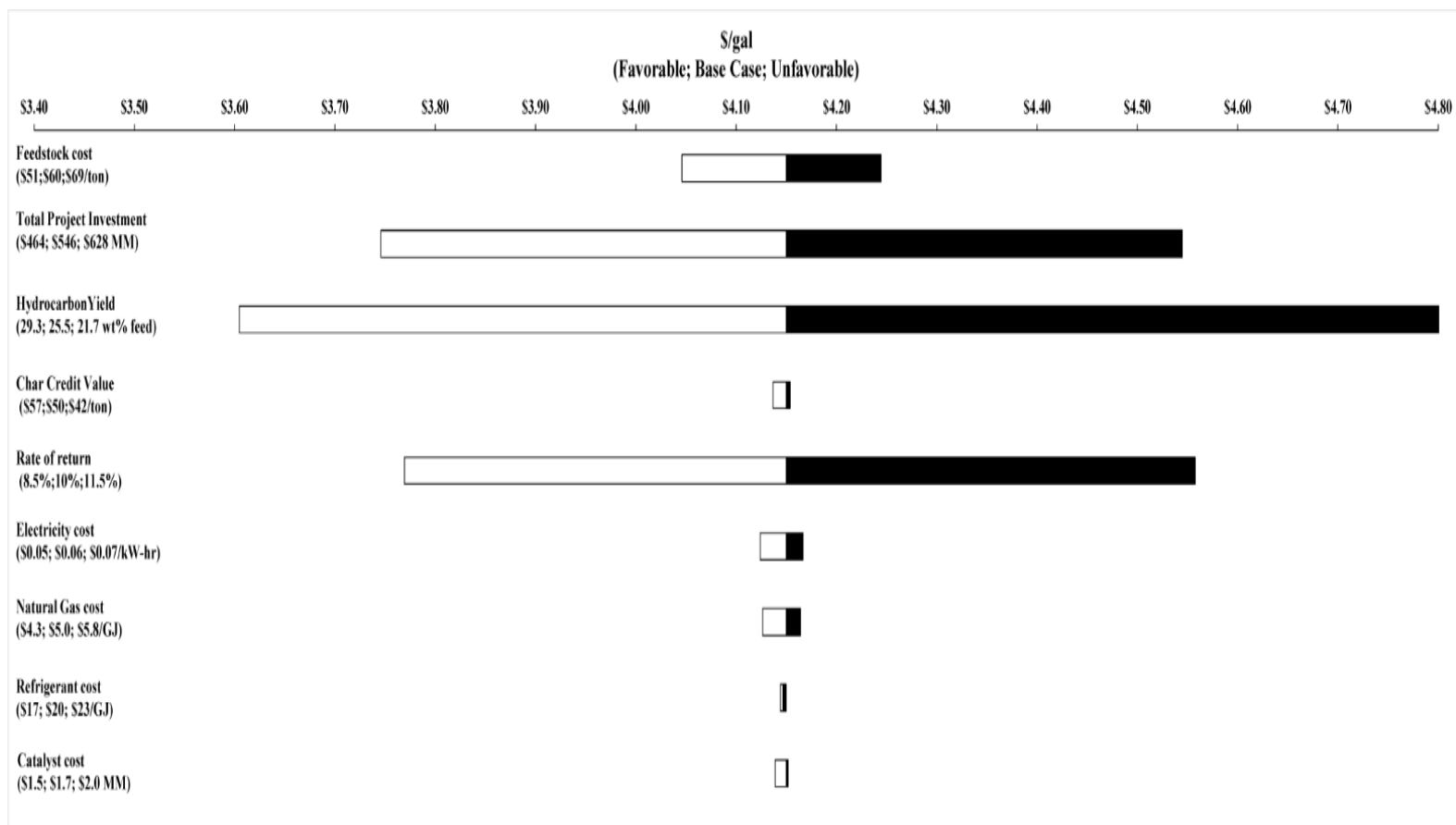
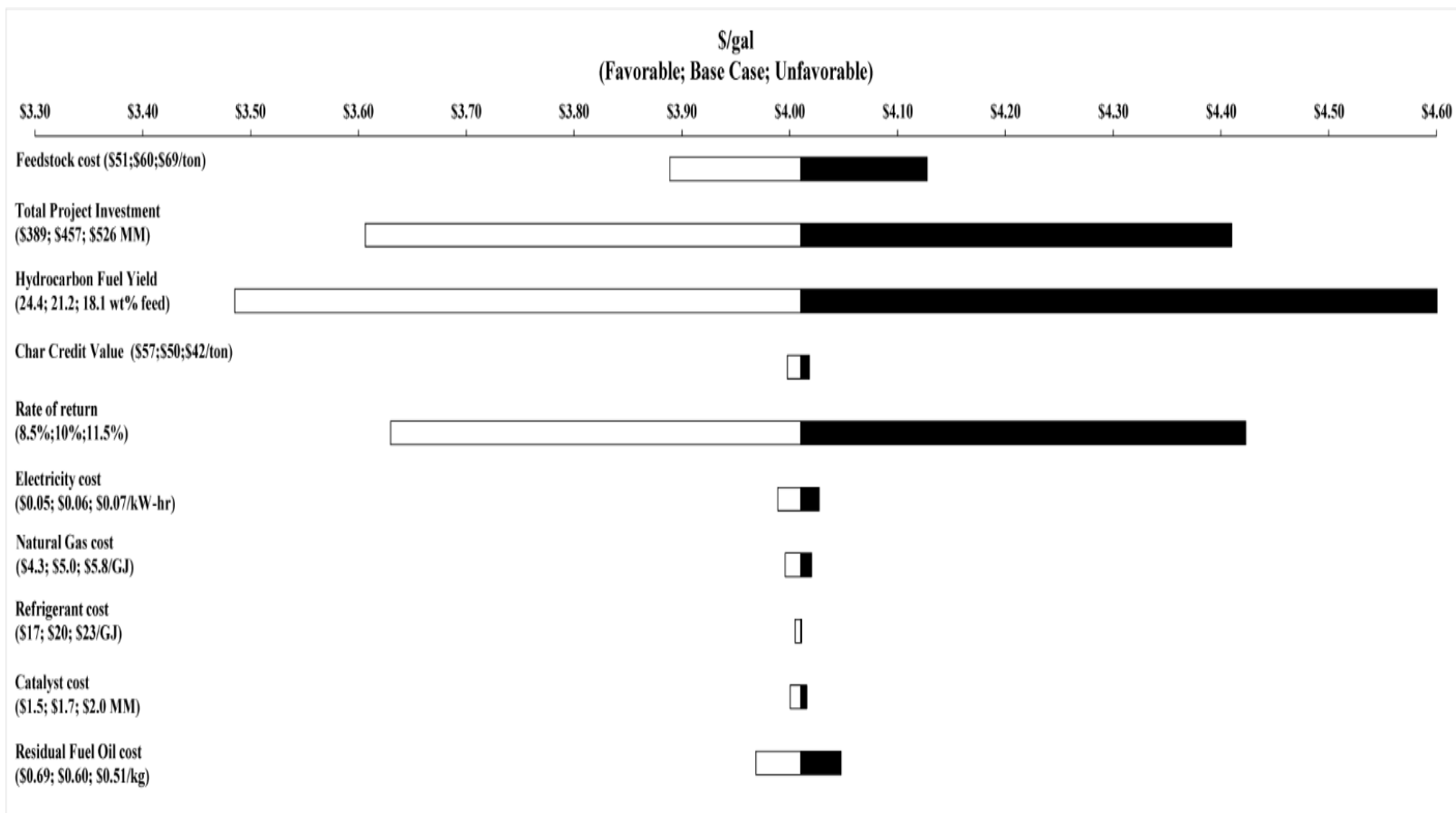


Figure 4.7. Sensitivity of the minimum selling price to some of the economic parameters. Two step conversion pathway scenario 1 at torrefaction temperature of 290°C with heat integration.



129

Figure 4.8. Sensitivity of the minimum selling price to some of the economic parameters. Two step conversion pathway scenario 3 at torrefaction temperature of 290°C with heat integration.

In conclusion, from the results of this study, MSP of hydrocarbon biofuel estimated for a one-step production pathway is almost the same with the MSP for a two-step pathway at 290°C torrefaction. Higher minimum selling prices were however estimated for hydrocarbon biofuel produced through the two-step pathway at higher torrefaction temperatures. The main conclusion of this study is the importance of heat integration for more favorable economics of the hydrocarbon biofuel pathway. The inclusion of torrefaction prior to pyrolysis showed almost the same MSP for two-step pathway at low torrefaction temperature of about 290°C. However, torrefaction does not appear to be an advantage on the cost of production for hydrocarbon fuels compared to a one-step process at high torrefaction temperatures. With heat integration, reduction in the cost of utilities outweighed the increase in capital cost, resulting in lower minimum selling price for the heat-integrated processes in comparison with the base case without heat integration. With heat integration, there is also an increase in revenue generated from the sale of unused co-products such as char and torrefaction condensed liquid. From the sensitivity analysis, it can be seen that the yield of bio-oil is the most sensitive parameter.

In a companion article, we will look at how the inclusion of torrefaction affects the greenhouse gas emissions from the hydrocarbon biofuel production pathway.¹¹It is worth mentioning that these results are based on loblolly pine as the biomass feedstock and for the data utilized in this study and may not be typical for other biomass feedstocks.

4.5 Acknowledgments

Financial support from the National Science Foundation MPS/CHE - ENG/ECCS – 1230803 Sustainable Energy Pathways (SEP) grant and the Richard and Bonnie Robbins Endowment is gratefully acknowledged. The authors will also like to acknowledge the contributions made by both Paul Langford and Jakob Nowicki of the Department of Chemical Engineering, Michigan Technological University to this study.

4.6 References

- (1) EIA, U. International energy outlook 2016. *US Energy Information Administration (EIA) 2016*.
- (2) Independence, E. Security Act of 2007. *Public law 2007, 110* (140), 19.
- (3) Bridgwater, A. V. Review of fast pyrolysis of biomass and product upgrading. *Biomass and bioenergy 2012*, 38, 68-94.
- (4) Graham, R.; Bergougnou, M.; Overend, R. Fast pyrolysis of biomass. *Journal of analytical and applied pyrolysis 1984*, 6 (2), 95-135.
- (5) Easterly, J. L. Assessment of bio-oil as a replacement for heating oil. *Northeast Regional Biomass Program 2002*, 1, 1-15.
- (6) Jones, S. B.; Valkenburg, C.; Walton, C. W.; Elliott, D. C.; Holladay, J. E.; Stevens, D. J.; Kinchin, C.; Czernik, S. *Production of gasoline and diesel from biomass via fast pyrolysis, hydrotreating and hydrocracking: a design case*, ed.; Pacific Northwest National Laboratory Richland, WA, 2009.
- (7) Wright, M. M.; Daugaard, D. E.; Satrio, J. A.; Brown, R. C. Techno-economic analysis of biomass fast pyrolysis to transportation fuels. *Fuel 2010*, 89, S2-S10.
- (8) Brown, T. R.; Thilakaratne, R.; Brown, R. C.; Hu, G. Techno-economic analysis of biomass to transportation fuels and electricity via fast pyrolysis and hydroprocessing. *Fuel 2013*, 106, 463-469.
- (9) Jones, S.; Meyer, P.; Snowden-Swan, L.; Padmaperuma, A.; Tan, E.; Dutta, A.; Jacobson, J.; Cafferty, K. *Process design and economics for the conversion of lignocellulosic biomass to hydrocarbon fuels: fast pyrolysis and hydrotreating bio-oil pathway*; Report No. 2013.

- (10) Winjobi, O.; Shonnard, D. R.; Bar-Ziv, E.; Zhou, W. Techno-economic assessment of the effect of torrefaction on fast pyrolysis of pine. *Biofuels, Bioproducts and Biorefining* **2016**.
- (11) Winjobi O., S. D. R., Kulas D., and Zhou W. Production of Hydrocarbon Fuel using Two-Step Torrefaction and Fast Pyrolysis of Pine. Part 2: Life-Cycle Carbon Footprint. *ACS Sustainable Chemistry & Engineering* **In Review**.
- (12) Phanphanich, M.; Mani, S. Impact of torrefaction on the grindability and fuel characteristics of forest biomass. *Bioresource technology* **2011**, *102* (2), 1246-1253.
- (13) Shankar Tumuluru, J.; Sokhansanj, S.; Hess, J. R.; Wright, C. T.; Boardman, R. D. REVIEW: A review on biomass torrefaction process and product properties for energy applications. *Industrial Biotechnology* **2011**, *7* (5), 384-401.
- (14) Bergman, P. C.; Kiel, J. H. Proc. 14th European Biomass Conference, Paris, France, 2005; p 17-21.
- (15) Arias, B.; Pevida, C.; Feroso, J.; Plaza, M. G.; Rubiera, F.; Pis, J. Influence of torrefaction on the grindability and reactivity of woody biomass. *Fuel Processing Technology* **2008**, *89* (2), 169-175.
- (16) Westerhof, R. J.; Brilman, D. W. F.; Garcia-Perez, M.; Wang, Z.; Oudenhoven, S. R.; Kersten, S. R. Stepwise fast pyrolysis of pine wood. *Energy & fuels* **2012**, *26* (12), 7263-7273.
- (17) Zheng, A.; Zhao, Z.; Chang, S.; Huang, Z.; He, F.; Li, H. Effect of torrefaction temperature on product distribution from two-staged pyrolysis of biomass. *Energy & Fuels* **2012**, *26* (5), 2968-2974.

- (18) Ji-Lu, Z. Bio-oil from fast pyrolysis of rice husk: Yields and related properties and improvement of the pyrolysis system. *Journal of Analytical and Applied Pyrolysis* **2007**, *80* (1), 30-35.
- (19) Chen, D.; Li, Y.; Deng, M.; Wang, J.; Chen, M.; Yan, B.; Yuan, Q. Effect of torrefaction pretreatment and catalytic pyrolysis on the pyrolysis poly-generation of pine wood. *Bioresource technology* **2016**, *214*, 615-622.
- (20) Boateng, A.; Mullen, C. Fast pyrolysis of biomass thermally pretreated by torrefaction. *Journal of Analytical and Applied Pyrolysis* **2013**, *100*, 95-102.
- (21) Park, J.; Meng, J.; Lim, K. H.; Rojas, O. J.; Park, S. Transformation of lignocellulosic biomass during torrefaction. *Journal of Analytical and Applied Pyrolysis* **2013**, *100*, 199-206.
- (22) He, Z.; Wang, X. Hydrodeoxygenation of model compounds and catalytic systems for pyrolysis bio-oils upgrading. *Catalysis for sustainable energy* **2012**, *1*, 28-52.
- (23) Zacher, A. H.; Olarte, M. V.; Santosa, D. M.; Elliott, D. C.; Jones, S. B. A review and perspective of recent bio-oil hydrotreating research. *Green Chemistry* **2014**, *16* (2), 491-515.
- (24) Furimsky, E. Catalytic hydrodeoxygenation. *Applied Catalysis A: General* **2000**, *199* (2), 147-190.
- (25) Odebunmi, E. O.; Ollis, D. F. Catalytic hydrodeoxygenation: I. Conversions of o-, p-, and m-cresols. *Journal of Catalysis* **1983**, *80* (1), 56-64.
- (26) Vispute, T. Pyrolysis oils: characterization, stability analysis, and catalytic upgrading to fuels and chemicals. **2011**.

- (27) Huber, G. W.; Chheda, J. N.; Barrett, C. J.; Dumesic, J. A. Production of liquid alkanes by aqueous-phase processing of biomass-derived carbohydrates. *Science* **2005**, *308* (5727), 1446-1450.
- (28) Bromaghim, G.; Gibeault, K.; Serfass, J.; Serfass, P.; Wagner, E. National Hydrogen Association, 2010.
- (29) Leiby, S. Options for refinery hydrogen. *A private report by the Process Economics Program, Report 1994*, (212).
- (30) Rostrup-Nielsen, J. R. In *Catalysis*; Springer, 1984.
- (31) Wagner, A. L.; Osborne, R. S.; Wagner, J. P. Prediction of deactivation rates and mechanisms of reforming catalysts. *Prepr. Pap.-Am. Chem. Soc., Div. Fuel Chem* **2003**, *48* (2), 748.
- (32) Peters, M. S.; Timmerhaus, K. D.; West, R. E.; Timmerhaus, K.; West, R. *Plant design and economics for chemical engineers*, ed.; McGraw-Hill New York, 1968.
- (33) CEPCI. Chemical Engineering Plant Cost Index. *Chem. Eng.* **2010**, 76.
- (34) Administration, U. S. E. I.; Vol. 2013.
- (35) Administration, U. S. E. I.; Vol. 2013.
- (36) Turton, R.; Bailie, R. C.; Whiting, W. B.; Shaeiwitz, J. A. *Analysis, synthesis and design of chemical processes*, ed.; Pearson Education, 2008.
- (37) Vol. 2016.
- (38) Administration, U. S. E. I.; Vol. 2013.
- (39) Sinnott, R.; Elsevier Butterworth Heinemann, Oxford, 20

5. Production of Hydrocarbon Fuel using Two-Step Torrefaction and Fast Pyrolysis of Pine. Part 2: Life Cycle Carbon Footprint.[§]

5.1. Abstract

This study, as part II of two companion papers, investigated the environmental performance of liquid hydrocarbon biofuel production via fast pyrolysis of pine through two pathways: a one-step pathway via fast pyrolysis only, and a two-step pathway that includes a torrefaction step prior to fast pyrolysis. Fast pyrolysis in all cases took place at a temperature of 530°C while for the two-step pathways, torrefaction was investigated at temperatures of 290, 310 and 330°C. Bio-oil produced was then catalytically upgraded to hydrocarbon biofuel. Different scenarios for providing the required process heat either by using fossil energy or renewable energy, as well as the effect of heat integration, were also investigated. Our life cycle analysis indicated that using the energy allocation approach, a two-step heat integrated pathway with torrefaction taking place at 330°C had the lowest global warming potential among all scenarios of about 29.0g CO₂ equivalent/MJ biofuel. Using the system expansion approach, significantly higher reductions in GHG emissions of about 56 to 265% relative to conventional gasoline were observed for the heat integrated processes. More modest percentage reduction in emissions of about 34 to 67% was observed across all scenarios using the energy allocation approach.

[§] Reprinted with permission from WINJOBI, O, ZHOU W, KULAS D, NOWICKI J, SHONNARD D. PRODUCTION OF HYDROCARBON FUEL USING TWO-STEP TORREFACTION AND FAST PYROLYSIS OF PINE.PART 2: LIFE CYCLE CARBON FOOTPRINT. Copyright (2017) American Chemical Society

5.2. Introduction

Concerns about energy security due to depleting crude oil reserves and volatility of oil prices, as well as global warming, have increased the focus on alternative energy sources that are potentially more environmental friendly. A potential alternative energy source, biomass is ubiquitous in nature ranging from woody biomass such as pine to agricultural waste such as rice husks. As a result, studies such as ‘The Billion Ton Vision’, have looked at potentially producing at least one billion dry tons of biomass annually in a sustainable manner to serve as feedstock for the production of biofuel, either through biochemical or thermochemical approaches to displace about 30% of the current petroleum consumption in the United States.¹

Of the various thermochemical conversion processes, fast pyrolysis is believed to offer significant advantages over conventional pyrolysis, flash pyrolysis and gasification process due to product yield quality and flexibility.² Fast pyrolysis thermally degrades biomass to produce non-condensable gases, char and the main product, liquid bio-oil. The bio-oil obtained from fast pyrolysis is typically chemically unstable, low in energy density, and acidic requiring an upgrade/refining step to be suitable as a ‘drop-in’ replacement for gasoline.³ In order to make biofuel production through fast pyrolysis more favorable, pretreatments such as torrefaction prior to fast pyrolysis are being investigated. The torrefaction pretreatment can potentially reduce the energy required for grinding biomass and improve the quality of the bio-oil.^{4,5} The improved bio-oil may require less hydrogen for the upgrade step, and by these steps potentially improve the economics and environmental impacts of hydrocarbon biofuel production. Techno-economic and life cycle

assessment can be used to evaluate the effect that the addition of torrefaction before fast pyrolysis has on the economics and greenhouse gas emissions from producing hydrocarbon biofuels.

While previously (Part I) we examined economic viability, here we will evaluate the environmental impacts of biofuel production via fast pyrolysis through two pathways; i. A one-step pathway with the loblolly pine undergoing fast pyrolysis followed by the upgrade of the pyrolysis bio-oil to hydrocarbon transportation biofuel, and ii. a two-step pathway with loblolly pine undergoing torrefaction then fast pyrolysis followed by the upgrade step to hydrocarbon biofuel.⁶

To be deemed sustainable and eligible for incentives, some countries have imposed minimum GHG emission levels for biofuels.^{7,8} As a result, this study aims to examine if the hydrocarbon biofuel modeled here will meet such emissions level in addition to the comparative assessment between one-step and two-step pathways. Using life cycle assessment (LCA), potential reductions that can be achieved from the production and combustion of biofuel can be evaluated. LCA is a standardized methodology used to study the potential environmental impacts throughout a product's or system's life cycle from raw material acquisition through production, use, and disposal.^{9,10} Previous works have used LCA to evaluate the environmental performance of bioenergy systems, as discussed next.

In their assessment of pyrolysis bio-oil from whole southern pine, Steele et al. achieved a 70 % reduction in emission compared to residual fuel oil based on equivalent energy value.¹¹ Winjobi et al. achieved an 80 % reduction in GHG relative to heavy fuel oil in their assessment of the effect of torrefaction on the GHG emissions from the production of

bio-oil from loblolly pine via fast pyrolysis.¹² While in their assessment of hydrocarbon transportation fuel from fast pyrolysis of short-rotation poplar biomass, Iribarren et al. achieved a GHG saving of 72% over conventional fossil fuel.¹³ Hsu estimated about 75% reduction in GHG emissions for biofuel produced via fast pyrolysis and hydroprocessing of hybrid poplar over conventional fossil gasoline.¹⁴ In their assessment of electric power generation from the combustion of pyrolysis oil, Fan et al. achieved GHG savings of 77 – 99% relative to combustion of fossil fuel for power generation. Also in the assessment of the use of the heavy end fraction of bio-oil derived from the fast pyrolysis of corn stover to co-fire with coal in power plants with biochar sequestration, Qi et al. achieved GHG emissions reduction ranging from 2.9 to 74.9% compared to traditional coal power plants.¹⁵ The differences in the results of these assessments can be attributed to the a number of factors such as differences in biomass feedstock utilized in these studies, the final primary product and the use of the final product which varied from hydrocarbon biofuel used as a transportation fuel, to pyrolysis bio-oil used in the generation of electric power among others. As a result, the functional unit used in carrying out these assessments also differed. To our knowledge, no work has investigated how the inclusion of torrefaction before fast pyrolysis in the production of hydrocarbon transportation biofuel affects the environmental performance of the production pathway.

This LCA study aims to carry out a comparative assessment to investigate how the inclusion of a torrefaction step before the fast pyrolysis step impacts the life cycle greenhouse gas emissions (carbon footprint) of hydrocarbon biofuel through the conversion of loblolly pine by fast pyrolysis via two production pathways.

5.3. Material and Methods

Process description

The biofuel production process is assumed to convert 1000 dry metric tons of biomass feedstock entering the pyrolyzer unit per day for both the one-step and two-step processes. For the one-step pathway, the feed is raw loblolly pine chips while for the two-step pathway the feed is torrefied loblolly pine wood chips. The hydrocarbon biofuel production pathway starts with the collection of the biomass, loblolly pine. A coarse size reduction step carried out on the harvest site reduces the biomass to chips of approximately 2.5cm in dimension before they are transported to the biofuel production facility. This study assumed the transportation of the chips to the facility includes road and rail transport. These operations before the delivery of the chips to the facility constitute the biomass logistic step in this study.

A schematic diagram of the biomass conversion at the biorefinery is shown in Figure 1, process conditions for the numbered streams are shown in Table D1 in section A of Appendix D. The received loblolly pine chips with an assumed moisture content of about 25% will be reduced to about 8% using an indirect contact rotary steam dryer. The dried biomass is then processed through an auger bed torrefaction unit for about 40 minutes for the two-step production pathway, producing non-condensable gases (NCG), torrefaction condensed liquid and bio-coal (torrefied biomass). Following the torrefaction step, the bio-coal is processed through hammer mills for further size reduction to about 2mm or smaller. For the one-step biofuel production pathway, the dried biomass exiting the dryer at 8% moisture content is processed through the hammer mills for the size reduction to about

2mm biomass size. Torrefied biomass from the size reduction step is processed through a circulating fluidized bed pyrolyzer producing NCG, char and pyrolysis bio-oil. The catalytic upgrade of the produced bio-oil to hydrocarbon fuel is achieved in two steps: stabilization of bio-oil and hydrotreatment to biofuels using compressed hydrogen. The high-pressure hydrogen required for the upgrade step is supplied in excess of the required hydrogen. As a result, the hydrogen required will be produced by steam reforming of the low molecular hydrocarbons produced from the upgrade of the bio-oil supplemented with natural gas supplied to the facility. Pressure swing adsorption (PSA) with an assumed recovery of about 85% will be used to produce a high purity hydrogen stream and an off-gas stream. The off-gas will contain mainly CO₂ (about 73 wt. %), with unreacted CH₄ (about 12 wt. %), CO (about 8.5 wt. %), H₂ (about 2.5 wt. %) and traces of other low molecular hydrocarbons. All units operations shown in Figure 5.1 for the two-step biofuel production pathway, are also present in the one-step pathway except the torrefaction step. A more detailed description of the process units can be found in the companion article part I.⁶ The processes analyzed are based on design cases modeled in Aspen Plus using yield data from the literature.¹⁶⁻¹⁹

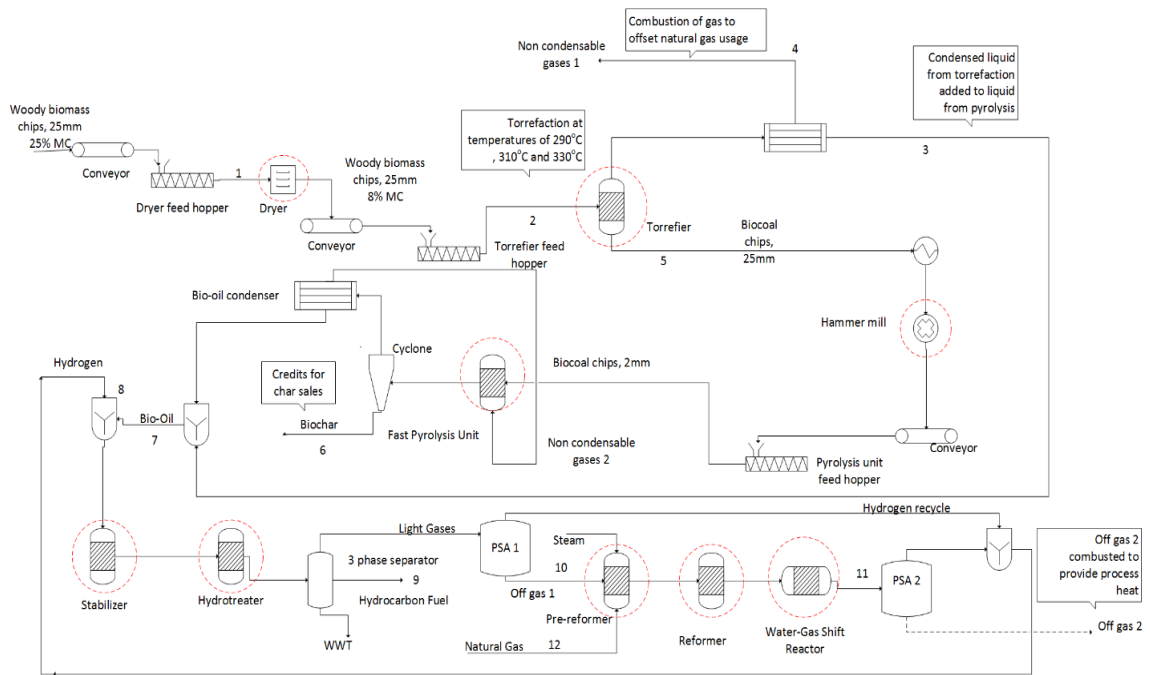


Figure 5.1. Schematic diagram for scenario 1 of a two-step hydrocarbon biofuel production pathway.

The life cycle assessment for the biofuel production pathway was carried out by investigating three scenarios. Each scenario has two objectives as shown in Table 5.1. The objectives of scenario 1 were met by using fossil energy inputs (natural gas) to provide the process heat required for the production pathway while the bio-oil yield was maximized by blending the torrefaction condensed liquid with the pyrolysis bio-oil. Process heat requirements were first satisfied by combusting the NCG from the torrefaction step and off-gas from the hydrogen production. Unmet heat requirements were then satisfied with natural gas. The blended bio-oil was then upgraded to the desired hydrocarbon biofuel. The co-product char produced from the pyrolysis step is carbon-rich and has a high-energy content. For this scenario, the char was exported to co-fire in coal power plants to improve environmental impacts for coal power plants^{20,21} The NCG from

the pyrolysis step has low heating value due to its dilution by nitrogen which served as the fluidizing agent. Thus, the NCG from pyrolysis was recirculated to the pyrolyzer rather than being combusted.

Table 5.1. Design objectives for different scenarios

Scenarios	Objective 1	Objective 2	Description
Scenario 1	Fossil energy inputs	Maximizing bio-oil yield	NCG and off-gas +NG, export biochar. Blend pyrolysis oil with torrefaction condensed liquid
Scenario 2	Minimize fossil energy inputs	Maximizing bio-oil yield	NCG and off-gas +NG, export biochar. Blend pyrolysis oil with torrefaction condensed liquid
Scenario 3	Renewable energy inputs	Maximizing bio-oil quality	NCG and off-gas + torrefaction condensed liquid +biochar.

NCG: non-condensable gas, NG: natural gas

Objective 1 of scenario 2 to minimize fossil energy inputs, was achieved by internally combusting the char produced from pyrolysis to meet some of the process heat required. For this scenario, the NCG from torrefaction, off-gas from hydrogen production and char from pyrolysis were first combusted to supply the process heat. Natural gas was then combusted to satisfy unmet process heat requirement. The second objective of maximizing bio-oil yield similarly to scenario 1 was achieved by blending the torrefaction condensed liquid with the pyrolysis bio-oil and then upgraded to hydrocarbon biofuel. The schematic diagram for this scenario is shown as Figure D1 in section A of Appendix D.

The objectives of scenario 3 of renewable energy inputs and maximizing bio-oil quality were met by internally combusting the torrefaction condensed liquid so that the use of fossil

energy inputs is totally offset. For this scenario, to entirely offset fossil energy inputs the order for the combustion of renewable energy sources for process heat was NCG from torrefaction, off-gas from hydrogen production, torrefaction condensed liquid and then char from pyrolysis. Depending on the process heat requirements, when only a portion of the torrefaction condensed liquid is required to be combusted to fully meet objective 1 of scenario 3, unused torrefaction condensed liquid will be blended with the pyrolysis bio-oil. Because the torrefaction condensed liquid was either not blended or partially blended with the pyrolysis bio-oil, objective 2 of maximizing bio-oil quality was met. The bio-oil from this scenario was then upgraded to hydrocarbon biofuel. Unused char from this scenario was also exported to co-fire in coal power plants. The schematic diagram for this scenario is shown as Figure D2 in section A of Appendix D.

Heat Integration

The significance of having an energy optimized process was investigated by carrying out heat integration on the biofuel production pathways described. Heat integration software Super Target® was used in performing this optimization. Stream temperatures and heat exchanger duties modeled in Aspen Plus® were input into the heat integration software to identify matches as explained in the companion article part I.⁶

LCA framework, system definition, and modeling assumptions

This study evaluates the ‘cradle-to-grave’ impact of hydrocarbon fuel production via fast pyrolysis followed by an upgrade of the intermediate bio-oil to hydrocarbon biofuel. SimaPro® version 8.0 is the LCA software used in this study. SimaPro® provides

accessible databases of environmental inventory data including ecoprofiles specific to the U.S.

Goal of the LCA study

The goal of this LCA study is to compare the greenhouse gas (GHG) emissions of hydrocarbon biofuel production and use from the fast pyrolysis of loblolly pine via two pathways, a one-step pathway and a two-step pathway using results obtained from process simulation of the pathways. The carbon footprint for the pathways were calculated by converting GHG emissions from the use of material and energy for the hydrocarbon biofuel production to CO₂ equivalents. The impacts from these pathways will also be compared with gasoline fuel produced from petroleum.

System boundary

The system boundary shows the sequence of unit processes in the pathway that is included in the assessment as shown in Figure 5.2. The hydrocarbon biofuel production chain is broken into two sections, biomass supply logistics, and biomass conversion. The biomass supply logistics includes the collection of biomass, coarse chipping of biomass in the forest, loading/unloading and transport of the biomass chips to the biofuel production site. This study assumes the biomass being converted is wood waste and logging residues. Thus CO₂ emissions due to direct and indirect land use changes are not considered in our assessment because we assume that sustainable practices will be adopted by leaving a portion of the logging residue in the forest to sustain soil C stocks. Emission factors for biomass logistics were based on values from the Greenhouse Gases, Regulated Emissions, and Energy Use in Transportation (GREET) model.²² Depending on the scenario being examined, the

outputs from the system boundary varies as shown in Table 5.2. Inputs into the system are similar in almost all scenarios except for scenario 3, where there is no input of natural gas for process heat. As earlier explained, for this scenario process heat was totally supplied internally by the combustion of renewable energy sources. Steam generated from the highly exothermic hydrotreatment reaction, an output for the pathways without heat integration, was utilized internally in the heat integrated processes.

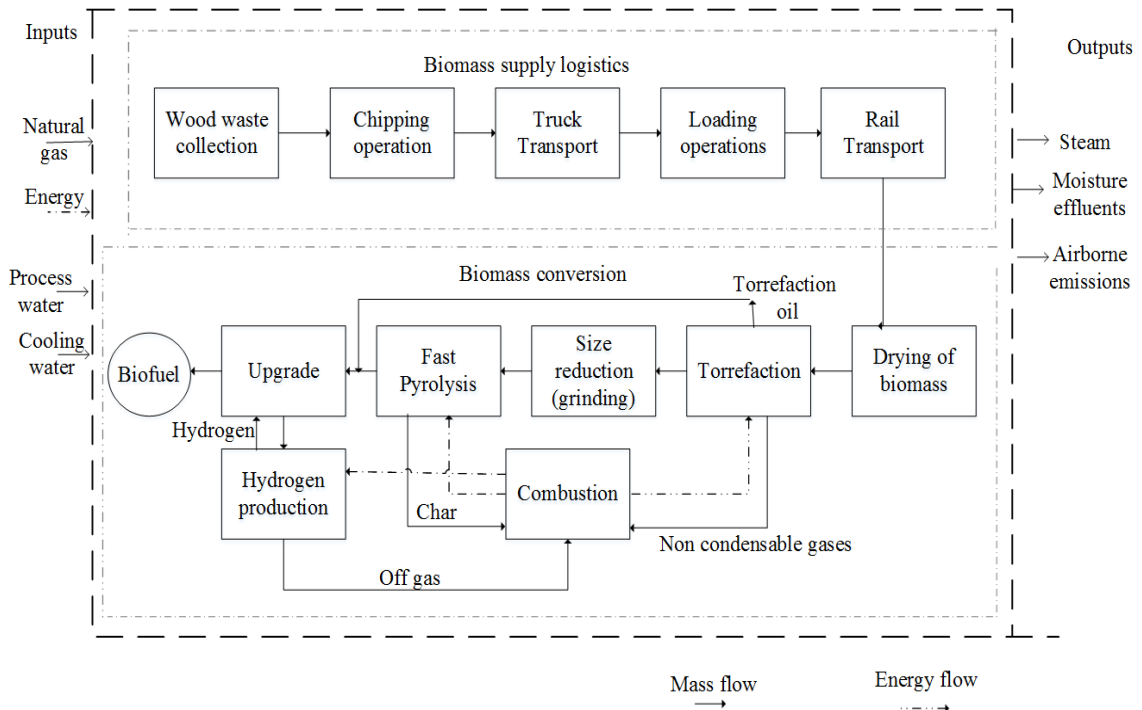


Figure 5.2. Cradle to grave system boundary for scenario 2 of a two-step hydrocarbon biofuel production.

Table 5.2. Inputs and outputs from each scenario of the hydrocarbon biofuel production pathway.

Inputs	Outputs		
	Scenario 1	Scenario 2	Scenario 3
Loblolly pine	Biofuel	Biofuel	Biofuel
Natural gas (for hydrogen production)	Char	Steam [†]	Steam [†]
Cooling water	Steam [†]	Off gas ^{††}	Char
Process water (for hydrogen production)	Off gas ^{††}		Off gas ^{††}
*Natural gas (for process heat)			Torr. condensed liquid ^{††}

*Applies to scenarios 1 & 2 only.

† Applies only to the scenarios without heat integration

†† Applies only to the heat integrated processes

Functional Unit

The functional unit provides the reference to which all results in the assessment are based.²³

For this comparative environmental assessment of one and two-step biofuel production pathways as well as the fossil gasoline pathway, the functional unit was set to 1 MJ of energy content of the biofuel produced and combusted.

Allocation methods

The pathways investigated in this study are multi-output pathways. For the base case without heat integration, co-products such as biochar and steam were produced and exported in addition to the main product (hydrocarbon biofuel) when applicable as shown

in Table 5.2. For such multi-output processes, allocation is carried out so that the environmental loadings are allocated to each product. This study looked at allocation using two approaches, a system expansion approach and an energy allocation approach. For the base case scenarios without heat integration, using the system expansion approach, biochar was assumed to displace coal to co-fire power plants while steam generated from cooling the highly exothermic hydrotreatment reaction is not utilized internally but exported to get credits for displacing the production of steam using natural gas. Torrefaction condensed liquid will be assumed to displace heavy fuel oil. Inventories of GHG emissions for the displaced product including their combustion emissions were obtained from ecoinvent™ database in SimaPro®.

For energy allocation, energy allocation factors were calculated using equation (1) and were used to partition the environmental loading of the produced hydrocarbon biofuel.

Allocation factor

$$= \frac{\dot{m}_{main\ product} LHV_{main\ product}}{\dot{m}_{main\ product} LHV_{main\ product} + \sum \dot{m}_{co-product} LHV_{co-product}} \quad (1)$$

In equation (1) $LHV_{main\ product}$ = lower heating value of the main product under study, $LHV_{co-product}$ = lower heating value of co-product and m = mass flowrates of the streams.

Due to the hydrocarbon biofuel and co-products existing at different stages of the production pathway, two or in some cases three allocation factors were calculated. This study applied the energy allocation approach to the heat integrated processes only. With heat integration, some co-products that were internally combusted to provide process heat in the base case scenarios were either partially combusted or not utilized internally at all.

As a result, potential co-products from the hydrocarbon biofuel production pathway includes torrefaction condensed liquid that is obtained from the torrefaction stage shown in Figure 2, from the condensation of torrefaction vapors for scenario 3, biochar produced from the fast pyrolysis stage, and unused off-gas produced from the hydrogen production stage (part of upgrading). Though the hydrocarbon biofuel exited the production pathway at the upgrade stage while unused off-gas exited from the hydrogen production stage, these stages were treated as an integrated stage as shown in Figure D3 in section F of Appendix D. The environmental burden from this integrated stage simply termed the hydrotreatment stage in this study will be allocated to both the hydrocarbon biofuel and the unused off-gas.

For the torrefaction, fast pyrolysis and the hydrotreatment stages, where the co-products exit the hydrocarbon biofuel production pathway, stage-specific allocation factors were calculated using equations (2) – (4).

$$\begin{aligned}
 & \textit{Allocation factor}_{\textit{torrefaction}} \\
 &= \frac{\dot{m}_{\textit{bio-coal}}LHV_{\textit{bio-coal}}}{\dot{m}_{\textit{bio-coal}}LHV_{\textit{bio-coal}} + \dot{m}_{\textit{torr. oil}}LHV_{\textit{torr.oil}}} \quad (2)
 \end{aligned}$$

$$\begin{aligned}
 & \textit{Allocation factor}_{\textit{fast pyrolysis}} \\
 &= \frac{\dot{m}_{\textit{bio-oil}}LHV_{\textit{bio-oil}}}{\dot{m}_{\textit{bio-oil}}LHV_{\textit{bio-oil}} + \dot{m}_{\textit{char}}LHV_{\textit{char}}} \quad (3)
 \end{aligned}$$

*Allocation factor*_{hydrotreatment}

$$= \frac{\dot{m}_{biofuel}LHV_{biofuel}}{\dot{m}_{biofuel}LHV_{biofuel} + \dot{m}_{off-gas}LHV_{off-gas}} \quad (4)$$

LHV_{biofuel} is the LHV of hydrocarbon biofuel and is assumed to be the same as that of conventional gasoline; 43.45 MJ/kg, LHV_{char} is the LHV of char produced estimated from its ultimate analysis as 29.98 MJ/kg using correlations as shown in section B of AppendixD. LHV_{torr. bio-oil} is the LHV of the torrefaction condensed liquid, and was estimated using the weight fractions and the LHV of the representative compounds in the torrefaction condensed liquid as shown in section B of Appendix D. LHV_{bio-coal} is the LHV of the torrefied biomass/bio-coal, and was estimated from its ultimate analysis as outlined for char and LHV_{off-gas} is the LHV of the off-gas which was estimated from the weight fractions and LHV of the low molecular hydrocarbon compounds in the off-gas.

An overall allocation factor, AF1 which was calculated as the product of all three stage-specific allocation factor as shown in Equation 5, was applied to all input and output streams up to and including the torrefaction step in Figure 5.2.

$$AF1 = Allocation\ factor_{torr.} \times Allocation\ factor_{pyrolysis} \times Allocation\ factor_{hydrotreatment} \quad (5)$$

AF2, which is the product of the fast pyrolysis allocation factor and the hydrotreatment allocation factor, was applied to the input and output streams for the size reduction and fast pyrolysis stages. The overall allocation factor AF3, which is the calculated allocation factor calculated for the hydrotreatment stage, was applied to the upgrade and hydrogen

production streams. A sample calculation for the allocation factors can be found in section F of Appendix D.

Life Cycle Inventory

The life cycle inventory includes all material and energy inputs to each stage in the life cycle as well as the cradle-to-gate inventory of greenhouse gas emissions and energy demand for those inputs.²⁴ The processes inventoried for the LCA in this study are described here. A more detailed description of the processes involved in the conversion step can be found in the companion article Part I.⁶

Biomass supply logistics

Wood collection

The collection of loblolly pine was modeled in this study as the collection of wood residues. Direct and indirect land use change emissions were not considered in this study. Emissions due to wood residue collection were obtained from the 2014 GREET model spreadsheet based on 1 dry metric ton of biomass. See section B of the Appendix D for the details on fuels use and emission factors of this step.

Coarse chipping of wood

Coarse size reduction of the biomass to chips was assumed to be done on the harvest site for easy transport of biomass to the biofuel facility. It was assumed that 0.5 kg of diesel was combusted per dry ton of biomass chipped based on the study by Maleche et al.²⁵ The inventory of greenhouse gas emissions was obtained from the GREET model for the production and combustion of diesel for the chipping step. See section B of the Appendix D for the details on fuels use and emission factors of this step.

Transport of wood chips to biofuel facility

This study looked at a ‘worst-case scenario’ scenario for the transportation of the wood chips to the biofuel facility. A 90-mile truck transport and a 490-mile rail transport was assumed based on the default distance from the GREET model. Emissions for the transportation step were obtained from the GREET model per dry ton of wood residue transported. When diesel was utilized such as in the transport by rail, emissions for both production and combustion of diesel were included. See section B of Appendix D for the details on fuels use and emission factors of this step.

Loading operations

Due to our assumption of truck and rail transport, three loading operations was modeled to take place for the forest-to-facility logistics. The loading operations include forest-to-truck, truck-to-train and finally rail to the facility. Handler et al. determined that 0.5 kg diesel/dry short ton of forest woody would be required for each loading step.²⁶ Emissions relating to the production and combustion of diesel were also factored into this step and were also obtained from the GREET model using diesel upstream and combustion emission factors. See section B of Appendix D for the details on fuels use and emission factors of this step.

Biomass conversion

Drying of biomass

Biomass received at the conversion facility is assumed to have a 25% moisture content. It is typically desired to reduce the moisture content to about 10% for the smooth operations of the hammer mills required for further size reduction step prior to fast pyrolysis. Bridgwater et al. also established that for optimal fast pyrolysis, the moisture content of

the biomass should be between 7 -10%.²⁷ This study assumed the drying operation reduced the moisture content of the biomass to 8%. The emissions from the drying step is based on the process heat required to generate the steam used in effecting the drying as explained in companion article part I.⁶ The drying step was modeled in Aspen Plus, and the estimated heat duty from the simulation was used to quantify the amount of either natural gas or renewable fuels required to generate the required steam. Previous studies have established the energy required for reducing the moisture content in biomass to range from about 2.9 to 4.0 MJ/kg of water removed.²⁸⁻³¹

Size reduction of loblolly pine chips

Further reduction in the size of the pine chips to a size of about 2mm is required to ensure that the biomass is processed in the pyrolyzer. The size reduction step for the dried loblolly pine and torrefied pine (bio-coal) were modeled in Aspen Plus using correlations established in the literature.³² The correlation established the grinding energy required as a function of torrefaction temperature. The size reduction was assumed to be carried out using hammer mills as described in companion article part I.⁶ The emissions from the size reduction step was quantified based on the estimated energy required to reduce the loblolly pine chips. A double pass through the hammer mill was assumed in this study. The hammer mill is assumed to be driven by electricity delivered to the plant using US grid electricity mix.

Torrefaction of biomass

For the two-step hydrocarbon fuel production pathway, the torrefaction step comes before the size reduction step. The effect of torrefaction on the fast pyrolysis of loblolly pine was

investigated by Westerhof et al. at torrefaction temperatures of 290, 310 and 330°C.¹⁶ The torrefaction step was modeled in Aspen Plus using a yield reactor based on literature data as described in part A of this study.^{16,18,19} Yields of non-condensable gases, condensed liquid and torrefied solid at different torrefaction temperatures and the yield distribution of the oil and gas for torrefaction are shown as Tables D7 and D8 in section C of Appendix D. Change in the structure of torrefied solid i.e. the ultimate and proximate analysis after torrefaction at the different temperatures based on literature data are shown in Tables D9 and D10, respectively, in section C of Appendix D.¹⁹ The emissions from this step are based on the estimated process heat required to effect the torrefaction at the different torrefaction temperatures investigated. In addition to the process heat supplied by either natural gas or renewable energy, emissions related to the amount of cooling water required to condense the torrefaction condensed liquid was also inventoried.

Fast Pyrolysis

Fast pyrolysis of the raw pine/torrefied pine, which took place at a temperature of 530°C was modeled using a yield reactor in Aspen Plus based on literature data.^{16,18,19} Yield data and yield distribution of the representative compounds in the bio-oil used in the model are as shown in Tables D11 and D12, respectively, in section C of Appendix D. A detailed description of the modeling of this step can be found in companion article part I.⁶ The emissions from this step are based on the amount of energy inputs (natural gas or renewable energy) required to satisfy the estimated process heat requirements to carry out fast pyrolysis. Cooling water required for quick quench of pyrolysis vapors is also inventoried for this step.

Upgrade of bio-oil

This study assumed whole bio-oil upgrade through catalytic hydrotreatment to remove the oxygen contained in the bio-oil as water by phase separation.³³ The upgrade of bio-oil to hydrocarbon fuel was achieved by a two-step upgrade step; a stabilization step followed by a hydrotreatment step. The upgrade steps were modeled in Aspen Plus using operating conditions from the literature.¹⁷ The conversion of representative compounds in bio-oil to hydrocarbon fuel by reacting with hydrogen were modeled using reaction pathways suggested in literature. The reaction pathways for the upgrade step are discussed in detail in companion article part I.⁶ The reaction pathways of the representative compounds are shown in section D of Appendix D, and the yield factors for modeling the hydrotreaters are shown as Tables D15 to D21 in Appendix D. The hydrotreatment is highly exothermic.²⁸ The emissions inventories for this step includes the process heat requirements by heat exchangers in this step and cooling water used in taking heat away from the hydrotreater.

Hydrogen production

The hydrogen required for the upgrade of bio-oil to biofuel was produced in the facility by steam methane reforming. The low molecular hydrocarbons such as ethane and propane generated during the upgrade of some of the representative compounds in bio-oil were first pre-reformed to methane followed by the steam reforming of methane to produce hydrogen. The pre-reforming, reforming and water-gas shift reactors were modeled as equilibrium reactors in Aspen Plus using operating conditions from literature.¹⁷ Natural gas was used to complement the off-gas from hydrotreatment to provide the amount of excess hydrogen required for the upgrade step. Pressure swing adsorption (PSA) operating at 85% H₂ recovery was used to separate the hydrogen from the unreacted methane as well as CO

and CO₂ produced during the pre-reforming and reforming steps. The off gas from the PSA was combusted to provide some of the process heat required. The emissions inventoried for this step includes the natural gas required to complement the off gas from hydrotreatment, energy inputs (natural gas or renewable energy) combusted to provide process heat for the highly endothermic pre-reforming and reforming reactions, cooling water required for the water-gas shift reaction, process water required to generate steam for the reactions, and CO₂ produced from the combustion of off-gas produced from the natural gas input. The life cycle inventory of the catalyst utilized for the catalytic upgrade was not accounted for in this study because previous studies have shown that the life cycle inventory of the catalyst has negligible effect on the overall life cycle emission of the pathway.^{17,34,35}

Combustion of char, torrefaction condensed liquid, and off-gas

Scenarios 2 and 3 either partially or entirely offset fossil energy inputs by internally combusting renewable energy sources to provide the process heat. These were achieved either through the combustion of char, or the combustion of torrefaction condensed liquid or in some cases combustion of both to fully offset natural gas. Combustion of off-gas from hydrogen production also took place to provide process heat. This study estimated energy from char based on its lower heating value (LHV) using an established correlation as shown in section B of Appendix D. The structure of the char based on its ultimate and proximate analysis shown in Table D14 of Appendix D. Energy from the combustion of torrefaction condensed liquid was estimated based on the LHVs of the representative compounds found in the oil and their mass fraction in the oil. LHVs of the representative compounds were obtained from the literature or estimated as shown in section B of Appendix D.^{36,37} A

sample calculation is also shown in section E of Appendix D. Energy from the combustion of off-gas was estimated using the LHVs of the combustible compounds in the off gas such as CO, H₂ and CH₄, and their mass fraction in the off gas. An efficiency of 80% was assumed for all combustion steps including when natural gas is utilized to supply process heat. Emissions from the combustion step for char and torrefaction condensed liquid were not included in our CO₂ accounting as they are biogenic. Only fossil carbon was included in the GHG emissions inventory. Description and sample calculation for the method used in evaluating the fossil carbon from the combustion of off-gas can be found in section G of Appendix D.

An inventory table for the conversion step for scenario 1 of a one-step hydrocarbon biofuel production pathway without heat integration is shown in Table 5.3. Inventory tables for other scenarios without heat integration are shown as Tables D26 to D35 in section G of Appendix D.

Table 5.3. Inputs including ecoprofile names, for scenario 1 of a one-step hydrocarbon biofuel production from pine wood chips without heat integration.

<i>Products</i>		
Hydrocarbon biofuel	1	MJ
Char (displaces coal)	0.009	kg
Fossil CO ₂ (from combustion of off-gas)	0.019	kg
Steam (displaces natural gas generated steam)	0.043	kg
<i>Material Inputs</i>		
Pine (8 % moisture content)	0.098	kg

Process water, ion exchange, production mix, at plant, from surface water RER S ^a (to generate steam for hydrogen production)	0.037	kg
Natural gas, from high pressure network (1-5 bar), at service station/US* US-EI U ^a (for hydrogen production)	0.007	kg
Water, completely softened, at plant ^a (cooling water, pyrolysis stage)	4.88	kg
Water, completely softened, at plant ^a (cooling water, hydrotreatment stage)	5.56	kg
Water, completely softened, at plant ^a (cooling water, hydrogen production stage)	4.73	kg
<i>Process Inputs or Displaced products (negative values)</i>		
Electricity, medium voltage US ^a (size reduction)	0.039	kWh
Electricity, medium voltage US ^a (hydrotreatment)	0.004	kWh
Electricity, medium voltage US ^a (hydrogen production)	0.011	kWh
Natural gas, burned in industrial furnace low-NO _x > 100kW ^a (biomass drying)	0.093	MJ
Natural gas, burned in industrial furnace low-NO _x > 100kW ^a (pyrolysis)	0.234	MJ
Natural gas, burned in industrial furnace low-NO _x > 100kW ^a (hydrotreatment)	0.056	MJ
Natural gas, burned in industrial furnace low-NO _x > 100kW ^a (hydrogen production)	0.400	MJ
Bituminous coal, combusted in industrial boiler NREL/US ^a	-0.008	kg

Steam, for chemical processes, at plant/US-US-EI U ^a	-0.043	kg
---	--------	----

a – These are names of ecoinvent profiles in SimaPro

Sensitivity Analysis

Using results from scenario 3 of the heat integrated two-step production pathway at torrefaction temperature of 290°C, significant LCA inputs were identified as parameters that can be varied for the sensitivity analysis. This study looked at the effects of +/- 15% changes in selected parameters on LCA results. A 15% variation is an appropriate uncertainty metric for a preliminary LCA that is based on laboratory experiments and process simulation rather than commercial process data.

5.4. Results

Hydrocarbon biofuel produced from the pathways in this study contained a significant amount of C6 (50%) and C7 (28%) range compounds which makes the modeled hydrocarbon biofuel suitable to be blended with gasoline. Also, the LHV of the modeled hydrocarbon biofuel ranged from 43.18 to 43.51 MJ/kg which is comparable to the LHV of gasoline of about 43.45 MJ/kg. As a result, the life cycle GHG emissions from the hydrocarbon biofuel was compared to that of gasoline. Typical composition of hydrocarbon biofuel modeled in this study is shown in Table D22 in section D of Appendix D.

Without Heat Integration

The GWP results for the hydrocarbon biofuel production pathways for the one-step and two-step scenarios are shown in Figure 5.3 for system expansion allocation without heat

integration. Net GHG emissions for the one-step scenarios are approximately equal to fossil gasoline, but decrease in comparison for two-step scenarios as torrefaction temperature increases. Among the two-step scenarios, scenario 3 exhibits the lowest emissions. In general, emissions from the hydrogen production step and size reduction steps were the major contributors to the net GWP for the one-step production pathway, while hydrogen production and char credits dominated the emissions for the two-step pathways. The GWP for the two-step pathway, at all torrefaction temperatures is lower than that of the one-step pathway mainly due to the significant reduction in emissions from size reduction and an increase in char credits.

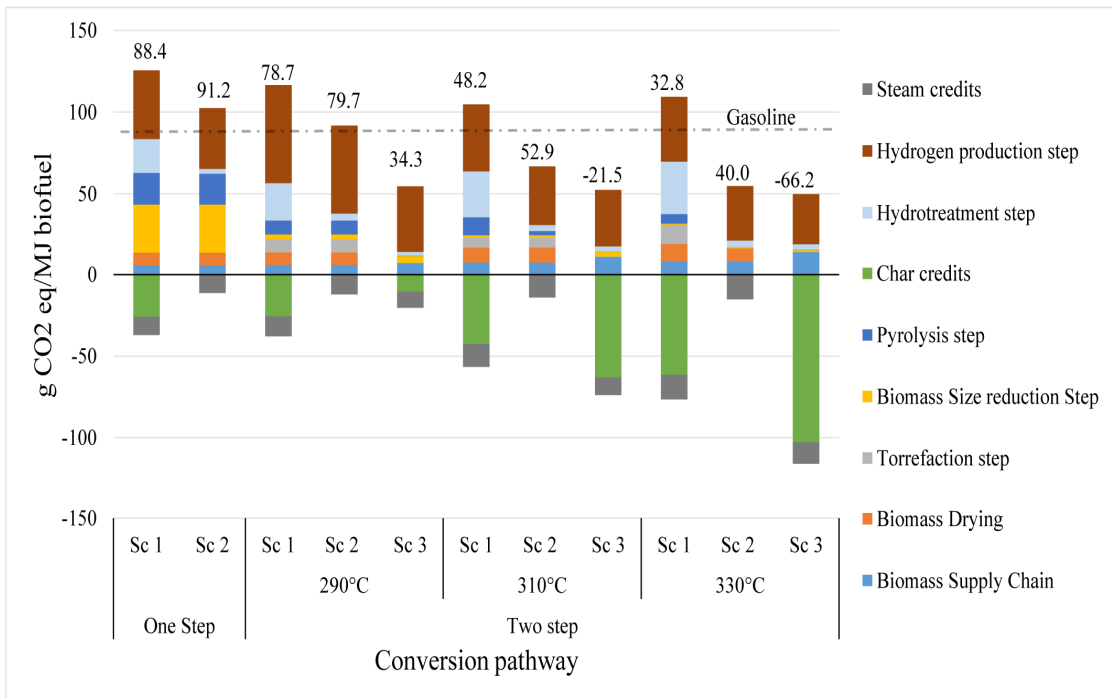


Figure 5.3. GWP of hydrocarbon fuel production pathway without heat integration (system expansion). Torrefaction temperature is shown for the two-step production pathways

A significant decrease in the net GWP was also observed as torrefaction temperature increased. This trend is due to the increase in the co-product char with increase in torrefaction temperature. Like other studies, the data used in our simulation shows that the fast pyrolysis of torrefied biomass favors production of biochar.^{5,38} A carbon conversion efficiency analysis of the biofuel conversion pathway shows an increase in the carbon conversion from biomass to biochar with increasing torrefaction temperature as shown in Table D23 in section D of Appendix D. About 63% reduction in GWP was observed for scenario 1 of a two-step production pathway with torrefaction taking place at 330 compared to scenario 1 of a one-step production pathway. Scenario 1 with char displacing coal to co-fire power plants achieved a more favorable result compared to scenario 2 where the char was internally combusted for process heat. This is because the credits from displacing the whole life cycle of a highly impactful energy source (coal) in scenario 1 outweigh the offset of comparative clean energy source (natural gas) for process heat in scenario 2. In addition, for each torrefaction temperature, the lowest emissions were observed for scenario 3 which has the objectives of using renewable energy for process heat and maximizing bio-oil quality, with export of maximum char. In our previous study where we considered bio-oil as the final product for these one and two-step pathways, similar trends of significant reduction in potential GHG emission but lower net GHG values were observed (about 36.3 gCO₂eq/MJ of bio-oil for the one-step pathway).¹² In comparison with gasoline, percent reduction ranged from about 8% for scenario 2 of the two-step at torrefaction temperature of 290°C to about 176% for scenario 3 at torrefaction temperature of 330°C.

With Heat Integration

With heat integration, a significant reduction in the net GWP can be achieved as shown in Figure 5.4. The hydrogen production stage and the credits from char are still the more dominant contributors to the overall net GWP for the heat integrated pathways. Though the process heat requirements were the same, by matching hot and cold streams through heat integration, fossil energy inputs for process heat were significantly reduced. Other operations such as size reduction were unchanged with heat integration.

For the heat integration case compared to without heat integration, reduction in potential GHG emission of about 56% for the one-step pathway to about 217% for the two-step pathway with torrefaction taking place at 330°C can be achieved in comparison to scenario 1 of the one-step pathway. In general, the highest reduction percentage was observed between scenario 1 of the one-step pathway without heat integration and scenario 3 of the two-step pathway with heat integration.

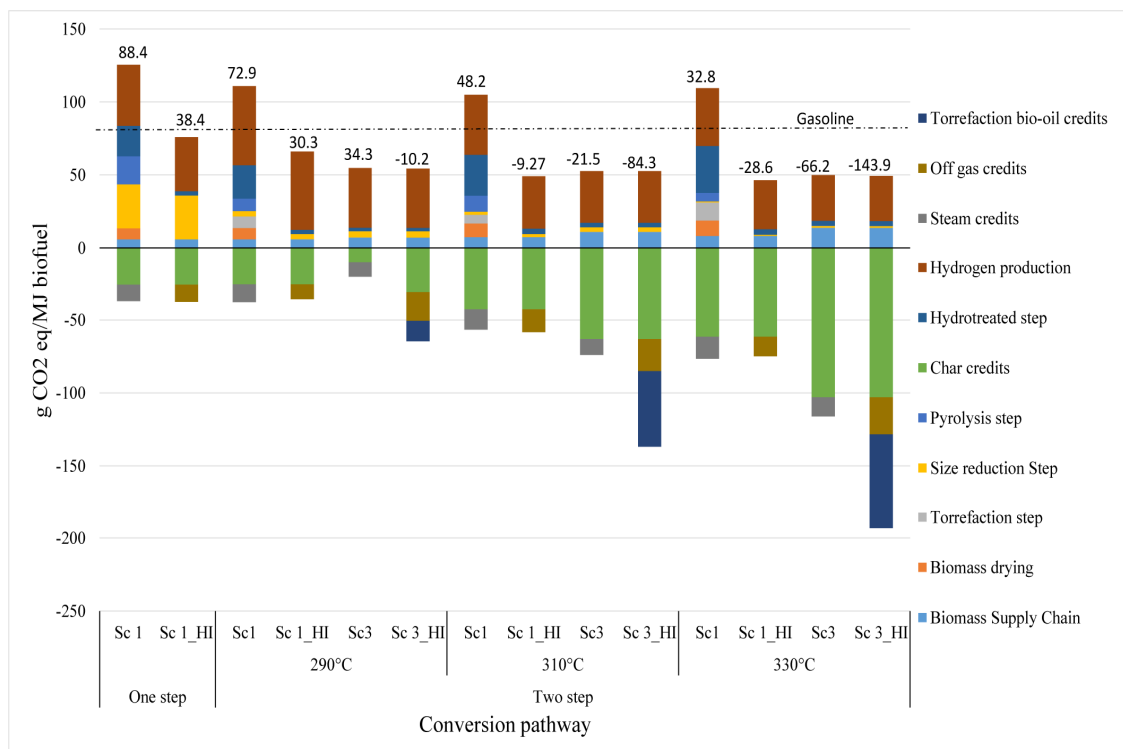


Figure 5.4. GWP comparison for base case and heat integrated hydrocarbon fuel production pathways (System expansion). Torrefaction temperatures are shown for the two-step pathways. HI denotes heat integrated process.

With increasing torrefaction temperature, there was an increase in credits from char and torrefaction condensed liquid displacing coal and heavy fuel oil respectively. In comparison with fossil gasoline, with heat integration percent reduction in GHG emissions ranged from about 56% for the heat integrated one-step production pathway to about 265% for the heat integrated two-step pathway at torrefaction temperature of 330°C.

Energy Allocation Cases

As shown in Figures 5.3 and 5.4, using system expansion, a large reduction in GHG emissions can be achieved as torrefaction temperature increased because of the significant amount of co-products. These co-products mitigate the release of large amount of GHGs

that could be released by the fuels replaced (coal, natural gas, and heavy residual fuel). With energy allocation, the input and output flows are partitioned between the main product, hydrocarbon biofuel, and the co-products (char, torrefaction condensed liquid, and off-gas). Calculated allocation factors are shown in Table 5.4 where subscripts 1, 2, and 3 refer to the torrefaction, fast pyrolysis and hydrotreatment stages respectively as described in the methods section.

Table 5.4. Estimated allocation factors for the heat-integrated biofuel production pathways.

	One Step	Two Step					
		290°C		310°C		330°C	
		Sc 1	Sc 3	Sc 1	Sc 3	Sc 1	Sc 3
AF ₁			0.53		0.37		0.28
AF ₂	0.67	0.68	0.57	0.57	0.44	0.53	0.35
AF ₃	0.85	0.87	0.77	0.81	0.75	0.83	0.72

Figure 5.5 shows the result of the GWP with the energy allocation approach for the heat integrated processes. As shown in the figure, modest reductions were achieved in comparison with the system allocation approach for the one-step pathway with heat integration. Similarly, to the system expansion approach, lower net GWP was achieved for the two-step production pathway compared with the one step. The hydrogen production and size reduction stages dominated the emissions for the one-step pathway while the main contributor for the two-step pathway is the hydrogen production stage. Relative to scenario 1 of the one-step biofuel production pathway, reduction in GHG emissions by 4%, 35%,

and 38% was achieved for scenario 1 of the two-step production pathways at torrefaction temperatures of 290, 310 and 330°C respectively.

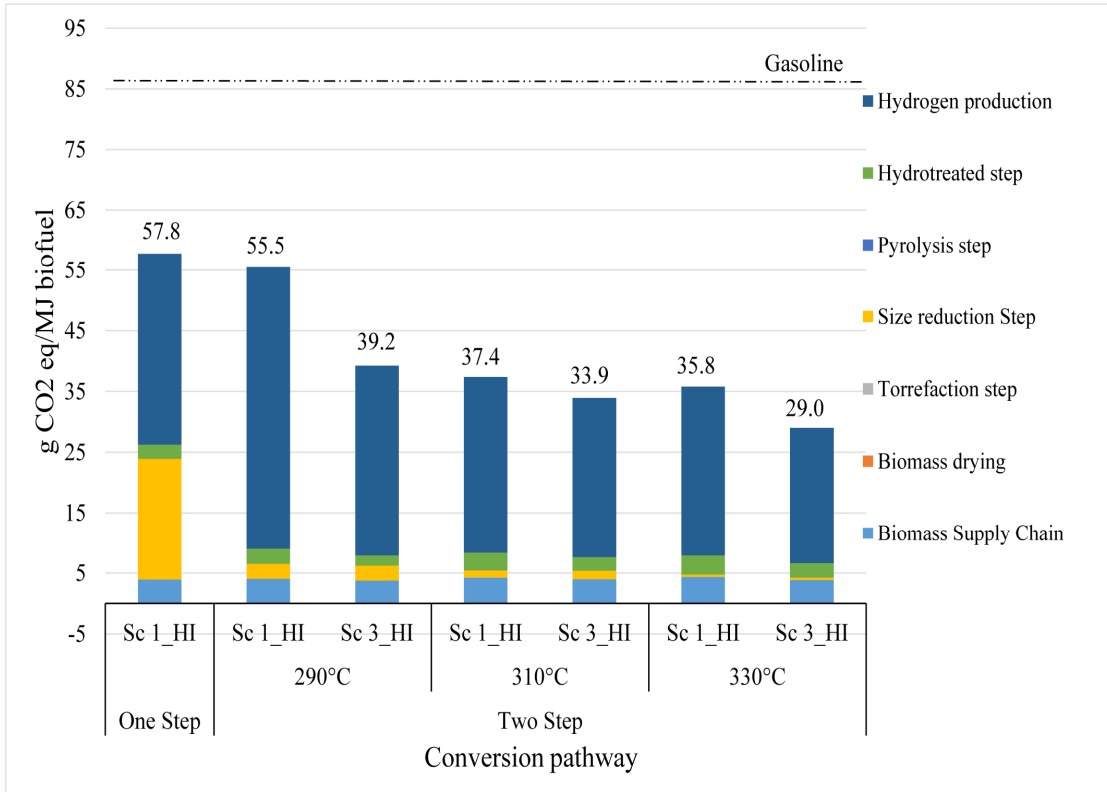


Figure 5.5. GWP for heat integrated hydrocarbon fuel production pathways (Energy allocation). Torrefaction temperatures are shown for the two-step pathways.

Sensitivity analyses are shown in Figures 5.6 and 5.7 respectively for scenario 1 of the heat integrated one-step biofuel production pathway and scenario 3 of the heat integrated two-step biofuel production pathway at 290°C torrefaction respectively. For the heat-integrated one-step pathway, the potential GWP was most sensitive to changes in the yield of hydrocarbon biofuel of all the variables investigated for a +/- 15% change (Figure 5.6). An increase in the yield resulted in lower GHG emissions in comparison with the base case. It should be noted that though changes in the yield of the hydrocarbon biofuel will have a

domino effect on other variables such as process heat requirements, the amount of char produced, etc. these potential changes were not considered for the hydrocarbon biofuel sensitivity in this study. The energy required for grinding of biomass supplied from the electricity grid mix was also observed to be very sensitive to a +/- 15% change. The LHV of char also showed significant sensitivity to a +/- 15 % change with higher values being favorable since it implies more coal being displaced. Since no torrefaction step was involved in the one-step pathway, changes in the estimated LHV of torrefaction condensed liquid has no effect on potential GWP from the one-step hydrocarbon biofuel production pathway.

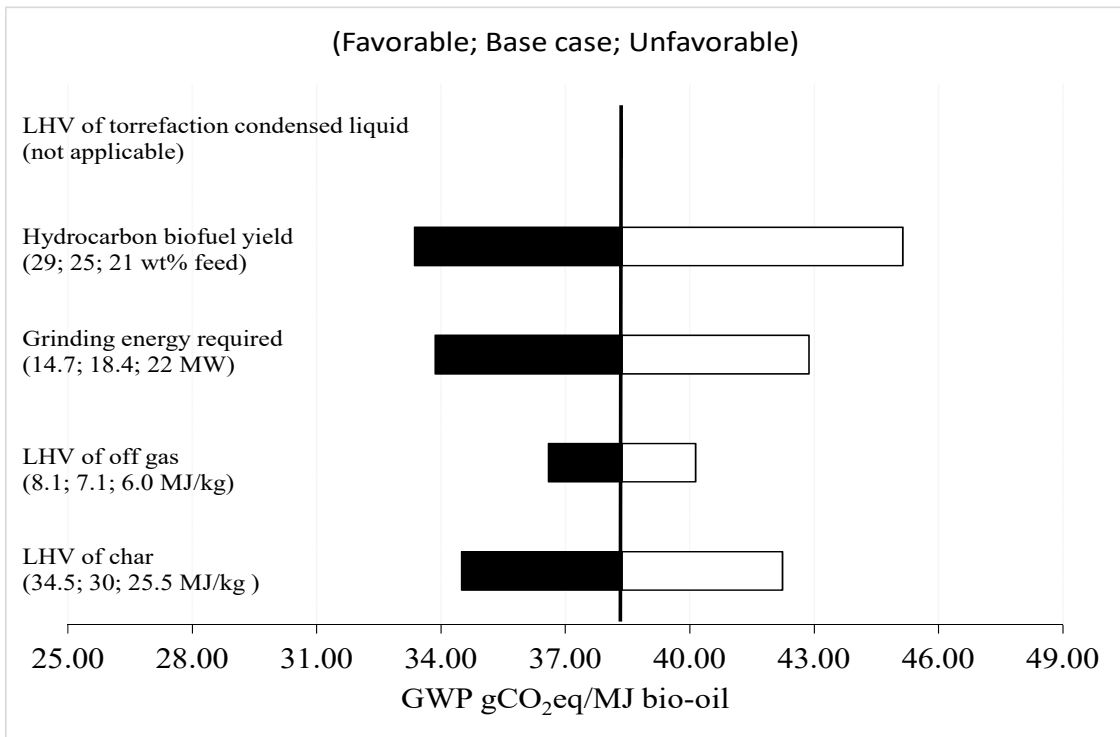


Figure 5.6. Sensitivity analysis for heat integrated one-step hydrocarbon biofuel production pathway. (System expansion)

For the sensitivity of the two-step shown in Figure 5.7, the GWP was most sensitive to changes in the LHV of the torrefaction condensed liquid of all the variables investigated. The sensitivity of the GWP to the changes in the LHV of char is comparable to the sensitivity observed for changes in the LHV of the torrefaction condensed liquid. The sensitivity of the GWP to the LHV of off-gas is more modest in comparison to that observed for the LHVs of the torrefaction condensed liquid and char. Though the flowrate of the off-gas co-product exceeds that of the char co-product, the significant sensitivity of the GWP to the LHV of char is because char displaces the more impactful coal energy source while the off gas displaced natural gas. Unlike the heat-integrated one-step where an increase in the hydrocarbon biofuel yield resulted in lower GHG emissions, for scenario 3 of the heat-integrated two-step pathway with 290°C torrefaction, increase in biofuel yield resulted in higher GHG emissions compared to the base case. As earlier pointed out, the change in biofuel yield was investigated without considering its effect on other variables. As a result, the increase in biofuel yield reduced the time required in producing 1MJ of the biofuel; this resulted in the reduction of potential credits from the export of biochar and torrefaction condensed liquid. The GWP was least sensitive to the estimated grinding energy for the two-step pathway. This may be because, with torrefaction, there is a significant reduction in the grinding energy required.

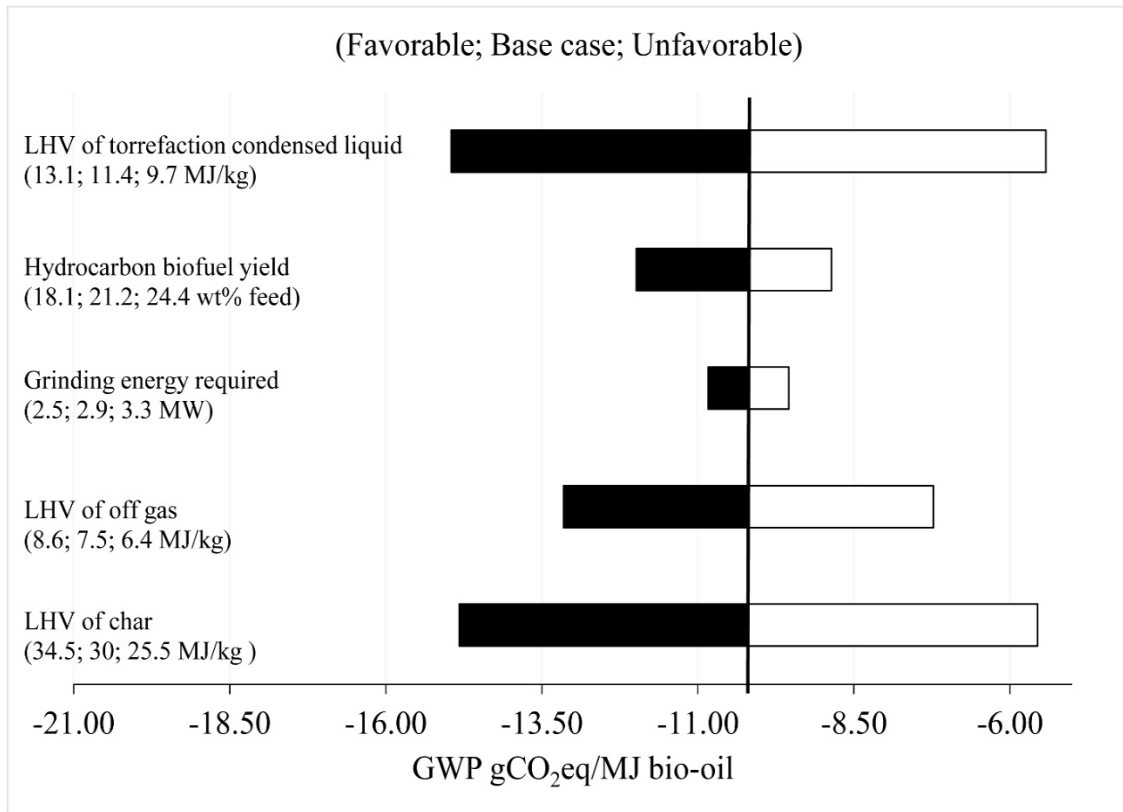


Figure 5.7. Sensitivity analysis for scenario 3 of heat integrated two-step pathway at torrefaction temperature of 290°C. (System expansion)

In conclusion, this study demonstrated the potential to reduce greenhouse gas emissions through a two-step hydrocarbon biofuel production pathway in comparison to a one-step pathway mainly due to the significant reduction in the energy required for size reduction prior to fast pyrolysis. Potential greenhouse gas emissions were reduced with increasing torrefaction temperature, however, more significant reductions can be achieved with the heat integrated processes. The trade of char to co-fire coal plants resulted in lower emissions relative to internally combusting char for process heat due to the avoidance of high impactful coal.

From our economic and environmental assessments, a two-step pathway at low torrefaction temperature of about 290°C which achieves almost the same minimum selling price and

significant GHG emission reduction relative to the one-step, will be the suggested pathway to produce hydrocarbon biofuel via fast pyrolysis of biomass.

5.5. Acknowledgements.

Financial support was provided by a National Science Foundation MPS/CHE - ENG/ECCS – 1230803 Sustainable Energy Pathways (SEP) grant and the Richard and Bonnie Robbins Endowment at Michigan Technological University.

Supporting Information

Detailed description of the emission inventory for biomass logistics, size reduction and combustion steps. Also contains the yield factors and representative compounds for modeling the reactors, proposed reaction pathways for the upgrade of bio-oil and carbon efficiency analysis.

5.6. References

- (1) Perlack, R. D.; Wright, L. L.; Turhollow, A. F.; Graham, R. L.; Stokes, B. J.; Erbach, D. C. *Biomass as feedstock for a bioenergy and bioproducts industry: the technical feasibility of a billion-ton annual supply*; Report No. 2005.
- (2) Graham, R.; Bergougnou, M.; Overend, R. Fast pyrolysis of biomass. *Journal of analytical and applied pyrolysis* **1984**, *6* (2), 95-135.
- (3) Regalbuto, J. R. Cellulosic biofuels—got gasoline? *Science* **2009**, *325* (5942), 822-824.
- (4) Neupane, S.; Adhikari, S.; Wang, Z.; Ragauskas, A.; Pu, Y. Effect of torrefaction on biomass structure and hydrocarbon production from fast pyrolysis. *Green Chemistry* **2015**, *17* (4), 2406-2417.
- (5) Boateng, A.; Mullen, C. Fast pyrolysis of biomass thermally pretreated by torrefaction. *Journal of Analytical and Applied Pyrolysis* **2013**, *100*, 95-102.
- (6) Winjobi O., S. D. R., and Zhou W. Production of Hydrocarbon Fuel using Two-Step Torrefaction and Fast Pyrolysis of Pine. Part 1: Techno-economic Analysis. *ACS Sustainable Chemistry & Engineering* **In Review**.
- (7) Van Dam, J.; Junginger, M.; Faaij, A.; Jürgens, I.; Best, G.; Fritsche, U. Overview of recent developments in sustainable biomass certification. *Biomass and Bioenergy* **2008**, *32* (8), 749-780.
- (8) Escobar, J. C.; Lora, E. S.; Venturini, O. J.; Yáñez, E. E.; Castillo, E. F.; Almazan, O. Biofuels: environment, technology and food security. *Renewable and sustainable energy reviews* **2009**, *13* (6), 1275-1287.

- (9) Standardization, I. O. f. *Environmental Management: Life Cycle Assessment: Principles and Framework*, ed.; ISO, 1997.
- (10) ISO, I. 14044: environmental management—life cycle assessment—requirements and guidelines. *International Organization for Standardization* **2006**.
- (11) Steele, P.; Puettmann, M. E.; Kanthi Penmetsa, V.; Cooper, J. E. Life-cycle assessment of pyrolysis bio-oil production. *Forest Products Journal* **2012**, *62* (4), 326.
- (12) Winjobi, O.; Shonnard, D. R.; Bar-Ziv, E.; Zhou, W. Life cycle greenhouse gas emissions of bio-oil from two-step torrefaction and fast pyrolysis of pine. *Biofuels, Bioproducts and Biorefining* **2016**, *10* (5), 576-588.
- (13) Iribarren, D.; Peters, J. F.; Dufour, J. Life cycle assessment of transportation fuels from biomass pyrolysis. *Fuel* **2012**, *97*, 812-821.
- (14) Hsu, D. D. Life cycle assessment of gasoline and diesel produced via fast pyrolysis and hydroprocessing. *Biomass and bioenergy* **2012**, *45*, 41-47.
- (15) Dang, Q.; Mba Wright, M.; Brown, R. C. Ultra-low carbon emissions from coal-fired power plants through bio-oil co-firing and biochar sequestration. *Environmental science & technology* **2015**, *49* (24), 14688-14695.
- (16) Westerhof, R. J.; Brilman, D. W. F.; Garcia-Perez, M.; Wang, Z.; Oudenhoven, S. R.; Kersten, S. R. Stepwise fast pyrolysis of pine wood. *Energy & fuels* **2012**, *26* (12), 7263-7273.
- (17) Jones, S.; Meyer, P.; Snowden-Swan, L.; Padmaperuma, A.; Tan, E.; Dutta, A.; Jacobson, J.; Cafferty, K. *Process design and economics for the conversion of*

lignocellulosic biomass to hydrocarbon fuels: fast pyrolysis and hydrotreating bio-oil pathway; Report No. 2013.

- (18) Zheng, A.; Zhao, Z.; Chang, S.; Huang, Z.; He, F.; Li, H. Effect of torrefaction temperature on product distribution from two-staged pyrolysis of biomass. *Energy & Fuels* **2012**, *26* (5), 2968-2974.
- (19) Park, J.; Meng, J.; Lim, K. H.; Rojas, O. J.; Park, S. Transformation of lignocellulosic biomass during torrefaction. *Journal of Analytical and Applied Pyrolysis* **2013**, *100*, 199-206.
- (20) Huang, Y.-F.; Syu, F.-S.; Chiueh, P.-T.; Lo, S.-L. Life cycle assessment of biochar cofiring with coal. *Bioresource technology* **2013**, *131*, 166-171.
- (21) Peters, J. F.; Iribarren, D.; Dufour, J. Biomass pyrolysis for biochar or energy applications? A life cycle assessment. *Environmental science & technology* **2015**, *49* (8), 5195-5202.
- (22) Wang, M. Q. *GREET 1.5-transportation fuel-cycle model-Vol. 1: methodology, development, use, and results*; Report No. 1999.
- (23) Weidema, B.; Wenzel, H.; Petersen, C.; Hansen, K. The product, functional unit and reference flows in LCA. *Environmental News* **2004**, *70*.
- (24) Owens, J. Life-cycle assessment: Constraints on moving from inventory to impact assessment. *Journal of industrial ecology* **1997**, *1* (1), 37-49.
- (25) Maleche, E. Life cycle assessment of biofuels produced by the new integrated hydrolysis-hydroconversion (IH 2) process. **2012**.
- (26) Handler, R. M.; Shonnard, D. R.; Lautala, P.; Abbas, D.; Srivastava, A. Environmental impacts of roundwood supply chain options in Michigan: Life-cycle

- assessment of harvest and transport stages. *Journal of Cleaner Production* **2014**, 76, 64-73.
- (27) Bridgwater, A.; Toft, A.; Brammer, J. A techno-economic comparison of power production by biomass fast pyrolysis with gasification and combustion. *Renewable and Sustainable Energy Reviews* **2002**, 6 (3), 181-246.
- (28) Wright, M. M.; Daugaard, D. E.; Satrio, J. A.; Brown, R. C. Techno-economic analysis of biomass fast pyrolysis to transportation fuels. *Fuel* **2010**, 89, S2-S10.
- (29) Koppejan, J.; Sokhansanj, S.; Melin, S.; Madrali, S. IEA bioenergy task, 2012; p 1-54.
- (30) Adams, P.; Shirley, J.; McManus, M. Comparative cradle-to-gate life cycle assessment of wood pellet production with torrefaction. *Applied Energy* **2015**, 138, 367-380.
- (31) Fagernäs, L.; Brammer, J.; Wilén, C.; Lauer, M.; Verhoeff, F. Drying of biomass for second generation synfuel production. *Biomass and Bioenergy* **2010**, 34 (9), 1267-1277.
- (32) Phanphanich, M.; Mani, S. Impact of torrefaction on the grindability and fuel characteristics of forest biomass. *Bioresource technology* **2011**, 102 (2), 1246-1253.
- (33) Wildschut, J.; Arentz, J.; Rasrendra, C.; Venderbosch, R.; Heeres, H. Catalytic hydrotreatment of fast pyrolysis oil: model studies on reaction pathways for the carbohydrate fraction. *Environmental progress & sustainable energy* **2009**, 28 (3), 450-460.

- (34) Snowden-Swan, L. J.; Spies, K. A.; Lee, G.; Zhu, Y. Life cycle greenhouse gas emissions analysis of catalysts for hydrotreating of fast pyrolysis bio-oil. *Biomass and Bioenergy* **2016**, *86*, 136-145.
- (35) Benavides, P. T.; Cronauer, D. C.; Adom, F.; Wang, Z.; Dunn, J. B. The influence of catalysts on biofuel life cycle analysis (LCA). *Sustainable Materials and Technologies* **2017**, *11*, 53-59.
- (36) Perry, R. H.; Green, D. W.; Maloney, J. O.; Abbott, M. M.; Ambler, C. M.; Amero, R. C. *Perry's chemical engineers' handbook*, ed.; McGraw-hill New York, 1997.
- (37) Domalski, E. S. Selected Values of Heats of Combustion and Heats of Formation of Organic Compounds Containing the Elements C, H, N, O, P, and S. *Journal of Physical and Chemical Reference Data* **1972**, *1* (2), 221-277.
- (38) Cen, K.; Chen, D.; Wang, J.; Cai, Y.; Wang, L. Effects of water washing and torrefaction pretreatments on corn stalk pyrolysis: A combined study using TG-FTIR and a fixed bed reactor. *Energy & Fuels* **2016**.

Chapter 6. TEA and LCA of hydrocarbon biofuel production via fast pyrolysis of poplar feedstock and catalytic upgrade

6.1. Introduction

Biomass-derived transportation biofuels have been promoted as a way to diversify energy supply, utilize indigenous and renewable resources, reduce reliance on imported oil, and mitigate the impact of energy on climate and the environment.[1] Plausible routes for the conversion biomass to biofuels includes biochemical, thermochemical and photobiological means. While there are no significant advantages of one conversion approach over the other, an added benefit of the thermochemical conversion approach is the ability to produce longer chain hydrocarbons suitable for aviation, marine or heavy road freight applications.[2] Among various thermochemical conversion methods, fast pyrolysis has been investigated widely and has been demonstrated as a feasible method to convert different biomass feedstocks to liquid biofuel.[3-6] Fast pyrolysis decomposes biomass feedstocks at atmospheric pressure, temperatures of about 450 to 600°C and a short residence time in an inert environment to produce vapors, permanent gases, and char. Condensation of the vapors produces the desired liquid, bio-oil. Bio-oil is a versatile feedstock that can be used as a substitute for heating oil, upgraded to hydrocarbon biofuel or utilized in the production of specialty chemicals.[7, 8]

Bio-oil directly obtained from fast pyrolysis cannot be used as a ‘drop-in’ transportation hydrocarbon fuel because it is corrosive, highly oxygenated and has a high-water content. Through catalytic upgrading, the bio-oil can be converted to a transportation hydrocarbon

biofuel. Due to the similarity between the removal of oxygen from bio-oil in the upgrade step and removal of sulfur in the refining of petroleum, it is believed that existing refining, and logistics infrastructure can be utilized in the upgrade of bio-oil. This adds to the attractiveness of hydrocarbon biofuel production through fast pyrolysis of biomass.

The high-energy intensity of the fast pyrolysis production pathway however adversely impacts the economics of the pathway. The high-energy intensity relates to the energy required in reducing the size of the biomass feedstock before the fast pyrolysis step and the energy required in removing the moisture contained in the biomass. To reduce the energy intensity of the biofuel production process, a torrefaction step before fast pyrolysis is being investigated. Torrefaction, another thermochemical conversion process like fast pyrolysis, takes place at atmospheric pressure, temperatures of about 250 to 330°C, and residence times of 20 to 40 minutes in an inert environment to produce bio-coal (torrefied biomass), vapors, and permanent gases. The solid bio-coal can then be further pyrolyzed to produce bio-oil, char, and permanent gases. Torrefaction potentially improves the grindability of the bio-coal thereby reducing the energy required for the size reduction step.[9-11] Aside from the improved grindability, torrefaction can also potentially improve the bio-oil quality.[12, 13] The partial degradation of biomass that takes place during torrefaction primarily degrades the hemicellulose portion of the biomass resulting in a lower yield of acidic components in the bio-oil produced from the fast pyrolysis of bio-coal.

With the potential benefits of improved grindability and bio-oil quality, the proposed torrefaction-fast pyrolysis (two-step) configuration needs to demonstrate competitive economics with the single fast pyrolysis (one-step) route and ultimately with conventional

hydrocarbon transportation fuel on a commercial scale. Techno-economic assessment (TEA) can be used in assessing the cost-competitiveness of competing and parallel production pathways. Researchers have utilized TEA to determine the minimum selling price (MSP) of biofuels to evaluate their economic viability. In the TEA studies, Wright et al. evaluated MSP of \$3.09 and \$2.11/gal (2012 dollars) for hydrocarbon biofuel produced from corn stover for hydrogen production and purchase scenarios respectively for a 2000 metric ton/day facility.[14] Jones et al. estimated MSP of \$2.04/gal (2007 dollars) for a 2000 metric ton/day plant processing hybrid poplar for hydrocarbon biofuel production.[8] In a more recent literature, Jones et al. estimated MSP of \$3.39 gallon gasoline equivalent (gge) for hydrocarbon biofuel for a 2000 metric ton/day facility.[15]

In addition to evaluating the cost competitiveness of biofuel pathways, it is also important to investigate the environmental impacts of biofuels. One of the most useful procedures for evaluating environmental impact is life cycle assessment (LCA).[16, 17] LCA is widely used to determine the environmental impacts of a product or system as it comprehensively assesses the impacts of a process or product for a whole set of impact categories.[18] Some studies, have used LCA to evaluate the environmental impact of hydrocarbon biofuel production from biomass. Peters et al. reported GHG savings of about 54% for a fuel mix produced from poplar compared to conventional gasoline and diesel.[19] Dang et al. reported a reduction in net GWP of about 69.1% for hydrocarbon biofuel derived from corn stover in contrast to conventional gasoline and diesel

The aim of this study is to carry out a comparative TEA and LCA study for a one-step and two-step biofuel production pathway using poplar biomass feedstock. In our previous

works, we investigated the one-step and two-step biofuel production pathway from loblolly pine biomass feedstock.[20, 21] MSP of \$4.82/gal was estimated for the one-step pathway and two-step pathway at low torrefaction temperature of about 290°C without heat integration and MSP of about \$4.01/gal in both cases with heat integration.[20] About 63% reduction in GWP was observed for the one-step scenario with a two-step pathway at torrefaction temperature at 330°C achieving a 176% reduction with heat integration. Higher reductions were observed with heat-integrated pathways.[21]

In contrast to our previous work which examined loblolly pine, a softwood; this study aims to investigate the one-step and two-step pathways using poplar, a hardwood as the biomass feedstock. Hardwoods typically have a higher proportion of cellulose, hemicellulose, and extractives than softwoods, but softwoods, as a result, have a high proportion of lignin. Table 6.1 compares the typical percentage of these components in these different biomass feedstocks.

Table 6.1. Typical content breakdown for softwood and hardwood

	Softwood	Hardwood
Cellulose	40 – 44%	43- 47%
Lignin	25 -31%	16 – 24%
Hemicellulose	25 -29%	25 – 35%
Extractives	1-5%	2-8%

6.2 Materials and methods

Process Description

The material and method employed in this chapter are same as used in the previous chapters in the production of hydrocarbon biofuel TEA (Chapter 4) and LCA (Chapter 5). The biorefinery is assumed to process about 1000 metric ton per day of feedstock through the pyrolysis unit. Poplar is processed through the pyrolysis unit for the one-step pathway while torrefied poplar is processed through the pyrolysis unit for the two-step pathway.

Size reduction of dried wood chips

The size reduction of poplar chips from the delivered size of about 25 mm to a size of about 2mm was modeled in Aspen Plus as described in Chapter 4. This study assumes the correlation used in Chapter 4 for loblolly pine chips will be applicable for the size reduction of poplar.

Torrefaction

Torrefaction of the poplar chips for the two-step pathway is assumed to take place at a temperature of 280°C. The description of the modeling of the torrefaction step is as described in Chapter 4. The yield factors used in modeling the torrefaction step are shown in Table 6.2. These yield factors were obtained using the mass yield of gases, bio-oil and char from the breakdown of poplar were obtained from the works of Fivga.[26] The speciation of the bio-oil into different compounds was carried out using the characterization work of Klementsruud et al. [27]

Table 6.2. Yield factors for the torrefaction of poplar at 280°C

% wt./wt. of biomass (dry basis)	
Water	10.13
Organics	8.35
Gases	5.35
Char	76.17
Total	100.00

Change in the structure of the poplar chips due to the torrefaction was accounted for through changes to the ultimate and proximate analysis of the torrefied poplar as shown in Table 6. 6. The breakdown of the representative compounds in the torrefaction organics and the composition of the permanent gases are given in Table 6.3.

Table 6.3. Composition of representative components obtained from torrefaction of poplar

Component	% wt./wt of biomass (dry basis)
CO	1.55
CO ₂	3.77
CH ₄	0.02
Water	10.13
Methanol	0.58
Acetic acid	4.08
Hydroxyacetaldehyde	0.78
Furanmethanol	0.78
Levoglucosan	0.00
Phenol	2.14
Char	76.17
Total	100.00

Fast Pyrolysis

For both the one-step and two-step pathway, fast pyrolysis was modeled to take place at 516°C according to literature data. The description of the modeling step is as described in Chapter 4. The yield factors used in modeling the pyrolysis step are shown in Table 6.4.

Raw and torrefied poplar processed through the pyrolyzer were modeled in Aspen Plus using their ultimate and proximate analysis as shown in Table 6.6.

Table 6.4. Pyrolysis yield factors for the one-step and two-step biofuel production pathways.

% wt./wt. of biomass (dry basis)		
	One-step	Two-step
Reaction water	9.36	12.30
Organics	68.59	52.49
Gases	9.72	11.24
Char	12.34	23.97

The composition of the organics and gases produced from the fast pyrolysis of the raw poplar (one-step) and the torrefied poplar (two-step) are shown in Table 6.5. The char produced from the pyrolysis step was also modeled using its ultimate and proximate analysis shown in Table 6.7.

Table 6.5. The composition of organics and gases produced from the one-step and two-step pathways.

% wt./wt. of biomass (wet basis)		
	One-step	Two-step
Hydrogen	0.09	0.11
CO	3.78	4.56
CO ₂	4.05	4.89
CH ₄	0.72	0.87
C ₂ H ₆	0.36	0.43
Water	16.07	15.22
Acetic acid	7.57	3.90
Acetaldehyde	1.30	0.64
Furfural	7.56	3.70
2-Furanmethanol	5.65	4.94
2-Methyl-2-cyclopenten-1-one	1.95	1.83
Hydroxyacetaldehyde	10.36	7.44
Vanillin	2.91	2.68
Levoglucosan	15.94	14.41

Phenol	3.09	2.83
Guaiacol	3.06	2.83
Syringol	4.12	5.55
Char	11.42	23.16
Total	100	100

This study assumed same properties i.e. ultimate and proximate analysis for the char produced from both the one-step and two-step pathways.

Table 6.6. Ultimate and proximate analysis of raw and torrefied poplar.

Ultimate Analysis			Proximate Analysis		
Wt. %			Wt. %		
	Raw poplar	Torrefied poplar		Raw poplar	Torrefied poplar
Carbon	46.8	54.96	Ash	1.16	2
Hydrogen	5.99	6.28	Volatile matter	98.84	98
Nitrogen	-	0.10	Fixed carbon	-	-
Sulfur	-	-	Moisture	25	3.45
Oxygen	46.05	36.66			
Ash	1.16	2.00			
Total	100	100	Total (dry basis)	100	100

Table 6.7. Ultimate and proximate analysis of char.

	Wt. %
Ash	4.6
Carbon	85.48
Hydrogen	0.76
Nitrogen	0.29
Chlorine	0
Sulfur	0
Oxygen	8.87
Total	100

Catalytic upgrading of bio-oil

The upgrade of bio-oil to hydrocarbon biofuel is assumed to occur over two upgrade stages, an initial stabilization step followed by the final hydrotreatment step. The catalytic upgrade step was modeled as described in Chapter 4

Definition of case studies

The TEA and LCA assessments of the hydrocarbon biofuel production were investigated under three scenarios as shown in Table 6.8. A detailed description of the scenarios and objectives can be found in Chapter 4.

Table 6.8. Assessment scenarios and objectives

Scenarios	Objective 1	Objective 2
Scenario 1	Fossil energy inputs	Maximizing bio-oil yield
Scenario 2	Minimize fossil energy inputs	Maximizing bio-oil yield
Scenario 3	Renewable energy inputs	Maximizing bio-oil quality

Techno-economic assessment of hydrocarbon fuel pathways

The TEA was carried out using mass and energy balances obtained from the simulation. The cost of most of the equipment was estimated from vendor quotes or literature data. Total project investment (TPI) was estimated from the total purchased equipment cost (TPEC) as described in Chapter 4.

LCA framework, system definition, and modeling assumptions

A functional unit of 1MJ of biofuel was used in carrying out the LCA. Framework, system boundary, and assumptions utilized in the LCA are described in detail in Chapter 5 of this dissertation.

Heat Integration

The effect of heat integration on the TEA and LCA was also investigated. The heat integration was carried out using the software, Super Target. A detailed description of the heat integration methodology can be found in Chapter 4.

6.3 Results

Table 6.9 shows the dry biomass input and major outputs for the different one-step and two-step scenarios of the biorefineries modeled. Based on the basis of 1000 dry metric tons of feed into the pyrolysis unit, the required biomass for the two-step pathway is higher to compensate for the mass loss due to the torrefaction step. Lower hydrocarbon biofuel yield was observed for the two-step production pathway compared to the one-step pathway.

Table 6.9. Feedstock Input and major outputs from the biofuel production pathway for one-step and two-step hydrocarbon biofuel production from poplar without heat integration.

	One-step		Two-step		
	Sc 1	Sc 2	Sc 1	Sc 2	Sc 3
Torrefaction temperature			280°C		
	Sc 1	Sc 2	Sc 1	Sc 2	Sc 3
Input of Biomass					
Biomass feedstock, 10 ⁶ kg/yr (dry basis)	352.8	352.8	459.3	459.3	459.3
Output of Biofuels					
Hydrocarbon biofuel, 10 ⁶ kg/yr (10 ⁶ gal/yr)	106.4 (37.7)	106.4 (37.7)	97.1 (34.5)	97.1 (34.5)	86.6 (30.7)
Hydrocarbon biofuel yield (% wt/wt feed dry basis) [†]	30.2	30.2	21.1	21.1	18.9
Bio-char , 10 ⁶ kg/yr	43.5	-	81.0	-	18.7
Bio-char yield (% wt./wt. feed dry basis) [†]	12.3	-	17.6	-	4.1
Torrefaction condensed liquid , 10 ⁶ kg/yr	-	-	-	-	--
Process Heat Inputs					
Combustion energy, 10 ⁶ GJ/yr	4.03	4.03	4.15	4.15	3.30
Combusted material					

Natural Gas, 10 ⁶ m ³ /yr	3096	1839	3200	854	-
Off-gas, 10 ⁶ kg/yr	193.4	193.4	173.8	173.8	137.7
Char, 10 ⁶ kg/yr	-	34.5	-	81.0	62.4
Torr. condensed liquid, 10 ⁶ kg/yr	-	-	-	-	-

† Based on dry biomass to the biorefinery

The lower yield of biofuel for the two-step pathway is believed to be due to the increase in the yield of char, gases, and water for the two-step pathway which led to reduced yield of organics that was upgraded. The high yield of char is in line with what is observed in the literature.[22, 23] High char yield from the pyrolysis of torrefied biomass is believed to be due to carbon-carbon crosslinks formed during the dehydration of carbohydrate polymers during torrefaction.[22] Scenario 3 of the two-step production pathway has the lowest overall yield of hydrocarbon biofuel because the torrefied condensed liquid was not blended with the pyrolysis bio-oil. As a result, this scenario has the least amount of bio-oil available to be upgraded to the hydrocarbon biofuel. The significant reduction in oil yield for the two-step pathway compared to the one-step pathway is, however, different from what is observed in the literature. Westerhof et al. found that the blended oil obtained from scenario 1 of the two-step pathway was equal to the oil yield of raw pine when the torrefaction temperature is below 290°C.[22, 24]

Similar yields were obtained in all cases for scenarios 1 and 2 of the one-step and two-step pathways except for the yield of biochar and the amount of natural gas combusted. With the design objective of minimizing the natural gas utilized for scenario 2, the combustion of the biochar results in the reduction of natural gas required to be combusted to provide process heat. In addition to the torrefaction condensed liquid combusted in scenario 3, bio-

char was partly combusted to entirely offset natural gas requirements for process heat as seen in Table 6.9.

With heat integration, it can be observed that the combustion energy, which is the energy needed by the pathway at steady state is significantly reduced as seen in Table 6.10. With or without heat integration, the yields of biofuel, char (when not used internally) remains unchanged. The yield of biogenic off-gas for the heat integrated scenarios shown in Table 6.10 when added to the off-gas combusted shown in Table 6.10 does not add up to the total off-gas combusted shown in Table 6.9 because the exported natural gas-derived off-gas was not included in the off-gas accounting in Table 6.10.

Table 6.10. Feedstock Input and major outputs from the biofuel production pathway for one-step and two-step hydrocarbon biofuel production from poplar with heat integration.

	One-step	Two-step	
Torrefaction temperature		280°C	
	Sc 1	Sc 1	Sc 3
Input of Biomass			
Biomass feedstock, 10 ⁶ kg/yr (dry basis)	352.8	459.3	459.3
Output of Biofuels			
Hydrocarbon biofuel, 10 ⁶ kg/yr (10 ⁶ gal/yr)	106.4 (37.7)	97.1 (34.5)	86.6 (30.7)
Hydrocarbon biofuel yield (% wt/wt feed dry basis) [†]	30.2	21.1	18.9
Bio-char , 10 ⁶ kg/yr	43.5	81.0	81.0
Bio-char yield (% wt./wt. feed dry basis) [†]	12.3	17.6	17.6
Torrefaction condensed liquid , 10 ⁶ kg/yr	-	-	--
Off-gas (biogenic), 10 ⁶ kg/yr	12.8	24.1	46.1
Off-gas (biogenic) yield (% wt./wt. feed, dry basis) [†]	4	5	10
Process Heat Inputs			
Combustion energy, 10 ⁶ GJ/yr	1.28	1.13	0.98

Combusted material			
Natural Gas, 10 ⁶ m ³ /yr	-	-	-
Off-gas, 10 ⁶ kg/yr	170.2	129.3	35.6
Char, 10 ⁶ kg/yr	-	-	-
Torr. condensed liquid, 10 ⁶ kg/yr	-	-	-

Hydrogen consumption

Table 6.11 shows the hydrogen consumed wt./wt. % of the bio-oil upgraded. The amount of hydrogen consumed in the upgrade of bio-oil to hydrocarbon fuel for a one-step hydrocarbon biofuel production pathway was estimated to be about 7.15 % wt./wt. of bio-oil. This value is higher than the 5.8 % wt./wt. of bio-oil estimated by Jones et al. and 6.38 % wt./wt. of bio-oil estimated by Winjobi et al. in their different one-step production pathway analyses.[15, 20] The result shows a higher hydrogen consumption for the one-step production pathway than two-step production pathway. The reason for this trend is believed to be because the water content of the blended bio-oil obtained from a two-step production pathway is higher than that of the bio-oil derived from a one-step pathway. This trend was also observed in the study done by Winjobi et al.[20] The higher water content is mainly due to the high-water content of the torrefaction condensed liquid that was blended with the pyrolysis bio-oil. Higher hydrogen consumption was also observed for scenario 3 compared to scenario 1 of the two-step production pathway. This trend is also mainly due to the water content of the upgraded oil, because the torrefaction condensed liquid was not blended with the pyrolysis bio-oil in scenario 3; the upgraded bio-oil in this scenario also has a relatively low water content.

Table 6.11. Hydrogen consumed for the upgrade of bio-oil to hydrocarbon biofuel.

Hydrogen consumption (% wt./wt. of upgraded bio-oil)		
Scenario	One-step	Two-step
1	7.15	5.30
2	7.15	5.30
3		6.86

Minimum Selling Price

The estimated minimum selling price (MSP) of the hydrocarbon biofuel is shown in Figure 6.1. In general, lower MSP was evaluated for the one-step biofuel pathway compared to the two-step pathway for all scenarios. The lowest MSP of about \$4.20/gal of hydrocarbon biofuel was obtained for scenario 2 of the one-step production pathway, which had the objective of minimizing fossil energy inputs for process heat, by combusting the produced bio-char internally.

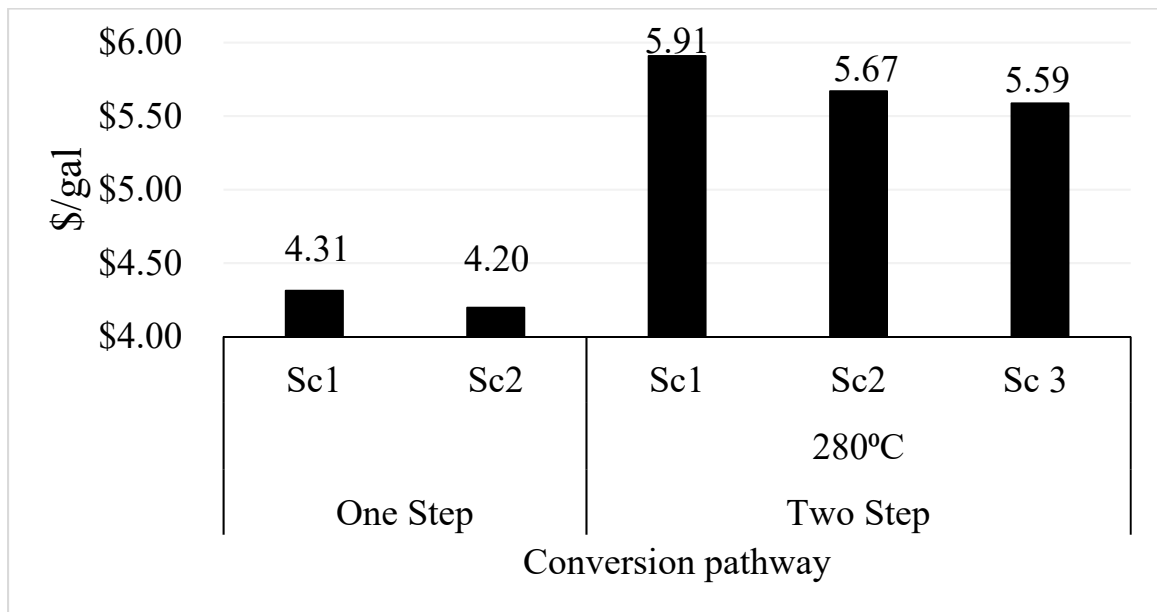


Figure 6.1. Minimum selling price of liquid hydrocarbon biofuel for one-step and two-step pathways without heat integration.

Higher MSP was estimated for the two-step pathway mainly due to the relatively low yield of hydrocarbon biofuel as earlier shown in Table 6.9. For the two-step pathway, the least MSP was observed for scenario 3. This scenario has the least throughput of bio-oil upgraded of all the three scenarios of the two-step pathway. This resulted in the lowest heating requirements as shown in Table 6.9, which was fully satisfied with some biochar exported for revenue. In comparison to our previous study that investigated loblolly pine at biomass feedstock, the one-step of the biofuel production pathway estimated more favorable economics for a one-step biofuel production from poplar. However, for the two-step pathways, loblolly pine feedstock demonstrated more favorable economics than the two-step pathway with poplar feedstock. This result is in contrast to literature result that shows favorable economics for two-step pathway where bio-oil is the final product.[25] Another recent literature observed comparable MSP for the one-step pathway and the two-step pathway at low torrefaction temperature of 290°C.[20] The main reason for this contrast is due to the relatively low yield of oil for the two-step pathways with poplar feedstocks compared to the yield obtained for the two-step pathway for loblolly pine feedstock.

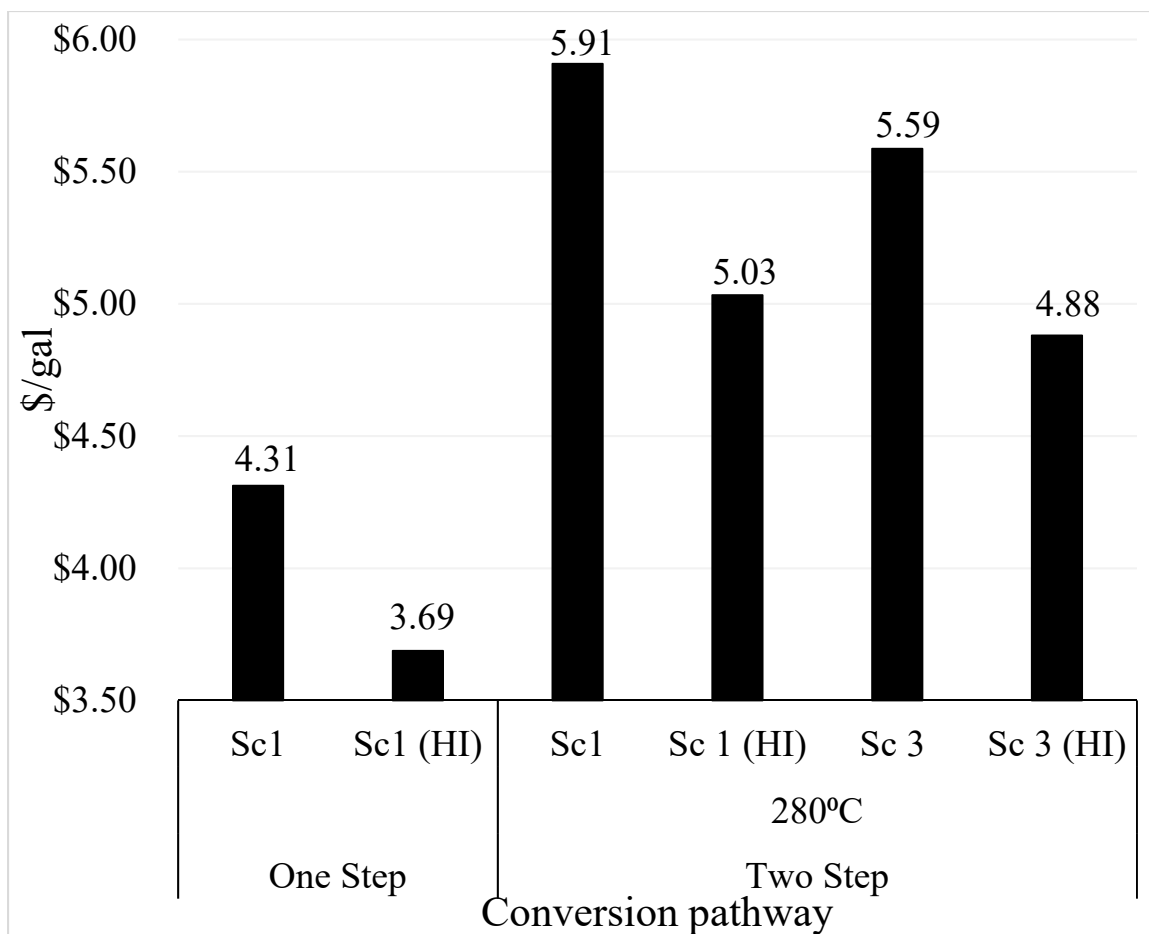


Figure 6.2. Minimum selling price comparison between heat-integrated and scenarios without heat integration.

With heat integration, further reduction in MSP were estimated as shown in Figure 6.2. The savings were mainly from the total offset of external natural gas requirements for process heat and minimized refrigerant requirement. Overall heat integration amounted for about \$0.62 reduction in the MSP compared to the scenarios without heat integration. Similar trends were observed in literature for the heat-integrated biofuel production pathways.

Life Cycle Carbon footprint

The GWP results for the biofuel production pathways without heat integration for the one-step and two-step routes are shown in Figure 6.3. The net GHG emissions for the one-step production pathways are slightly higher than GHG emissions from the utilization of fossil gasoline for transportation. However, lower GHG emissions were observed for the two-step pathways. In general, the emissions related to the hydrogen production step and credits from char where applicable dominates the emissions over the life cycle of the hydrocarbon biofuel.

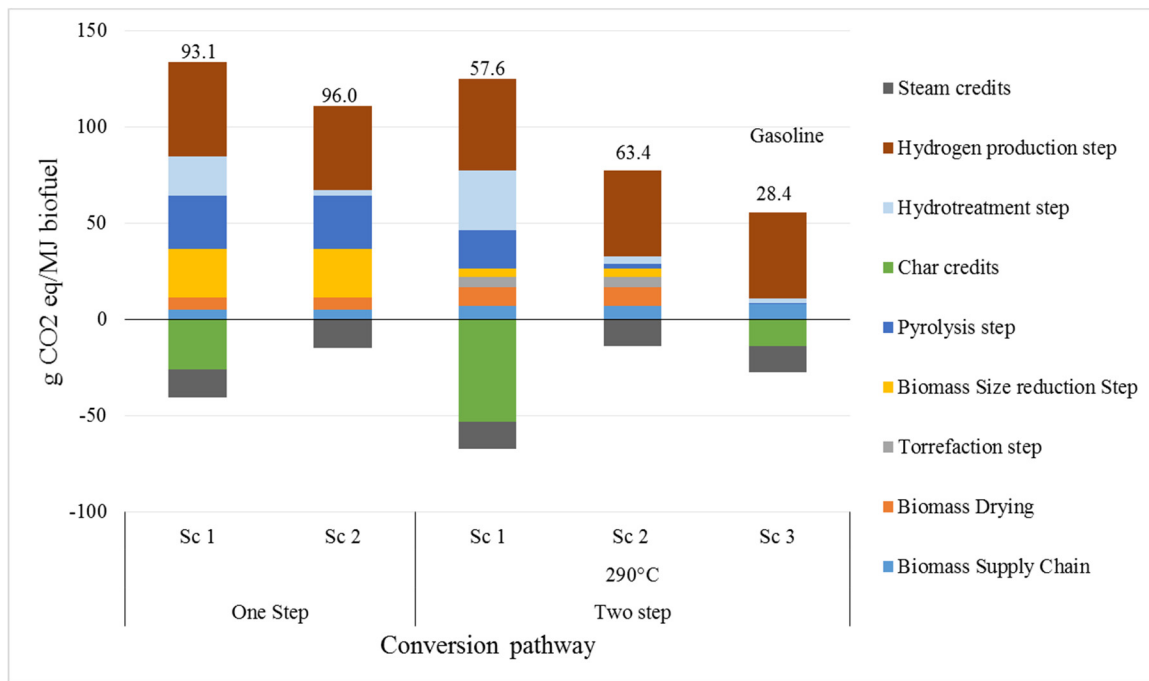


Figure 6.3. GWP of the one-step and two-step pathways without heat integration.

The GWP for scenario one of the two-step pathway is lower than that of scenario one of the one-step mainly due to the significant reduction in the emissions associated with size reduction and the increase in credits from char displacing coal to co-fire power plants.

Relative to fossil gasoline, about 67% reduction in GHG can be achieved for scenario 3 of

the two-step pathway. In line with trends found in the literature, the export of char to displace coal as investigated in scenarios 1 estimates lower GHG emissions than scenarios 2 when the char was combusted internally for process heat.

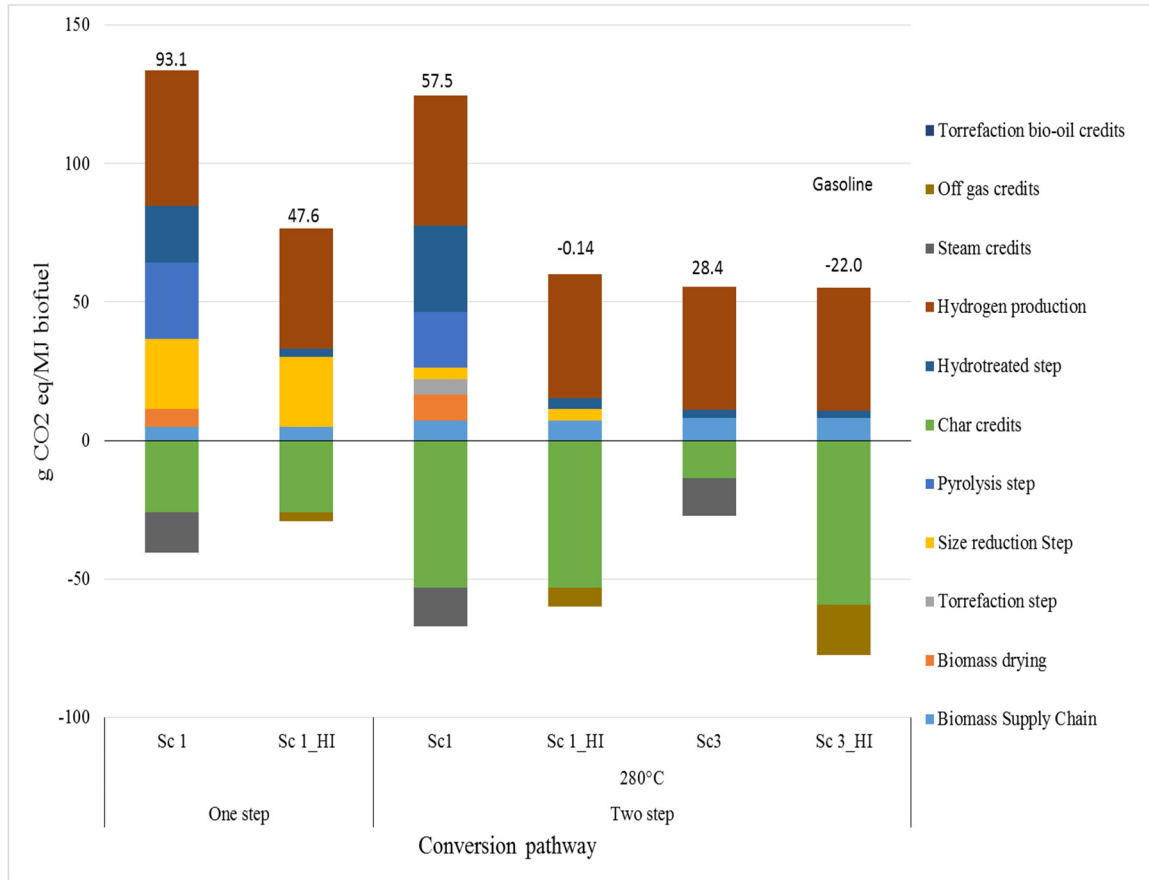


Figure 6.4. Comparison of GWP for hydrocarbon biofuel production pathway for the one-step and two-step pathways with and without heat integration.

With heat integration as shown in Figure 6.4, higher reduction in the GHG emissions were estimated. Scenario 3 of the heat integrated two-step pathway shows very low GWP and can potentially act as a carbon sink. With heat integration, reduction in GHG emissions of about 45%, 100% and 125% were estimated for the one-step, scenario 1 of the two-step and scenario 3 of the two-step respectively.

6.4 Conclusions

From the results of this study, MSP of hydrocarbon biofuel estimated for a one-step production pathway is significantly lower than the MSP for a two-step pathway at 280°C torrefaction. However, in terms of the environmental impacts, the two-step pathway has lower impact on the environment. The main conclusion of this study is the importance of heat integration for more favorable economics of the hydrocarbon biofuel pathway. Based on the assumptions, designs and parameters used in this study, torrefaction does not appear to be an advantage on the cost of production for hydrocarbon fuels compared to a one-step process at high torrefaction temperatures however it demonstrates significant advantage on the environmental impact of the biofuel production pathway. With heat integration, reduction in the cost of utilities outweighed the increase in capital cost, resulting in lower minimum selling price for the heat-integrated processes in comparison with the base case without heat integration.

6.5 References

1. Anex, R.P., et al., *Techno-economic comparison of biomass-to-transportation fuels via pyrolysis, gasification, and biochemical pathways*. Fuel, 2010. **89**: p. S29-S35.
2. Sims, R.E., et al., *An overview of second generation biofuel technologies*. Bioresource technology, 2010. **101**(6): p. 1570-1580.
3. Dang, Q., C. Yu, and Z. Luo, *Environmental life cycle assessment of bio-fuel production via fast pyrolysis of corn stover and hydroprocessing*. Fuel, 2014. **131**: p. 36-42.
4. Bridgwater, A.V., *Review of fast pyrolysis of biomass and product upgrading*. Biomass and bioenergy, 2012. **38**: p. 68-94.
5. Mohan, D., C.U. Pittman, and P.H. Steele, *Pyrolysis of wood/biomass for bio-oil: a critical review*. Energy & fuels, 2006. **20**(3): p. 848-889.
6. Butler, E., et al., *A review of recent laboratory research and commercial developments in fast pyrolysis and upgrading*. Renewable and Sustainable Energy Reviews, 2011. **15**(8): p. 4171-4186.
7. Yoder, J., et al., *Economic tradeoff between biochar and bio-oil production via pyrolysis*. biomass and bioenergy, 2011. **35**(5): p. 1851-1862.
8. Jones, S.B., et al., *Production of gasoline and diesel from biomass via fast pyrolysis, hydrotreating and hydrocracking: a design case*. 2009: Pacific Northwest National Laboratory Richland, WA.

9. Phanphanich, M. and S. Mani, *Impact of torrefaction on the grindability and fuel characteristics of forest biomass*. *Bioresource technology*, 2011. **102**(2): p. 1246-1253.
10. Arias, B., et al., *Influence of torrefaction on the grindability and reactivity of woody biomass*. *Fuel Processing Technology*, 2008. **89**(2): p. 169-175.
11. Shankar Tumuluru, J., et al., *REVIEW: A review on biomass torrefaction process and product properties for energy applications*. *Industrial Biotechnology*, 2011. **7**(5): p. 384-401.
12. Meng, J., et al., *The effect of torrefaction on the chemistry of fast-pyrolysis bio-oil*. *Bioresource technology*, 2012. **111**: p. 439-446.
13. Chen, D., et al., *Torrefaction of biomass stalk and its effect on the yield and quality of pyrolysis products*. *Fuel*, 2015. **159**: p. 27-32.
14. Wright, M.M., et al., *Techno-economic analysis of biomass fast pyrolysis to transportation fuels*. *Fuel*, 2010. **89**, **Supplement 1**(0): p. S2-S10.
15. Jones, S., et al., *Process design and economics for the conversion of lignocellulosic biomass to hydrocarbon fuels: fast pyrolysis and hydrotreating bio-oil pathway*. 2013, National Renewable Energy Laboratory (NREL), Golden, CO.
16. Morselli, L., et al., *Environmental impacts of waste incineration in a regional system (Emilia Romagna, Italy) evaluated from a life cycle perspective*. *Journal of Hazardous Materials*, 2008. **159**(2): p. 505-511.
17. Ning, S.-K., et al., *Benefit assessment of cost, energy, and environment for biomass pyrolysis oil*. *Journal of Cleaner Production*, 2013. **59**: p. 141-149.

18. de Haes, H.A.U. and R. Heijungs, *Life-cycle assessment for energy analysis and management*. Applied Energy, 2007. **84**(7): p. 817-827.
19. Peters, J.F., D. Iribarren, and J. Dufour, *Simulation and life cycle assessment of biofuel production via fast pyrolysis and hydrougrading*. Fuel, 2015. **139**: p. 441-456.
20. Winjobi O., S.D.R., and Zhou W., *Production of Hydrocarbon Fuel using Two-Step Torrefaction and Fast Pyrolysis of Pine. Part 1: Techno-economic Analysis*. ACS Sustainable Chemistry & Engineering, In Review.
21. Winjobi O., S.D.R., Kulas D., and Zhou W., *Production of Hydrocarbon Fuel using Two-Step Torrefaction and Fast Pyrolysis of Pine. Part 2: Life-Cycle Carbon Footprint*. ACS Sustainable Chemistry & Engineering In Review.
22. Wigley, T.B., *Improving the quality of bio-oil by fast pyrolysis of acid leached and torrefied Pinus radiata*. 2015.
23. Boateng, A. and C. Mullen, *Fast pyrolysis of biomass thermally pretreated by torrefaction*. Journal of Analytical and Applied Pyrolysis, 2013. **100**: p. 95-102.
24. Westerhof, R.J., et al., *Stepwise fast pyrolysis of pine wood*. Energy & fuels, 2012. **26**(12): p. 7263-7273.
25. Winjobi, O., et al., *Techno-economic assessment of the effect of torrefaction on fast pyrolysis of pine*. Biofuels, Bioproducts and Biorefining, 2016.
26. Fivga A. *Comparison of the effect of pre-treatment and catalysts on liquid quality from fast pyrolysis of biomass* (Doctoral dissertation, Aston University).

27. Klemetsrud B, Ukaew S, Thompson VS, Thompson DN, Klinger J, Li L, Eatherton D, Puengprasert P, Shonnard D. *Characterization of products from fast micropyrolysis of municipal solid waste biomass*. ACS Sustainable Chemistry & Engineering. 2016 Sep 15;4(10):5415-23.

Chapter 7. Conclusions and Recommendations for Future Work

This dissertation research investigated the sustainability of biofuel production through two routes: a one-step fast pyrolysis of biomass and a two-step torrefaction-fast pyrolysis of biomass using the product's minimum selling price and the life cycle GHG emissions of the pathways as the indicators for sustainability. In addition, this research examined the impact of heat integration on these sustainability indicators.

A good understanding of how design changes, use of by-products and other related factors is necessary to establish a viable and sustainable biofuel production route. A proposed torrefaction-fast pyrolysis design has the potential benefit of reducing the energy required for size reduction and improving the quality of bio-oil. However, drawbacks such as increased capital cost and loss of mass because of the torrefaction reinforces the need to adequately understand and navigate the trade-offs prior to commercialization of such design approaches.

In the production of bio-oil from pine, as shown in Figure 7.1, the two-step approach in most cases exhibited better economics and lower environmental impacts compared to the one-step approach. In Figure 7.1, a shift towards the red star designates approaches to the worst-case scenario based on the trade-offs between the MSP and the GHG emissions while the green star designates the best-case scenario. From Figure 7.1, if bio-oil is the final product and used in boilers or as a substitute for heating oil, scenario 2 of a two-step pathway at torrefaction temperature of 330°C designated as point 'A' will be the optimum pathway to produce bio-oil from pyrolysis of loblolly pine. This scenario shows the closest

approach to the best-case scenario based on the trade-offs between the MSP and the GHG emissions.

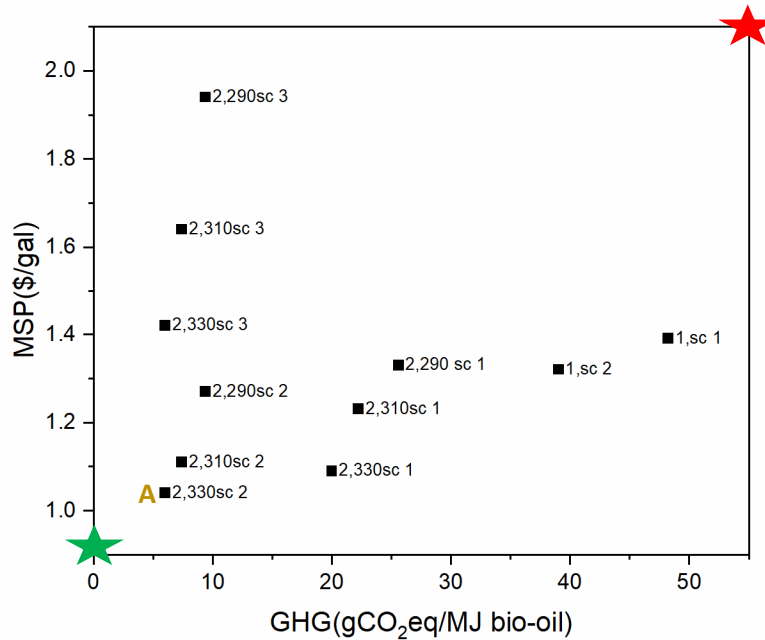


Figure 7.1. Minimum Selling Price vs Greenhouse gas emissions (energy allocation) for bio-oil production from pine: one- and two-step pathways.

As observed in Figure 7.1, in general the two-step pathway resulted in the reduction of the potential GHG emissions from the bio-oil production process relative to the one-step pathway because of the significant reduction in the use of US average grid electricity for the size reduction step as a result of the improved grindability of the torrefied biomass. Comparing the different scenarios for the two-step pathways, generally scenarios 2 show the closest approach to the best-case scenario for each torrefaction temperature because in this scenario, renewable energy inputs were used to offset fossil energy inputs while maximizing the yield of bio-oil. Because of the avoided cost of natural gas for process heat

and maximized yield of bio-oil by combusting biochar to provide the process heat led to a significant drop in the MSP and potential GHG emissions for this scenario. Scenario 3 for the two-step pathway shows comparable GHG emissions to scenario 2 but higher MSP of bio-oil. This is because the use of fossil energy inputs was totally offset with renewable energy inputs in both scenarios. However, in scenario 3 the offset was achieved by utilizing the oil from torrefaction. Because the same fossil energy inputs were avoided, GHG emissions in scenarios 2 and 3 are similar, however the lower yield of bio-oil for scenario 3 (maximizing bio-oil quality), relative to scenario 2 (maximizing bio-oil yield) results in significantly higher MSP for scenarios 3 relative to scenarios 2. In general, the highest potential GHG emissions for the two-step pathways was obtained for scenario 1 because of the fossil energy inputs required to satisfy process heat relative to scenarios 2 and 3 which used renewable energy inputs. The MSP of the bio-oil for these scenarios is however not significantly higher than those obtained for scenarios 2 because both scenarios maximized the yield of bio-oil. The main reason for the difference in MSP for these scenarios can be attributed to the trade-off between generating revenue through the sale of biochar to displace cheap coal as modeled in scenarios 1 and reducing the operating cost associated with the purchase of fossil-derived natural gas for process heat by internally combusting biochar. It can be inferred that minimizing the use of a slightly more expensive natural gas relative to coal is the major driver for the difference in MSP between scenarios 1 and 2 of the two-step pathway.

If the production of hydrocarbon biofuel is the desired final product, as shown in Figure 7.2, scenario 3 of a heat-integrated two-step pathway at torrefaction temperature of 290°C, designated as point A, and scenario 2 of a heat-integrated two-step pathway at torrefaction

temperature of 330°C are the closest approaches to the best-case scenario. Point A has the lowest MSP while point B has the lowest GHG emissions.

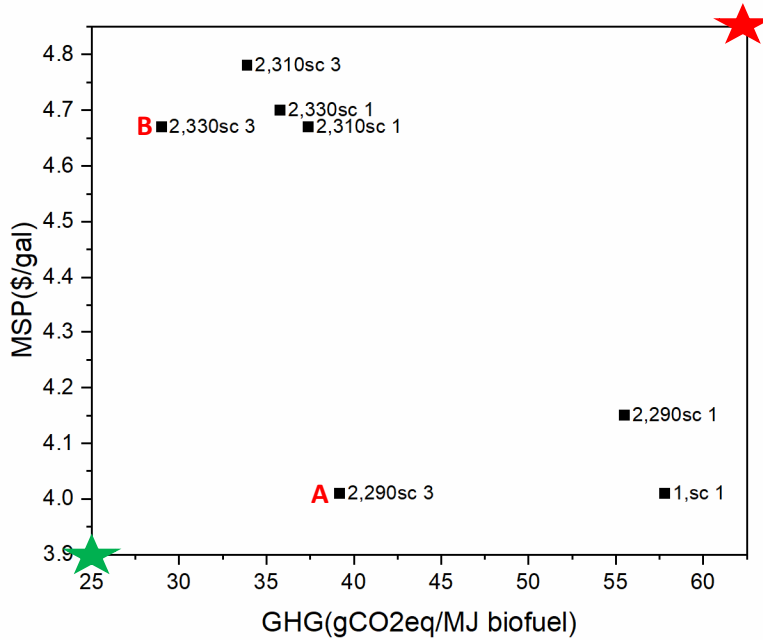


Figure 7.2. Minimum Selling Price vs Greenhouse gas emissions (energy allocation) for biofuel production from pine with heat integration: one- and two-step pathways.

For the heat-integrated pathways to produce transportation hydrocarbon biofuel, the lowest MSP was evaluated for the one-step pathway and scenario 3 of the two-step pathway at 290°C (point A) while the lowest potential GHG emissions was evaluated for scenario 3 of the two-step pathway at 330°C. In general, all the two-step pathways showed lower potential GHG emissions relative to the one-step pathway. With heat-integration, process heat requirements were satisfied by using renewable energy inputs and heat exchange, resulting in zero emissions associated with process heat. However, the emissions related to

size reduction and hydrotreatment (CO₂ produced from combustion of off-gas from fossil-derived natural gas) remain significant. The potential GHG emissions evaluated for hydrotreatment step for the heat-integrated pathway using the energy allocation approach is dictated by the amount of CO₂ generated and the allocation factor for the hydrotreatment step.

Comparing points A and B, both scenario 3 with objectives of utilizing renewable energy inputs and maximizing bio-oil quality, a significant swing in MSP and GHG can be observed. This is because as torrefaction temperature increased, the ratio of pyrolysis bio-oil to torrefaction bio-oil produced from the pathway reduced from 1.72 to 1 at torrefaction temperature of 290°C to 0.26 to 1 at torrefaction temperature of 330°C. Due to maximizing bio-oil quality for both points A and B, only the bio-oil from pyrolysis was upgraded resulting in point A having more hydrocarbon biofuel produced compared to point B. With heat-integration, the torrefaction bio-oil not utilized for process heat was assumed to be sold to generate revenue in addition to the off-gas from hydrogen production and biochar. The revenue generated from the sale of more of these by-products for point B however did not fully offset the lower hydrocarbon biofuel yield compared to point A, resulting in the lower MSP of point A. Because point B has a lower yield of bio-oil that is upgraded to hydrocarbon biofuel, the natural gas required to generate hydrogen is lower compared to point A. The lower fossil-derived natural gas requirement for hydrogen production for point B relative to point A led to lower fossil associated CO₂ from the potential combustion of the off-gas from the hydrogen production stage. Also, due to the lower biofuel yield and slightly higher off-gas produced from point B compared to point A, the allocation factor

for point B is slightly lower, which combined with the lower fossil CO₂ led to the lower GHG of point B relative to A.

The largest swing in MSP and potential GHG emissions between different scenarios of a two-step pathway at a specific temperature was observed at torrefaction temperature of 290°C as shown in Figure 7.2. Scenario 3 at this temperature (shown as point A) with the objectives of utilizing renewable energy inputs and maximizing bio-oil quality showed a significant reduction in potential GHG emissions and modest reduction in MSP relative to scenario 1 at this temperature. Though a lower yield (about 20%) of hydrocarbon biofuel was observed for scenario 3 relative to scenario 1, the lower throughput of bio-oil that was upgraded in scenario 3 resulted in lower process heat requirement downstream of the pyrolysis stage. Combined with heat-integration, the lower process heat requirement resulted in scenario 3 having more revenue generated from the sale of by-products compared to scenario 1. Because the process heat not satisfied through heat-integration was first satisfied using the bio-oil from torrefaction in scenario 3, all the off-gas and biochar produced in this scenario were totally sold to generate revenue in addition with unused torrefaction bio-oil while only a portion of the off-gas and all of the char were sold to generate revenue in scenario 1. Revenue generated from the sale of these by-products totally off-set the lower yield of biofuel resulting in lower MSP for scenario 3 relative to scenario 1. Because of maximizing the quality of bio-oil in scenario 3, a lower amount of natural gas was required to produce the complementary hydrogen required for the upgrade step leading to a lower CO₂ production from the combustion of the off-gas from the hydrogen production step. The higher yield of by-products, specifically off-gas from hydrogen production for scenario 3 relative to scenario 1 of the heat-integrated pathway at

290°C resulted in lower allocation factor for scenario 3. The combination of the lower CO₂ produced and lower allocation factor resulted in the significantly lower GHG emission for scenario 3 relative to scenario 1 at torrefaction temperature of 290°C.

From Figure 7.2, the optimum production pathway between points A and B cannot be easily inferred however the MSP of point B, with the lower GHG emission and higher MSP compared to point A, can be further reduced through incentives and tax credits because of its lower GHG emissions. In general, changes that leads to lower CO₂ production and lower allocation factor such as observed in scenario 3 can be achieved through pathways with low natural gas requirements for hydrogen production and high yield of by-products specifically off-gas resulting in low GHG emissions while low MSP is observed based on the trade-off between lower yield of biofuel and revenue generated from sale of by-products.

Results obtained for biofuel production from poplar highlight the sensitivity of the economics and environmental impacts to yield of biofuel, showing the need for extensive study and experiments on the fast pyrolysis of woody biomass before broad conclusions can be drawn on the cost competitiveness of proposed innovative technologies. Further reductions to the MSP of the biofuel can be achieved by utilizing the by-products from the pathway to displace high-value products instead of low-value products. The use of the char generated from the pathways for soil amendment or generating activated carbon are such high-value products that can potentially reduce the MSP of the biofuel instead of the low-value coal considered in this study. How displacing such high-value products potentially

affects the GHG emissions from the pathways also needs to be investigated to determine the trade-offs and an optimum production pathway.

To further improve the analysis done in this study, kinetic models that gives a better insight into the processes in the reactor should be developed. The inclusion of kinetic models in the torrefaction, fast pyrolysis, and hydrotreatment reactors, will give a better insight into how variables like reaction temperature and solid or vapor residence time affect biofuel product distribution and species concentrations, and as a result better economic and environmental impact assessments. In this case, kinetic reactors within Aspen Plus will be superior to the yield reactors used in this study. The kinetic models will also make it possible to explore other opportunities for optimizing the processes beyond the heat-integration that was examined in this study.

In general, the two-step production pathway offers more flexibility to either focus on biofuel or biochar production depending on market forces. Also, the significant reduction in energy required for the size reduction of the biomass results in significant reduction in the GHG emissions from the two-step pathway relative to the one-step pathway. With heat integration, the inclusion of a torrefaction step in the fast pyrolysis pathway results in significant lowering of the carbon footprint with little (at torrefaction temperature of 310°C and 330°C) to no (torrefaction temperature of 290°C) impact on the economic performance of the process.

Appendix A: Techno-economic assessment of the effect of torrefaction on fast pyrolysis of pine Supplementary Information

A.1. Supplementary material from Chapter 2

Section A. MODEL DESCRIPTION OF SOME UNIT OPERATIONS

A.1 Drying

Biomass inherently contains moisture, and it is assumed here that the delivered pine wood has a moisture content of about 25% which will be dried to about 7% which is recommended for fast pyrolysis. The set-up in this study has the drying step prior to size reduction for a couple of reasons that includes being able to gain the benefit of reduced energy requirement as a result of a torrefaction pre-treatment step and also prevent plugging of screens. Moisture content higher than 15% may affect the size reduction step due to plugging or blinding of the small diameter screen openings that would be employed to attain the desired particle size. The drying step will be modeled in Aspen Plus using a stoichiometric reactor and a STEAM thermodynamic package. This calculates the energy required for drying by estimating the specific energy required to raise the temperature of the biomass and its inherent moisture to the target temperature and also the latent heat required to vaporize the moisture in the biomass.

A.2 Size Reduction

The correlation obtained from literature given as follows for pine was used in evaluating the reduction in energy consumption to attain required size to effect fast pyrolysis.⁽¹⁾

$$E_g = -0.756T + 260.0 \quad (1)$$

where E_g is specific energy consumption for grinding in kW-hr/ton, T is Temperature in °C

The size reduction step was then modeled in Aspen Plus® as a hammer mill with the estimated specific energy consumed for grinding estimated at different torrefaction temperatures, while the untreated raw pine's energy was estimated using ambient temperature of 25°C. The work index required for grinding was also calculated using

$$E_g = 10 * W_i * \left(\frac{1}{\sqrt{P}} - \frac{1}{\sqrt{F}} \right) \quad (2)$$

where E_g Specific energy consumption for grinding in kW-hr/ton, W_i is work index in kW-hr/ton, P is final particle size in microns and F is Initial particle size in microns

A.3 Combustion

Combustion of products, when considered in this study, was not modeled using the process simulation software. However, the heat released during combustion was estimated from correlations obtained from the literature as shown below:

A.3.1 Combustion of char

Heat released from the combustion of char was evaluated based on the lower heating value of char, which was estimated from its higher heating value based on correlation from literature given below:⁽²⁾

$$LHV = HHV \left(1 - \frac{w}{100} \right) - 2.444 * \frac{w}{100} - 2.444 * \frac{h}{100} * 8.936 \left(1 - \frac{w}{100} \right) \left[\frac{MJ}{kg}, w. b. \right]$$

(3)

Where

2.444 = enthalpy difference between gaseous and liquid water at 25°C

8.936 = M_{H_2O}/M_{H_2} ; i.e. the molecular mass ratio between H₂O and H₂

LHV = lower heating value

HHV = higher heating value

w = moisture content of the fuel in wt% (w.b.)

h = concentration of hydrogen in wt% (d.b.)

The higher value utilized in equation above was also estimated from empirical formula as well as shown below.⁽³⁾

$$HHV = 0.3491X_C + 1.1783X_H + 0.1005X_S - 0.0151X_N - 0.1034X_O - 0.0211X_{ash} \left[\frac{MJ}{kg}, d. b. \right] \quad (4)$$

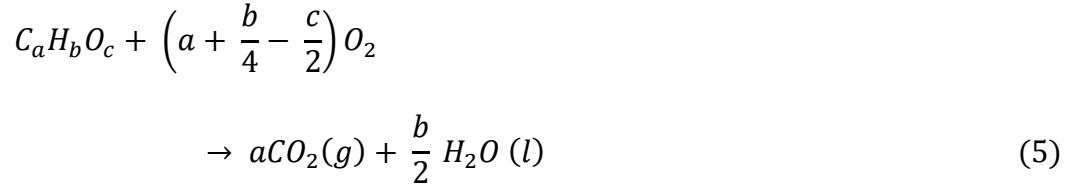
Where X_i is the content of carbon (C), hydrogen (H), etc. from the ultimate analysis of the solid fuel.

A.3.2 Combustion of condensates from torrefaction

The energy released from the combustion of condensates from torrefaction when such step takes place in this study was estimated by obtaining from the literature the lower heating value of the individual components in the condensates.⁽⁴⁾ Based on the lower heating value of the individual components and their weight fraction in the liquid, the lower heating value of the liquid was estimated. For high molecular compounds produced from either the torrefaction or pyrolysis step whose lower heating values were not found in the

literature, their lower heating values were estimated using correlation obtained from the literature as shown below:⁽⁵⁾

For compounds containing only carbon, hydrogen and oxygen, general combustion reaction was given as



The standard heat of combustion is then given as

$$\begin{aligned} \Delta_c H^\circ &= -a\Delta_f H^\circ(CO_2, g) - \frac{1}{2}b\Delta_f H^\circ(H_2O, l) + \Delta_f H^\circ(C_aH_bO_c) \\ (6) \\ &= 393.51a + 142.915b + \Delta_f H^\circ(C_aH_bO_c) \\ (7) \end{aligned}$$

Where $\Delta_f H^\circ$ is the enthalpy of formation. When the heat of formation is not available from literature, it was estimated based on the structure of the component by using the Joback method which is based on group contribution.^(4, 6)

A.3.3 Combustion of non-condensable gas from torrefaction

Heat generated from combustion of non-condensable gas from torrefaction was estimated using the lower heating value of the components present in the non-condensable gas phase. Severity of torrefaction usually determines the components contained in the non-condensable gas. However, for this study the components were assumed to be essentially

CO₂ and CO in an 80 to 20 ratio. Hence heat released from combustion is due to the CO component only. The assumption is supported by the report of Tumuluru et al which showed energy released from the combustion of volatiles from torrefaction is mainly from CO.⁽⁷⁾

A.3.4 Bioe correlation for heat of combustion estimation

One of the correlations used in Aspen Plus® to estimate the heat of combustion of unconventional solids such as biomass was based on the ultimate analysis is as shown:

$$\Delta_c h_i^{dm} = [a_{1i}w_{C,i}^{dm} + a_{2i}w_{H,i}^{dm} + a_{3i}w_{S,i}^{dm} + a_{4i}w_{O,i}^{dm} + a_{5i}w_{N,i}^{dm}]10^2 + a_{6i} \quad (8)$$

Where $w_{C,i}^{dm}$ is the weight fraction of carbon.

Values of the parameters as given by Aspen Plus® are as follows⁽⁸⁾

$$a_{1i} = 151.2, a_{2i} = 499.77, a_{3i} = 45.0, a_{4i} = -47.7, a_{5i} = 27.0 \text{ and } a_{6i} = -189$$

A.4 Conveyance

Biomass movement across the plant is assumed to be carried out using conveyor belts, and the energy required for this conveyance was estimated by firstly using the guidelines by CEMA as shown by Couper et al.^(9, 10) The conveyance is assumed to be carried out using a 24 inch, 45° troughed belt conveyor of length, 33.5m and up a longitudinal incline of 22°. The running angle of repose of the woodchips is taken to be about 30° and the required power is estimated by using equation 7.

$$Power (hp) = P_{horizontal} + P_{vertical} + P_{empty} \quad (9)$$

Where $P_{\text{horizontal}} = (0.4+L/300)(W/100)$, $P_{\text{vertical}} = 0.001HW$, and P_{empty} obtained based on desired conveyor length from the literature.⁽¹⁰⁾

A.5 Energy Return on Energy Invested (EROEI)

$$EROEI = \frac{Energy_{out}}{Energy_{in}} = \frac{E_{bo} + E_{char}}{E_{thermal} + E_{electricity}} = \frac{\dot{m}_{bo}LHV_{bo} + \dot{m}_{char}LHV_{char}}{E_{thermal} + E_{electricity}} \quad (10)$$

Where E_{bo} is the energy obtainable from bio-oil estimated based on its lower heating value (LHV); E_{char} is the energy obtainable from char also obtained from its lower heating value. \dot{m} is the mass flowrate while $E_{thermal}$ is the required process heat required over the whole process and $E_{electricity}$ is the energy associated with size reduction and conveyance across the process. Energy due to electricity was converted to thermal assuming an efficiency of about 35% for the conversion of steam to electricity.

SECTION B. INPUT DATA TABLES USED IN MODELING

Table A1. Torrefaction component distribution (wt % organics) of organics from torrefaction of pine at different torrefaction temperatures.

Component (wt/wt organics)	Torrefaction temperature		
	290°C	310°C	330°C
Acetic Acid	8.01	11.92	13.09
Propionic Acid	0.25	0.42	0.48
Acetol	2.47	5.08	6.43
Fufural	1.01	1.26	1.95
2-Furanmethanol	0.09	0.11	0.21
5-(hydroxymethyl)-2-furancarboxaldehyde	0.00	0.00	0.00
Levoglucosan	0.40	2.43	3.00
Xylose	0.40	1.22	1.32
Hydrolysable Oligomers(cellobiose)	0.00	0.15	0.36
Glucose	0.10	0.61	0.60
Isoeugenol	0.33	0.76	1.83
Eugenol	0.05	0.13	0.27
Vanillin	0.21	0.32	0.31
2-methoxy-4-vinylphenol(p-vinylguaiacol)	0.00	0.00	0.00
Catechol(benze-1,2-diol)	0.00	0.00	0.00
Phenol	0.00	0.00	0.00
2-methoxyphenol (guaiacol)	0.49	0.83	1.48
4-methylphenol(p-cresol)	0.00	0.00	0.00
3-methylphenol (m-cresol)	0.00	0.00	0.00
4-ethylphenol	0.00	0.00	0.00
2-methoxy-4-methylphenol (creosol)	0.00	0.00	0.00
Low MW Lignin-Derived Compound A(Dimethoxy stilbenzene)	0.95	1.24	1.87
Low MW Lignin Derived Compound B (Dibenzofuran)	0.19	0.25	0.38
High MW Lignin-Derived Compound A	0.79	1.04	1.56
High MW Lignin Derived Compound B	0.17	0.23	0.34

Table A2. Ultimate analysis data (wt %) for torrefied pine chips at different torrefaction temperatures.

Torrefaction Temperature	290°C	310°C	330°C
Component	Wt %		
Ash	0.6	0.6	0.8
Carbon	55.05	57.27	65.75
Hydrogen	5.94	5.79	4.87
Chlorine	-	-	-
Nitrogen	0.11	0.14	0.28
Sulfur	-	-	-
Oxygen	38.3	36.0	27.6

Table A3. Proximate analysis data (wt %) for torrefied pine chips at different torrefaction temperatures.

Torrefaction Temperature	290°C	310°C	330°C
Component	Wt %		
Ash	0.60	0.80	1.4
Moisture Content	0	0	0
Volatile Matter	78.6	76.4	60
Fixed Carbon	20.8	22.8	38.6

Table A4. Pyrolysis component distribution of organics (wt/wt organics) for one step and two step pyrolysis of pine.

		One Step	Two Step		
Component (wt %)	Torrefaction temperature		290°C	310°C	330°C
Acetic Acid		7.59	4.42	2.96	1.11
Propionic Acid		3.69	0.00	0.00	0.00
Acetol		3.11	3.28	2.39	0.85
Fufural		1.00	0.29	0.15	0.38
2-Furanmethanol		0.12	0.07	0.04	0.11
5-(hydroxymethyl)-2-furancarboxaldehyde		0.23	0.28	0.15	0.45
Levoglucosan		7.24	7.91	6.04	8.45
Xylose		2.19	2.05	1.01	0.94
Cellobiose		3.29	5.28	4.70	0.00
Glucose		1.10	1.17	0.34	0.00
Isoeugenol		0.54	0.58	0.58	0.50

Eugenol	0.12	0.36	0.20	0.17
Vanillin	0.42	0.14	0.15	0.12
P-vinylguaiacol	0.79	0.37	0.25	0.21
Catechol	2.53	4.88	2.32	2.08
Phenol	0.19	0.33	0.24	0.23
Guaiacol	0.46	0.46	0.37	0.30
P-cresol	0.06	0.12	0.10	0.06
M-cresol	0.02	0.06	0.13	0.09
4-ethylphenol	0.07	0.14	0.05	0.07
Creosol	0.46	0.85	0.50	0.59
Low MW Lignin-Derived Compound A(Dimethoxy stilbenzene)	7.11	6.50	6.00	3.05
Low MW Lignin Derived Compound B (Dibenzofuran)	1.43	1.31	1.21	0.62
High MW Lignin-Derived Compound A	5.94	5.43	5.02	2.55
High MW Lignin Derived Compound B	1.30	1.18	1.10	0.56

Table A5. Ultimate and proximate data (wt %) for char obtained after pyrolysis.

Ultimate Analysis		Proximate Analysis	
Components	Wt. %	Components	Wt. %
Ash	7.67	Ash	4.60
Carbon	83.03	Moisture Content	-
Hydrogen	1.14	Volatile matter	7.40
Nitrogen	1.37	Fixed carbon	88.0
Chlorine	-		
Sulfur	-		
Oxygen	6.56		

Table A6. Estimated number of employees and their wages rate.

Employee	Annual Salary	Number Required
Plant/General Manager	\$136,830.00	1
Plant Engineer	\$108,630.00	1
Maintenance Supervisor	\$76,480.00	1
Lab Manager/Chemist	\$77,970.00	1
Shift Supervisor	\$74,470.00	5
Maintenance Tech	\$70,450.00	6
Shift Operators	\$55,980.00	23
Admin Assistants	\$43,440.00	2

SECTION C. SCHEMATIC DIAGRAMS FOR SCENARIOS 2 & 3 OF THE DESIGN OBJECTIVES.

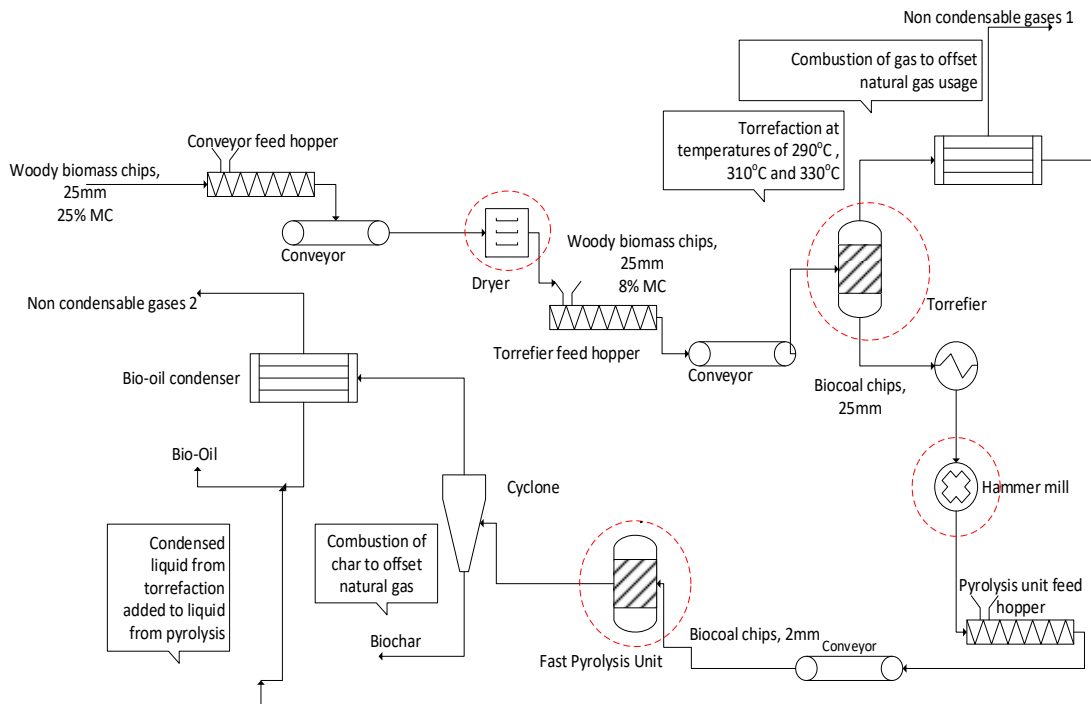


Figure A1. Schematic diagram for scenario 2 of a two-step conversion route.

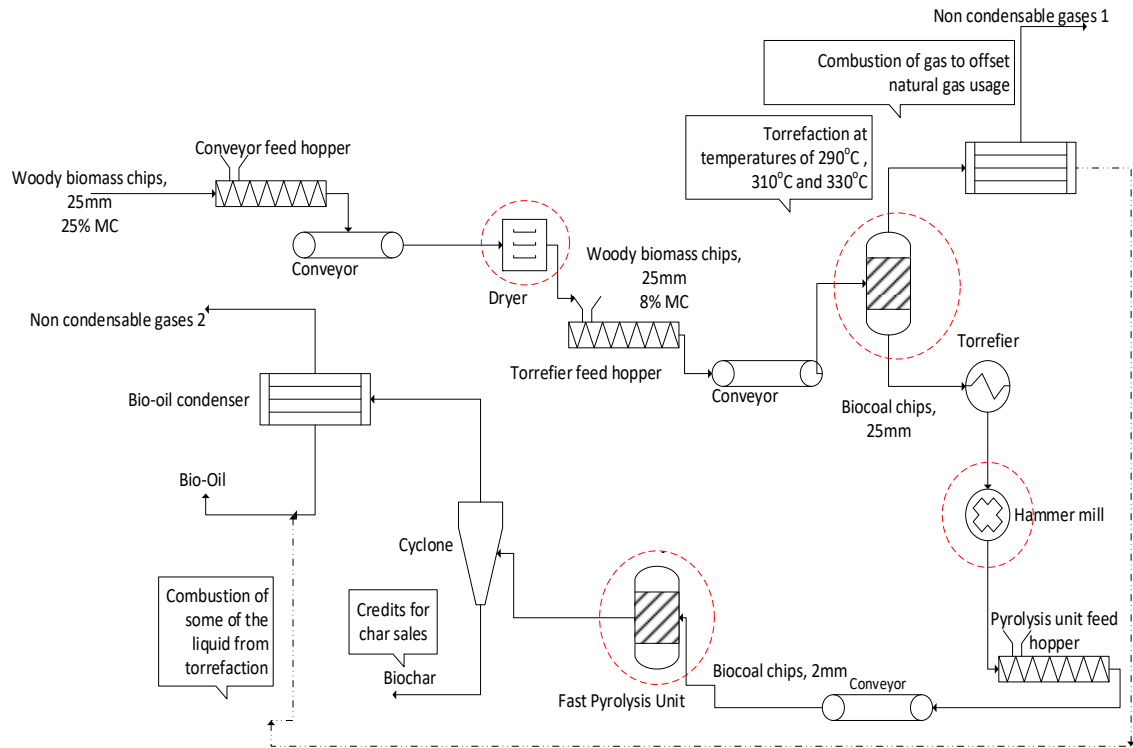


Figure A2. Schematic diagram for scenario 3 of a two-step conversion route for pine biomass to bio-oil.

SECTION D. FIGURES FOR SENSITIVITY ANALYSIS RESULTS.

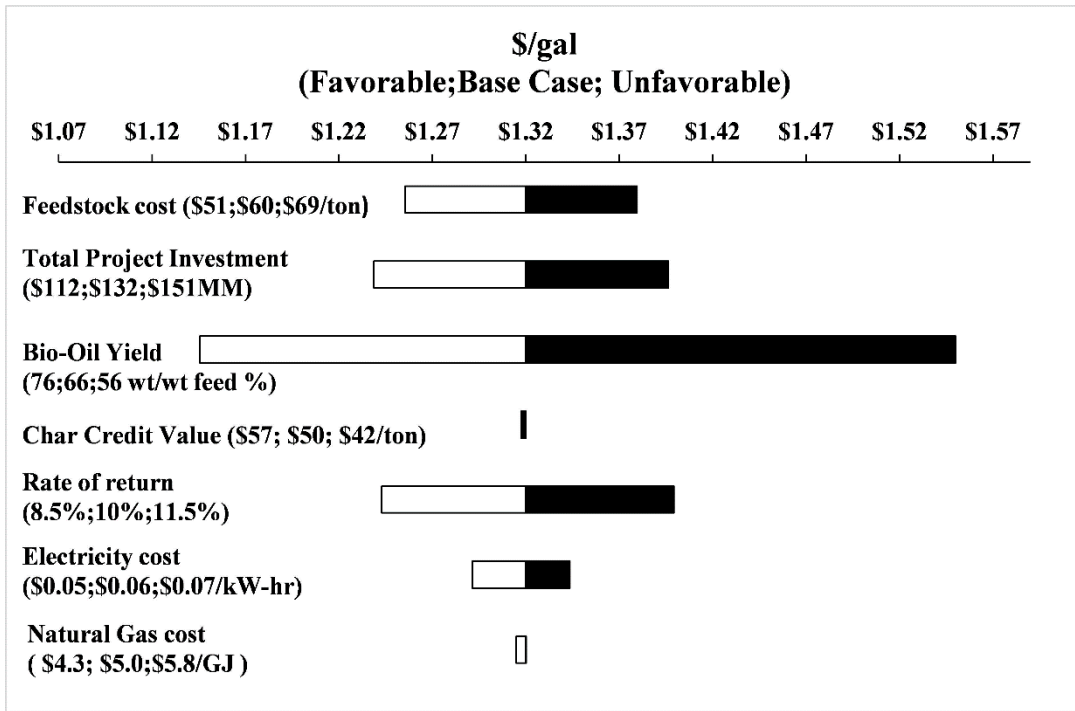


Figure A3. Sensitivity analysis for scenario 2 of a one-step conversion of pine to bio-oil

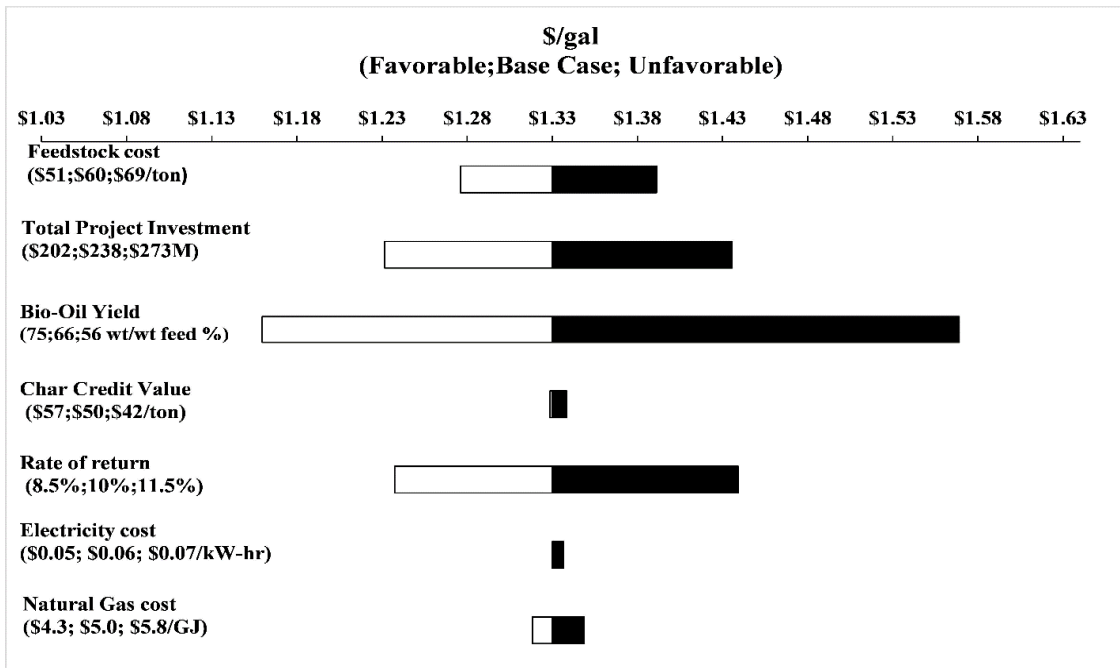


Figure A4. Sensitivity analysis for scenario 1 of a two-step conversion process of pine to bio-oil at torrefaction temperature of 290°C.

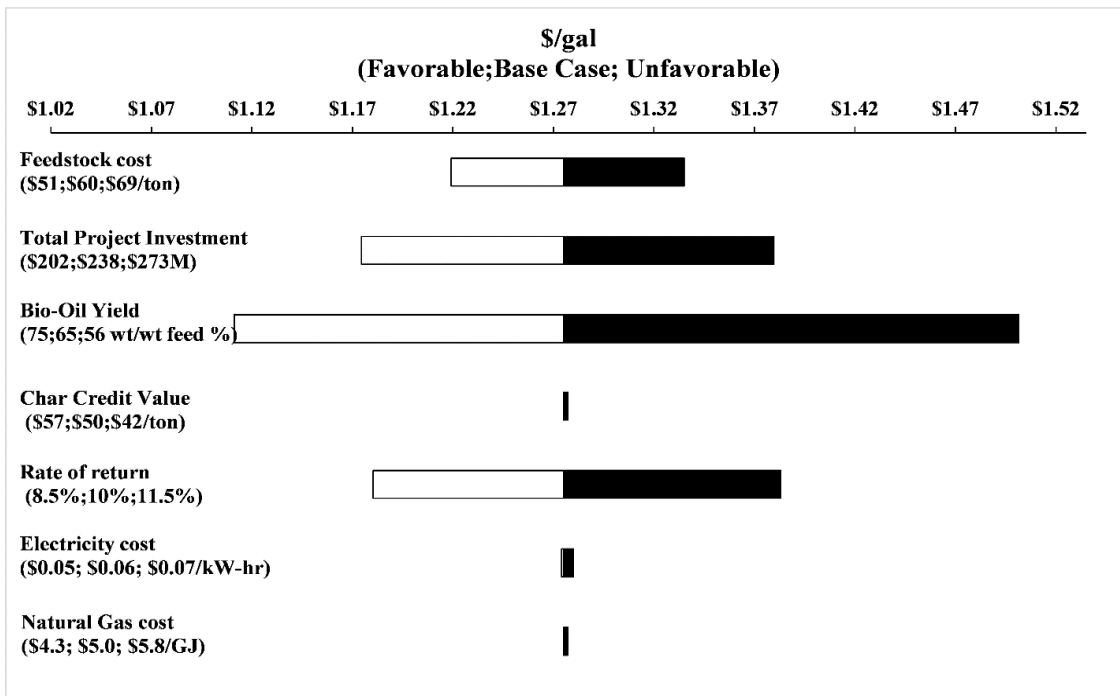


Figure A5. Sensitivity analysis for scenario 2 of a two-step conversion process of pine to bio-oil at torrefaction temperature of 290°C.

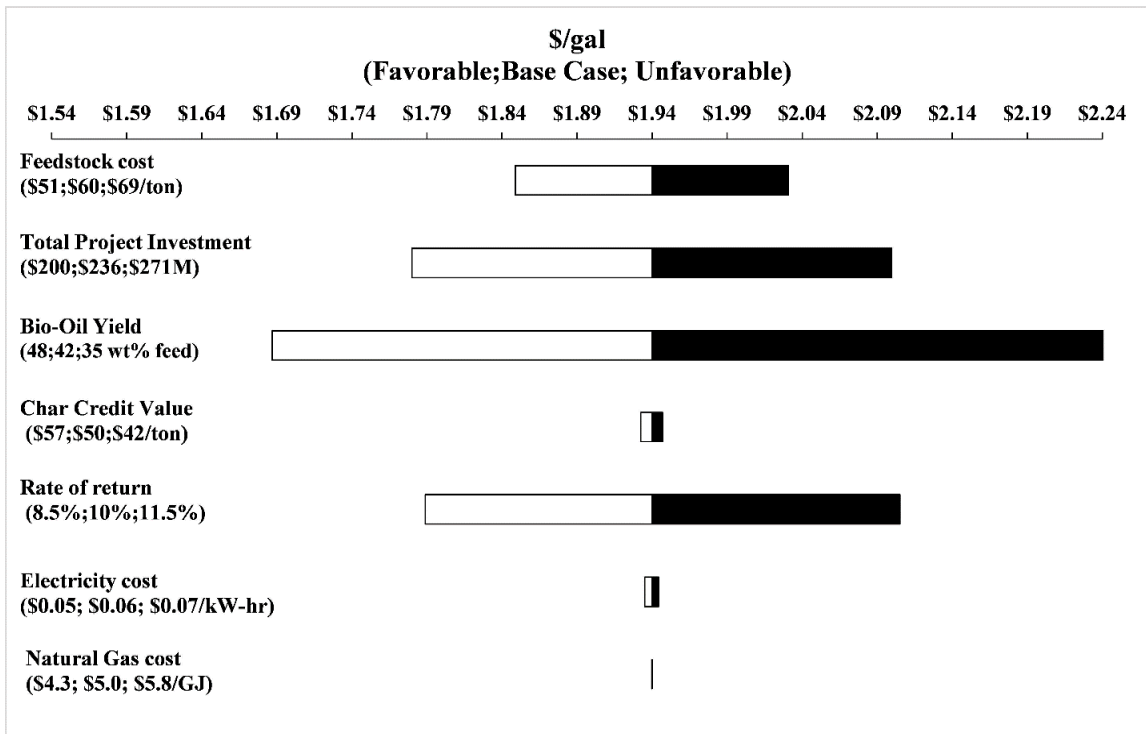


Figure A6. Sensitivity analysis for scenario 3 of a two-step conversion process of pine to bio-oil at torrefaction temperature of 290°C.

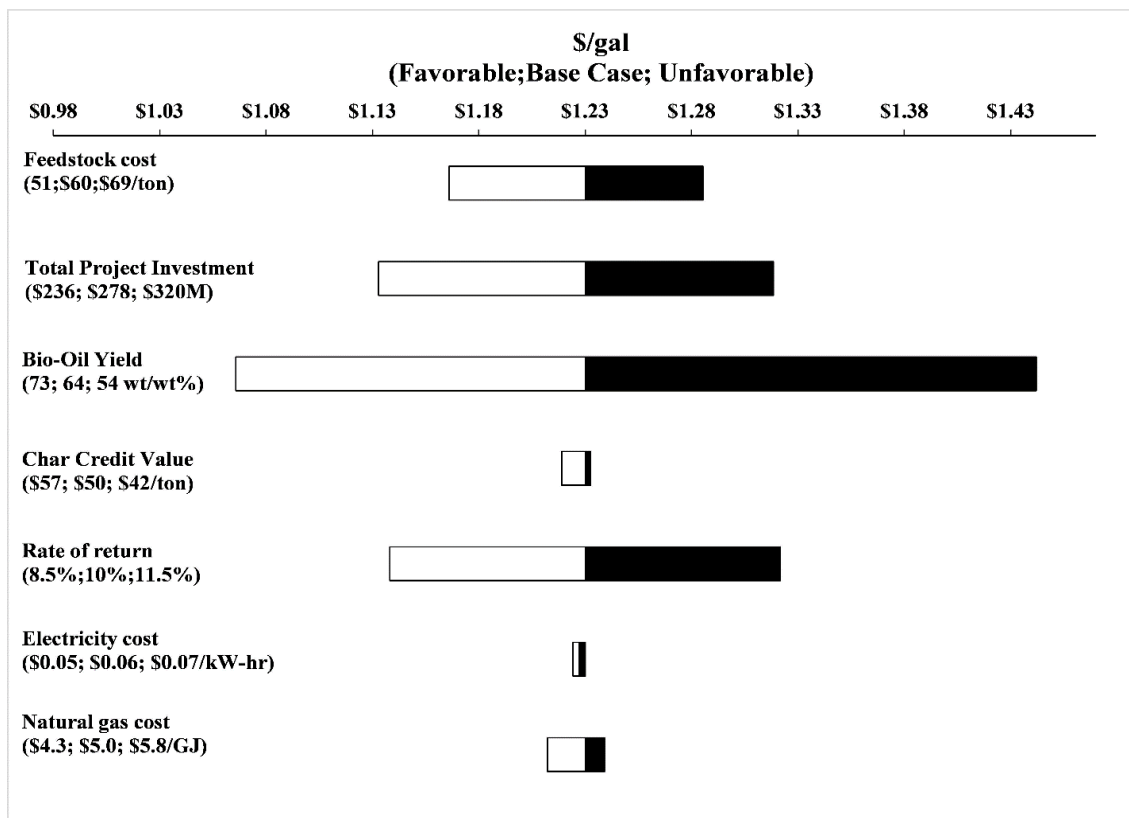


Figure A7. Sensitivity analysis for scenario 1 of a two-step conversion process of pine to bio-oil at torrefaction temperature of 310°C.

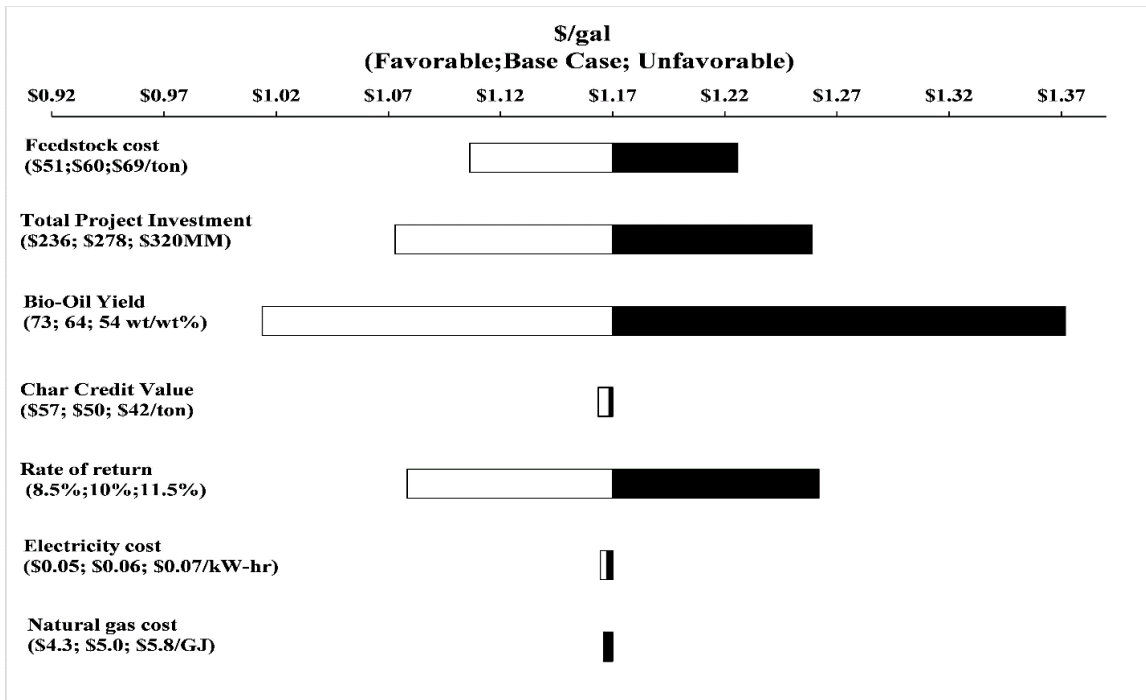


Figure A8. Sensitivity analysis for scenario 2 of a two-step conversion process of pine to bio-oil at torrefaction temperature of 310°C.

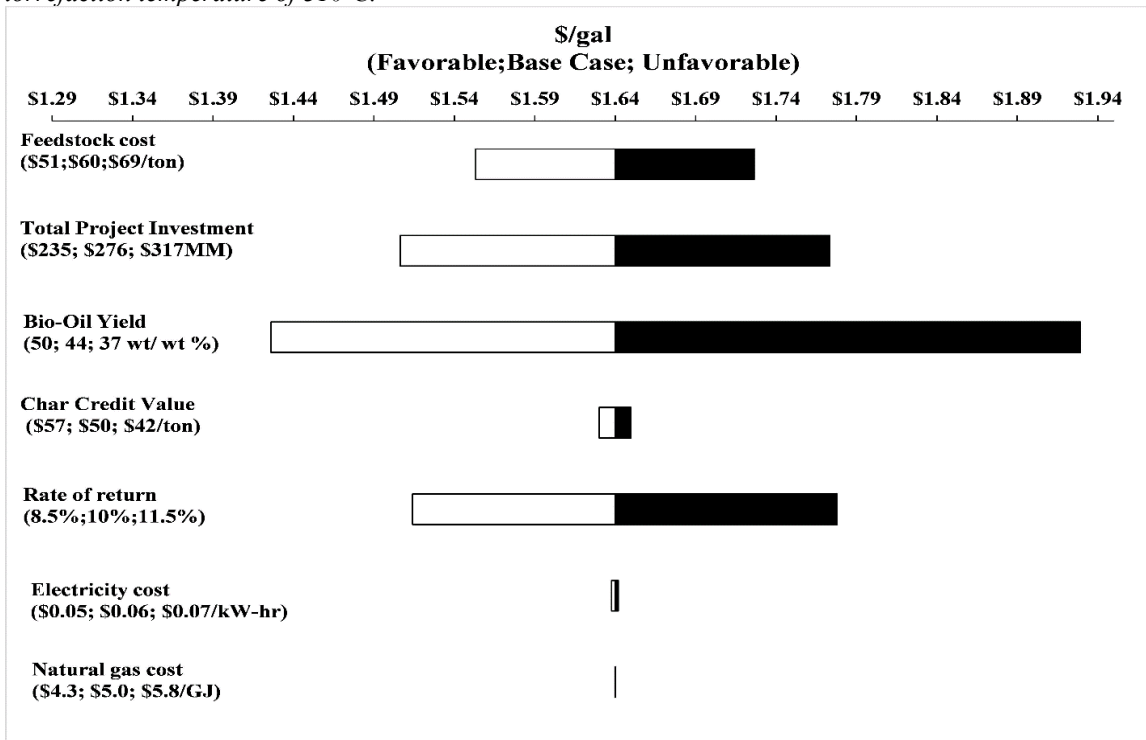


Figure A9. Sensitivity analysis for scenario 3 of a two-step conversion process of pine to bio-oil at torrefaction temperature of 310°C.

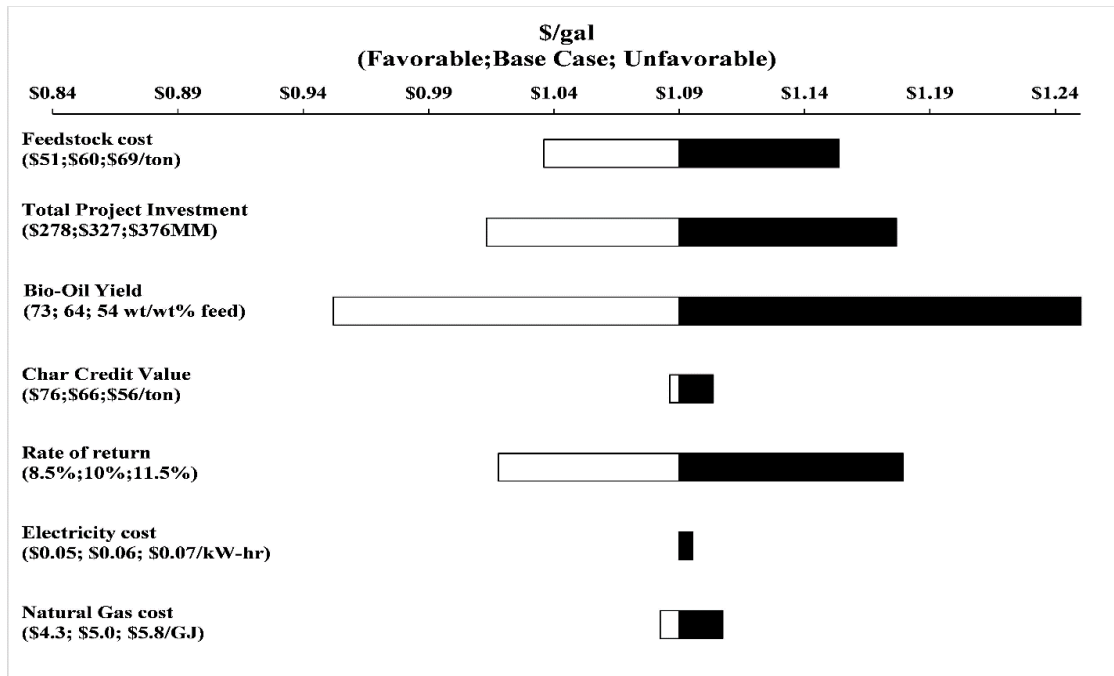


Figure A10. Sensitivity analysis for scenario 1 of a two-step conversion process of pine to bio-oil at torrefaction temperature of 330°C.

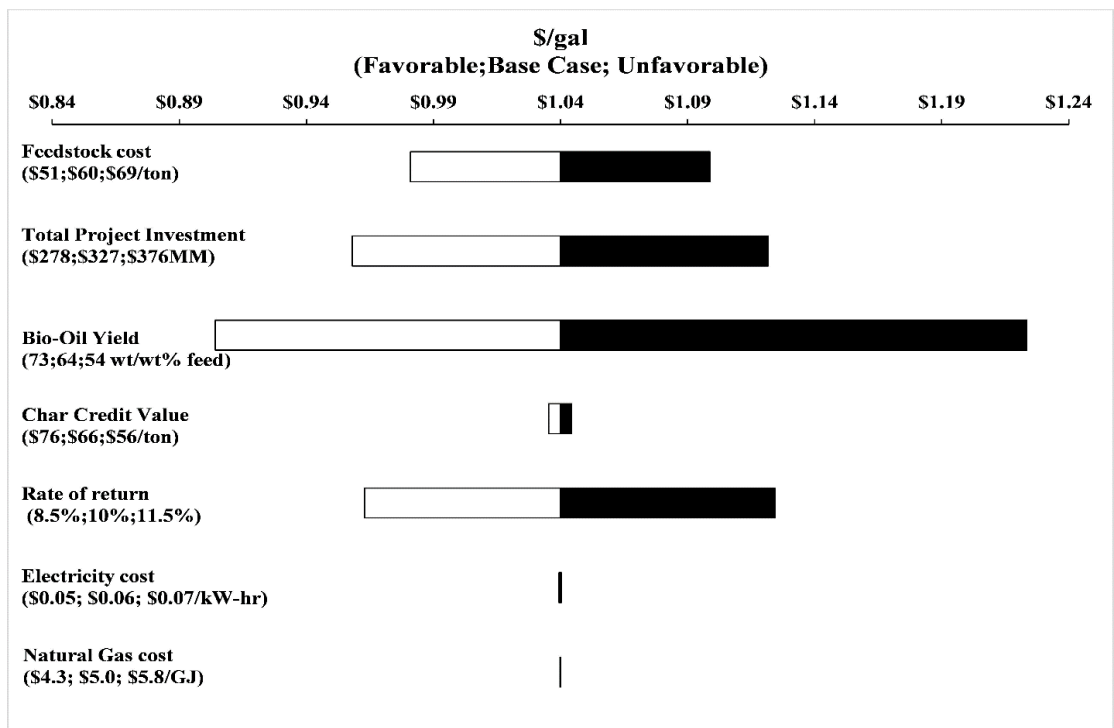


Figure A11. Sensitivity analysis for scenario 2 of a two-step conversion process of pine to bio-oil at torrefaction temperature of 330°C.

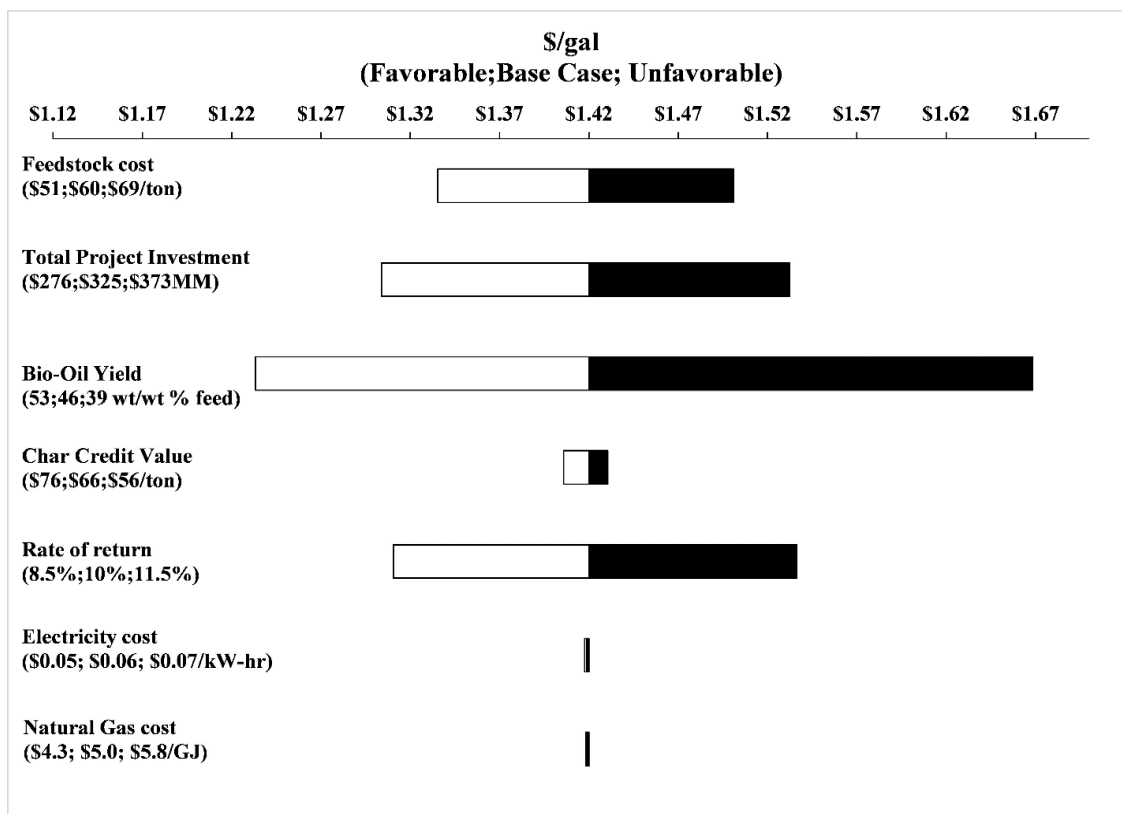


Figure A12. Sensitivity analysis for scenario 3 of a two-step conversion process of pine to bio-oil at torrefaction temperature of 330°C.

A.2. References

1. Phanphanich M, Mani S. Impact of torrefaction on the grindability and fuel characteristics of forest biomass. *Bioresource technology*. 2011;102(2):1246-53.
2. Koppejan J, Van Loo S. *The handbook of biomass combustion and co-firing*: Routledge; 2012.
3. Gaur S, Reed TB. *An atlas of thermal data for biomass and other fuels*. National Renewable Energy Lab., Golden, CO (United States), 1995.
4. Perry RH, Green DW, Maloney JO, Abbott MM, Ambler CM, Amero RC. *Perry's chemical engineers' handbook*: McGraw-hill New York; 1997.
5. Haynes WM. *CRC handbook of chemistry and physics*: CRC press; 2013.
6. Joback KG, Reid RC. Estimation of pure-component properties from group-contributions. *Chemical Engineering Communications*. 1987;57(1-6):233-43.
7. Shankar Tumuluru J, Sokhansanj S, Hess JR, Wright CT, Boardman RD. REVIEW: A review on biomass torrefaction process and product properties for energy applications. *Industrial Biotechnology*. 2011;7(5):384-401.
8. Plus A. Aspen Technology. Inc, version. 2009;11.
9. Conference CEMAE. *Belt conveyors for bulk materials: Conveyor Equipment Manufacturers Association*; 1997.
10. Couper JR, Penney WR, Fair JR. *Chemical Process Equipment revised 2E: Selection and Design*: Gulf Professional Publishing; 2009.

Appendix B: Life cycle assessment for greenhouse gas emissions of two-step torrefaction and fast pyrolysis of pine supplementary information

B.1 Supplementary material from Chapter 3

Section A. SCHEMATIC DIAGRAMS FOR RMBY & RMBQ OF THE DESIGN OBJECTIVES.

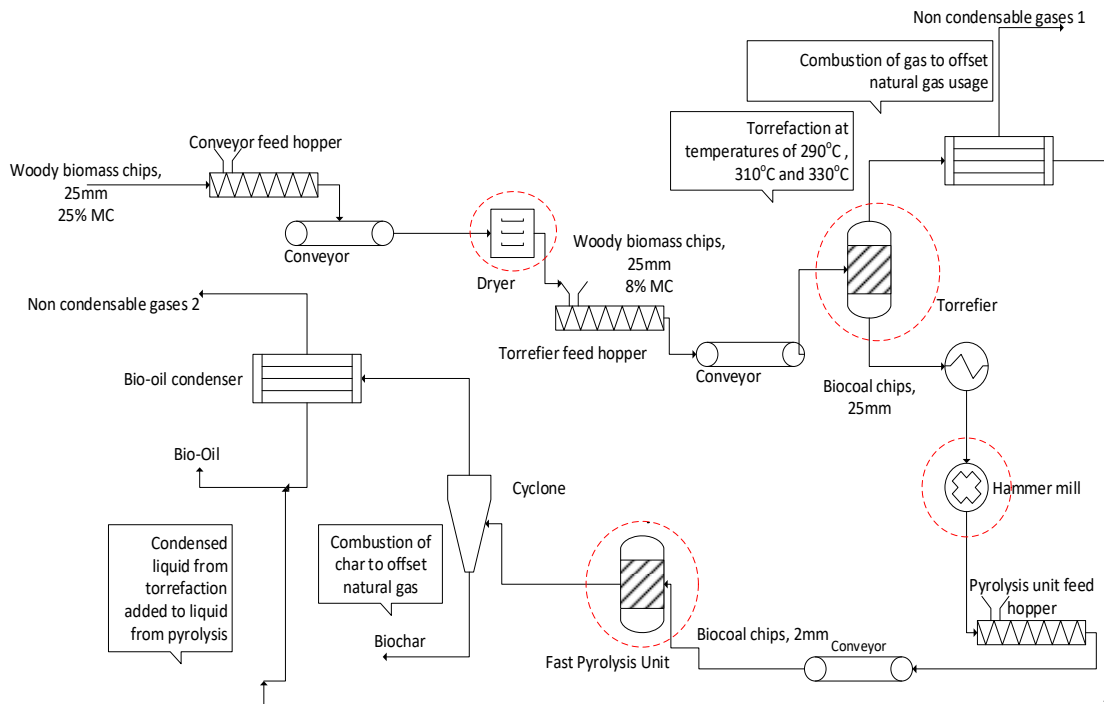


Figure B1. Schematic diagram for RMBY of a two-step conversion route.

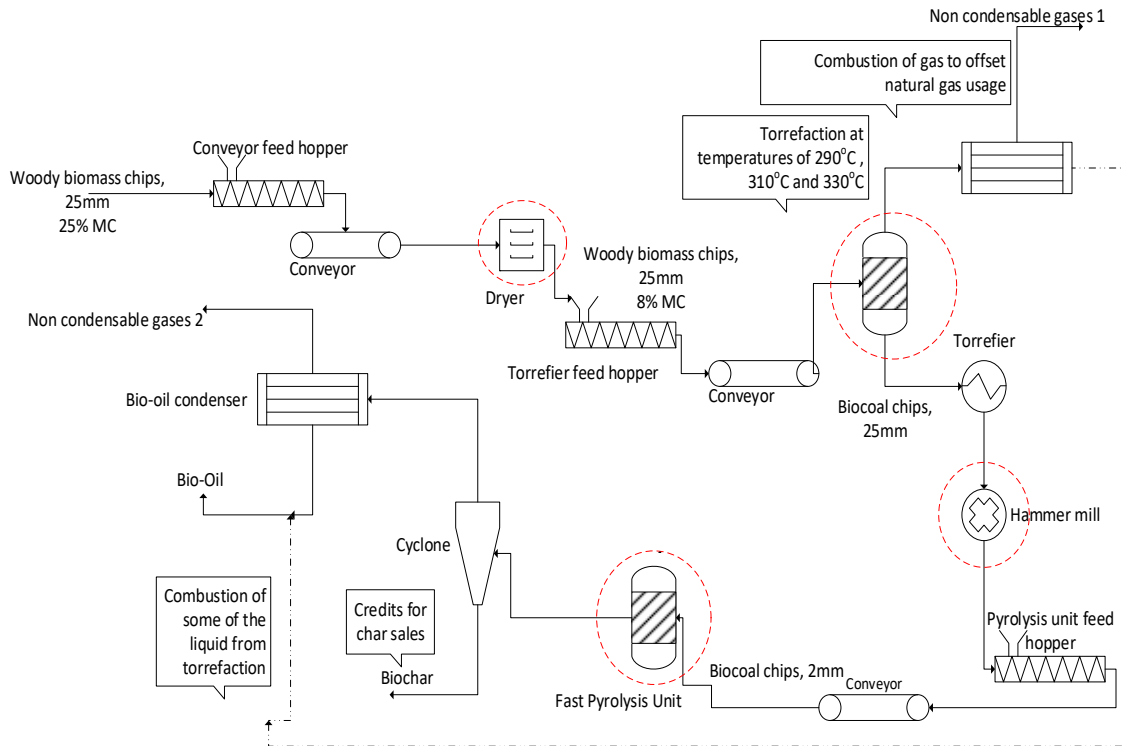


Figure B2. Schematic diagram for RMBQ of a two-step conversion route for pine biomass to bio-oil.

Section B. BIOMASS SUPPLY CHAIN EMISSIONS USING GREET MODEL 2014.

B.1 Wood collection

The emissions due to the collection of wood were obtained from the EtOH tab of the GREET model as shown below. (1) The emission factors given in grams/dry ton were input into SimaPro®.

Table B1. GREET emission factors for wood collection. (1)

Wood collection	
grams/dry ton	EtOH tab DU 454:464
VOC	11.803
CO	60.833
CH ₄	18.67

N ₂ O	0.156
CO ₂	12009

B.2 Biomass chipping

For the coarse chipping of biomass at the forest, emission factors were determined for the production of diesel used in running the stationary reciprocating diesel engine. The factors obtained from the GREET model as shown in Table below were given in grams/mmBtu of diesel burned.(1)

Table B2. GREET emission factors for coarse chipping at forest.(1)

Chipping- Stationary Reciprocating Diesel Engine		
grams/mmBtu Diesel burned	Petroleum tab BI 127:140 Production	EF tab R6:16 Combustion
VOC	0.978	2.027
CO	2.873	657.005
CH ₄	18.406	4.221
N ₂ O	0.1	0.6
CO ₂	2485	77149

These factors were converted to grams/ short ton by multiplying by 0.129488 mmBtu/gal LSD (Fuel_Specs tab B18), the lower heating value (LHV) of diesel. Then divided by 3.206 kg LSD/ gal LSD (Fuel_Specs tab E18), the density of low sulfur diesel. This was then multiplied by a factor of 0.5 kg LSD combusted/ dry short ton of biomass, based on the amount of diesel required per dry ton of biomass given by Maleche et al.(2)

B.3 Truck Transport

Emission factors for truck transport obtained from the GREET model are shown below for a 90-mile truck transport (T&D tab GP 107).(1)

Table B3. GREET emission factors for truck transport of biomass.(1)

Truck transport (90 miles)	
grams/dry short ton	EtOH tab DV 454:464
VOC	8.993
CO	30.676
CH4	53.645
N2O	0.486
CO2	32626

B.4 Loading operations

Three loading operations were considered in the biomass supply chain. The loading operations were achieved using front loading trucks. The emission factors obtained from the GREET database includes the emissions for the production of diesel and combustion of diesel in the front loading trucks.(1)

Table B4. GREET emission factors for loading operations of biomass.(1)

Loading operations		
grams/mmBtu Diesel burned	Petroleum tab K 265:275 Production	EF tab AD37:47 Combustion
VOC	4.156	16.785
CO	7.021	69.368
CH4	19.18	19.224
N2O	0.16	0.083
CO2	8125	77985

These factors were converted to grams/ short ton by multiplying by 0.129488 mmBtu/gal LSD (Fuel_Specs tab B18), the lower heating value (LHV) of diesel. Then divided by 3.206 kg LSD/ gal LSD (Fuel_Specs tab E18), the density of low sulfur diesel. Then multiplied by 1.5 kg/short ton, based on 0.5 kg diesel/ dry short ton reported for each loading operations by Handler et al.(3)

B.5 Rail transport

Table B5. GREET emission factors for rail transport of biomass.(1)

Rail transport (490 miles)		
grams/mmBtu Diesel burned	T&D J 181:191 Production	EF S37:J47 Combustion
VOC	0.241	58.388
CO	0.805	206.53
CH4	0.532	6.825
N2O	0.009	2.132
CO2	329	77674

A distance of 490 miles (T&D tab J16) was assumed for rail transport. Emissions were evaluated for the production and consumption of diesel. To convert the factors given in grams/mmBtu Diesel burned to grams/dry ton of biomass, the factors were multiplied by the rail intensity 274 Btu/ton-mile (T&D tab E122) and then multiplied by the distance of 156 traveled.

B.6 Size reduction

The energy required to reduce the pine chips to the required size for pyrolysis was evaluated using a correlation obtained from the literature given as follows:(4)

$$E_g = -0.756T + 260.0 \quad (1)$$

where E_g is specific energy consumption for grinding in kW-hr/ton, T is Temperature in °C

The size reduction step was then modeled in Aspen Plus® as a hammer mill with the estimated specific energy consumed for grinding estimated at different torrefaction temperatures, while the untreated raw pine's energy was estimated using ambient temperature of 25°C. The work index required for grinding was also calculated using

$$E_g = 10 * W_i * \left(\frac{1}{\sqrt{P}} - \frac{1}{\sqrt{F}} \right) \quad (2)$$

where E_g Specific energy consumption for grinding in kW-hr/ton, W_i is work index in kW-hr/ton, P is final particle size in microns and F is Initial particle size in microns

B.7 Combustion

Combustion of products, when considered in this study, was not modeled using the process simulation software. However, the heat released during combustion were estimated from correlations obtained from literature as shown below:

B.7.1 Combustion of char

Heat released from the combustion of char was evaluated based on the lower heating value of char, which was estimated from its higher heating value based on correlation from literature given below:⁽⁵⁾

$$LHV = HHV \left(1 - \frac{w}{100}\right) - 2.444 * \frac{w}{100} - 2.444 * \frac{h}{100} * 8.936 \left(1 - \frac{w}{100}\right) \left[\frac{MJ}{kg}, w. b.\right]$$

(3)

Where

2.444 = enthalpy difference between gaseous and liquid water at 25°C

8.936 = M_{H_2O}/M_{H_2} ; i.e. the molecular mass ratio between H₂O and H₂

LHV = lower heating value in MJ/kg fuel (w.b.)

HHV = higher heating value in MJ/kg fuel (d.b.)

w = moisture content of the fuel in wt% (w.b.)

h = concentration of hydrogen in wt% (d.b.)

The higher value utilized in equation above was also estimated from empirical formula as well as shown below.⁽⁶⁾

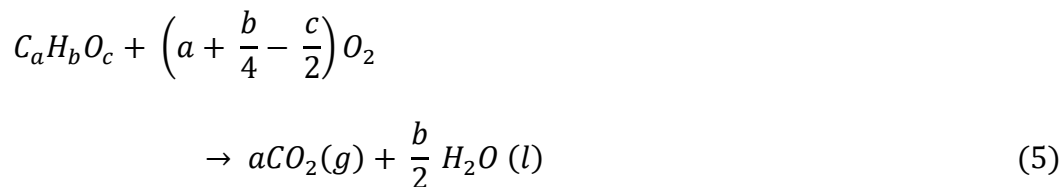
$$HHV = 0.3491X_C + 1.1783X_H + 0.1005X_S - 0.0151X_N - 0.1034X_O - 0.0211X_{ash} \left[\frac{MJ}{kg}, d. b.\right] \quad (4)$$

Where X_i is the content of carbon (C), hydrogen (H), etc. from the ultimate analysis of the solid fuel.

B.7.2 Combustion of condensates from torrefaction

The energy released from the combustion of condensates from torrefaction when such step takes place in this study was estimated by obtaining from the literature the lower heating value of the individual components in the condensates.⁽⁷⁾ Based on the lower heating value of the individual components and their weight fraction in the liquid, the lower heating value of the liquid was estimated. For high molecular compounds produced from either the torrefaction or pyrolysis step whose lower heating values were not found in the literature, their lower heating values were estimated using correlation obtained from the literature as shown below:⁽⁸⁾

For compounds containing only carbon, hydrogen and oxygen, general combustion reaction was given as



The standard heat of combustion is then given as

$$\Delta_c H^\circ = -a \Delta_f H^\circ(CO_2, g) - \frac{1}{2} b \Delta_f H^\circ(H_2O, l) + \Delta_f H^\circ(C_a H_b O_c) \quad (6)$$

$$= 393.51a + 142.915b + \Delta_f H^\circ(C_a H_b O_c) \quad (7)$$

where $\Delta_f H^\circ$ is the enthalpy of formation. When the heat of formation is not available from the literature, it was estimated based on the structure of the component by using the Joback method which is based on group contribution.^(7, 9)

B.7.3 Combustion of non-condensable gas from torrefaction

Heat generated from combustion of non-condensable gas from torrefaction was estimated using the lower heating value of the components present in the non-condensable gas phase. Severity of torrefaction usually determines the components contained in the non-condensable gas. However, for this study the components were assumed to be essentially CO₂ and CO in an 80 to 20 ratio hence heat released from combustion is due to the CO component only. This assumption is supported by the report of Tumuluru et al. which showed energy released from the combustion of volatiles from torrefaction is mainly from CO.⁽¹⁰⁾

B.7.4 Bioe correlation for heat of combustion estimation

One of the correlations used in Aspen Plus® to estimate the heat of combustion of unconventional solids such as biomass based on the ultimate analysis is as shown:

$$\Delta_c h_i^{dm} = [a_{1i} w_{C,i}^{dm} + a_{2i} w_{H,i}^{dm} + a_{3i} w_{S,i}^{dm} + a_{4i} w_{O,i}^{dm} + a_{5i} w_{N,i}^{dm}] 10^2 + a_{6i} \quad (8)$$

Where $w_{C,i}^{dm}$ is the weight fraction of carbon.

Values of the parameters as given by Aspen Plus® are as follows⁽¹¹⁾

$$a_{1i} = 151.2, a_{2i} = 499.77, a_{3i} = 45.0, a_{4i} = -47.7, a_{5i} = 27.0 \text{ and } a_{6i} = -189$$

B. 8 Enthalpy of reaction (torrefaction & pyrolysis)

The heat of reaction for both processes modeled using a yield reactor was calculated using equation

$$\Delta h_{reaction} = h_{products}^f - h_{reactants}^f$$

Where h^f is the heat of formation.

$$Q_{reaction} = \Delta h_{reaction} + h_{sensible}$$

Where $h_{sensible}$ is the heat required to raise feed to reactor temperature.

SECTION C. INPUT DATA TABLES USED IN MODELING

Table B6. Torrefaction yield data (kg/kg intake pine × 100 %) at different torrefaction temperatures.⁽¹²⁾

Torrefaction Temperature	290°C	310°C	330°C
Material	Wt %		
Gas	6	8	11
Condensed Liquid	17	33	46
Torrefied Solid	78	56	43

Table B7. Torrefaction component distribution (wt % organics) of organics from torrefaction of pine at different torrefaction temperatures.^(12, 13)

Component (wt/wt organics)	Torrefaction temperature		
	290°C	310°C	330°C
Acetic Acid	8.01	11.92	13.09
Propionic Acid	0.25	0.42	0.48
Acetol	2.47	5.08	6.43
Fufural	1.01	1.26	1.95
2-Furanmethanol	0.09	0.11	0.21
5-(hydroxymethyl)-2-furancarboxaldehyde	0.00	0.00	0.00
Levoglucozan	0.40	2.43	3.00
Xylose	0.40	1.22	1.32

Hydrolysable Oligomers(cellobiose)	0.00	0.15	0.36
Glucose	0.10	0.61	0.60
Isoeugenol	0.33	0.76	1.83
Eugenol	0.05	0.13	0.27
Vanillin	0.21	0.32	0.31
2-methoxy-4-vinylphenol(p-vinylguaiacol)	0.00	0.00	0.00
Catechol(benze-1,2-diol)	0.00	0.00	0.00
Phenol	0.00	0.00	0.00
2-methoxyphenol (guaiacol)	0.49	0.83	1.48
4-methylphenol(p-cresol)	0.00	0.00	0.00
3-methylphenol (m-cresol)	0.00	0.00	0.00
4-ethylphenol	0.00	0.00	0.00
2-methoxy-4-methylphenol (creosol)	0.00	0.00	0.00
Low MW Lignin-Derived Compound A(Dimethoxy stilbene	0.95	1.24	1.87
Low MW Lignin Derived Compound B (Dibenzofuran)	0.19	0.25	0.38
High MW Lignin-Derived Compound A	0.79	1.04	1.56
High MW Lignin Derived Compound B	0.17	0.23	0.34

Table B8. Ultimate analysis data (wt %) for torrefied pine chips at different torrefaction temperatures in (14)

Torrefaction Temperature	290°C	310°C	330°C
Element	Value (wt %)		
Ash	0.6	0.6	0.8
Carbon	55.05	57.27	65.75
Hydrogen	5.94	5.79	4.87
Chlorine	-	-	-
Nitrogen	0.11	0.14	0.28
Sulfur	-	-	-
Oxygen	38.3	36.0	27.6

Table B9. Proximate analysis data (wt %) for torrefied pine chips at different torrefaction temperatures in (14)

Torrefaction Temperature	290°C	310°C	330°C
Element	Value (wt %)		
Ash	0.60	0.80	1.4
Moisture Content	0	0	0
Volatile Matter	78.6	76.4	60
Fixed Carbon	20.8	22.8	38.6

Table B10. Pyrolysis yield data (kg/ kg pyrolyzer feed intake × 100 %) for one and two-step pyrolysis taking place at 530°C. (The yields are based on the feed entering the pyrolyzer on a dry ash free basis-one step is raw pine; two-step is torrefied pine)⁽¹²⁾

Material	Wt %			
	One Step	Two Step (290°C)	Two Step (310°C)	Two Step (330°C)
Gas	28	24.4	26.8	23.3
Liquid	59	57.7	46.4	32.6
Solid/Char	10	12.8	23.2	39.5

Table B11. Pyrolysis bio-oil component distribution of organics (wt/wt organics) for one step and two step pyrolysis of pine.^(12, 13)

		One Step (wt/wt organics)	Two Step (wt/wt organics)		
Component	Torrefaction temperature		290°C	310°C	330°C
Acetic Acid		7.59	4.42	2.96	1.11
Propionic Acid		3.69	0.00	0.00	0.00
Acetol		3.11	3.28	2.39	0.85
Fufural		1.00	0.29	0.15	0.38
2-Furanmethanol		0.12	0.07	0.04	0.11

5-(hydroxymethyl)-2-furancarboxaldehyde	0.23	0.28	0.15	0.45
Levogluconan	7.24	7.91	6.04	8.45
Xylose	2.19	2.05	1.01	0.94
Cellobiose	3.29	5.28	4.70	0.00
Glucose	1.10	1.17	0.34	0.00
Isoeugenol	0.54	0.58	0.58	0.50
Eugenol	0.12	0.36	0.20	0.17
Vanillin	0.42	0.14	0.15	0.12
P-vinylguaiacol	0.79	0.37	0.25	0.21
Catechol	2.53	4.88	2.32	2.08
Phenol	0.19	0.33	0.24	0.23
Guaiacol	0.46	0.46	0.37	0.30
P-cresol	0.06	0.12	0.10	0.06
M-cresol	0.02	0.06	0.13	0.09
4-ethylphenol	0.07	0.14	0.05	0.07
Creosol	0.46	0.85	0.50	0.59
Low MW Lignin-Derived Compound A(Dimethoxy stilbene)	7.11	6.50	6.00	3.05
Low MW Lignin Derived Compound B (Dibenzofuran)	1.43	1.31	1.21	0.62
High MW Lignin-Derived Compound A	5.94	5.43	5.02	2.55
High MW Lignin Derived Compound B	1.30	1.18	1.10	0.56

Table B12. Ultimate and proximate analysis (wt %) for raw pine chips.

Ultimate Analysis		Proximate Analysis (wet basis)	
Element	Value (wt %)	Element	Value (wt %)
Ash	0.6	Ash	0.60
Carbon	50.45	Moisture Content	25
Hydrogen	6.26	Volatile Matter	84.6
Chlorine	-	Fixed Carbon	14.8
Nitrogen	0.09		
Sulfur	-		
Oxygen	42.6		

Table B13. Ultimate and proximate data (wt %) for char obtained after pyrolysis.

Ultimate Analysis		Proximate Analysis	
Components	Wt. %	Components	Wt. %
Ash	7.67	Ash	4.60
Carbon	83.03	Moisture Content	-
Hydrogen	1.14	Volatile matter	7.40
Nitrogen	1.37	Fixed carbon	88.0
Chlorine	-		
Sulfur	-		
Oxygen	6.56		

SECTION D: INVENTORY DATA TABLE FOR BIOMASS CONVERSION

Table B14. Life cycle inventory to produce 1MJ of bio-oil for RMBY of a one-step conversion

Products		
Bio-oil	1	MJ
Char (combusted in the process)	0.09	kg
Material Inputs		
Pine (8% moisture content)	0.095	kg
Water, completely softened, at plant	9.4	kg
Process Inputs or Displaced Products (negative values)		
Electricity, medium voltage US (size reduction)	0.039	kWh
Natural gas, burned in industrial furnace low-NO _x > 100kW (biomass drying)	0.035	MJ
Natural gas, burned in industrial furnace low-NO _x > 100kW (pyrolysis)	0	MJ
Bituminous coal, combusted in industrial boiler NREL/US	0	kg

Table B15. Life cycle inventory to produce 1MJ of bio-oil for a two-step conversion, FMBY at torrefaction temperature of 290°C (biomass conversion step)

Products		
Bio-oil (pyrolysis)	0.745	MJ
Bio-oil (torrefaction)	0.255	MJ
Char (exported to displace coal)	0.009	kg
Non-condensable gases (pyrolysis – recycled for fluidizing)		
Non-condensable gases (torrefaction – combusted internally)	0.015	kg
Material Inputs		
Pine (8% moisture content)	0.094	Kg
Water, completely softened, at plant (pyrolysis)	6.1	Kg
Water, completely softened, at plant (torrefaction)	2.02	Kg
Process Inputs or Displaced Products (negative values)		
Electricity, medium voltage US (size reduction)	0.004	kWh
Natural gas, burned in industrial furnace low-NOx> 100kW (biomass drying)	0.089	MJ
Natural gas, burned in industrial furnace low-NOx> 100kW (torrefaction)	0.094	MJ
Natural gas, burned in industrial furnace low-NOx> 100kW (pyrolysis)	0.099	MJ
Bituminous coal, combusted in industrial boiler NREL/US	-0.008	Kg

Table B16. Life cycle inventory to produce 1MJ of bio-oil for a two-step conversion, RMBY at torrefaction temperature of 290°C (biomass conversion step)

Products		
Bio-oil (pyrolysis)	0.747	MJ
Bio-oil (torrefaction)	0.253	MJ
Char (combusted in the process)	0.009	Kg
Non-condensable gases (pyrolysis – recycled for fluidizing)		
Non-condensable gases (torrefaction – combusted internally)	0.015	Kg
Material Inputs		
Pine (8% moisture content)	0.094	Kg
Water, completely softened, at plant (pyrolysis)	6.1	Kg
Water, completely softened, at plant (torrefaction)	2.02	Kg
Process Inputs or Displaced Products (negative values)		
Electricity, medium voltage US (size reduction)	0.004	kWh
Natural gas, burned in industrial furnace low-NOx> 100kW (biomass drying)	0	MJ
Natural gas, burned in industrial furnace low-NOx> 100kW (torrefaction)	0	MJ
Natural gas, burned in industrial furnace low-NOx> 100kW (pyrolysis)	0.079	MJ
Bituminous coal, combusted in industrial boiler NREL/US	0	Kg

Table B17. Life cycle inventory to produce 1MJ of bio-oil for a two-step conversion, RMBQ at torrefaction temperature of 290°C (biomass conversion step)

Products		
Bio-oil (pyrolysis)	1	MJ
Bio-oil (torrefaction)	-	MJ
Char (exported to displace coal)	0.011	Kg
Non-condensable gases (pyrolysis – recycled for fluidizing)		
Non-condensable gases (torrefaction – combusted internally)	0.021	Kg
Material Inputs		
Pine (8% moisture content)	0.126	Kg
Water, completely softened, at plant (pyrolysis)	8.31	Kg
Water, completely softened, at plant (torrefaction)	2.71	Kg
Process Inputs or Displaced Products (negative values)		
Electricity, medium voltage US (size reduction)	0.006	kWh
Natural gas, burned in industrial furnace low-NOx> 100kW (biomass drying)	0	MJ
Natural gas, burned in industrial furnace low-NOx> 100kW (torrefaction)	0	MJ
Natural gas, burned in industrial furnace low-NOx> 100kW (pyrolysis)	0	MJ
Bituminous coal, combusted in industrial boiler NREL/US	-0.010	Kg

Table B18. Life cycle inventory to produce 1MJ of bio-oil for a two-step conversion, FMBY at torrefaction temperature of 310°C (biomass conversion step)

Products		
Bio-oil (pyrolysis)	0.486	MJ
Bio-oil (torrefaction)	0.514	MJ
Char (exported to displace coal)	0.013	Kg
Non-condensable gases (pyrolysis – recycled for fluidizing)		
Non-condensable gases (torrefaction – combusted internally)	0.020	Kg
Material Inputs		
Pine (8% moisture content)	0.105	Kg
Water, completely softened, at plant (pyrolysis)	4.78	Kg
Water, completely softened, at plant (torrefaction)	3.40	Kg
Process Inputs or Displaced Products (negative values)		
Electricity, medium voltage US (size reduction)	0.002	kWh
Natural gas, burned in industrial furnace low-NOx> 100kW (biomass drying)	0.1	MJ
Natural gas, burned in industrial furnace low-NOx> 100kW (torrefaction)	0.063	MJ

Natural gas, burned in industrial furnace low-NO _x > 100kW (pyrolysis)	0.115	MJ
Bituminous coal, combusted in industrial boiler NREL/US	-0.012	Kg

Table B19. Life cycle inventory to produce 1MJ of bio-oil for a two-step conversion, RMBY at torrefaction temperature of 310°C (biomass conversion step)

Products		
Bio-oil (pyrolysis)	0.486	MJ
Bio-oil (torrefaction)	0.514	MJ
Char (Combusted, with excess exported to displace coal)	0.013	Kg
Non-condensable gases (pyrolysis – recycled for fluidizing)		
Non-condensable gases (torrefaction – combusted internally)	0.020	Kg
Material Inputs		
Pine (8% moisture content)	0.105	Kg
Water, completely softened, at plant (pyrolysis)	4.78	Kg
Water, completely softened, at plant (torrefaction)	3.40	Kg
Process Inputs or Displaced Products (negative values)		
Electricity, medium voltage US (size reduction)	0.002	kWh
Natural gas, burned in industrial furnace low-NO _x > 100kW (biomass drying)	0	MJ
Natural gas, burned in industrial furnace low-NO _x > 100kW (torrefaction)	0	MJ
Natural gas, burned in industrial furnace low-NO _x > 100kW (pyrolysis)	0	MJ
Bituminous coal, combusted in industrial boiler NREL/US	-0.004	Kg

Table B20. Life cycle inventory to produce 1MJ of bio-oil for a two-step conversion, RMBQ at torrefaction temperature of 310°C (biomass conversion step)

Products		
Bio-oil (pyrolysis)	0.657	MJ
Bio-oil (torrefaction)	0.343	MJ
Char (Combusted, with excess exported to displace coal)	0.018	Kg
Non-condensable gases (pyrolysis – recycled for fluidizing)		
Non-condensable gases (torrefaction – combusted internally)	0.027	Kg
Material Inputs		
Pine (8% moisture content)	0.142	Kg
Water, completely softened, at plant (pyrolysis)	6.45	Kg
Water, completely softened, at plant (torrefaction)	4.59	Kg
Process Inputs or Displaced Products (negative values)		
Electricity, medium voltage US (size reduction)	0.003	kWh
Natural gas, burned in industrial furnace low-NO _x > 100kW (biomass drying)	0	MJ

Natural gas, burned in industrial furnace low-NO _x > 100kW (torrefaction)	0	MJ
Natural gas, burned in industrial furnace low-NO _x > 100kW (pyrolysis)	0	MJ
Bituminous coal, combusted in industrial boiler NREL/US	-0.017	Kg

Table B21. Life cycle inventory to produce 1MJ of bio-oil for a two-step conversion, FMBY at torrefaction temperature of 330°C (biomass conversion step)

Products		
Bio-oil (pyrolysis)	0.251	MJ
Bio-oil (torrefaction)	0.749	MJ
Char (exported to displace coal)	0.019	Kg
Non-condensable gases (pyrolysis – recycled for fluidizing)		
Non-condensable gases (torrefaction – combusted internally)	0.016	Kg
Material Inputs		
Pine (8% moisture content)	0.113	Kg
Water, completely softened, at plant (pyrolysis)	3.50	Kg
Water, completely softened, at plant (torrefaction)	4.60	Kg
Process Inputs or Displaced Products (negative values)		
Electricity, medium voltage US (size reduction)	0.001	kWh
Natural gas, burned in industrial furnace low-NO _x > 100kW (biomass drying)	0.104	MJ
Natural gas, burned in industrial furnace low-NO _x > 100kW (torrefaction)	0.125	MJ
Natural gas, burned in industrial furnace low-NO _x > 100kW (pyrolysis)	0.058	MJ
Bituminous coal, combusted in industrial boiler NREL/US	-0.017	Kg

Table B22. Life cycle inventory to produce 1MJ of bio-oil for a two-step conversion, RMBY at torrefaction temperature of 330°C (biomass conversion step)

Products		
Bio-oil (pyrolysis)	0.251	MJ
Bio-oil (torrefaction)	0.749	MJ
Char (Combusted, with excess exported to displace coal)	0.019	Kg
Non-condensable gases (pyrolysis – recycled for fluidizing)		
Non-condensable gases (torrefaction – combusted internally)	0.016	Kg
Material Inputs		
Pine (8% moisture content)	0.113	Kg
Water, completely softened, at plant (pyrolysis)	3.50	Kg
Water, completely softened, at plant (torrefaction)	4.60	Kg
Process Inputs or Displaced Products (negative values)		
Electricity, medium voltage US (size reduction)	0.001	kWh

Natural gas, burned in industrial furnace low-NO _x > 100kW (biomass drying)	0	MJ
Natural gas, burned in industrial furnace low-NO _x > 100kW (torrefaction)	0	MJ
Natural gas, burned in industrial furnace low-NO _x > 100kW (pyrolysis)	0	MJ
Bituminous coal, combusted in industrial boiler NREL/US	-0.009	Kg

Table B23. Life cycle inventory to produce 1MJ of bio-oil for a two-step conversion, RMBQ at torrefaction temperature of 330°C (biomass conversion step)

Products		
Bio-oil (pyrolysis)	0.345	MJ
Bio-oil (torrefaction)	0.655	MJ
Char (Combusted, with excess exported to displace coal)	0.026	Kg
Non-condensable gases (pyrolysis – recycled for fluidizing)		
Non-condensable gases (torrefaction – combusted internally)	0.022	Kg
Material Inputs		
Pine (8% moisture content)	0.156	Kg
Water, completely softened, at plant (pyrolysis)	4.80	Kg
Water, completely softened, at plant (torrefaction)	6.32	Kg
Process Inputs or Displaced Products (negative values)		
Electricity, medium voltage US (size reduction)	0.001	kWh
Natural gas, burned in industrial furnace low-NO _x > 100kW (biomass drying)	0	MJ
Natural gas, burned in industrial furnace low-NO _x > 100kW (torrefaction)	0	MJ
Natural gas, burned in industrial furnace low-NO _x > 100kW (pyrolysis)	0	MJ
Bituminous coal, combusted in industrial boiler NREL/US	-0.023	Kg

SECTION E: SAMPLE CALCULATION OF THE LHV OF BIO-OIL OBTAINED FROM SIMULATION FOR A ONE-STEP PYROLYSIS PATHWAY

Table B24. Calculated allocation factors for energy allocation approach. Torrefaction temperatures shown for two-step processes

Scenario	One-step	Two-step		
		290°C	310°C	330°C
1	0.785	0.789	0.713	0.641
2	1.000	1.000	0.874	0.777
3		0.747	0.647	0.566

Table B25. Sample calculation of the LHV of bio-oil for one-step conversion pathway using the heat of combustion of representative compounds found in the literature.

	wt frac	Heat of combustion (MJ/kg)	Heat of combustion	Source
N2	0.00039	-	0	
CO2	0.001039	-	0	
CO	0.000117	-	0	
H2	0	-	0	
CH4	0	-	0	
C2H6	0	-	0	
H2O	0.221533	-	0	(7)
ACETIC ACID	0.109078	-13.5647	-1.47961	(7)
PROPIONIC ACID	0.056227	-18.8312	-1.05883	(7)
ACETOL	0.047267	-22.5708	-1.06686	*
ISOEUGENOL	0.008311	-32.6024	-0.27095	(15)
EUGENOL	0.001818	-32.8317	-0.05969	(15)
VANILLIN	0.006493	-25.1678	-0.16341	(15)
P-VINYLGUAIACOL	0.012206			
CATECHOL (BENZE-1,2 DIOL)	0.037528	-26.03	-0.97685	
PHENOL	0.002987	-31.0372	-0.0927	(7)
GUAIACOL	0.007142			
P-CRESOL	0.001039	-32.5741	-0.03384	(7)
M-CRESOL	0.00026	-32.6228	-0.00847	(7)
4-ETYLPHENOL	0.001039	-35.6322	-0.03702	(16)
O-CRESOL	0.007272	-32.6244	-0.23724	(7)
FUFURAL	0.014154	-24.3674	-0.3449	(16)
2-FURANMETHANOL	0.001818	-26.0091	-0.04728	(16)

5-(HYDROXYMETHYL)-2-FURANCARBOXALDEHYDE	0.00350 6		0	
LEVOGLUCOSAN	0.11219 5	-17.4747	-1.96056	(16)
XYLOSE	0.03402 2	-15.5924	-0.53048	(16)
CELLBOISE	0.05103 3	-16.4864	-0.84135	(16)
GLUCOSE	0.01701 1	-15.6072	-0.26549	(16)
LOW MW LIGNIN DERIVED COMPOUND A (DIMETHOXY STILBENZENE)	0.11024 7	-35.4908	-3.91275	*
LOW MW LIGNIN DERIVED COMPOUND B (DIBENZOFURANN)	0.02220 5	-35.2318	-0.78233	*
HIGH MW LIGNIN DERIVED COMPOUND A	0.09206 7	-26.4613	-2.43622	*
HIGH MW LIGNIN DERIVED COMPOUND B	0.01999 8	-26.6643	-0.53322	*
Total	1	LHV	-17.1401	

- Calculated based on the composition of carbon, hydrogen, and oxygen using the method described in section B above.

$$\Delta_c H^\circ = 393.51a + 142.915b + \Delta_f H^\circ(C_a H_b O_c)$$

Acetol – C₃H₆O₂ (74.049g/mol)

$$\begin{aligned} \Delta_c H^\circ (\text{Acetol}) &= (393.51 * 3) + (142.915 * 6) + (-366) \\ &= -1672.02 \text{ kJ/mol} \\ &= - 22.57 \text{ MJ/kg} \end{aligned}$$

B.2 References

1. Wang M. The Greenhouse Gases, Regulated Emissions, and Energy Use in Transportation (GREET) Model: Version 1.5. Center for Transportation Research, Argonne National Laboratory. 2008.
2. Maleche E. Life cycle assessment of biofuels produced by the new integrated hydrolysis-hydroconversion (IH 2) process. 2012.
3. Handler RM, Shonnard DR, Lautala P, Abbas D, Srivastava A. Environmental impacts of roundwood supply chain options in Michigan: Life-cycle assessment of harvest and transport stages. *Journal of Cleaner Production*. 2014;76:64-73.
4. Phanphanich M, Mani S. Impact of torrefaction on the grindability and fuel characteristics of forest biomass. *Bioresource technology*. 2011;102(2):1246-53.
5. Koppejan J, Van Loo S. *The handbook of biomass combustion and co-firing*: Routledge; 2012.
6. Gaur S, Reed TB. *An atlas of thermal data for biomass and other fuels*. National Renewable Energy Lab., Golden, CO (United States), 1995.
7. Perry RH, Green DW, Maloney JO, Abbott MM, Ambler CM, Amero RC. *Perry's chemical engineers' handbook*: McGraw-hill New York; 1997.
8. Haynes WM. *CRC handbook of chemistry and physics*: CRC press; 2013.
9. Joback KG, Reid RC. Estimation of pure-component properties from group-contributions. *Chemical Engineering Communications*. 1987;57(1-6):233-43.
10. Shankar Tumuluru J, Sokhansanj S, Hess JR, Wright CT, Boardman RD. REVIEW: A review on biomass torrefaction process and product properties for energy applications. *Industrial Biotechnology*. 2011;7(5):384-401.

11. Plus A. Aspen Technology. Inc, version. 2009;11.
12. Westerhof RJ, Brilman DWF, Garcia-Perez M, Wang Z, Oudenhoven SR, Kersten SR. Stepwise fast pyrolysis of pine wood. *Energy & Fuels*. 2012;26(12):7263-73.
13. Zheng A, Zhao Z, Chang S, Huang Z, He F, Li H. Effect of Torrefaction Temperature on Product Distribution from Two-Staged Pyrolysis of Biomass. *Energy & Fuels*. 2012;26(5):2968-74.
14. Park J, Meng J, Lim KH, Rojas OJ, Park S. Transformation of lignocellulosic biomass during torrefaction. *Journal of Analytical and Applied Pyrolysis*. 2013;100:199-206.
15. Kharasch MS. Heats of combustion of organic compounds: US Government Printing Office; 1929.
16. Domalski ES. Selected Values of Heats of Combustion and Heats of Formation of Organic Compounds Containing the Elements C, H, N, O, P, and S. *Journal of Physical and Chemical Reference Data*. 1972;1(2):221-77.

Appendix C: Production of Hydrocarbon Fuel using Two-Step Torrefaction and Fast Pyrolysis of Pine. Part 1: Techno-economic Analysis

C.1 Supplementary material from Chapter 4

Section A. MODEL DESCRIPTION OF SOME UNIT OPERATIONS

This section and its sub-sections were presented in our prior study.¹

A.1 Drying

Biomass inherently contains moisture, and it is assumed here that the delivered pine wood has a moisture content of about 25% which will be dried to about 7% which is recommended for fast pyrolysis. The set-up in this study has the drying step prior to size reduction for a couple of reasons that includes being able to gain the benefit of reduced energy requirement as a result of a torrefaction pre-treatment step and also prevent plugging of screens. Moisture content higher than 15% may affect the size reduction step due to plugging or blinding of the small diameter screen openings that would be employed to attain the desired particle size. The drying step will be modeled in Aspen Plus using a stoichiometric reactor and a STEAM thermodynamic package. This calculates the energy required for drying by estimating the specific energy required to raise the temperature of the biomass and its inherent moisture to the target temperature, and also the latent heat required to vaporize the moisture in the biomass.

A.2 Size Reduction

The correlation obtained from literature given as follows for pine was used in evaluating the reduction in energy consumption to attain required size to effect fast pyrolysis.²

$$E_g = -0.756T + 260.0 \quad (1)$$

where E_g is specific energy consumption for grinding in kW-hr/ton, T is Temperature in °C

The size reduction step was then modeled in Aspen Plus® as a hammer mill with the estimated specific energy consumed for grinding estimated at different torrefaction temperatures, while the untreated raw pine's energy was estimated using ambient temperature of 25°C.

Work index, a function of the specific energy consumption, as well as the initial and final biomass particle size is required to model the size reduction step. The work index required for grinding was calculated from the specific energy (calculated in equation 1) and size of initial and final biomass particle using equation 2.

$$E_g = 10 * W_i * \left(\frac{1}{\sqrt{P}} - \frac{1}{\sqrt{F}} \right) \quad (2)$$

where E_g is specific energy consumption for grinding in kW-hr/ton, W_i is work index in kW-hr/ton, P is final particle size in microns and F is Initial particle size in microns

A.3 Combustion

Combustion of products, when considered in this study, was not modeled using the process simulation software. However, the heat released during combustion were estimated from correlations obtained from the literature as shown below:

A.3.1 Combustion of char

Heat released from the combustion of char was evaluated based on the lower heating value of char, which was estimated from its higher heating value based on correlation from literature given below:³

$$LHV = HHV \left(1 - \frac{w}{100}\right) - 2.444 * \frac{w}{100} - 2.444 * \frac{h}{100} * 8.936 \left(1 - \frac{w}{100}\right) \left[\frac{MJ}{kg}, w. b.\right]$$

(3)

Where

2.444 = enthalpy difference between gaseous and liquid water at 25°C

8.936 = M_{H_2O}/M_{H_2} ; i.e. the molecular mass ratio between H₂O and H₂

LHV = lower heating value

HHV = higher heating value

w = moisture content of the fuel in wt% (wet basis)

h = concentration of hydrogen in wt% (dry basis)

The higher heating value utilized in the equation above was also estimated from empirical formula as well as shown below.⁴

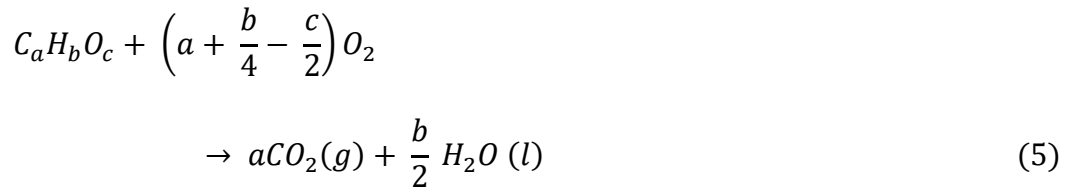
$$HHV = 0.3491X_C + 1.1783X_H + 0.1005X_S - 0.0151X_N - 0.1034X_O - 0.0211X_{ash} \left[\frac{MJ}{kg}, d. b. \right] \quad (4)$$

X_i is the content of carbon (C), hydrogen (H), sulfur (S), nitrogen (N), oxygen (O), etc. from the ultimate analysis of the solid fuel.

A.3.2 Combustion of condensates from torrefaction

The energy released from the combustion of condensates from torrefaction when such steps take place in this study was estimated by obtaining from literature the lower heating value of the individual components in the condensates.⁵ Based on the lower heating value of the individual components and their weight fraction in the liquid, the lower heating value of the liquid was estimated. For high molecular compounds produced from either the torrefaction or pyrolysis step whose lower heating values were not found in the literature, their lower heating values were estimated using correlation obtained from the literature as shown below:⁶

For compounds containing only carbon, hydrogen and oxygen, a general combustion reaction was given as



The standard heat of combustion is then given as

$$\Delta_c H^\circ = -a\Delta_f H^\circ(CO_2, g) - \frac{1}{2}b\Delta_f H^\circ(H_2O, l) + \Delta_f H^\circ(C_a H_b O_c)$$

(6)

$$= 393.51a + 142.915b + \Delta_f H^\circ(C_a H_b O_c)$$

(7)

where $\Delta_f H^\circ$ is the enthalpy of formation. When the heat of formation is not available from literature, it was estimated based on the structure of the component by using the Joback method which is based on group contribution.^{5,7}

A.3.3 Combustion of non-condensable gas from torrefaction

Heat generated from combustion of non-condensable gas from torrefaction was estimated using the lower heating value of the components present in the non-condensable gas phase. Severity of torrefaction usually determines the components contained in the non-condensable gas. However for this study, the components were assumed to be essentially CO₂, and CO in an 80 to 20 ratio hence heat released from combustion is due to the CO component only, and this assumption is supported by the report of Tumuluru et al. which showed energy released from the combustion of volatiles from torrefaction is mainly from CO.⁸

A.3.4 Boie correlation for heat of combustion estimation

One of the correlations used in Aspen Plus® to estimate the heat of combustion of unconventional solids such as biomass based on the ultimate analysis is as shown⁹:

$$\Delta_c h_i^{dm} = [a_{1i}w_{C,i}^{dm} + a_{2i}w_{H,i}^{dm} + a_{3i}w_{S,i}^{dm} + a_{4i}w_{O,i}^{dm} + a_{5i}w_{N,i}^{dm}]10^2 + a_{6i} \quad (8)$$

Where $w_{c,i}^{dm}$ is the weight fraction of carbon.

Values of the parameters as given by Aspen Plu® are as follows¹⁰

$$a_{1i} = 151.2, a_{2i} = 499.77, a_{3i} = 45.0, a_{4i} = -47.7, a_{5i} = 27.0 \text{ and } a_{6i} = -189$$

A.4 Conveyance

Biomass movement across the plant is assumed to be carried out using conveyor belts, and the energy required for this conveyance was estimated by firstly using the guidelines as shown by Couper et al.^{11,12} The conveyance is assumed to be carried out using a 24 inch, 45° troughed belt conveyor of length, 33.5m and up a longitudinal incline of 22°. The running angle of repose of the woodchips is taken to be about 30° and the required power is estimated by using equation 7.

$$Power (hp) = P_{horizontal} + P_{vertical} + P_{empty} \quad (9)$$

Where $P_{horizontal} = (0.4+L/300)(W/100)$, $P_{vertical} = 0.001HW$, and P_{empty} obtained based on desired conveyor length from literature.¹²

SECTION B. INPUT DATA TABLES USED IN MODELING

Tables C1 to C7 found in this section were presented in our prior study, but repeated here for completeness.¹

Table C1. Component distribution of organics for one step and two step pyrolysis of pine.^{13,14}

		One Step	Two Step		
Component (wt %)	Torrefaction temperature		290°C	310°C	330°C
Acetic Acid		7.59	4.42	2.96	1.11
Propionic Acid		3.69	0.00	0.00	0.00
Acetol		3.11	3.28	2.39	0.85

Fufural	1.00	0.29	0.15	0.38
2-Furanmethanol	0.12	0.07	0.04	0.11
5-(hydroxymethyl)-2-furancarboxaldehyde	0.23	0.28	0.15	0.45
Levoglucosan	7.24	7.91	6.04	8.45
Xylose	2.19	2.05	1.01	0.94
Cellobiose	3.29	5.28	4.70	0.00
Glucose	1.10	1.17	0.34	0.00
Isoeugenol	0.54	0.58	0.58	0.50
Eugenol	0.12	0.36	0.20	0.17
Vanillin	0.42	0.14	0.15	0.12
P-vinylguaiacol	0.79	0.37	0.25	0.21
Catechol	2.53	4.88	2.32	2.08
Phenol	0.19	0.33	0.24	0.23
Guaiacol	0.46	0.46	0.37	0.30
P-cresol	0.06	0.12	0.10	0.06
M-cresol	0.02	0.06	0.13	0.09
4-ethylphenol	0.07	0.14	0.05	0.07
Creosol	0.46	0.85	0.50	0.59
Low MW Lignin Derived Compound A (Dimethoxy stilbenzene)	7.11	6.50	6.00	3.05
Low MW Lignin Derived Compound B (Dibenzofuran)	1.43	1.31	1.21	0.62
High MW Lignin Derived Compound A	5.94	5.43	5.02	2.55
High MW Lignin Derived Compound B	1.30	1.18	1.10	0.56

Table C2. Ultimate analysis data for torrefied pine chips at different torrefaction temperatures.¹⁵

Torrefaction Temperature	Raw pine	290°C	310°C	330°C
Component	Wt %			
Ash	0.6	0.6	0.6	0.8
Carbon	50.45	55.05	57.27	65.75
Hydrogen	6.26	5.94	5.79	4.87
Chlorine	-	-	-	-
Nitrogen	0.09	0.11	0.14	0.28
Sulfur	-	-	-	-

Oxygen	42.6	38.3	36.0	27.6
--------	------	------	------	------

Table C3. Proximate analysis data for torrefied pine chips at different torrefaction temperatures.¹⁵

Torrefaction Temperature	Raw pine	290°C	310°C	330°C
Component	Wt %			
Ash	0.6	0.60	0.80	1.4
Moisture Content	25	0	0	0
Volatile Matter	84.6	78.6	76.4	60
Fixed Carbon	14.8	20.8	22.8	38.6

Table C4. Product distribution for organics from torrefaction of pine at different torrefaction temperatures.^{13,14}

Component (wt %)	290°C	310°C	330°C
Acetic Acid	8.01	11.92	13.09
Propionic Acid	0.25	0.42	0.48
Acetol	2.47	5.08	6.43
Fufural	1.01	1.26	1.95
2-Furanmethanol	0.09	0.11	0.21
5-(hydroxymethyl)-2-furancarboxaldehyde	0.00	0.00	0.00
Levoglucosan	0.40	2.43	3.00
Xylose	0.40	1.22	1.32
Hydrolysable Oligomers(cellobiose)	0.00	0.15	0.36
Glucose	0.10	0.61	0.60
Isoeugenol	0.33	0.76	1.83
Eugenol	0.05	0.13	0.27
Vanillin	0.21	0.32	0.31
2-methoxy-4-vinylphenol(p-vinylguaiacol)	0.00	0.00	0.00
Catechol(benze-1,2-diol)	0.00	0.00	0.00
Phenol	0.00	0.00	0.00
2-methoxyphenol (guaiacol)	0.49	0.83	1.48
4-methylphenol(p-cresol)	0.00	0.00	0.00

3-methylphenol (m-cresol)	0.00	0.00	0.00
4-ethylphenol	0.00	0.00	0.00
2-methoxy-4-methylphenol (creosol)	0.00	0.00	0.00
Low MW Lignin Derived Compound A(Dimethoxy stilbenzene)	0.95	1.24	1.87
Low MW Lignin Derived Compound B (Dibenzofuran)	0.19	0.25	0.38
High MW Lignin Derived Compound A	0.79	1.04	1.56
High MW Lignin Derived Compound B	0.17	0.23	0.34

Table C5. Ultimate and proximate data for char obtained after pyrolysis.

Ultimate Analysis		Proximate Analysis	
Components	Wt. %	Components	Wt. %
Ash	7.67	Ash	4.60
Carbon	83.03	Moisture Content	-
Hydrogen	1.14	Volatile matter	7.40
Nitrogen	1.37	Fixed carbon	88.0
Chlorine	-		
Sulfur	-		
Oxygen	6.56		

Table C6. Estimated number of employees and their wages rate.

Employee	Annual Salary	Number Required
Plant/General Manager	\$136,830.00	1
Plant Engineer	\$108,630.00	1
Maintenance Supervisor	\$76,480.00	1
Lab Manager/Chemist	\$77,970.00	1
Shift Supervisor	\$74,470.00	5
Maintenance Tech	\$70,450.00	6
Shift Operators	\$55,980.00	23
Admin Assistants	\$43,440.00	2

Table C7. Yield factors for upgrade step for the one-step pathway.

Stabilizer		Hydrotreater	
Component	(wt. %)	Component	(wt. %)
N2	0.033	N2	0.033
CO2	0.068	CO2	0.068
CO	0.001	CO	0.895
H2	14.708	H2	9.743
H2O	21.247	CH4	2.637
Acetaldehyde	6.574	C2H6	5.098
Propanal	3.784	H2O	45.227
Propylene Glycol	4.170	Propane	5.475
Isoeugenol	0.724	Butane	1.851
Eugenol	0.158	Pentane	0.291
Vanillyl alcohol	0.575	Hexane	8.186
Vinylguaiacol	1.071	Cyclohexane	3.895
Catechol	3.294	Methylcyclohexane	5.954
Phenol	0.257	Ethylcyclohexane	0.755
Guaiacol	0.628	Propylcyclohexane	1.794
4-methylphenol	0.087	Benzene	1.477
3-methylphenol	0.026	Toulene	4.573
4-ethylphenol	0.096	Propylbenzene	1.107
2-methoxy-4-methylphenol	0.636	Vinylbenzene	0.334
Furfural	1.155	Propenylbenzene	0.301

2-Furanmethanol	0.15 2	Ethylbenzene	0.24 4
5-Hydromethylfufural	0.31 3		
Levoglucosan	9.84 1		
Xylose	2.98 2		
Cellobiose	4.47 3		
Glucose	1.49 1		
Low MW Lignin Derived Compound A(Dimethoxy stilbene C16H16O2)	9.66 9		
Low MW Lignin Derived Compound B (Dibenzofuran)	1.95 1		
High MW Lignin Derived Compound A (C20H26O8) [‡]	8.07 9		
High MW Lignin Derived Compound B (C21H26O8) [‡]	1.75 7		

[‡] Chemical structure obtained from literature

Table C8. Yield factors for upgrade step for scenario 1 of a two-step pathway at torrefaction temperature of 290°C.

Stabilizer		Hydrotreater	
Component	(wt. %)	Component	(wt. %)
N2	0.03 8	N2	0.03 8
CO2	0.17 4	CO	0.93 0
CO	0.00 3	CO2	0.17 4
H2	14.6 47	H2	9.99 6
H2O	24.9 78	CH4	2.12 4
Acetaldehyde	9.61 0	C2H6	7.02 1
Propanal	0.23 2	H2O	48.1 29
Propylene Glycol	6.10 6	Propane	3.85 6

Isoeugenol	0.94 2	Butane	1.79 9
Eugenol	0.40 1	Pentane	0.27 6
Vanillyl alcohol	0.36 3	Hexane	7.43 5
Vinylguaiacol	0.35 4	Cyclohexane	4.14 0
Catechol	4.69 3	Methylcyclohexane	4.67 6
Phenol	0.31 3	Ethylcyclohexane	0.41 4
Guaiacol	1.01 4	Propylcyclohexane	1.64 9
4-methylphenol	0.11 1	Benzene	2.01 7
3-methylphenol	0.05 5	Toulene	3.59 2
4-ethylphenol	0.13 0	Propylbenzene	0.82 9
2-methoxy-4-methylphenol	0.81 6	Vinylbenzene	0.11 0
Furfural	1.41 5	propenylbenzene	0.43 5
2-Furanmethanol	0.16 9	Ethylbenzene	0.20 8
5-Hydromethylfufural	0.26 5		
Levoglucozan	8.07 9		
Xylose	2.44 1		
Cellobiose	5.07 4		
Glucose	1.24 5		
Low MW Lignin Derived Compound A(Dimethoxy stilbene C ₁₆ H ₁₆ O ₂)	7.36 0		
Low MW Lignin Derived Compound B (Dibenzofuran)	1.48 5		
High MW Lignin Derived Compound A (C ₂₀ H ₂₆ O ₈)	6.15 0		
High MW Lignin Derived Compound B (C ₂₁ H ₂₆ O ₈)	1.33 8		

Table C9. Yield factors for upgrade step for scenario 3 of a two-step pathway at torrefaction temperature of 290°C.

Stabilizer		Hydrotreater	
Component	(wt. %)	Component	(wt. %)
N2	0.027	N2	0.027
CO2	0.061	CO	0.794
CO	0.001	CO2	0.061
H2	14.919	H2	9.561
H2O	15.224	CH4	2.732
Acetaldehyde	4.441	C2H6	3.656
Propanal	0.000	H2O	42.442
Propylene Glycol	4.969	Propane	3.071
Isoeugenol	0.885	Butane	1.450
Eugenol	0.548	Pentane	0.315
Vanillyl alcohol	0.213	Hexane	11.267
Vinylguaiacol	0.559	Cyclohexane	5.815
Catechol	7.414	Methylcyclohexane	6.276
Phenol	0.495	Ethylcyclohexane	0.606
Guaiacol	0.699	Propylcyclohexane	2.057
4-methylphenol	0.175	Benzene	2.903
3-methylphenol	0.088	Toulene	4.820
4-ethylphenol	0.205	Propylbenzene	1.112
2-methoxy-4-methylphenol	1.290	Vinylbenzene	0.174

Furfural	0.40 5	propenylbenzene	0.46 4
2-Furanmethanol	0.10 3	Ethylbenzene	0.29 1
5-Hydromethylfufural	0.41 8		
Levoglucosan	12.0 25		
Xylose	3.11 8		
Cellobiose	8.01 7		
Glucose	1.78 1		
Low MW Lignin Derived Compound A(Dimethoxy stilbene C16H16O2)	9.87 9		
Low MW Lignin Derived Compound B (Dibenzofuran)	1.99 4		
High MW Lignin Derived Compound A (C20H26O8)	8.25 5		
High MW Lignin Derived Compound B (C21H26O8)	1.79 5		

Table C10. Yield factors for upgrade step for scenario 1 of a two-step pathway at torrefaction temperature of 310°C.

Stabilizer		Hydrotreater	
Component	(wt. %)	Component	(wt. %)
N2	0.03 9	N2	0.03 9
CO2	0.27 0	CO	0.94 6
CO	0.00 5	CO2	0.27 0
H2	14.4 48	H2	10.0 31
H2O	28.0 86	CH4	1.83 7

Acetaldehyde	12.4 23	C2H6	8.85 1
Propanal	0.42 2	H2O	50.5 46
Propylene Glycol	8.36 3	Propane	5.27 9
Isoeugenol	1.39 7	Butane	1.90 1
Eugenol	0.30 6	Pentane	0.18 0
Vanillyl alcohol	0.52 2	Hexane	6.31 1
Vinylguaiacol	0.18 2	Cyclohexane	2.62 6
Catechol	1.70 5	Methylcyclohexane	3.80 8
Phenol	0.17 4	Ethylcyclohexane	0.25 7
Guaiacol	1.32 5	Propylcyclohexane	1.59 9
4-methylphenol	0.07 3	Benzene	1.07 8
3-methylphenol	0.09 2	Toulene	2.92 5
4-ethylphenol	0.03 4	Propylbenzene	0.67 4
2-methoxy-4-methylphenol	0.43 9	Vinylbenzene	0.05 7
Furfural	1.68 4	propenylbenzene	0.55 2
2-Furanmethanol	0.16 2	Ethylbenzene	0.14 1
5-Hydromethylfufural	0.10 6		
Levoglucozan	7.52 2		
Xylose	2.28 3		
Cellobiose	3.64 1		
Glucose	1.01 9		
Low MW Lignin Derived Compound A(Dimethoxy stilbene C16H16O2)	5.98 3		

Low MW Lignin Derived Compound B (Dibenzofuran)	1.20 7		
High MW Lignin Derived Compound A (C ₂₀ H ₂₆ O ₈)	4.99 9		
High MW Lignin Derived Compound B (C ₂₁ H ₂₆ O ₈)	1.08 7		

Table C11. Yield factors for upgrade step for scenario 3 of a two-step pathway at torrefaction temperature of 310°C.

Stabilizer		Hydrotreater	
Component	(wt. %)	Component	(wt. %)
N ₂	0.03 4	N ₂	0.03 4
CO ₂	0.15 1	CO	0.66 7
CO	0.00 3	CO ₂	0.15 1
H ₂	14.7 65	H ₂	9.88 6
H ₂ O	22.2 39	CH ₄	2.58 9
Acetaldehyde	7.05 7	C ₂ H ₆	5.40 3
Propanal	0.16 3	H ₂ O	46.4 08
Propylene Glycol	6.00 2	Propane	3.78 2
Isoeugenol	1.21 9	Butane	1.27 9
Eugenol	0.34 7	Pentane	0.19 9
Vanillyl alcohol	0.38 1	Hexane	9.10 0
Vinylguaiacol	0.35 8	Cyclohexane	3.99 9
Catechol	3.35 8	Methylcyclohexane	5.87 0
Phenol	0.34 3	Ethylcyclohexane	0.43 7

Guaiacol	0.94 7	Propylcyclohexane	2.02 7
4-methylphenol	0.14 4	Benzene	1.61 4
3-methylphenol	0.18 2	Toulene	4.50 9
4-ethylphenol	0.06 7	Propylbenzene	1.04 6
2-methoxy-4-methylphenol	0.86 5	Vinylbenzene	0.11 2
Furfural	0.80 4	propenylbenzene	0.50 7
2-Furanmethanol	0.10 7	Ethylbenzene	0.22 5
5-Hydromethylfufural	0.20 9		
Levoglucozan	9.92 9		
Xylose	2.05 3		
Cellobiose	6.86 8		
Glucose	0.78 4		
Low MW Lignin Derived Compound A(Dimethoxy stilbene C ₁₆ H ₁₆ O ₂)	9.29 2		
Low MW Lignin Derived Compound B (Dibenzofuran)	1.87 5		
High MW Lignin Derived Compound A (C ₂₀ H ₂₆ O ₈)	7.76 5		
High MW Lignin Derived Compound B (C ₂₁ H ₂₆ O ₈)	1.68 9		

Table C12. Yield factors for upgrade step for scenario 1 of a two-step pathway at torrefaction temperature of 330°C.

Stabilizer		Hydrotreater	
Component	(wt. %)	Component	(wt. %)
N2	0.038	N2	0.038
CO2	0.391	CO	1.268
CO	0.007	CO2	0.391
H2	14.411	H2	10.227
H2O	30.592	CH4	1.629
Acetaldehyde	12.812	C2H6	8.999
Propanal	0.491	H2O	51.747
Propylene Glycol	9.048	Propane	5.693
Isoeugenol	2.668	Butane	2.497
Eugenol	0.451	Pentane	0.389
Vanillyl alcohol	0.480	Hexane	5.206
Vinylguaiacol	0.118	Cyclohexane	2.259
Catechol	1.171	Methylcyclohexane	2.677
Phenol	0.127	Ethylcyclohexane	0.182
Guaiacol	2.098	Propylcyclohexane	1.927
4-methylphenol	0.035	Benzene	1.080
3-methylphenol	0.051	Toulene	2.056
4-ethylphenol	0.039	Propylbenzene	0.467
2-methoxy-4-methylphenol	0.330	Vinylbenzene	0.037

Furfural	2.695	propenylbenzene	1.010
2-Furanmethanol	0.334	Ethylbenzene	0.104
5-Hydromethylfufural	0.250		
Levoglucosan	8.659		
Xylose	2.248		
Cellobiose	0.469		
Glucose	0.782		
Low MW Lignin Derived Compound A(Dimethoxy stilbene C16H16O2)	4.147		
Low MW Lignin Derived Compound B (Dibenzofuran)	0.837		
High MW Lignin Derived Compound A (C20H26O8)	3.466		
High MW Lignin Derived Compound B (C21H26O8)	0.754		

Table C13. Yield factors for upgrade step for scenario 3 of a two-step pathway at torrefaction temperature of 330°C.

Stabilizer		Hydrotreater	
Component	(wt. %)	Component	(wt. %)
N2	0.038	N2	0.038
CO2	0.313	CO	1.203
CO	0.005	CO2	0.313
H2	14.580	H2	10.204

H2O	28.3 56	CH4	1.84 3
Acetaldehyde	10.1 51	C2H6	7.25 2
Propanal	0.37 1	H2O	50.2 64
Propylene Glycol	7.38 6	Propane	4.66 0
Isoeugenol	2.35 0	Butane	2.25 5
Eugenol	0.45 5	Pentane	0.52 0
Vanillyl alcohol	0.44 5	Hexane	6.96 0
Vinylguaiacol	0.23 1	Cyclohexane	2.90 6
Catechol	2.29 3	Methylcyclohexane	3.41 8
Phenol	0.25 0	Ethylcyclohexane	0.27 7
Guaiacol	1.78 5	Propylcyclohexane	1.94 8
4-methylphenol	0.06 9	Benzene	1.41 2
3-methylphenol	0.10 1	Toulene	2.62 6
4-ethylphenol	0.07 6	Propylbenzene	0.58 5
2-methoxy-4-methylphenol	0.64 6	Vinylbenzene	0.07 2
Furfural	2.24 1	propenylbenzene	0.90 8
2-Furanmethanol	0.32 6	Ethylbenzene	0.14 1
5-Hydromethylfufural	0.49 0		
Levogluconan	12.2 46		
Xylose	2.33 0		
Cellobiose	0.35 4		
Glucose	0.59 0		

Low MW Lignin Derived Compound A(Dimethoxy stilbene C16H16O2)	5.19 2		
Low MW Lignin Derived Compound B (Dibenzofuran)	1.04 8		
High MW Lignin Derived Compound A (C20H26O8)	4.33 8		
High MW Lignin Derived Compound B (C21H26O8)	0.94 4		

Table C14. Natural Gas composition

Component	Mole fraction.
Methane	0.95
Ethane	0.032
Propane	0.002
Nitrogen	0.01
Carbon dioxide	0.005
n-Butane	0.0003
i-Butane	0.0003
n-Pentane	0.0001
n-Hexane	0.0001
Oxygen	0.0002

SECTION C. SCHEMATIC DIAGRAMS FOR SCENARIOS 2 & 3 OF THE DESIGN OBJECTIVES.

269

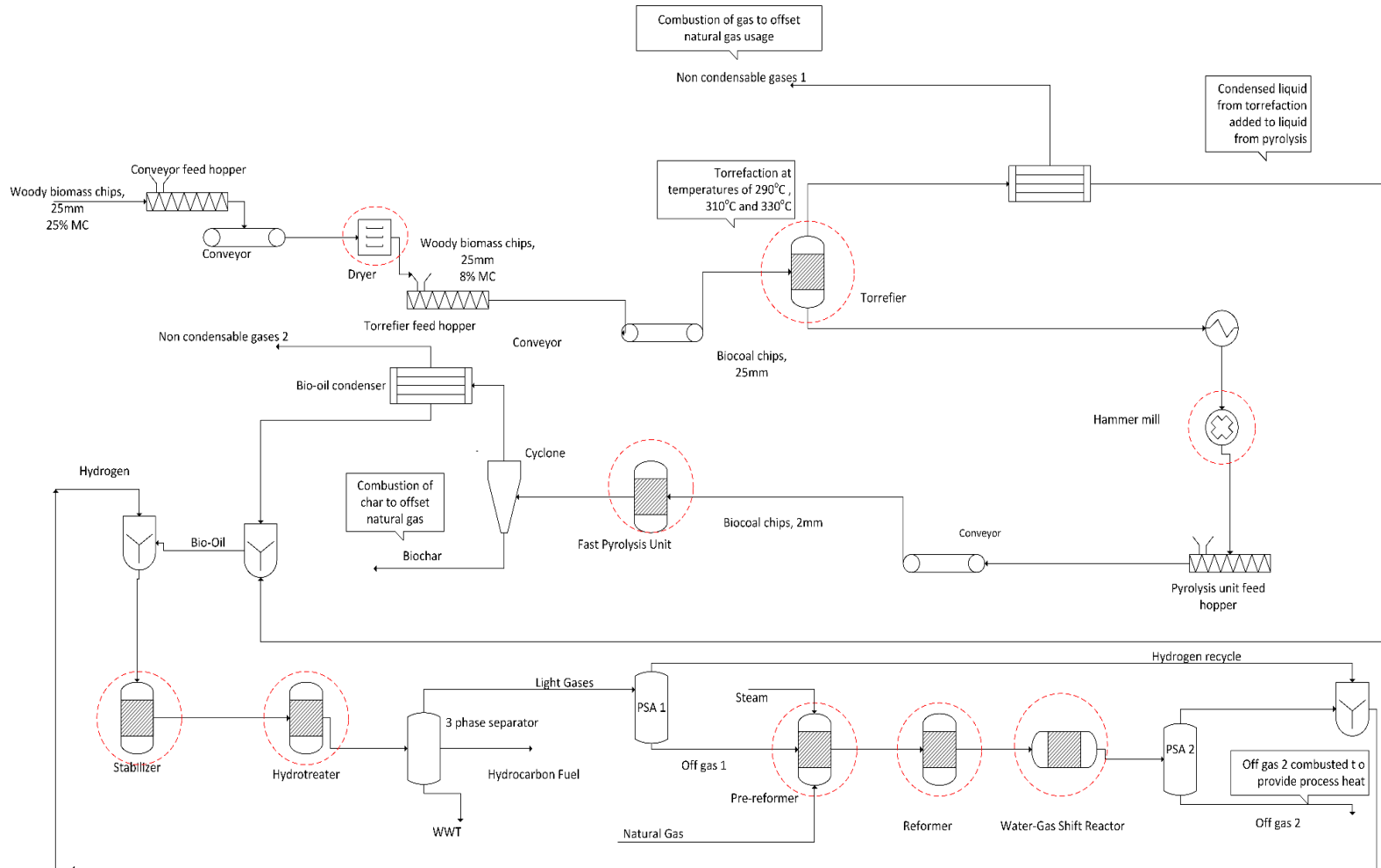


Figure C1. Schematic diagram for scenario 2 of a two-step conversion route for pine biomass to hydrocarbon biofuel.

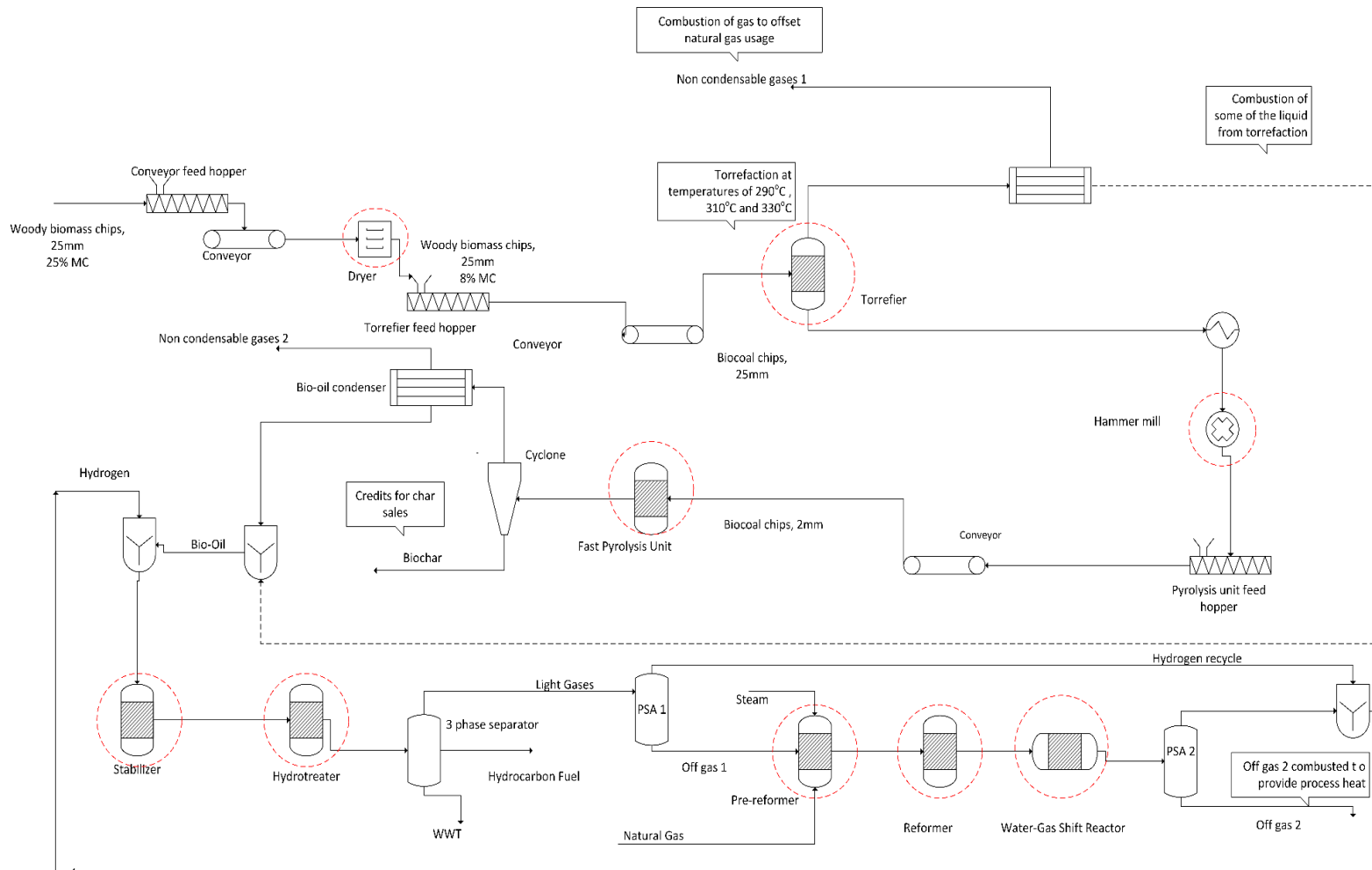


Figure C2. Schematic diagram for scenario 3 of a two-step conversion route for pine biomass to hydrocarbon biofuel.

SECTION D: SAMPLE CALCULATION OF THE LHV OF BIO-OIL OBTAINED FROM SIMULATION FOR A ONE-STEP PYROLYSIS PATHWAY

Table C15. Sample calculation of the LHV of bio-oil for one-step conversion pathway using the heat of combustion of representative compounds found in literature.

	Wt. frac	Heat of combustion (MJ/kg)	Heat of combustion	Source
N2	0.00039	-	0	
CO2	0.001039	-	0	
CO	0.000117	-	0	
H2	0	-	0	
CH4	0	-	0	
C2H6	0	-	0	
H2O	0.221533	-	0	⁵
ACETIC ACID	0.109078	-13.5647	-1.47961	⁵
PROPIONIC ACID	0.056227	-18.8312	-1.05883	⁵
ACETOL	0.047267	-22.5708	-1.06686	*
ISOEUGENOL	0.008311	-32.6024	-0.27095	¹⁶
EUGENOL	0.001818	-32.8317	-0.05969	¹⁶
VANILLIN	0.006493	-25.1678	-0.16341	¹⁶
P-VINYLGUAIACOL	0.012206		0	
CATECHOL (BENZE-1,2 DIOL)	0.037528	-26.03	-0.97685	
PHENOL	0.002987	-31.0372	-0.0927	⁵
GUAIACOL	0.007142		0	
P-CRESOL	0.001039	-32.5741	-0.03384	⁵
M-CRESOL	0.00026	-32.6228	-0.00847	⁵
4-ETYLPHENOL	0.001039	-35.6322	-0.03702	¹⁷
O-CRESOL	0.007272	-32.6244	-0.23724	⁵
FUFURAL	0.014154	-24.3674	-0.3449	¹⁷

2-FURANMETHANOL	0.00181 8	-26.0091	-0.04728	17
5-(HYDROXYMETHYL)-2-FURANCARBOXALDEHYDE	0.00350 6		0	
LEVOGLUCOSAN	0.11219 5	-17.4747	-1.96056	17
XYLOSE	0.03402 2	-15.5924	-0.53048	17
CELLBOISE	0.05103 3	-16.4864	-0.84135	17
GLUCOSE	0.01701 1	-15.6072	-0.26549	17
LOW MW LIGNIN DERIVED COMPOUND A (DIMETHOXY STILBENZENE)	0.11024 7	-35.4908	-3.91275	*
LOW MW LIGNIN DERIVED COMPOUND B (DIBENZOFURANN)	0.02220 5	-35.2318	-0.78233	*
HIGH MW LIGNIN DERIVED COMPOUND A	0.09206 7	-26.4613	-2.43622	*
HIGH MW LIGNIN DERIVED COMPOUND B	0.01999 8	-26.6643	-0.53322	*
Total	1	LHV	-17.1401	

- Calculated based on the composition of carbon, hydrogen, and oxygen using the method described in section B above.

$$\Delta_c H^\circ = 393.51a + 142.915b + \Delta_f H^\circ (C_a H_b O_c)$$

Acetol – C₃H₆O₂ (74.049g/mol)

$$\begin{aligned} \Delta_c H^\circ (\text{Acetol}) &= (393.51 * 3) + (142.915 * 6) + (-366) \\ &= -1672.02 \text{ kJ/mol} \\ &= -22.57 \text{ MJ/kg} \end{aligned}$$

Table C16. LHV of bio-oil from one-stage and two-stage processes.

LHV (MJ/kg)				
Scenario	One-step	Two-step		
		290°C	310°C	330°C
1	17.14	16.33	14.95	13.93
2	17.14	16.33	14.95	13.93
3		19.22	17.30	14.76

Table C17. Overall heat-transfer coefficients.¹⁸

Process stream	U (W/m ² °C)
Bio-oil (c)	255
Water-gas shift product stream (h)	160
Torrefaction feed stream (c)	500
Pyrolysis feed stream (c)	500
PSA-1 feed stream (c)	110
Stabilizer product stream (h)	255
Hydrotreater feed stream (c)	175
Pre-reformer feed stream (c)	65
Recycled hydrogen feed stream (h)	160
Pyrolysis vapor (h)	600
Hydrotreater product stream (h)	60
Reformer product stream (h)	160
Stabilizer feed stream (c)	255
Reformer feed stream (c)	65
Generated steam stream (h)	2750
SMR steam stream (c)	65
Dryer effluent steam stream (c)	65
Torrefaction vapor (h)	600

(h) denotes hot stream being cooled by cold utility while (c) denotes cold utility heated by hot fluid.

SECTION E: CORRELATION FOR PURCHASED COST OF HEAT EXCHANGERS¹⁹

Purchase cost of heat exchangers in 2001 dollars was estimated using correlation below

$$\log_{10}C_p^o = K_1 + K_2\log_{10}(A) + K_3[\log_{10}(A)]^2 \quad (10)$$

Where $K_1 = 4.1884$, $K_2 = -0.2503$, $K_3 = 0.1974$ and $A =$ calculated heat exchanger area in m^2

Pressure effect on the cost of heat exchanger was accounted for using the correlation

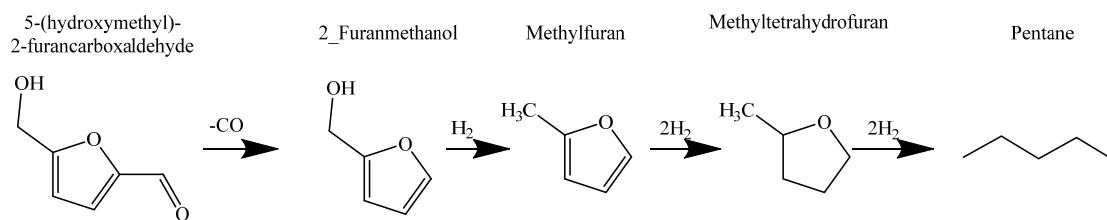
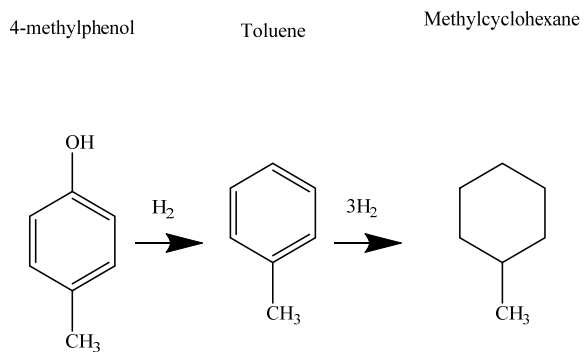
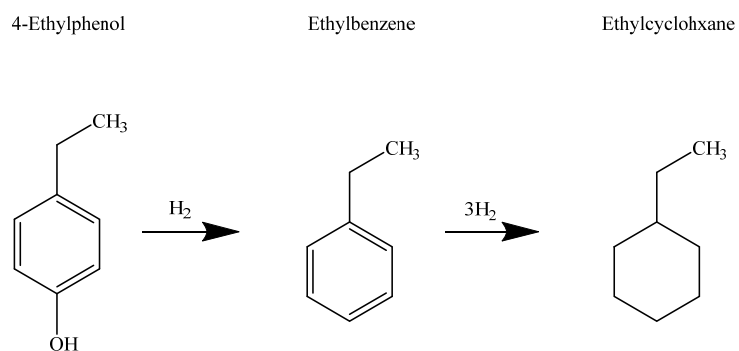
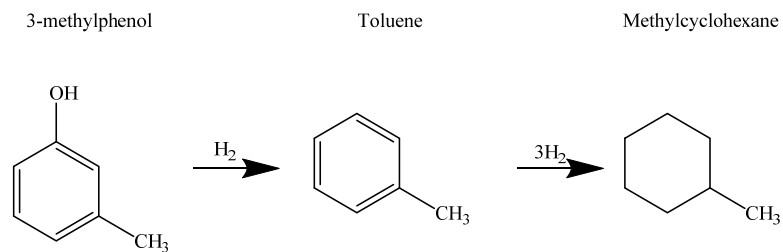
$$\log_{10}F_p = C_1 + C_2\log_{10}(P) + C_3[\log_{10}(P)]^2 \quad (11)$$

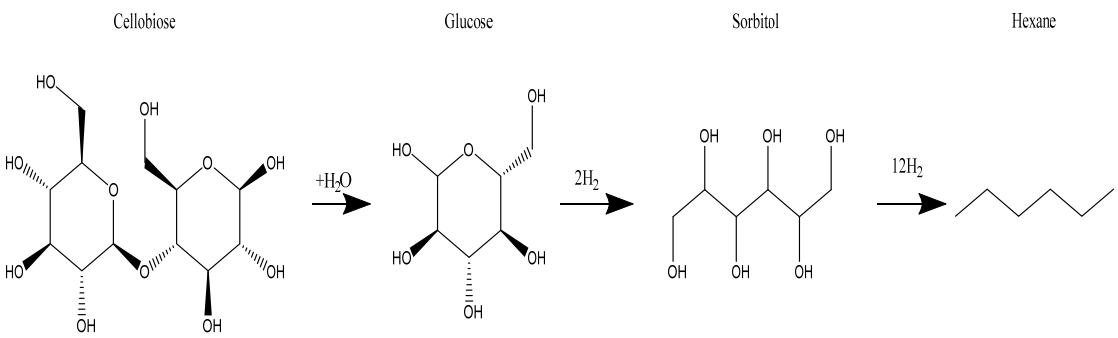
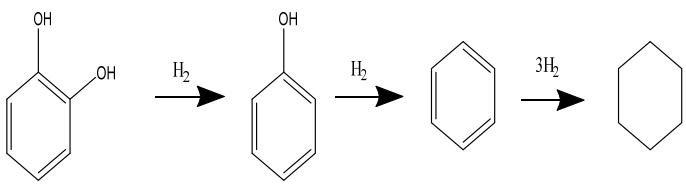
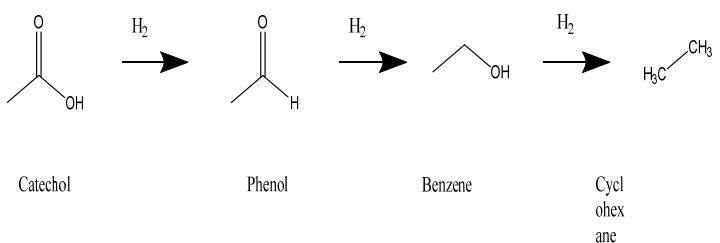
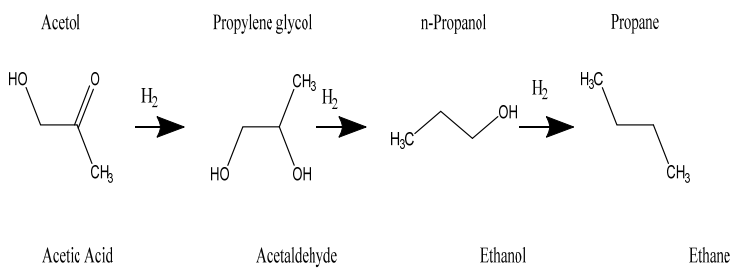
Where $K_1 = 4.1884$, $K_2 = -0.2503$, $K_3 = 0.1974$ and $P =$ operating pressure in bar guage

$$\text{Cost of heat exchanger with pressure effects in 2001 dollars} = C_p^o \times F_p \quad (12)$$

SECTION F: REACTION PATHWAYS FOR BIO-OIL MODEL COMPOUNDS

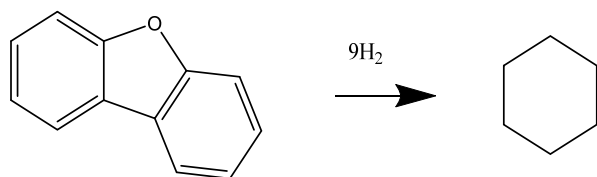
UPGRADE





Dibenzofuran

Cyclohexane

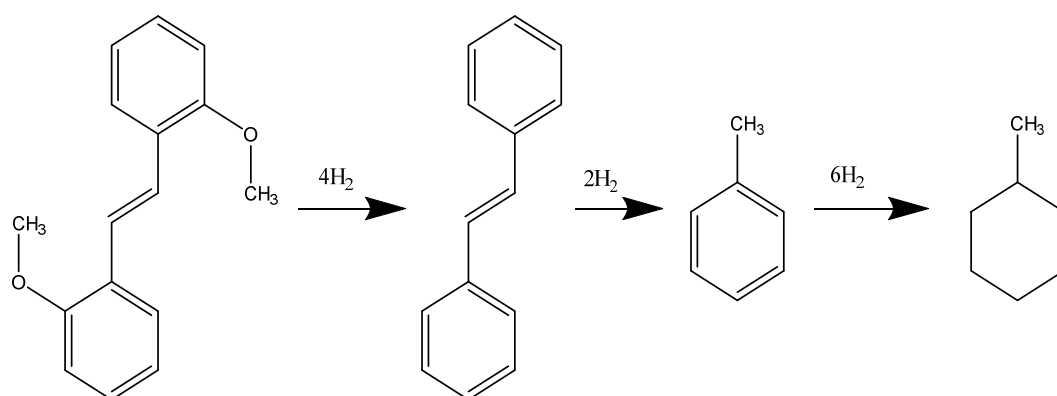


Dimethoxy Stilbene

Trans-Stilbene

Toluene

Methylcyclohexane

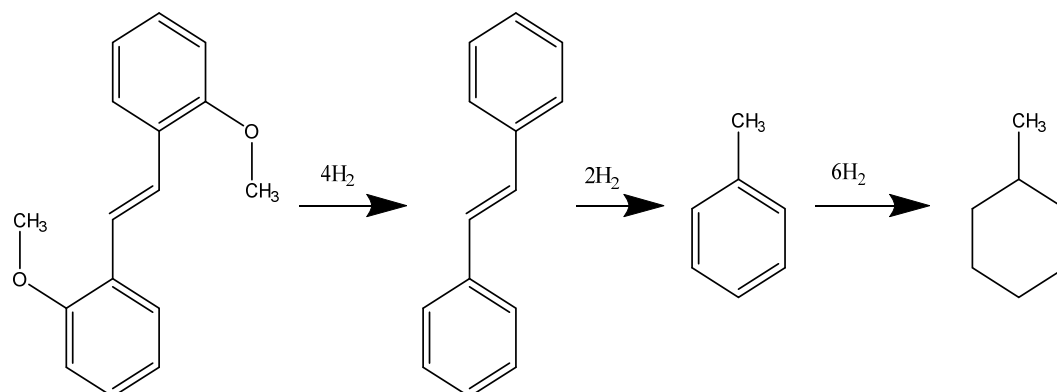


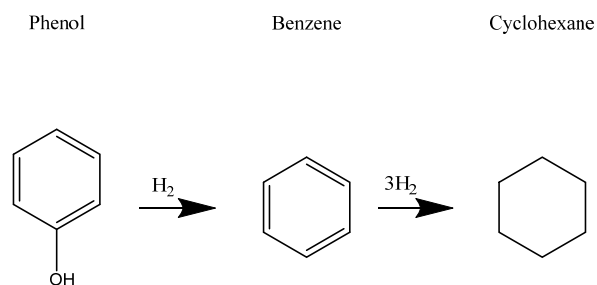
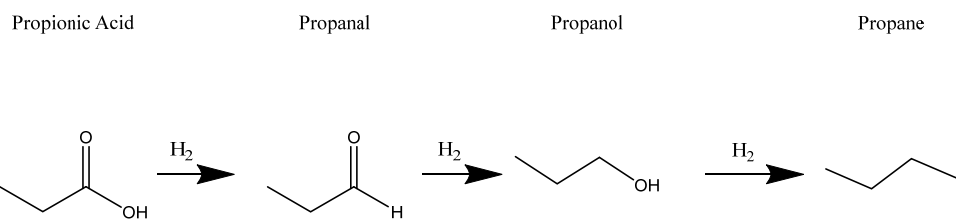
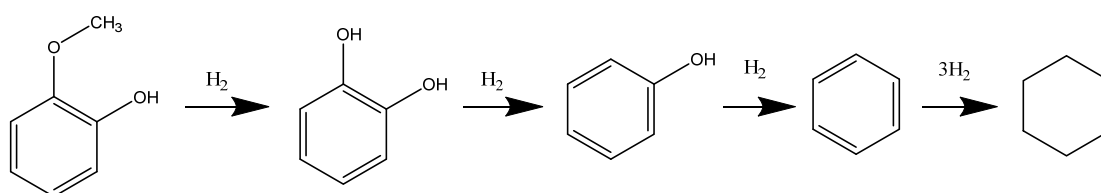
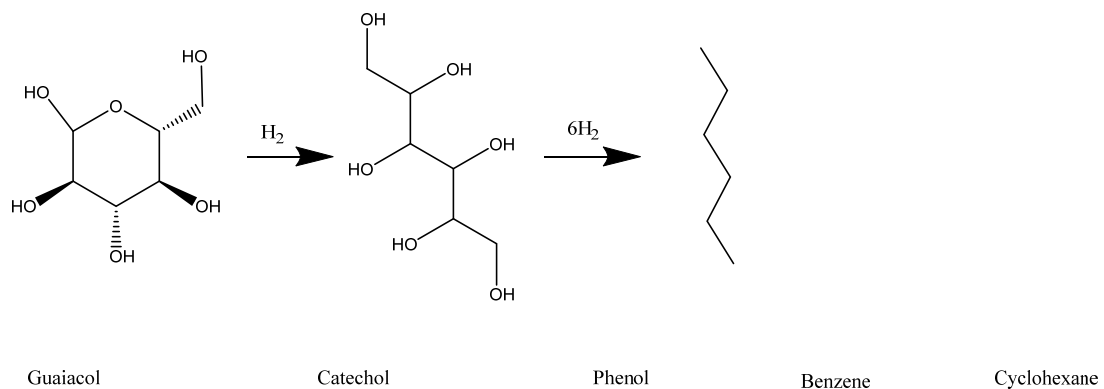
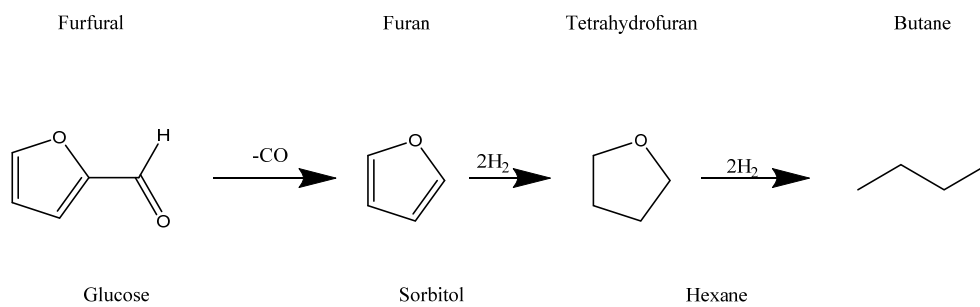
Dimethoxy Stilbene

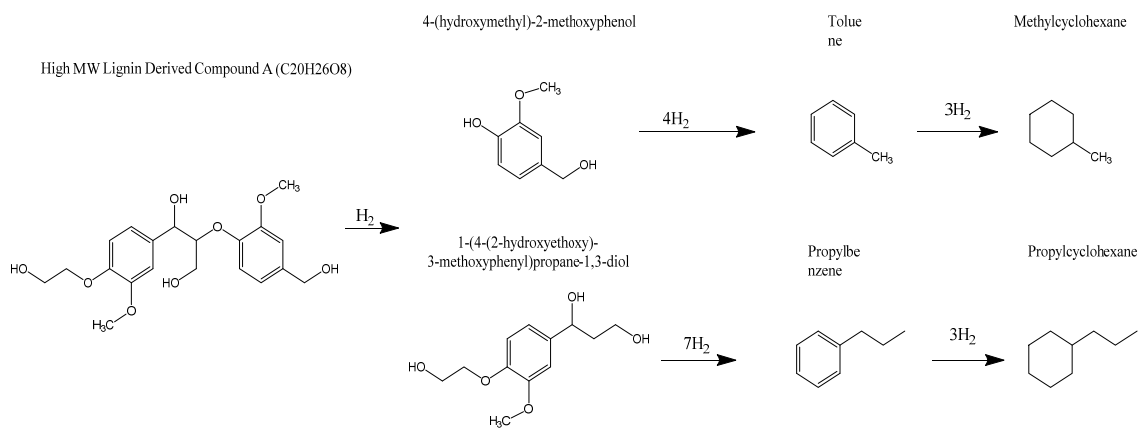
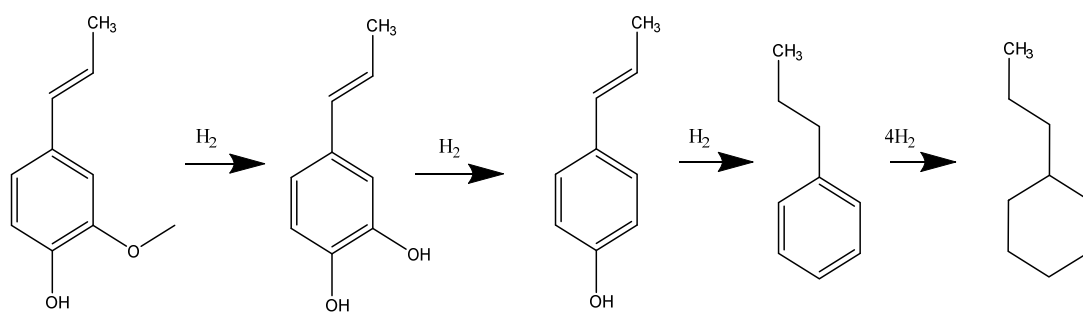
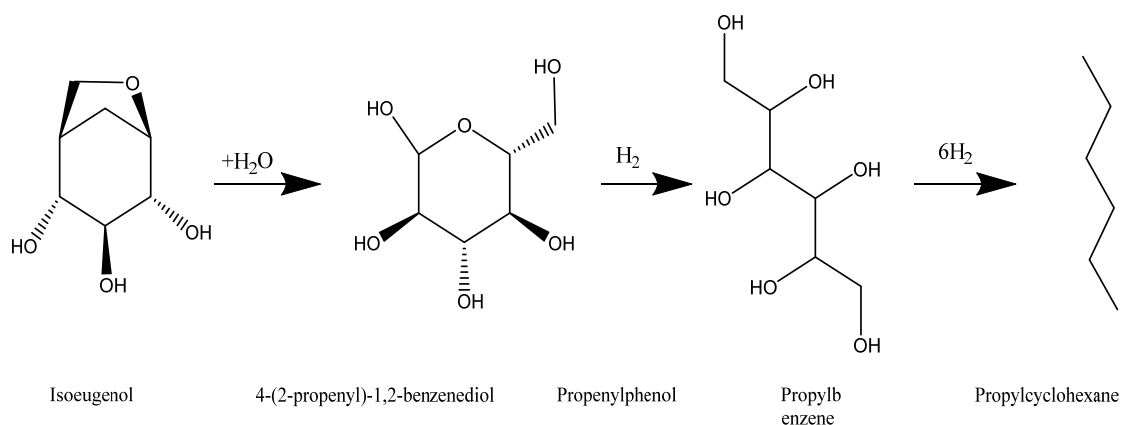
Trans-Stilbene

Toluene

Methylcyclohexane







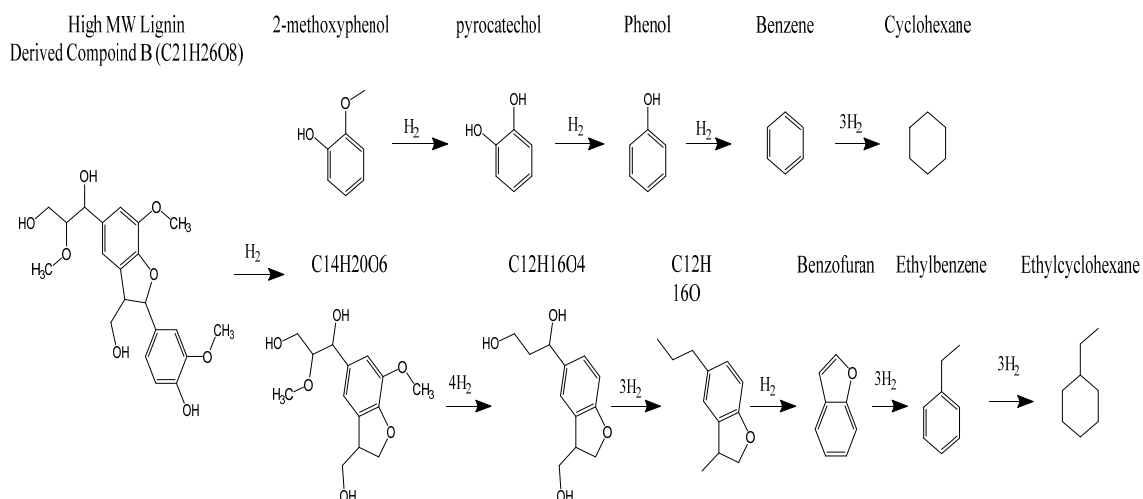


Table C18. Purchase cost of major equipment.

Equipment name	Stream flow	Stream flow units	Original base year	Cost (2015 U.S. dollars)	Source
CFB Pyrolyzer, quench and auxiliaries	1000	Metric tons/day	2009	24,055,830.11	²⁰
Torrefaction reactor	5	Metric tons/hr	2012	22,667,380.24	²¹
Steam Reformer System	31.27	MMscfd H ₂	2007	27,568,866.19	²⁰
Hammer Mill	42	Metric tons/hr	2013	130,000.00	*
Biomass dryer + Exhaust fan	1000	Metric tons/day	2013	954,264.15	*
Stabilization bed	1653	Liquid scfh	2011	7,052,876.18	²⁰
Hydrotreater	1271	Liquid scfh	2011	3,318,730.08	²⁰

* Vendor quotes

C.2 References

- (1) Winjobi, O.; Shonnard, D. R.; Bar-Ziv, E.; Zhou, W. Techno-economic assessment of the effect of torrefaction on fast pyrolysis of pine. *Biofuels, Bioproducts and Biorefining* **2016**.
- (2) Phanphanich, M.; Mani, S. Impact of torrefaction on the grindability and fuel characteristics of forest biomass. *Bioresource technology* **2011**, *102* (2), 1246-1253.
- (3) Koppejan, J.; Van Loo, S. *The handbook of biomass combustion and co-firing*, ed.; Routledge, 2012.
- (4) Gaur, S.; Reed, T. B. *An atlas of thermal data for biomass and other fuels*; Report No. 1995.
- (5) Perry, R. H.; Green, D. W.; Maloney, J. O.; Abbott, M. M.; Ambler, C. M.; Amero, R. C. *Perry's chemical engineers' handbook*, ed.; McGraw-hill New York, 1997.
- (6) Haynes, W. M. *CRC handbook of chemistry and physics*, ed.; CRC press, 2013.
- (7) Joback, K. G.; Reid, R. C. Estimation of pure-component properties from group-contributions. *Chemical Engineering Communications* **1987**, *57* (1-6), 233-243.
- (8) Shankar Tumuluru, J.; Sokhansanj, S.; Hess, J. R.; Wright, C. T.; Boardman, R. D. REVIEW: A review on biomass torrefaction process and product properties for energy applications. *Industrial Biotechnology* **2011**, *7* (5), 384-401.
- (9) Rönsch, S.; Wagner, H. DBFZ Workshop Fließschemasimulation in der Energietechnik, Leipzig, 2012; p 1-7.
- (10) Plus, A. Aspen Technology. *Inc., version 2009, 11*.

- (11) Conference, C. E. M. A. E. *Belt conveyors for bulk materials*, ed.; Conveyor Equipment Manufacturers Association, 1997.
- (12) Couper, J. R.; Penney, W. R.; Fair, J. R. *Chemical Process Equipment revised 2E: Selection and Design*, ed.; Gulf Professional Publishing, 2009.
- (13) Westerhof, R. J.; Brilman, D. W. F.; Garcia-Perez, M.; Wang, Z.; Oudenhoven, S. R.; Kersten, S. R. Stepwise fast pyrolysis of pine wood. *Energy & fuels* **2012**, *26* (12), 7263-7273.
- (14) Zheng, A.; Zhao, Z.; Chang, S.; Huang, Z.; He, F.; Li, H. Effect of torrefaction temperature on product distribution from two-staged pyrolysis of biomass. *Energy & Fuels* **2012**, *26* (5), 2968-2974.
- (15) Park, J.; Meng, J.; Lim, K. H.; Rojas, O. J.; Park, S. Transformation of lignocellulosic biomass during torrefaction. *Journal of Analytical and Applied Pyrolysis* **2013**, *100*, 199-206.
- (16) Kharasch, M. S. *Heats of combustion of organic compounds*, ed.; US Government Printing Office, 1929.
- (17) Domalski, E. S. Selected Values of Heats of Combustion and Heats of Formation of Organic Compounds Containing the Elements C, H, N, O, P, and S. *Journal of Physical and Chemical Reference Data* **1972**, *1* (2), 221-277.
- (18) Sinnott, R.; Elsevier Butterworth Heinemann, Oxford, 2005.
- (19) Turton, R.; Bailie, R. C.; Whiting, W. B.; Shaeiwitz, J. A. *Analysis, synthesis and design of chemical processes*, ed.; Pearson Education, 2008.
- (20) Jones, S.; Meyer, P.; Snowden-Swan, L.; Padmaperuma, A.; Tan, E.; Dutta, A.; Jacobson, J.; Cafferty, K. *Process design and economics for the conversion of*

lignocellulosic biomass to hydrocarbon fuels: fast pyrolysis and hydrotreating bio-oil pathway; Report No. 2013.

- (21) Batidzirai, B.; Mignot, A.; Schakel, W.; Junginger, H.; Faaij, A. Biomass torrefaction technology: Techno-economic status and future prospects. *Energy* **2013**, *62*, 196-214.

Appendix D: Production of Hydrocarbon Fuel using Two-Step Torrefaction and Fast Pyrolysis of Pine. Part 2: Life Cycle Carbon Footprint

D.1 Supplementary material from Chapter 5

The present document is prepared to complement the manuscript and provide additional information. The features of interest include the process description of other unit operations and the flow diagrams of the scenarios described in the manuscript.

Section A. SCHEMATIC DIAGRAMS FOR SCENARIOS 2 & 3 OF THE DESIGN OBJECTIVES.

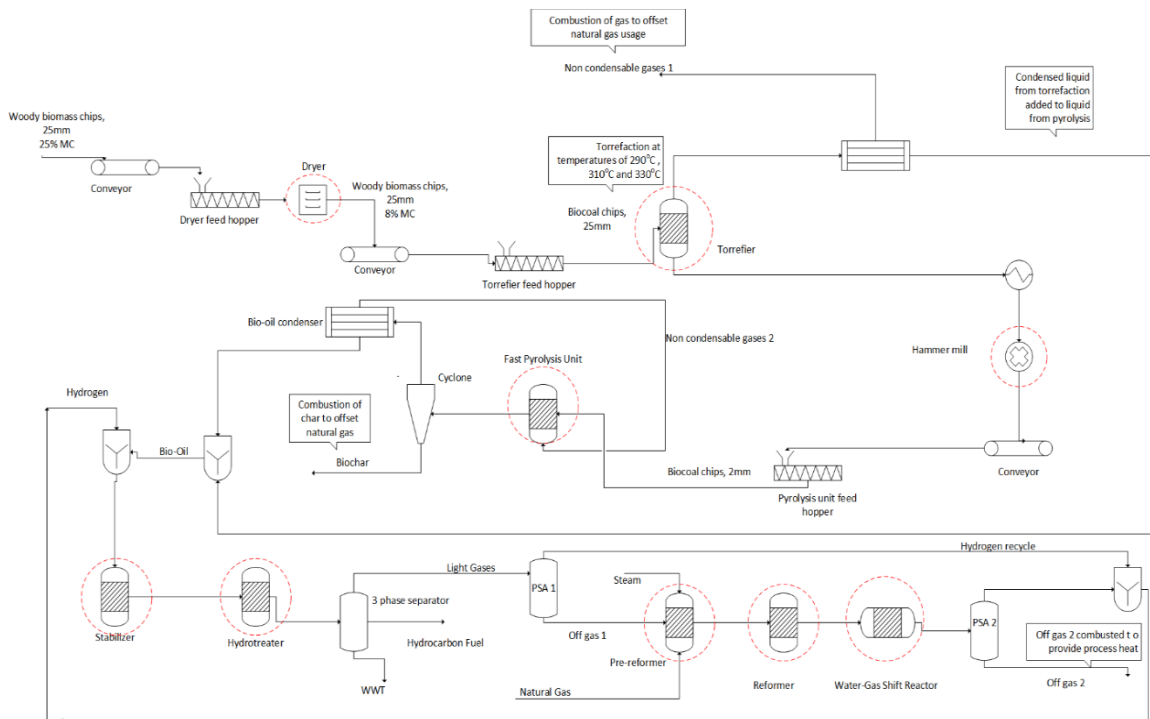


Figure D1. Schematic diagram for scenario 2 of a two-step conversion route.

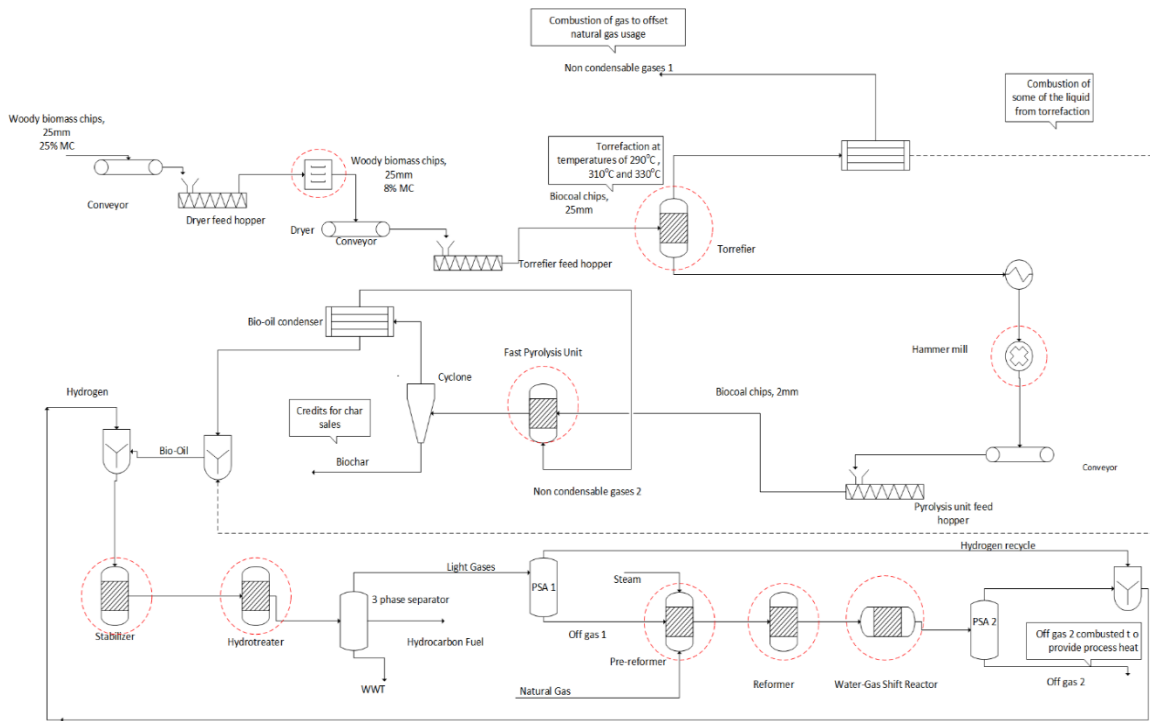


Figure D2. Schematic diagram for scenario 3 of a two-step conversion pathway.

Table D1. Process conditions of some selected streams for the two-step pathway at 290°C, scenario 3.

Stream	Pressure (bar)	Temperature (°C)	Flowrate (kg/hr)
1	1	25	72560.00
2	1	110	59152.17
3	1	20	14206.27
4	1	20	9661.99
5	1	290	41655.92
6	1	530	5629.18
7	1	20	24482.98
8	82.7	65.6	4406.94
9	52	34.9	11564.013
10	1.4	35	2790.44
11	20.2	65.6	22295.21
12	28.6	337.8	4237.75

Section B. BIOMASS SUPPLY CHAIN EMISSIONS USING GREET MODEL 2014.

This section was presented in our prior study, but repeated here for completeness.¹

B.1 Wood collection

The emissions due to the collection of wood was obtained from the EtOH tab of the GREET model as shown below.² The emission factors given in grams/dry ton were input into SimaPro®.

Table D2. GREET emission factors for wood collection.²

Wood collection	
grams/dry ton	EtOH tab DU 454:464
VOC	11.803
CO	60.833
CH ₄	18.67
N ₂ O	0.156
CO ₂	12009

B.2 Biomass chipping

For the coarse chipping of biomass at the forest, emission factors were determined for the production of diesel used in running the stationary reciprocating diesel engine. The factors obtained from the GREET model as shown in Table below were given in grams/mmBtu of diesel burned.²

Table D3. GREET emission factors for coarse chipping at forest.²

Chipping- Stationary Reciprocating Diesel Engine		
grams/mmBtu Diesel burned	Petroleum tab BI 127:140 Production	EF tab R6:16 Combustion
VOC	0.978	2.027
CO	2.873	657.005
CH4	18.406	4.221
N2O	0.1	0.6
CO2	2485	77149

These factors were converted to grams/ short ton by multiplying by 0.129488 mmBtu/gal LSD (Fuel_Specs tab B18), the lower heating value (LHV) of diesel. Then divided by 3.206 kg LSD/ gal LSD (Fuel_Specs tab E18), the density of low sulfur diesel. This was then multiplied by a factor of 0.5 kg LSD combusted/ dry short ton of biomass, based on the amount of diesel required per dry ton of biomass given by Maleche et al.³

B.3 Truck Transport

Emission factors for truck transport obtained from the GREET model are shown below for a 90 mile truck transport (T&D tab GP 107).²

Table D4. GREET emission factors for truck transport of biomass.²

Truck transport (90 miles)	
grams/dry short ton	EtOH tab DV 454:464
VOC	8.993
CO	30.676
CH4	53.645
N2O	0.486
CO2	32626

B.4 Loading operations

Three loading operations were considered in the biomass supply chain. The loading operations were achieved using front loading trucks. The emission factors obtained from the GREET database includes the emissions for the production of diesel and combustion of diesel in the front loading trucks.²

Table D5. GREET emission factors for loading operations of biomass.²

Loading operations		
grams/mmBtu Diesel burned	Petroleum tab K 265:275 Production	EF tab AD37:47 Combustion
VOC	4.156	16.785
CO	7.021	69.368
CH4	19.18	19.224
N2O	0.16	0.083
CO2	8125	77985

These factors were converted to grams/ short ton by multiplying by 0.129488 mmBtu/gal LSD (Fuel_Specs tab B18), the lower heating value (LHV) of diesel. Then divided by 3.206 kg LSD/ gal LSD (Fuel_Specs tab E18), the density of low sulfur diesel. Then multiplied by 1.5 kg/short ton, based on 0.5 kg diesel/ dry short ton reported for each loading operations by Handler et al.⁴

B.5 Rail transport

Table D6. GREET emission factors for rail transport of biomass.²

Rail transport (490 miles)		
grams/mmBtu Diesel burned	T&D J 181:191 Production	EF S37:J47 Combustion
VOC	0.241	58.388
CO	0.805	206.53
CH4	0.532	6.825
N2O	0.009	2.132
CO2	329	77674

A distance of 490 miles (T&D tab J16) was assumed for rail transport. Emissions were evaluated for the production and consumption of diesel. To convert the factors given in grams/mmBtu Diesel burned to grams/dry ton of biomass, the factors were multiplied by the rail intensity 274 Btu/ton-mile (T&D tab E122) and then multiplied by the distance of 156 travelled.

B.6 Size reduction

The correlation obtained from literature given as follows for pine was used in evaluating the reduction in energy consumption to attain required size to effect fast pyrolysis.⁵

$$E_g = -0.756T + 260.0 \quad (1)$$

where E_g is specific energy consumption for grinding in kW-hr/ton, T is Temperature in °C

The size reduction step was then modeled in Aspen Plus® as a hammer mill with the estimated specific energy consumed for grinding estimated at different torrefaction temperatures while the untreated raw pine's energy was estimated using ambient temperature of 25°C.

Work index, a function of the specific energy consumption, as well as the initial and final biomass particle size is required to model the size reduction step. The work index required for grinding was calculated from the specific energy (calculated in equation 1) and size of initial and final biomass particle using equation 2.

$$E_g = 10 * W_i * \left(\frac{1}{\sqrt{P}} - \frac{1}{\sqrt{F}} \right) \quad (2)$$

where E_g Specific energy consumption for grinding in kW-hr/ton, W_i is work index in kW-hr/ton, P is final particle size in microns and F is Initial particle size in microns

B.7 Combustion

Combustion of products when considered in this study was not modeled using the process simulation software, however the heat released during combustion were estimated from correlations obtained from literature as shown below:

B.7.1 Combustion of char

Heat released from the combustion of char was evaluated based on the lower heating value of char, which was estimated from its higher heating value based on correlation from literature given below:⁶

$$LHV = HHV \left(1 - \frac{w}{100}\right) - 2.444 * \frac{w}{100} - 2.444 * \frac{h}{100} * 8.936 \left(1 - \frac{w}{100}\right) \left[\frac{MJ}{kg}, w. b.\right]$$

(3)

Where

2.444 = enthalpy difference between gaseous and liquid water at 25°C

8.936 = M_{H_2O}/M_{H_2} ; i.e. the molecular mass ratio between H₂O and H₂

LHV = lower heating value in MJ/kg fuel (w.b.)

HHV = higher heating value in MJ/kg fuel (d.b.)

w = moisture content of the fuel in wt% (w.b.)

h = concentration of hydrogen in wt% (d.b.)

The higher value utilized in equation above was also estimated from empirical formula as well as shown below.⁷

$$HHV = 0.3491X_C + 1.1783X_H + 0.1005X_S - 0.0151X_N - 0.1034X_O - 0.0211X_{ash} \left[\frac{MJ}{kg}, d. b.\right] \quad (4)$$

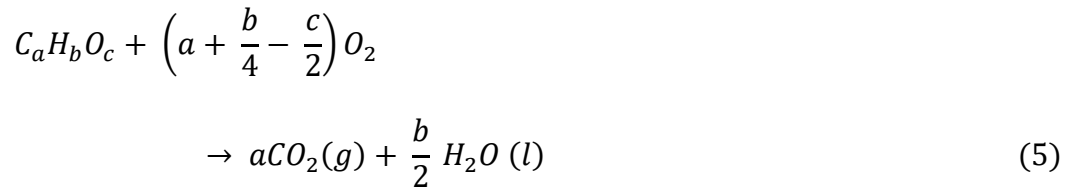
Where X_i is the content of carbon (C), hydrogen (H), etc. from the ultimate analysis of the solid fuel.

B.7.2 Combustion of condensates from torrefaction

Energy released from the combustion of condensates from torrefaction when such step takes place in this study was estimated by obtaining from literature the lower heating value of the individual components in the condensates.⁸ Based on the lower heating value of the

individual components and their weight fraction in the liquid, the lower heating value of the liquid was estimated. For high molecular compounds produced from either the torrefaction or pyrolysis step whose lower heating values were not found in literature, their lower heating values were estimated using correlation obtained from literature as shown below:⁹

For compounds containing only carbon, hydrogen and oxygen, general combustion reaction was given as



The standard heat of combustion is then given as

$$\Delta_c H^\circ = -a\Delta_f H^\circ(CO_2, g) - \frac{1}{2}b\Delta_f H^\circ(H_2O, l) + \Delta_f H^\circ(C_aH_bO_c) \quad (6)$$

$$= 393.51a + 142.915b + \Delta_f H^\circ(C_aH_bO_c) \quad (7)$$

where $\Delta_f H^\circ$ is the enthalpy of formation. When the heat of formation is not available from literature, it was estimated based on the structure of the component by using the Joback method which is based on group contribution.^{8,10}

B.7.3 Combustion of non-condensable gas from torrefaction

Heat generated from combustion of non-condensable gas from torrefaction was estimated using the lower heating value of the components present in the non-condensable gas phase. Severity of torrefaction usually determines the components contained in the non-condensable gas, however for this study, the components were assumed to be essentially CO₂ and CO in a 80 to 20 ratio hence heat released from combustion is due to the CO component only, this assumption is supported by the report of Tumuluru et al which showed energy released from the combustion of volatiles from torrefaction is mainly from CO.¹¹

B.7.4 Bioe correlation for heat of combustion estimation

One of the correlation used in Aspen Plus® to estimate the heat of combustion of unconventional solids such as biomass based on the ultimate analysis is as shown:

$$\Delta_c h_i^{dm} = [a_{1i}w_{C,i}^{dm} + a_{2i}w_{H,i}^{dm} + a_{3i}w_{S,i}^{dm} + a_{4i}w_{O,i}^{dm} + a_{5i}w_{N,i}^{dm}]10^2 + a_{6i} \quad (8)$$

Where $w_{C,i}^{dm}$ is the weight fraction of carbon.

Values of the parameters as given by Aspen Plus® are as follows¹²

$$a_{1i} = 151.2, a_{2i} = 499.77, a_{3i} = 45.0, a_{4i} = -47.7, a_{5i} = 27.0 \text{ and } a_{6i} = -189$$

B. 8 Enthalpy of reaction (torrefaction & pyrolysis)

The heat of reaction for both processes modeled using a yield reactor was calculated using equation

$$\Delta h_{reaction} = h_{products}^f - h_{reactants}^f \quad (9)$$

Where h^f is the heat of formation.

$$Q_{reaction} = \Delta h_{reaction} + h_{sensible} \quad (10)$$

Where $h_{sensible}$ is the heat required to raise feed to reactor temperature.

SECTION C. INPUT DATA TABLES USED IN MODELING

Tables D7 to 8c found in this section were presented in our prior study, but repeated here for completeness.¹

Table D7. Torrefaction yield data (kg/kg intake pine × 100 %) at different torrefaction temperatures.¹³

Torrefaction Temperature	290°C	310°C	330°C
Material	Wt %		
Gas	6	8	11
Condensed Liquid	17	33	46
Torrefied Solid	78	56	43

TableD8. Torrefaction component distribution (wt % organics) of organics from torrefaction of pine at different torrefaction temperatures.^{13,14}

Component (wt/wt organics)	Torrefaction temperature		
	290°C	310°C	330°C
Acetic Acid	8.01	11.92	13.09
Propionic Acid	0.25	0.42	0.48
Acetol	2.47	5.08	6.43
Fufural	1.01	1.26	1.95
2-Furanmethanol	0.09	0.11	0.21
5-(hydroxymethyl)-2-furancarboxaldehyde	0.00	0.00	0.00
Levogluosan	0.40	2.43	3.00
Xylose	0.40	1.22	1.32
Hydrolysable Oligomers(cellobiose)	0.00	0.15	0.36
Glucose	0.10	0.61	0.60

Isoeugenol	0.33	0.76	1.83
Eugenol	0.05	0.13	0.27
Vanillin	0.21	0.32	0.31
2-methoxy-4-vinylphenol(p-vinylguaiacol)	0.00	0.00	0.00
Catechol(benze-1,2-diol)	0.00	0.00	0.00
Phenol	0.00	0.00	0.00
2-methoxyphenol (guaiacol)	0.49	0.83	1.48
4-methylphenol(p-cresol)	0.00	0.00	0.00
3-methylphenol (m-cresol)	0.00	0.00	0.00
4-ethylphenol	0.00	0.00	0.00
2-methoxy-4-methylphenol (creosol)	0.00	0.00	0.00
Low MW Lignin-Derived Compound A(Dimethoxy stilbene)	0.95	1.24	1.87
Low MW Lignin Derived Compound B (Dibenzofuran)	0.19	0.25	0.38
High MW Lignin-Derived Compound A	0.79	1.04	1.56
High MW Lignin Derived Compound B	0.17	0.23	0.34

Table D9. Ultimate analysis data (wt %) for torrefied pine chips at different torrefaction temperatures in .¹⁵

Torrefaction Temperature	290°C	310°C	330°C
Element	Value (wt %)		
Ash	0.6	0.6	0.8
Carbon	55.05	57.27	65.75
Hydrogen	5.94	5.79	4.87
Chlorine	-	-	-
Nitrogen	0.11	0.14	0.28
Sulfur	-	-	-
Oxygen	38.3	36.0	27.6

Table D10. Proximate analysis data (wt %) for torrefied pine chips at different torrefaction temperatures in .¹⁵

Torrefaction Temperature	290°C	310°C	330°C
Element	Value (wt %)		
Ash	0.60	0.80	1.4
Moisture Content	0	0	0

Volatile Matter	78.6	76.4	60
Fixed Carbon	20.8	22.8	38.6

Table D11. Pyrolysis yield data (kg/ kg pyrolyzer feed intake × 100 %) for one and two-step pyrolysis taking place at 530°C. (The yields are based on the feed entering the pyrolyzer on a dry ash free basis-one step is raw pine; two-step is torrefied pine)¹³

Material	Wt %			
	One Step	Two Step (290°C)	Two Step (310°C)	Two Step (330°C)
Gas	28	24.4	26.8	23.3
Liquid	59	57.7	46.4	32.6
Solid/Char	10	12.8	23.2	39.5

TableD12. Pyrolysis bio-oil component distribution of organics (wt/wt organics) for one step and two step pyrolysis of pine.^{13,14}

		One Step (wt/wt organics)	Two Step (wt/wt organics)		
Component	Torrefaction temperature		290°C	310°C	330°C
Acetic Acid		7.59	4.42	2.96	1.11
Propionic Acid		3.69	0.00	0.00	0.00
Acetol		3.11	3.28	2.39	0.85
Fufural		1.00	0.29	0.15	0.38
2-Furanmethanol		0.12	0.07	0.04	0.11
5-(hydroxymethyl)-2-furancarboxaldehyde		0.23	0.28	0.15	0.45
Levoglucosan		7.24	7.91	6.04	8.45
Xylose		2.19	2.05	1.01	0.94
Cellobiose		3.29	5.28	4.70	0.00
Glucose		1.10	1.17	0.34	0.00
Isoeugenol		0.54	0.58	0.58	0.50
Eugenol		0.12	0.36	0.20	0.17
Vanillin		0.42	0.14	0.15	0.12
P-vinylguaiacol		0.79	0.37	0.25	0.21

Catechol	2.53	4.88	2.32	2.08
Phenol	0.19	0.33	0.24	0.23
Guaiacol	0.46	0.46	0.37	0.30
P-cresol	0.06	0.12	0.10	0.06
M-cresol	0.02	0.06	0.13	0.09
4-ethylphenol	0.07	0.14	0.05	0.07
Creosol	0.46	0.85	0.50	0.59
Low MW Lignin-Derived Compound A(Dimethoxy stilbene)	7.11	6.50	6.00	3.05
Low MW Lignin Derived Compound B (Dibenzofuran)	1.43	1.31	1.21	0.62
High MW Lignin-Derived Compound A	5.94	5.43	5.02	2.55
High MW Lignin Derived Compound B	1.30	1.18	1.10	0.56

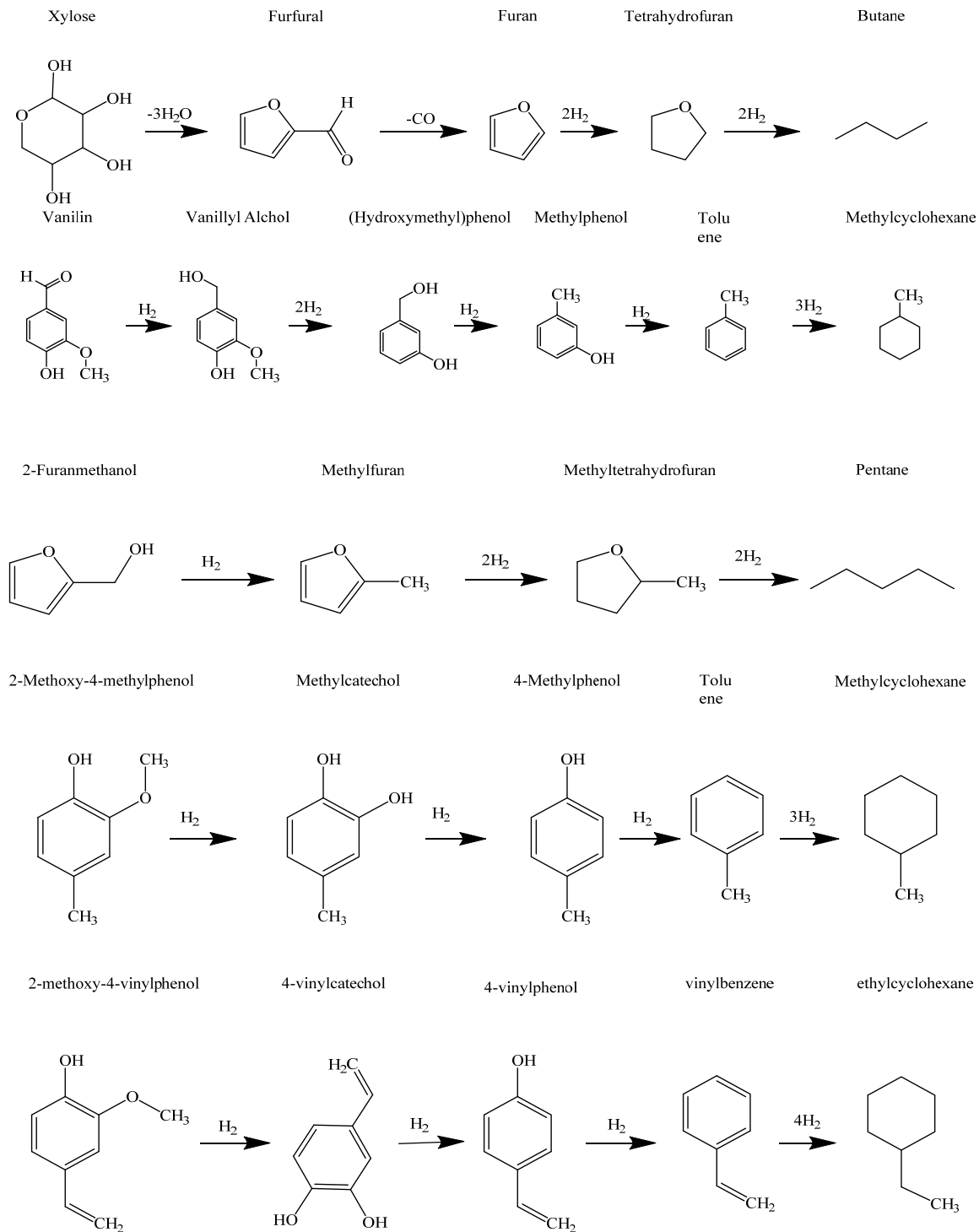
TableD13. Ultimate and proximate analysis (wt %) for raw pine chips.

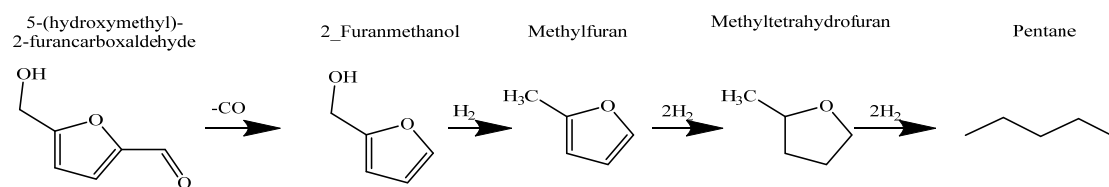
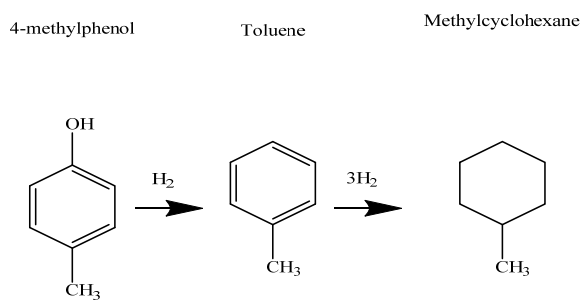
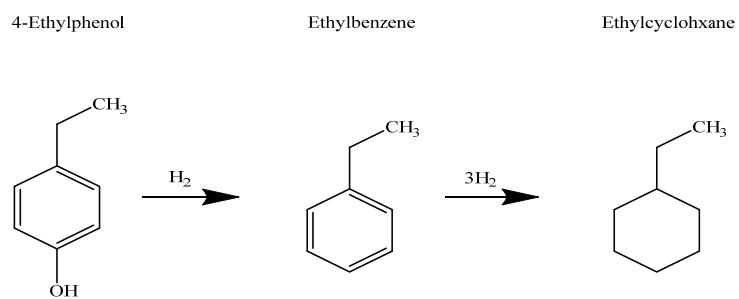
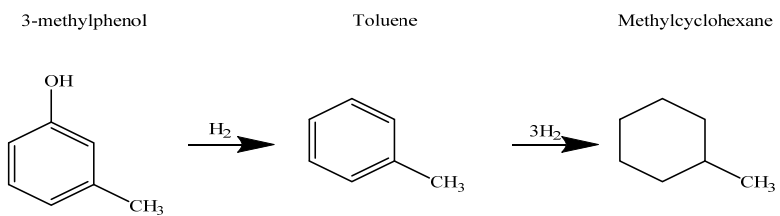
Ultimate Analysis		Proximate Analysis (wet basis)	
Element	Value (wt %)	Element	Value (wt %)
Ash	0.6	Ash	0.60
Carbon	50.45	Moisture Content	25
Hydrogen	6.26	Volatile Matter	84.6
Chlorine	-	Fixed Carbon	14.8
Nitrogen	0.09		
Sulfur	-		
Oxygen	42.6		

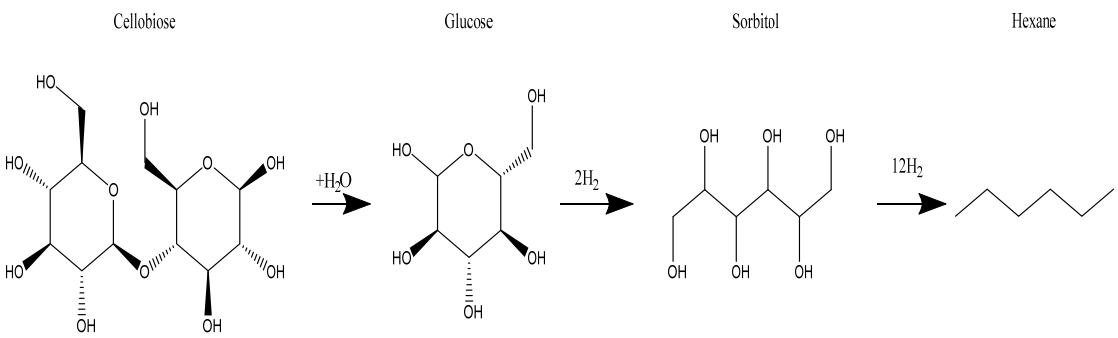
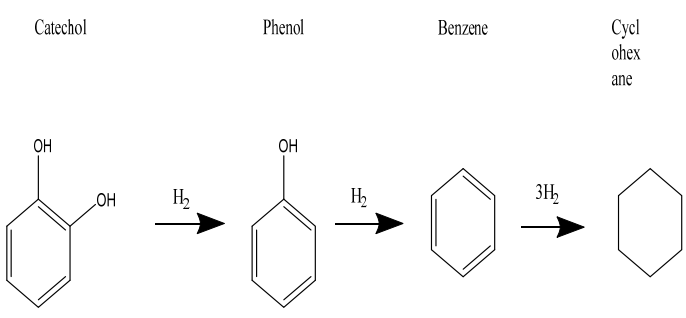
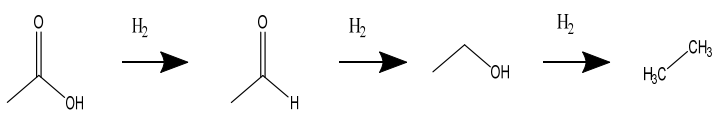
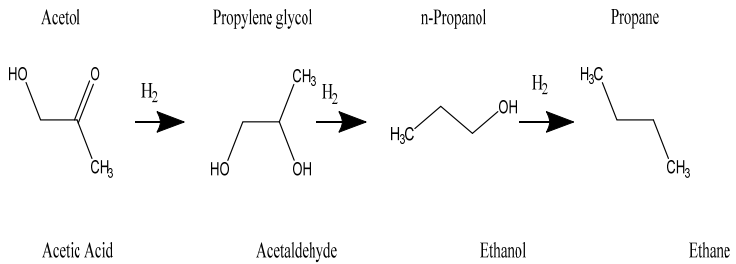
TableD14. Ultimate and proximate data (wt %) for char obtained after pyrolysis.

Ultimate Analysis		Proximate Analysis	
Components	Wt. %	Components	Wt. %
Ash	7.67	Ash	4.60
Carbon	83.03	Moisture Content	-
Hydrogen	1.14	Volatile matter	7.40
Nitrogen	1.37	Fixed carbon	88.0
Chlorine	-		
Sulfur	-		
Oxygen	6.56		

SECTION D: REACTION PATHWAYS FOR BIO-OIL MODEL COMPOUNDS
UPGRADE

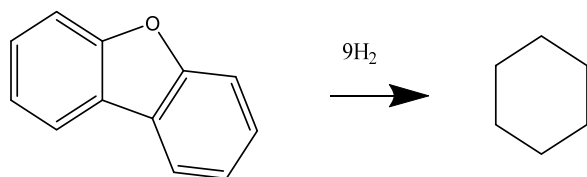






Dibenzofuran

Cyclohexane

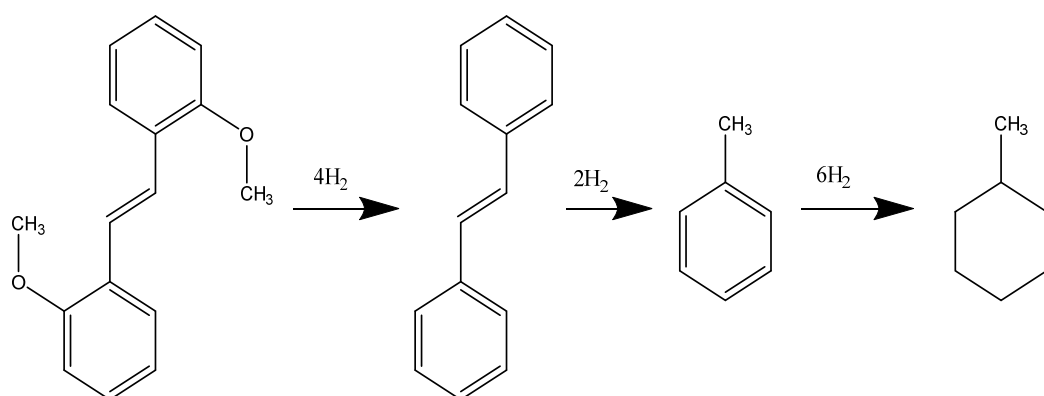


Dimethoxy Stilbene

Trans-Stilbene

Toluene

Methylcyclohexane

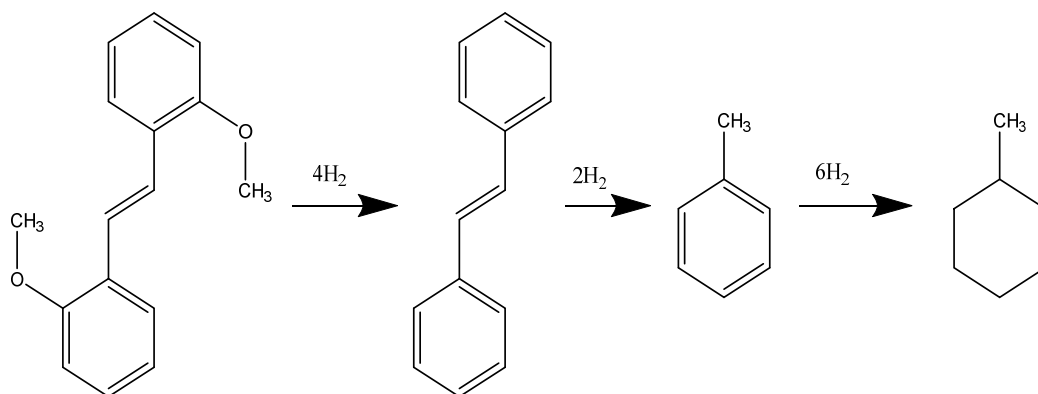


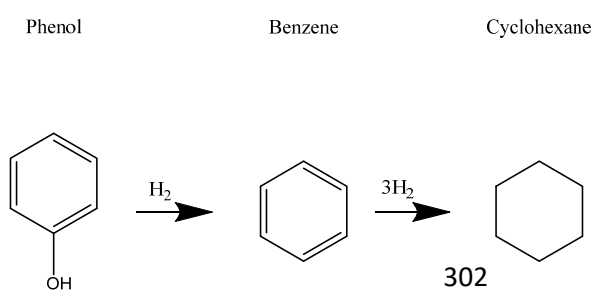
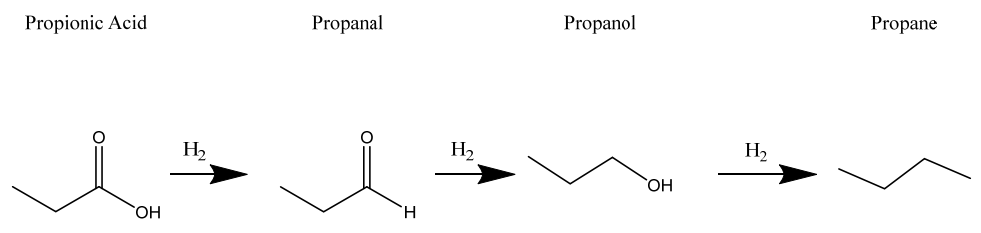
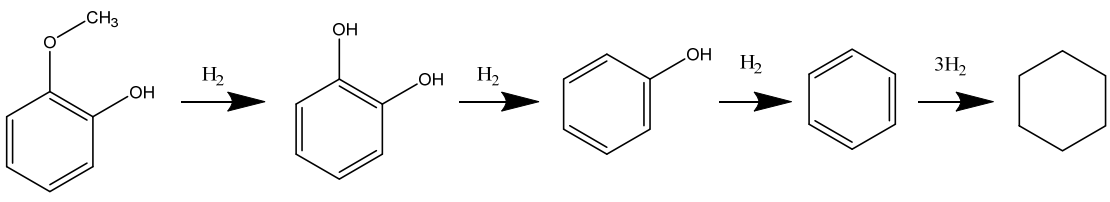
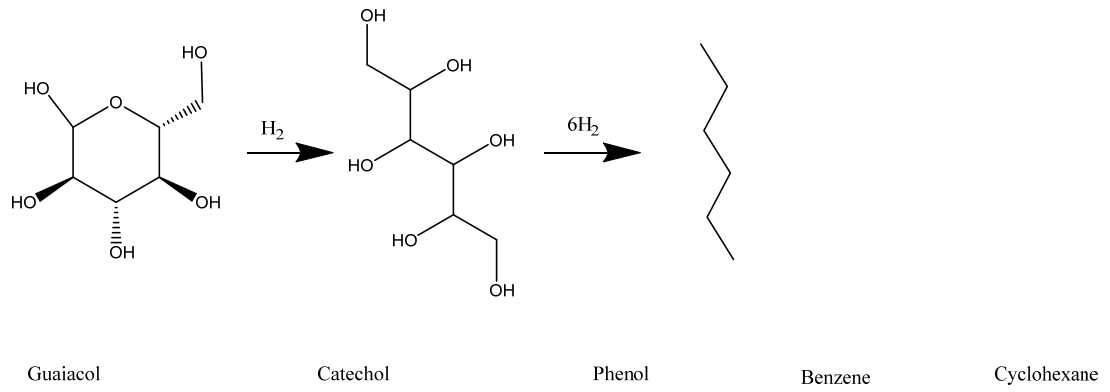
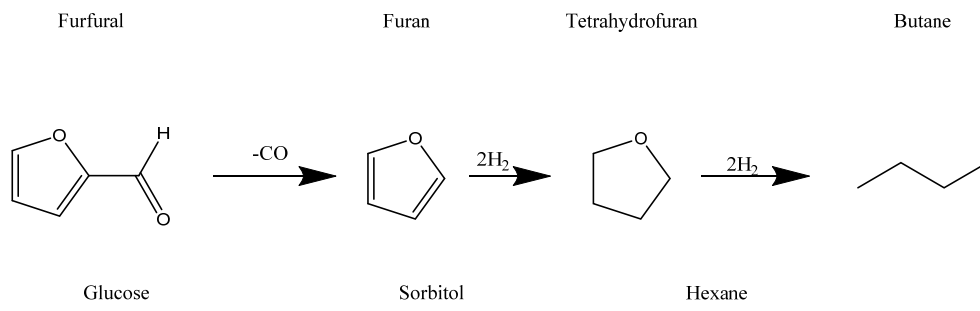
Dimethoxy Stilbene

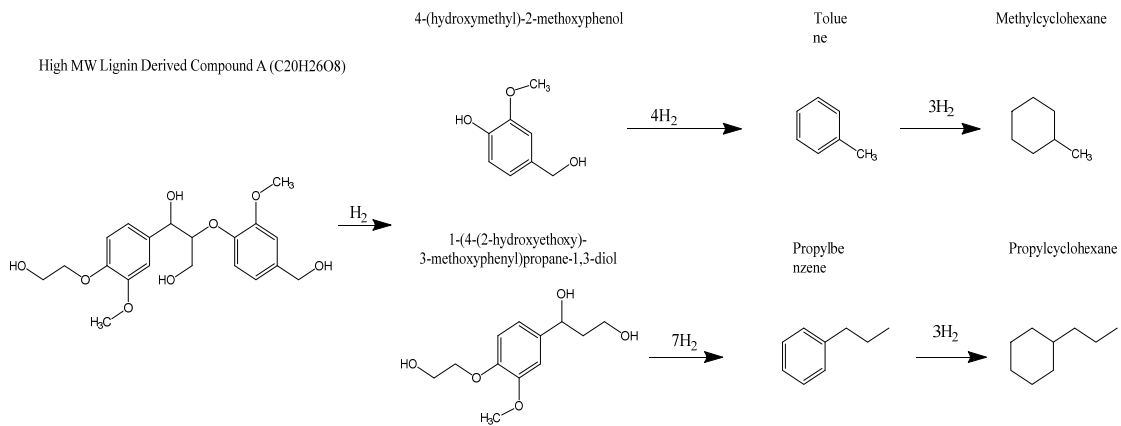
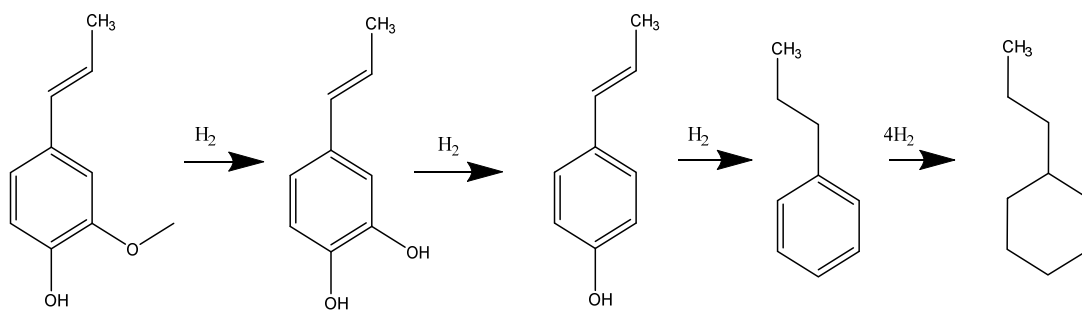
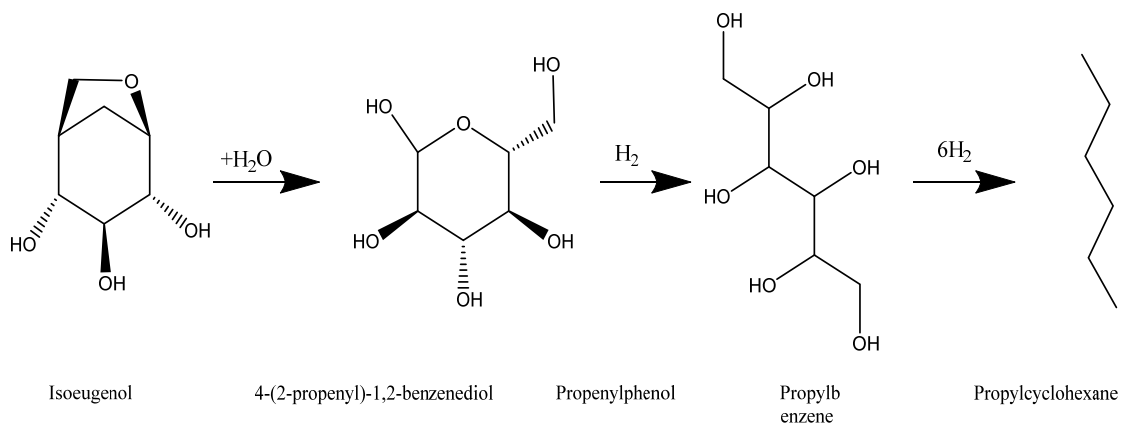
Trans-Stilbene

Toluene

Methylcyclohexane







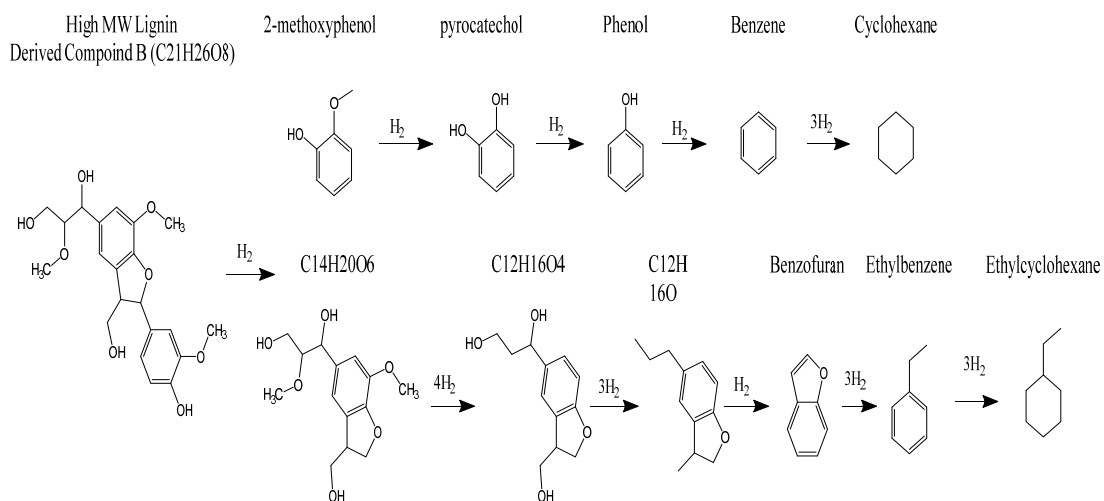


Table D15. Yield factors for upgrade step for the one-step pathway.

Stabilizer		Hydrotreater	
Component	(wt. %)	Component	(wt. %)
N2	0.033	N2	0.033
CO2	0.068	CO2	0.068
CO	0.001	CO	0.895
H2	14.708	H2	9.743
H2O	21.247	CH4	2.637
Acetaldehyde	6.574	C2H6	5.098
Propanal	3.784	H2O	45.227
Propylene Glycol	4.170	Propane	5.475
Isoeugenol	0.724	Butane	1.851
Eugenol	0.158	Pentane	0.291
Vanillyl alcohol	0.575	Hexane	8.186
Vinylguaiacol	1.071	Cyclohexane	3.895
Catechol	3.294	Methylcyclohexane	5.954
Phenol	0.257	Ethylcyclohexane	0.755
Guaiacol	0.628	Propylcyclohexane	1.794
4-methylphenol	0.087	Benzene	1.477
3-methylphenol	0.026	Toulene	4.573
4-ethylphenol	0.096	Propylbenzene	1.107
2-methoxy-4-methylphenol	0.636	Vinylbenzene	0.334
Furfural	1.155	Propenylbenzene	0.301

2-Furanmethanol	0.15 2	Ethylbenzene	0.24 4
5-Hydromethylfufural	0.31 3		
Levoglucosan	9.84 1		
Xylose	2.98 2		
Cellobiose	4.47 3		
Glucose	1.49 1		
Low MW Lignin-Derived Compound A(Dimethoxy stilbene C16H16O2)	9.66 9		
Low MW Lignin-Derived Compound B (Dibenzofuran)	1.95 1		
High MW Lignin-Derived Compound A (C20H26O8) [‡]	8.07 9		
High MW Lignin-Derived Compound B (C21H26O8) [‡]	1.75 7		

[‡] Chemical structure obtained from literature¹⁶

Table D16. Yield factors for upgrade step for scenario 1 of a two-step pathway at torrefaction temperature of 290°C.

Stabilizer		Hydrotreater	
Component	(wt. %)	Component	(wt. %)
N2	0.03 8	N2	0.03 8
CO2	0.17 4	CO	0.93 0
CO	0.00 3	CO2	0.17 4
H2	14.6 47	H2	9.99 6
H2O	24.9 78	CH4	2.12 4
Acetaldehyde	9.61 0	C2H6	7.02 1

Propanal	0.23 2	H2O	48.1 29
Propylene Glycol	6.10 6	Propane	3.85 6
Isoeugenol	0.94 2	Butane	1.79 9
Eugenol	0.40 1	Pentane	0.27 6
Vanillyl alcohol	0.36 3	Hexane	7.43 5
Vinylguaiacol	0.35 4	Cyclohexane	4.14 0
Catechol	4.69 3	Methylcyclohexane	4.67 6
Phenol	0.31 3	Ethylcyclohexane	0.41 4
Guaiacol	1.01 4	Propylcyclohexane	1.64 9
4-methylphenol	0.11 1	Benzene	2.01 7
3-methylphenol	0.05 5	Toulene	3.59 2
4-ethylphenol	0.13 0	Propylbenzene	0.82 9
2-methoxy-4-methylphenol	0.81 6	Vinylbenzene	0.11 0
Furfural	1.41 5	propenylbenzene	0.43 5
2-Furanmethanol	0.16 9	Ethylbenzene	0.20 8
5-Hydromethylfufural	0.26 5		
Levoglucozan	8.07 9		
Xylose	2.44 1		
Cellobiose	5.07 4		
Glucose	1.24 5		
Low MW Lignin-Derived Compound A(Dimethoxy stilbene C16H16O2)	7.36 0		
Low MW Lignin-Derived Compound B (Dibenzofuran)	1.48 5		

High MW Lignin-Derived Compound A (C ₂₀ H ₂₆ O ₈)	6.15 0		
High MW Lignin-Derived Compound B (C ₂₁ H ₂₆ O ₈)	1.33 8		

Table D17. Yield factors for upgrade step for scenario 3 of a two-step pathway at torrefaction temperature of 290°C.

Stabilizer		Hydrotreater	
Component	(wt. %)	Component	(wt. %)
N ₂	0.02 7	N ₂	0.02 7
CO ₂	0.06 1	CO	0.79 4
CO	0.00 1	CO ₂	0.06 1
H ₂	14.9 19	H ₂	9.56 1
H ₂ O	15.2 24	CH ₄	2.73 2
Acetaldehyde	4.44 1	C ₂ H ₆	3.65 6
Propanal	0.00 0	H ₂ O	42.4 42
Propylene Glycol	4.96 9	Propane	3.07 1
Isoeugenol	0.88 5	Butane	1.45 0
Eugenol	0.54 8	Pentane	0.31 5
Vanillyl alcohol	0.21 3	Hexane	11.2 67
Vinylguaiacol	0.55 9	Cyclohexane	5.81 5
Catechol	7.41 4	Methylcyclohexane	6.27 6
Phenol	0.49 5	Ethylcyclohexane	0.60 6
Guaiacol	0.69 9	Propylcyclohexane	2.05 7

4-methylphenol	0.17 5	Benzene	2.90 3
3-methylphenol	0.08 8	Toulene	4.82 0
4-ethylphenol	0.20 5	Propylbenzen e	1.11 2
2-methoxy-4-methylphenol	1.29 0	Vinylbenzene	0.17 4
Furfural	0.40 5	propenylbenze ne	0.46 4
2-Furanmethanol	0.10 3	Ethylbenzene	0.29 1
5-Hydromethylfufural	0.41 8		
Levoglucozan	12.0 25		
Xylose	3.11 8		
Cellobiose	8.01 7		
Glucose	1.78 1		
Low MW Lignin-Derived Compound A(Dimethoxy stilbene C16H16O2)	9.87 9		
Low MW Lignin-Derived Compound B (Dibenzofuran)	1.99 4		
High MW Lignin-Derived Compound A (C20H26O8)	8.25 5		
High MW Lignin-Derived Compound B (C21H26O8)	1.79 5		

Table D18. Yield factors for upgrade step for scenario 1 of a two-step pathway at torrefaction temperature of 310°C.

Stabilizer		Hydrotreater	
Component	(wt. %)	Component	(wt. %)
N2	0.039	N2	0.039
CO2	0.270	CO	0.946
CO	0.005	CO2	0.270
H2	14.448	H2	10.031
H2O	28.086	CH4	1.837
Acetaldehyde	12.423	C2H6	8.851
Propanal	0.422	H2O	50.546
Propylene Glycol	8.363	Propane	5.279
Isoeugenol	1.397	Butane	1.901
Eugenol	0.306	Pentane	0.180
Vanillyl alcohol	0.522	Hexane	6.311
Vinylguaiacol	0.182	Cyclohexane	2.626
Catechol	1.705	Methylcyclohexane	3.808
Phenol	0.174	Ethylcyclohexane	0.257
Guaiacol	1.325	Propylcyclohexane	1.599
4-methylphenol	0.073	Benzene	1.078
3-methylphenol	0.092	Toulene	2.925
4-ethylphenol	0.034	Propylbenzene	0.674
2-methoxy-4-methylphenol	0.439	Vinylbenzene	0.057

Furfural	1.68 4	propenylbenzene	0.55 2
2-Furanmethanol	0.16 2	Ethylbenzene	0.14 1
5-Hydromethylfufural	0.10 6		
Levoglucosan	7.52 2		
Xylose	2.28 3		
Cellobiose	3.64 1		
Glucose	1.01 9		
Low MW Lignin-Derived Compound A(Dimethoxy stilbene C16H16O2)	5.98 3		
Low MW Lignin-Derived Compound B (Dibenzofuran)	1.20 7		
High MW Lignin-Derived Compound A (C20H26O8)	4.99 9		
High MW Lignin-Derived Compound B (C21H26O8)	1.08 7		

Table D19. Yield factors for upgrade step for scenario 3 of a two-step pathway at torrefaction temperature of 310°C.

Stabilizer		Hydrotreater	
Component	(wt. %)	Component	(wt. %)
N2	0.03 4	N2	0.03 4
CO2	0.15 1	CO	0.66 7
CO	0.00 3	CO2	0.15 1
H2	14.7 65	H2	9.88 6
H2O	22.2 39	CH4	2.58 9
Acetaldehyde	7.05 7	C2H6	5.40 3

Propanal	0.16 3	H2O	46.4 08
Propylene Glycol	6.00 2	Propane	3.78 2
Isoeugenol	1.21 9	Butane	1.27 9
Eugenol	0.34 7	Pentane	0.19 9
Vanillyl alcohol	0.38 1	Hexane	9.10 0
Vinylguaiacol	0.35 8	Cyclohexane	3.99 9
Catechol	3.35 8	Methylcyclohexane	5.87 0
Phenol	0.34 3	Ethylcyclohexane	0.43 7
Guaiacol	0.94 7	Propylcyclohexane	2.02 7
4-methylphenol	0.14 4	Benzene	1.61 4
3-methylphenol	0.18 2	Toulene	4.50 9
4-ethylphenol	0.06 7	Propylbenzene	1.04 6
2-methoxy-4-methylphenol	0.86 5	Vinylbenzene	0.11 2
Furfural	0.80 4	propenylbenzene	0.50 7
2-Furanmethanol	0.10 7	Ethylbenzene	0.22 5
5-Hydromethylfufural	0.20 9		
Levoglucosan	9.92 9		
Xylose	2.05 3		
Cellobiose	6.86 8		
Glucose	0.78 4		
Low MW Lignin-Derived Compound A(Dimethoxy stilbene C16H16O2)	9.29 2		
Low MW Lignin-Derived Compound B (Dibenzofuran)	1.87 5		

High MW Lignin-Derived Compound A (C ₂₀ H ₂₆ O ₈)	7.76 5		
High MW Lignin-Derived Compound B (C ₂₁ H ₂₆ O ₈)	1.68 9		

Table D20. Yield factors for upgrade step for scenario 1 of a two-step pathway at torrefaction temperature of 330°C.

Stabilizer		Hydrotreater	
Component	(wt. %)	Component	(wt. %)
N ₂	0.03 8	N ₂	0.03 8
CO ₂	0.39 1	CO	1.26 8
CO	0.00 7	CO ₂	0.39 1
H ₂	14.4 11	H ₂	10.2 27
H ₂ O	30.5 92	CH ₄	1.62 9
Acetaldehyde	12.8 12	C ₂ H ₆	8.99 9
Propanal	0.49 1	H ₂ O	51.7 47
Propylene Glycol	9.04 8	Propane	5.69 3
Isoeugenol	2.66 8	Butane	2.49 7
Eugenol	0.45 1	Pentane	0.38 9
Vanillyl alcohol	0.48 0	Hexane	5.20 6
Vinylguaiacol	0.11 8	Cyclohexane	2.25 9
Catechol	1.17 1	Methylcyclohexane	2.67 7
Phenol	0.12 7	Ethylcyclohexane	0.18 2
Guaiacol	2.09 8	Propylcyclohexane	1.92 7
4-methylphenol	0.03 5	Benzene	1.08 0

3-methylphenol	0.051	Toulene	2.056
4-ethylphenol	0.039	Propylbenzene	0.467
2-methoxy-4-methylphenol	0.330	Vinylbenzene	0.037
Furfural	2.695	propenylbenzene	1.010
2-Furanmethanol	0.334	Ethylbenzene	0.104
5-Hydromethylfufural	0.250		
Levoglucosan	8.659		
Xylose	2.248		
Cellobiose	0.469		
Glucose	0.782		
Low MW Lignin-Derived Compound A(Dimethoxy stilbene C ₁₆ H ₁₆ O ₂)	4.147		
Low MW Lignin-Derived Compound B (Dibenzofuran)	0.837		
High MW Lignin-Derived Compound A (C ₂₀ H ₂₆ O ₈)	3.466		
High MW Lignin-Derived Compound B (C ₂₁ H ₂₆ O ₈)	0.754		

Table D21. Yield factors for upgrade step for scenario 3 of a two-step pathway at torrefaction temperature of 330°C.

Stabilizer		Hydrotreater	
Component	(wt. %)	Component	(wt. %)
N2	0.038	N2	0.038

CO2	0.31 3	CO	1.20 3
CO	0.00 5	CO2	0.31 3
H2	14.5 80	H2	10.2 04
H2O	28.3 56	CH4	1.84 3
Acetaldehyde	10.1 51	C2H6	7.25 2
Propanal	0.37 1	H2O	50.2 64
Propylene Glycol	7.38 6	Propane	4.66 0
Isoeugenol	2.35 0	Butane	2.25 5
Eugenol	0.45 5	Pentane	0.52 0
Vanillyl alcohol	0.44 5	Hexane	6.96 0
Vinylguaiacol	0.23 1	Cyclohexane	2.90 6
Catechol	2.29 3	Methylcyclohexane	3.41 8
Phenol	0.25 0	Ethylcyclohexane	0.27 7
Guaiacol	1.78 5	Propylcyclohexane	1.94 8
4-methylphenol	0.06 9	Benzene	1.41 2
3-methylphenol	0.10 1	Toulene	2.62 6
4-ethylphenol	0.07 6	Propylbenzene	0.58 5
2-methoxy-4-methylphenol	0.64 6	Vinylbenzene	0.07 2
Furfural	2.24 1	propenylbenzene	0.90 8
2-Furanmethanol	0.32 6	Ethylbenzene	0.14 1
5-Hydromethylfufural	0.49 0		
Levogluosan	12.2 46		

Xylose	2.33 0		
Cellobiose	0.35 4		
Glucose	0.59 0		
Low MW Lignin-Derived Compound A(Dimethoxy stilbene C16H16O2)	5.19 2		
Low MW Lignin-Derived Compound B (Dibenzofuran)	1.04 8		
High MW Lignin-Derived Compound A (C20H26O8)	4.33 8		
High MW Lignin-Derived Compound B (C21H26O8)	0.94 4		

Table D22. Typical weight fractions of components in the modeled hydrocarbon biofuel.

Nitrogen	N2	0%
Carbon Monoxide	CO	0%
Carbon Dioxide	CO2	0%
Hydrogen	H2	0%
Methane	CH4	0%
Ethane	C2H6	2%
Water	H2O	1%
Propane	C3H8	4%
Butane	C4H10	3%
Pentane	C5H12	1%
Hexane	C6H14	28%
Cyclohexane	C6H12	15%
Methylcyclohexane	C7H14	16%
Ethylcyclohexane	C8H16	2%
Propylcyclohexane	C9H18	5%
Benzene	C6H6	7%
Toulene	C7H8	12%
Propylbenzene	C9H12	3%
Vinylbenzene	C8H8	0%
propenylbenzene	C9H10	1%
Ethylbenzene	C8H10	1%

Table D23. % carbon conversion of biomass to hydrocarbon biofuel and co-products

	One -step	Two-step					
	Sc1	Sc1	Sc3	Sc1	Sc3	Sc1	Sc3
Hydrocarbon biofuel	43%	43%	36%	35%	24%	31%	19%
Biochar	17%	17%	17%	23%	23%	29%	29%
Low molecular HC	14%	14%	6%	18%	6%	18%	8%
NCG _{torrefaction}	-	4%	4%	5%	5%	7%	7%
Wastewater	0%	0%	0%	0%	0%	0%	0%
NCG _{pyrolysis}	18%	12%	12%	10%	10%	6%	6%
Torrefaction condensed liquid	-	-	15%	-	22%	-	23%
Total C Closure	92%	90%	90%	90%	90%	92%	92%

HC = hydrocarbons from hydrotreatment, NCG = non-condensable gas from torrefaction or pyrolysis.

C closure is achieved to $\geq 90\%$ in all scenarios. Total closure of carbon is not achieved due to the assumed bio-oil compounds in the unidentified fraction of the bio-oil in the literature source used in this study of conversion of pine.¹³ Considering this, overall mass balance closure of streams was achieved in our Aspen simulations.

SECTION E: SAMPLE CALCULATION OF THE LHV OF BIO-OIL OBTAINED FROM SIMULATION FOR A ONE-STEP PYROLYSIS PATHWAY

This section and its sub-sections were presented in our prior study.¹

Table D24. Sample calculation of the LHV of bio-oil for one-step conversion pathway using the heat of combustion of representative compounds found in literature.

	Wt. frac	Heat of combustion (MJ/kg)	Heat of combustion	Source
N2	0.00039	-	0	
CO2	0.001039	-	0	
CO	0.000117	-	0	
H2	0	-	0	
CH4	0	-	0	
C2H6	0	-	0	
H2O	0.221533	-	0	⁸

ACETIC ACID	0.10907 8	-13.5647	-1.47961	8
PROPIONIC ACID	0.05622 7	-18.8312	-1.05883	8
ACETOL	0.04726 7	-22.5708	-1.06686	*
ISOEUGENOL	0.00831 1	-32.6024	-0.27095	17
EUGENOL	0.00181 8	-32.8317	-0.05969	17
VANILLIN	0.00649 3	-25.1678	-0.16341	17
P-VINYLGUAIACOL	0.01220 6			
CATECHOL (BENZE-1,2_DIOL)	0.03752 8	-26.03	-0.97685	
PHENOL	0.00298 7	-31.0372	-0.0927	8
GUAIACOL	0.00714 2			
P-CRESOL	0.00103 9	-32.5741	-0.03384	8
M-CRESOL	0.00026	-32.6228	-0.00847	8
4-ETYLPHENOL	0.00103 9	-35.6322	-0.03702	18
O-CRESOL	0.00727 2	-32.6244	-0.23724	8
FUFURAL	0.01415 4	-24.3674	-0.3449	18
2-FURANMETHANOL	0.00181 8	-26.0091	-0.04728	18
5-(HYDROXYMETHYL)-2-FURANCARBOXALDEHYDE	0.00350 6		0	
LEVOGLUCOSAN	0.11219 5	-17.4747	-1.96056	18
XYLOSE	0.03402 2	-15.5924	-0.53048	18
CELLBOISE	0.05103 3	-16.4864	-0.84135	18
GLUCOSE	0.01701 1	-15.6072	-0.26549	18
LOW MW LIGNIN DERIVED COMPOUND A (DIMETHOXY STILBENZENE)	0.11024 7	-35.4908	-3.91275	*
LOW MW LIGNIN DERIVED COMPOUND B (DIBENZOFURANN)	0.02220 5	-35.2318	-0.78233	*

HIGH MW LIGNIN DERIVED COMPOUND A	0.09206 7	-26.4613	-2.43622	*
HIGH MW LIGNIN DERIVED COMPOUND B	0.01999 8	-26.6643	-0.53322	*
Total	1	LHV	-17.1401	

- Calculated based on the composition of carbon, hydrogen, and oxygen using the method described in section B above.

$$\Delta_c H^\circ = 393.51a + 142.915b + \Delta_f H^\circ(C_a H_b O_c) \quad (11)$$

Acetol – C₃H₆O₂ (74.049g/mol)

$$\begin{aligned} \Delta_c H^\circ (\text{Acetol}) &= (393.51 * 3) + (142.915 * 6) + (-366) \\ &= -1672.02 \text{kJ/mol} \\ &= - 22.57 \text{ MJ/kg} \end{aligned}$$

SECTION F: SAMPLE CALCULATION OF THE ENERGY ALLOCATION FACTORS

The allocation factors used in our study were calculated as shown in the sample calculation below for scenario 3 of a heat integrated two-step hydrocarbon biofuel production pathway with torrefaction taking place at 290°C. Figure D3 is a simplified schematic for the production pathway. Co-products torrefaction bio-oil, char, and off-gas exited the production pathway at the torrefaction, fast pyrolysis, and hydrogen production stages respectively.

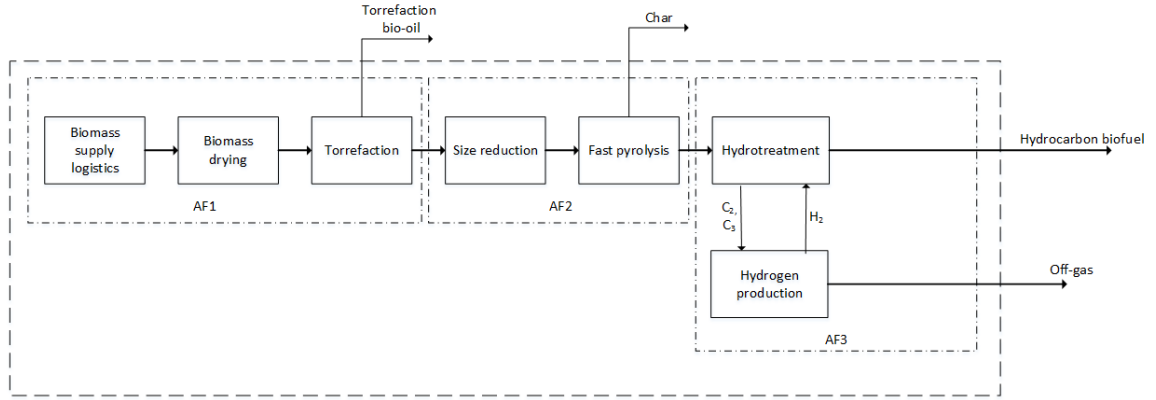


Figure D3. Simple schematic diagram for a two-step production pathway

Stage-specific allocation factors were calculated for these three stages using equations 12-14. Mass flowrates and the LHV of the main product, biofuel and the co-products obtained from the model simulation for scenario 3 of a two-step pathway at torrefaction temperature of 290°C are shown in Table D25. The calculated stage-specific allocation factor for the three stages are also shown in Table D25.

$$\text{Allocation factor}_{\text{torrefaction}} = \frac{\dot{m}_{\text{bio-coal}} H_{\text{bio-coal}}}{\dot{m}_{\text{bio-coal}} H_{\text{bio-coal}} + \dot{m}_{\text{torr. oil}} H_{\text{torr.oil}}} \quad (12)$$

$$\text{Allocation factor}_{\text{fast pyrolysis}} = \frac{\dot{m}_{\text{bio-oil}} H_{\text{bio-oil}}}{\dot{m}_{\text{bio-oil}} H_{\text{bio-oil}} + \dot{m}_{\text{char}} H_{\text{char}}} \quad (13)$$

$$\begin{aligned} \text{Allocation factor}_{\text{hydrogen production}} \\ = \frac{\dot{m}_{\text{biofuel}} H_{\text{biofuel}}}{\dot{m}_{\text{biofuel}} H_{\text{biofuel}} + \dot{m}_{\text{off-gas}} H_{\text{off-gas}}} \end{aligned} \quad (14)$$

Overall allocation factor AF1 shown in Table D25 obtained as the product of all three stage-wise allocation factors was applied to all the inputs and outputs for all the stages prior to and including the torrefaction stage as shown in Figure F1. Overall allocation factor AF2

shown in Table 16a obtained as the product of the fast pyrolysis and hydrogen production stage-wise allocation factors was applied to all the inputs and outputs from the size reduction and fast pyrolysis stages. Allocation factor AF3 is the allocation factor for the hydrogen production stage was applied to the inputs and outputs from the hydrotreatment and hydrogen production stages.

Table D25. Flow rates and LHV values for scenario 3 of a heat integrated two-step hydrocarbon biofuel production pathway at torrefaction temperature of 290°C

	Mass flowrate (kg/hr)	LHV (MJ/kg)
Volatiles	6252	11.362
Torrefied pine/bio-coal	41655	24.537
Biochar	5629	29.988
Bio-oil	24482	19.216
Off-gas	20206	7.498
Hydrocarbon biofuel	11564	43.448
Allocation factor		
Allocation factor _{torrefaction}	0.935016	
Allocation factor _{fast pyrolysis}	0.735936	
Allocation factor _{hydrotreatment}	0.768319	
AF1	0.52869	
AF2	0.565434	
AF3	0.768319	

SECTION G: LCA INVENTORY TABLES FOR ONE AND TWO-STEP PATHWAYS WITHOUT HEAT INTEGRATION

Table D26. Inputs including ecoprofile names, for scenario 2 of a one-step hydrocarbon biofuel production from pine wood chips without heat integration

<i>Products</i>		
Hydrocarbon biofuel	1	MJ
Char (displaces coal)	-	kg
Fossil CO ₂ (from combustion of off-gas)	0.019	kg
Steam (displaces natural gas generated steam)	0.043	kg
<i>Material Inputs</i>		
Pine (8 % moisture content)	0.098	kg
Process water, ion exchange, production mix, at plant, from surface water RER S ^a (to generate steam for hydrogen production)	0.037	kg
Natural gas, from high pressure network (1-5 bar), at service station/US* US-EI U ^a (for hydrogen production)	0.007	kg
Water, completely softened, at plant ^a (cooling water, pyrolysis stage)	4.88	kg
Water, completely softened, at plant ^a (cooling water, hydrotreatment stage)	5.56	kg
Water, completely softened, at plant ^a (cooling water, hydrogen production stage)	4.73	kg
<i>Process Inputs or Displaced products (negative values)</i>		
Electricity, medium voltage US ^a (size reduction)	0.04	kWh
Electricity, medium voltage US ^a (hydrotreatment)	0.004	kWh
Electricity, medium voltage US ^a (hydrogen production)	0.011	kWh
Natural gas, burned in industrial furnace low-NO _x > 100kW ^a (biomass drying)	0.093	MJ
Natural gas, burned in industrial furnace low-NO _x > 100kW ^a (pyrolysis)	0.230	MJ
Natural gas, burned in industrial furnace low-NO _x > 100kW ^a (hydrotreatment)	-	MJ
Natural gas, burned in industrial furnace low-NO _x > 100kW ^a (hydrogen production)	-	MJ
Bituminous coal, combusted in industrial boiler NREL/US ^a	-	kg
Steam, for chemical processes, at plant/US-US-EI U ^a	-0.043	kg

Table D27. Inputs including ecoprofile names, for scenario 1 of a two-step hydrocarbon biofuel production from pine wood chips without heat integration at 290°C without heat integration

<i>Products</i>		
Hydrocarbon biofuel	1	MJ
Char (displaces coal)	0.009	kg
Fossil CO ₂ (from combustion of off-gas)	0.019	kg
Steam (displaces natural gas generated steam)	0.046	kg
<i>Material Inputs</i>		
Pine (8 % moisture content)	0.097	kg
Process water, ion exchange, production mix, at plant, from surface water RER S ^a (to generate steam for hydrogen production)	0.039	kg
Natural gas, from high pressure network (1-5 bar), at service station/US* US-EI U ^a (for hydrogen production)	0.007	kg
Water, completely softened, at plant ^a (cooling water, torrefaction stage)	1.07	kg
Water, completely softened, at plant ^a (cooling water, pyrolysis stage)	3.27	kg
Water, completely softened, at plant ^a (cooling water, hydrotreatment stage)	6.03	kg
Water, completely softened, at plant ^a (cooling water, hydrogen production stage)	4.97	kg
<i>Process Inputs or Displaced products (negative values)</i>		
Electricity, medium voltage US ^a (size reduction)	0.005	kWh
Electricity, medium voltage US ^a (hydrotreatment)	0.004	kWh
Electricity, medium voltage US ^a (hydrogen production)	0.012	kWh
Natural gas, burned in industrial furnace low-NO _x > 100kW ^a (biomass drying)	0.093	MJ
Natural gas, burned in industrial furnace low-NO _x > 100kW ^a (torrefaction)	0.10	MJ
Natural gas, burned in industrial furnace low-NO _x > 100kW ^a (pyrolysis)	0.10	MJ
Natural gas, burned in industrial furnace low-NO _x > 100kW ^a (hydrotreatment)	0.24	MJ
Natural gas, burned in industrial furnace low-NO _x > 100kW ^a (hydrogen production)	0.05	MJ
Bituminous coal, combusted in industrial boiler NREL/US ^a	-0.008	kg
Steam, for chemical processes, at plant/US-US-EI U ^a	-0.046	kg

Table D28. Inputs including ecoprofile names, for scenario 2 of a two-step hydrocarbon biofuel production from pine wood chips without heat integration at 290°C without heat integration

<i>Products</i>		
Hydrocarbon biofuel	1	MJ
Char (displaces coal)	-	kg
Fossil CO ₂ (from combustion of off-gas)	0.019	kg
Steam (displaces natural gas generated steam)	0.046	kg
<i>Material Inputs</i>		
Pine (8 % moisture content)	0.097	kg
Process water, ion exchange, production mix, at plant, from surface water RER S ^a (to generate steam for hydrogen production)	0.039	kg
Natural gas, from high pressure network (1-5 bar), at service station/US* US-EI U ^a (for hydrogen production)	0.007	kg
Water, completely softened, at plant ^a (cooling water, torrefaction stage)	1.07	kg
Water, completely softened, at plant ^a (cooling water, pyrolysis stage)	3.27	kg
Water, completely softened, at plant ^a (cooling water, hydrotreatment stage)	6.03	kg
Water, completely softened, at plant ^a (cooling water, hydrogen production stage)	4.97	kg
<i>Process Inputs or Displaced products (negative values)</i>		
Electricity, medium voltage US ^a (size reduction)	0.005	kWh
Electricity, medium voltage US ^a (hydrotreatment)	0.004	kWh
Electricity, medium voltage US ^a (hydrogen production)	0.012	kWh
Natural gas, burned in industrial furnace low-NO _x > 100kW ^a (biomass drying)	0.093	MJ
Natural gas, burned in industrial furnace low-NO _x > 100kW ^a (torrefaction)	0.10	MJ
Natural gas, burned in industrial furnace low-NO _x > 100kW ^a (pyrolysis)	0.10	MJ
Natural gas, burned in industrial furnace low-NO _x > 100kW ^a (hydrotreatment)	0.016	MJ
Natural gas, burned in industrial furnace low-NO _x > 100kW ^a (hydrogen production)	-	MJ
Bituminous coal, combusted in industrial boiler NREL/US ^a	-	kg
Steam, for chemical processes, at plant/US-US-EI U ^a	-0.046	kg

Table D29. Inputs including ecoprofile names, for scenario 3 of a two-step hydrocarbon biofuel production from pine wood chips without heat integration at 290°C without heat integration

<i>Products</i>		
Hydrocarbon biofuel	1	MJ
Char (displaces coal)	0.004	kg
Fossil CO ₂ (from combustion of off-gas)	0.03	kg
Steam (displaces natural gas generated steam)	0.038	kg
<i>Material Inputs</i>		
Pine (8 % moisture content)	0.097	kg
Process water, ion exchange, production mix, at plant, from surface water RER S ^a (to generate steam for hydrogen production)	0.030	kg
Natural gas, from high pressure network (1-5 bar), at service station/US* US-EI U ^a (for hydrogen production)	0.008	kg
Water, completely softened, at plant ^a (cooling water, torrefaction stage)	1.28	kg
Water, completely softened, at plant ^a (cooling water, pyrolysis stage)	3.93	kg
Water, completely softened, at plant ^a (cooling water, hydrotreatment stage)	4.38	kg
Water, completely softened, at plant ^a (cooling water, hydrogen production stage)	3.91	kg
<i>Process Inputs or Displaced products (negative values)</i>		
Electricity, medium voltage US ^a (size reduction)	0.006	kWh
Electricity, medium voltage US ^a (hydrotreatment)	0.003	kWh
Electricity, medium voltage US ^a (hydrogen production)	0.009	kWh
Natural gas, burned in industrial furnace low-NO _x > 100kW ^a (biomass drying)	-	MJ
Natural gas, burned in industrial furnace low-NO _x > 100kW ^a (torrefaction)	-	MJ
Natural gas, burned in industrial furnace low-NO _x > 100kW ^a (pyrolysis)	-	MJ
Natural gas, burned in industrial furnace low-NO _x > 100kW ^a (hydrotreatment)	-	MJ
Natural gas, burned in industrial furnace low-NO _x > 100kW ^a (hydrogen production)	-	MJ
Bituminous coal, combusted in industrial boiler NREL/US ^a	-0.003	kg
Steam, for chemical processes, at plant/US-US-EI U ^a	-0.038	kg

Table D30. Inputs including ecoprofile names, for scenario 1 of a two-step hydrocarbon biofuel production from pine wood chips without heat integration at 310°C without heat integration

<i>Products</i>		
Hydrocarbon biofuel	1	MJ
Char (displaces coal)	0.015	kg
Fossil CO ₂ (from combustion of off-gas)	0.017	kg
Steam (displaces natural gas generated steam)	0.053	kg
<i>Material Inputs</i>		
Pine (8 % moisture content)	0.121	kg
Process water, ion exchange, production mix, at plant, from surface water RER S ^a (to generate steam for hydrogen production)	0.048	kg
Natural gas, from high pressure network (1-5 bar), at service station/US* US-EI U ^a (for hydrogen production)	0.006	kg
Water, completely softened, at plant ^a (cooling water, torrefaction stage)	1.97	kg
Water, completely softened, at plant ^a (cooling water, pyrolysis stage)	2.77	kg
Water, completely softened, at plant ^a (cooling water, hydrotreatment stage)	7.33	kg
Water, completely softened, at plant ^a (cooling water, hydrogen production stage)	5.97	kg
<i>Process Inputs or Displaced products (negative values)</i>		
Electricity, medium voltage US ^a (size reduction)	0.002	kWh
Electricity, medium voltage US ^a (hydrotreatment)	0.004	kWh
Electricity, medium voltage US ^a (hydrogen production)	0.014	kWh
Natural gas, burned in industrial furnace low-NO _x > 100kW ^a (biomass drying)	0.115	MJ
Natural gas, burned in industrial furnace low-NO _x > 100kW ^a (torrefaction)	0.072	MJ
Natural gas, burned in industrial furnace low-NO _x > 100kW ^a (pyrolysis)	0.133	MJ
Natural gas, burned in industrial furnace low-NO _x > 100kW ^a (hydrotreatment)	0.30	MJ
Natural gas, burned in industrial furnace low-NO _x > 100kW ^a (hydrogen production)	0.062	MJ
Bituminous coal, combusted in industrial boiler NREL/US ^a	-0.014	kg
Steam, for chemical processes, at plant/US-US-EI U ^a	-0.053	kg

Table D31. Inputs including ecoprofile names, for scenario 2 of a two-step hydrocarbon biofuel production from pine wood chips without heat integration at 310°C without heat integration

<i>Products</i>		
Hydrocarbon biofuel	1	MJ
Char (displaces coal)	-	kg
Fossil CO ₂ (from combustion of off-gas)	0.017	kg
Steam (displaces natural gas generated steam)	0.053	kg
<i>Material Inputs</i>		
Pine (8 % moisture content)	0.121	kg
Process water, ion exchange, production mix, at plant, from surface water RER S ^a (to generate steam for hydrogen production)	0.048	kg
Natural gas, from high pressure network (1-5 bar), at service station/US* US-EI U ^a (for hydrogen production)	0.006	kg
Water, completely softened, at plant ^a (cooling water, torrefaction stage)	1.97	kg
Water, completely softened, at plant ^a (cooling water, pyrolysis stage)	2.77	kg
Water, completely softened, at plant ^a (cooling water, hydrotreatment stage)	7.33	kg
Water, completely softened, at plant ^a (cooling water, hydrogen production stage)	5.97	kg
<i>Process Inputs or Displaced products (negative values)</i>		
Electricity, medium voltage US ^a (size reduction)	0.002	kWh
Electricity, medium voltage US ^a (hydrotreatment)	0.004	kWh
Electricity, medium voltage US ^a (hydrogen production)	0.014	kWh
Natural gas, burned in industrial furnace low-NO _x > 100kW ^a (biomass drying)	0.115	MJ
Natural gas, burned in industrial furnace low-NO _x > 100kW ^a (torrefaction)	0.072	MJ
Natural gas, burned in industrial furnace low-NO _x > 100kW ^a (pyrolysis)	0.031	MJ
Natural gas, burned in industrial furnace low-NO _x > 100kW ^a (hydrotreatment)	-	MJ
Natural gas, burned in industrial furnace low-NO _x > 100kW ^a (hydrogen production)	-	MJ
Bituminous coal, combusted in industrial boiler NREL/US ^a	-	kg
Steam, for chemical processes, at plant/US-US-EI U ^a	-0.053	kg

Table D32. Inputs including ecoprofile names, for scenario 1 of a two-step hydrocarbon biofuel production from pine wood chips without heat integration at 310°C without heat integration

<i>Products</i>		
Hydrocarbon biofuel	1	MJ
Char (displaces coal)	0.023	kg
Fossil CO ₂ (from combustion of off-gas)	0.016	kg
Steam (displaces natural gas generated steam)	0.041	kg
<i>Material Inputs</i>		
Pine (8 % moisture content)	0.179	kg
Process water, ion exchange, production mix, at plant, from surface water RER S ^a (to generate steam for hydrogen production)	0.035	kg
Natural gas, from high pressure network (1-5 bar), at service station/US* US-EI U ^a (for hydrogen production)	0.008	kg
Water, completely softened, at plant ^a (cooling water, torrefaction stage)	2.92	kg
Water, completely softened, at plant ^a (cooling water, pyrolysis stage)	4.10	kg
Water, completely softened, at plant ^a (cooling water, hydrotreatment stage)	5.40	kg
Water, completely softened, at plant ^a (cooling water, hydrogen production stage)	4.49	kg
<i>Process Inputs or Displaced products (negative values)</i>		
Electricity, medium voltage US ^a (size reduction)	0.004	kWh
Electricity, medium voltage US ^a (hydrotreatment)	0.004	kWh
Electricity, medium voltage US ^a (hydrogen production)	0.012	kWh
Natural gas, burned in industrial furnace low-NO _x > 100kW ^a (biomass drying)	-	MJ
Natural gas, burned in industrial furnace low-NO _x > 100kW ^a (torrefaction)	-	MJ
Natural gas, burned in industrial furnace low-NO _x > 100kW ^a (pyrolysis)	-	MJ
Natural gas, burned in industrial furnace low-NO _x > 100kW ^a (hydrotreatment)	-	MJ
Natural gas, burned in industrial furnace low-NO _x > 100kW ^a (hydrogen production)	-	MJ
Bituminous coal, combusted in industrial boiler NREL/US ^a	-0.021	kg
Steam, for chemical processes, at plant/US-US-EI U ^a	-0.041	kg

Table D33. Inputs including ecoprofile names, for scenario 1 of a two-step hydrocarbon biofuel production from pine wood chips without heat integration at 330°C without heat integration

<i>Products</i>		
Hydrocarbon biofuel	1	MJ
Char (displaces coal)	0.022	kg
Fossil CO ₂ (from combustion of off-gas)	0.015	kg
Steam (displaces natural gas generated steam)	0.057	kg
<i>Material Inputs</i>		
Pine (8 % moisture content)	0.133	kg
Process water, ion exchange, production mix, at plant, from surface water RER S ^a (to generate steam for hydrogen production)	0.053	kg
Natural gas, from high pressure network (1-5 bar), at service station/US* US-EI U ^a (for hydrogen production)	0.006	kg
Water, completely softened, at plant ^a (cooling water, torrefaction stage)	2.88	kg
Water, completely softened, at plant ^a (cooling water, pyrolysis stage)	2.10	kg
Water, completely softened, at plant ^a (cooling water, hydrotreatment stage)	8.13	kg
Water, completely softened, at plant ^a (cooling water, hydrogen production stage)	6.50	kg
<i>Process Inputs or Displaced products (negative values)</i>		
Electricity, medium voltage US ^a (size reduction)	0.001	kWh
Electricity, medium voltage US ^a (hydrotreatment)	0.005	kWh
Electricity, medium voltage US ^a (hydrogen production)	0.015	kWh
Natural gas, burned in industrial furnace low-NO _x > 100kW ^a (biomass drying)	0.129	MJ
Natural gas, burned in industrial furnace low-NO _x > 100kW ^a (torrefaction)	0.151	
Natural gas, burned in industrial furnace low-NO _x > 100kW ^a (pyrolysis)	0.070	MJ
Natural gas, burned in industrial furnace low-NO _x > 100kW ^a (hydrotreatment)	0.344	MJ
Natural gas, burned in industrial furnace low-NO _x > 100kW ^a (hydrogen production)	0.072	MJ
Bituminous coal, combusted in industrial boiler NREL/US ^a	-0.020	kg
Steam, for chemical processes, at plant/US-US-EI U ^a	-0.057	kg

Table D34. Inputs including ecoprofile names, for scenario 1 of a two-step hydrocarbon biofuel production from pine wood chips without heat integration at 310°C without heat integration

<i>Products</i>		
Hydrocarbon biofuel	1	MJ
Char (displaces coal)	-	kg
Fossil CO ₂ (from combustion of off-gas)	0.015	kg
Steam (displaces natural gas generated steam)	0.057	kg
<i>Material Inputs</i>		
Pine (8 % moisture content)	0.133	kg
Process water, ion exchange, production mix, at plant, from surface water RER S ^a (to generate steam for hydrogen production)	0.053	kg
Natural gas, from high pressure network (1-5 bar), at service station/US* US-EI U ^a (for hydrogen production)	0.006	kg
Water, completely softened, at plant ^a (cooling water, torrefaction stage)	2.88	kg
Water, completely softened, at plant ^a (cooling water, pyrolysis stage)	2.10	kg
Water, completely softened, at plant ^a (cooling water, hydrotreatment stage)	8.13	kg
Water, completely softened, at plant ^a (cooling water, hydrogen production stage)	6.50	kg
<i>Process Inputs or Displaced products (negative values)</i>		
Electricity, medium voltage US ^a (size reduction)	0.001	kWh
Electricity, medium voltage US ^a (hydrotreatment)	0.005	kWh
Electricity, medium voltage US ^a (hydrogen production)	0.015	kWh
Natural gas, burned in industrial furnace low-NO _x > 100kW ^a (biomass drying)	0.097	MJ
Natural gas, burned in industrial furnace low-NO _x > 100kW ^a (torrefaction)	-	MJ
Natural gas, burned in industrial furnace low-NO _x > 100kW ^a (pyrolysis)	-	MJ
Natural gas, burned in industrial furnace low-NO _x > 100kW ^a (hydrotreatment)	-	MJ
Natural gas, burned in industrial furnace low-NO _x > 100kW ^a (hydrogen production)	-	MJ
Bituminous coal, combusted in industrial boiler NREL/US ^a	-	kg
Steam, for chemical processes, at plant/US-US-EI U ^a	-0.057	kg

Table D35. Inputs including ecoprofile names, for scenario 1 of a two-step hydrocarbon biofuel production from pine wood chips without heat integration at 310°C without heat integration

<i>Products</i>		
Hydrocarbon biofuel	1	MJ
Char (displaces coal)	0.037	kg
Fossil CO ₂ (from combustion of off-gas)	0.012	kg
Steam (displaces natural gas generated steam)	0.049	kg
<i>Material Inputs</i>		
Pine (8 % moisture content)	0.223	kg
Process water, ion exchange, production mix, at plant, from surface water RER S ^a (to generate steam for hydrogen production)	0.039	kg
Natural gas, from high pressure network (1-5 bar), at service station/US* US-EI U ^a (for hydrogen production)	0.007	kg
Water, completely softened, at plant ^a (cooling water, torrefaction stage)	4.82	kg
Water, completely softened, at plant ^a (cooling water, pyrolysis stage)	3.52	kg
Water, completely softened, at plant ^a (cooling water, hydrotreatment stage)	6.91	kg
Water, completely softened, at plant ^a (cooling water, hydrogen production stage)	5.52	kg
<i>Process Inputs or Displaced products (negative values)</i>		
Electricity, medium voltage US ^a (size reduction)	0.002	kWh
Electricity, medium voltage US ^a (hydrotreatment)	0.004	kWh
Electricity, medium voltage US ^a (hydrogen production)	0.013	kWh
Natural gas, burned in industrial furnace low-NO _x > 100kW ^a (biomass drying)	-	MJ
Natural gas, burned in industrial furnace low-NO _x > 100kW ^a (torrefaction)	-	MJ
Natural gas, burned in industrial furnace low-NO _x > 100kW ^a (pyrolysis)	-	MJ
Natural gas, burned in industrial furnace low-NO _x > 100kW ^a (hydrotreatment)	-	MJ
Natural gas, burned in industrial furnace low-NO _x > 100kW ^a (hydrogen production)	-	MJ
Bituminous coal, combusted in industrial boiler NREL/US ^a	-0.034	kg
Steam, for chemical processes, at plant/US-US-EI U ^a	-0.049	kg

SECTION H: FOSSIL CARBON ACCOUNTING FROM COMBUSTION OF OFF-GAS

Off-gas produced from the hydrogen production step utilizes biogenic low molecular weight hydrocarbons from hydrotreatment step and fossil natural gas. To partition the CO₂ produced from the combustion of the off-gas to biogenic and fossil-derived CO₂, our initial simulation run evaluated the biogenic CO₂ by having the biogenic low molecular and steam in a steam to carbon ratio of 3:1 be the feed into the hydrogen production stage starting from the pre-reformer for run 1. A sample calculation using flows from the one step is shown in Table S1g.

Assuming 100% conversion of off-gas components to CO₂ during combustion, total CO₂ produced was estimated to be about 10,518kg/hr as shown in Table S1h. With run 2, natural gas was added to the hydrogen production inlet feed and the steam flowrate was adjusted to maintain a 3:1 steam to carbon ratio. Total CO₂ produced from complete combustion was estimated to be about 19,552kg/hr as shown in Table S1h. Fossil derived CO₂ was then evaluated by subtracting total CO₂ produced from run 1 from the total CO₂ produced from run 2.

Table D36. Sample calculation for fossil derived CO₂ from combustion of off-gas from H₂ production

Run	Biogenic hydrocarbons (kg/hr)	Natural gas (kg/hr)	Steam (kg/hr)	Off-gas (kg/hr)		Total CO ₂ produced (kg/hr)
				Component	Flowrate (kg/hr)	
1	4273.89	-	10509.56	N ₂	10.66	10517.95
				CO ₂	6779.30	
				CO	671.22	
				H ₂	238.49	
				CH ₄	975.70	
				C ₂ H ₆	0.23	
2	4273.89	3360	17229.56	N ₂	66.53	19551.51
				CO ₂	11989.88	
				CO	1400.32	
				H ₂	401.77	
				CH ₄	1948.97	
				C ₂ H ₆	0.50	
						9033.56

D.2 References

- (1) Winjobi, O.; Shonnard, D. R.; Bar-Ziv, E.; Zhou, W. Life cycle greenhouse gas emissions of bio-oil from two-step torrefaction and fast pyrolysis of pine. *Biofuels, Bioproducts and Biorefining* **2016**, *10* (5), 576-588.
- (2) Wang, M. The Greenhouse Gases, Regulated Emissions, and Energy Use in Transportation (GREET) Model: Version 1.5. *Center for Transportation Research, Argonne National Laboratory* **2008**.
- (3) Maleche, E. Life cycle assessment of biofuels produced by the new integrated hydrolysis-hydroconversion (IH 2) process. **2012**.
- (4) Handler, R. M.; Shonnard, D. R.; Lautala, P.; Abbas, D.; Srivastava, A. Environmental impacts of roundwood supply chain options in Michigan: Life-cycle assessment of harvest and transport stages. *Journal of Cleaner Production* **2014**, *76*, 64-73.
- (5) Phanphanich, M.; Mani, S. Impact of torrefaction on the grindability and fuel characteristics of forest biomass. *Bioresource technology* **2011**, *102* (2), 1246-1253.
- (6) Koppejan, J.; Van Loo, S. *The handbook of biomass combustion and co-firing*, ed.; Routledge, 2012.
- (7) Gaur, S.; Reed, T. B. *An atlas of thermal data for biomass and other fuels*; Report No. 1995.
- (8) Perry, R. H.; Green, D. W.; Maloney, J. O.; Abbott, M. M.; Ambler, C. M.; Amero, R. C. *Perry's chemical engineers' handbook*, ed.; McGraw-hill New York, 1997.
- (9) Haynes, W. M. *CRC handbook of chemistry and physics*, ed.; CRC press, 2013.

- (10) Joback, K. G.; Reid, R. C. Estimation of pure-component properties from group-contributions. *Chemical Engineering Communications* **1987**, *57* (1-6), 233-243.
- (11) Shankar Tumuluru, J.; Sokhansanj, S.; Hess, J. R.; Wright, C. T.; Boardman, R. D. REVIEW: A review on biomass torrefaction process and product properties for energy applications. *Industrial Biotechnology* **2011**, *7* (5), 384-401.
- (12) Plus, A. Aspen Technology. *Inc., version 2009, 11*.
- (13) Westerhof, R. J.; Brilman, D. W. F.; Garcia-Perez, M.; Wang, Z.; Oudenhoven, S. R.; Kersten, S. R. Stepwise fast pyrolysis of pine wood. *Energy & fuels* **2012**, *26* (12), 7263-7273.
- (14) Zheng, A.; Zhao, Z.; Chang, S.; Huang, Z.; He, F.; Li, H. Effect of torrefaction temperature on product distribution from two-staged pyrolysis of biomass. *Energy & Fuels* **2012**, *26* (5), 2968-2974.
- (15) Park, J.; Meng, J.; Lim, K. H.; Rojas, O. J.; Park, S. Transformation of lignocellulosic biomass during torrefaction. *Journal of Analytical and Applied Pyrolysis* **2013**, *100*, 199-206.
- (16) Jones, S.; Meyer, P.; Snowden-Swan, L.; Padmaperuma, A.; Tan, E.; Dutta, A.; Jacobson, J.; Cafferty, K. *Process design and economics for the conversion of lignocellulosic biomass to hydrocarbon fuels: fast pyrolysis and hydrotreating bio-oil pathway*; Report No. 2013.
- (17) Kharasch, M. S. *Heats of combustion of organic compounds*, ed.; US Government Printing Office, 1929.

- (18) Domalski, E. S. Selected Values of Heats of Combustion and Heats of Formation of Organic Compounds Containing the Elements C, H, N, O, P, and S. *Journal of Physical and Chemical Reference Data* **1972**, *1* (2), 221-277.

Appendix E: Copyright Clearance

8/11/2017

RightsLink Printable License

JOHN WILEY AND SONS LICENSE TERMS AND CONDITIONS

Aug 11, 2017

This Agreement between Olumide Winjobi ("You") and John Wiley and Sons ("John Wiley and Sons") consists of your license details and the terms and conditions provided by John Wiley and Sons and Copyright Clearance Center.

License Number	4166151388206
License date	Aug 11, 2017
Licensed Content Publisher	John Wiley and Sons
Licensed Content Publication	Biotechnology Progress
Licensed Content Title	Process Design and Costing of Bioethanol Technology: A Tool for Determining the Status and Direction of Research and Development
Licensed Content Author	Robert Wooley,Mark Ruth,David Glassner,John Sheehan
Licensed Content Date	Sep 4, 2008
Licensed Content Pages	10
Type of use	Dissertation/Thesis
Requestor type	University/Academic
Format	Print and electronic
Portion	Figure/table
Number of figures/tables	1
Original Wiley figure/table number(s)	Figure 1
Will you be translating?	No
Title of your thesis / dissertation	TECHNO-ECONOMIC AND LIFE CYCLE ASSESSMENTS OF BIOFUEL PRODUCTION FROM WOODY BIOMASS THROUGH TORREFACTION-FAST PYROLYSIS AND CATALYTIC UPGRADING
Expected completion date	Apr 2017
Expected size (number of pages)	320
Requestor Location	Olumide Winjobi 1800 Townsend Drive Dept of Chemical Engineering Michigan Technological University HOUGHTON, MI 49931 United States Attn: Olumide Winjobi
Publisher Tax ID	EU826007151
Billing Type	Invoice
Billing Address	Olumide Winjobi 1800 Townsend Drive Dept of Chemical Engineering Michigan Technological University HOUGHTON, MI 49931 United States Attn: Olumide Winjobi
Total	0.00 USD

<https://s100.copyright.com/AppDispatchServlet>

1/5

Figure E.1: Copyright clearance for Figure 1.5

**JOHN WILEY AND SONS LICENSE
TERMS AND CONDITIONS**

Mar 17, 2017

This Agreement between Olumide Winjobi ("You") and John Wiley and Sons ("John Wiley and Sons") consists of your license details and the terms and conditions provided by John Wiley and Sons and Copyright Clearance Center.

License Number	4071541360062
License date	Mar 17, 2017
Licensed Content Publisher	John Wiley and Sons
Licensed Content Publication	Biofuels, Bioproducts and Biorefining
Licensed Content Title	Techno-economic assessment of the effect of torrefaction on fast pyrolysis of pine
Licensed Content Author	Olumide Winjobi,David R. Shonnard,Ezra Bar-Ziv,Wen Zhou
Licensed Content Date	Jan 8, 2016
Licensed Content Pages	12
Type of use	Dissertation/Thesis
Requestor type	Author of this Wiley article
Format	Print and electronic
Portion	Full article
Will you be translating?	No
Title of your thesis / dissertation	TECHNO-ECONOMIC AND LIFE CYCLE ASSESSMENTS OF BIOFUEL PRODUCTION FROM WOODY BIOMASS THROUGH TORREFACTION-FAST PYROLYSIS AND CATALYTIC UPGRADING
Expected completion date	Apr 2017
Expected size (number of pages)	320
Requestor Location	Olumide Winjobi 1800 Townsend Drive Dept of Chemical Engineering Michigan Technological University HOUGHTON, MI 49931 United States Attn: Olumide Winjobi
Publisher Tax ID	EU826007151
Billing Type	Invoice
Billing Address	Olumide Winjobi 1800 Townsend Drive Dept of Chemical Engineering Michigan Technological University HOUGHTON, MI 49931 United States Attn: Olumide Winjobi
Total	0.00 USD
Terms and Conditions	

TERMS AND CONDITIONS

<https://s100.copyright.com/AppDispatchServlet>

1/5

Figure E.2: Copyright clearance for Chapter 2

**JOHN WILEY AND SONS LICENSE
TERMS AND CONDITIONS**

Mar 17, 2017

This Agreement between Olumide Winjobi ("You") and John Wiley and Sons ("John Wiley and Sons") consists of your license details and the terms and conditions provided by John Wiley and Sons and Copyright Clearance Center.

License Number	4071540996500
License date	Mar 17, 2017
Licensed Content Publisher	John Wiley and Sons
Licensed Content Publication	Biofuels, Bioproducts and Biorefining
Licensed Content Title	Life cycle greenhouse gas emissions of bio-oil from two-step torrefaction and fast pyrolysis of pine
Licensed Content Author	Olumide Winjobi,David R Shonnard,Ezra Bar-Ziv,Wen Zhou
Licensed Content Date	Jun 17, 2016
Licensed Content Pages	13
Type of use	Dissertation/Thesis
Requestor type	Author of this Wiley article
Format	Electronic
Portion	Full article
Will you be translating?	No
Title of your thesis / dissertation	TECHNO-ECONOMIC AND LIFE CYCLE ASSESSMENTS OF BIOFUEL PRODUCTION FROM WOODY BIOMASS THROUGH TORREFACTION-FAST PYROLYSIS AND CATALYTIC UPGRADING
Expected completion date	Apr 2017
Expected size (number of pages)	320
Requestor Location	Olumide Winjobi 1800 Townsend Drive Dept of Chemical Engineering Michigan Technological University HOUGHTON, MI 49931 United States Attn: Olumide Winjobi
Publisher Tax ID	EU826007151
Billing Type	Invoice
Billing Address	Olumide Winjobi 1800 Townsend Drive Dept of Chemical Engineering Michigan Technological University HOUGHTON, MI 49931 United States Attn: Olumide Winjobi
Total	0.00 USD
Terms and Conditions	

TERMS AND CONDITIONS

<https://s100.copyright.com/AppDispatchServlet>

1/5

Figure E.3: Copyright clearance for Chapter 3

**JOHN WILEY AND SONS LICENSE
TERMS AND CONDITIONS**

Aug 16, 2017

This Agreement between Olumide Winjobi ("You") and John Wiley and Sons ("John Wiley and Sons") consists of your license details and the terms and conditions provided by John Wiley and Sons and Copyright Clearance Center.

License Number	4170590417367
License date	Aug 16, 2017
Licensed Content Publisher	John Wiley and Sons
Licensed Content Publication	Biofuels, Bioproducts and Biorefining
Licensed Content Title	Techno-economic assessment of the effect of torrefaction on fast pyrolysis of pine
Licensed Content Author	Olumide Winjobi,David R. Shonnard,Ezra Bar-Ziv,Wen Zhou
Licensed Content Date	Jan 8, 2016
Licensed Content Pages	12
Type of use	Dissertation/Thesis
Requestor type	Author of this Wiley article
Format	Print and electronic
Portion	Figure/table
Number of figures/tables	1
Original Wiley figure/table number(s)	Figure 2
Will you be translating?	No
Title of your thesis / dissertation	TECHNO-ECONOMIC AND LIFE CYCLE ASSESSMENTS OF BIOFUEL PRODUCTION FROM WOODY BIOMASS THROUGH TORREFACTION-FAST PYROLYSIS AND CATALYTIC UPGRADING
Expected completion date	Apr 2017
Expected size (number of pages)	320
Requestor Location	Olumide Winjobi 1800 Townsend Drive Dept of Chemical Engineering Michigan Technological University HOUGHTON, MI 49931 United States Attn: Olumide Winjobi
Publisher Tax ID	EU826007151
Billing Type	Invoice
Billing Address	Olumide Winjobi 1800 Townsend Drive Dept of Chemical Engineering Michigan Technological University HOUGHTON, MI 49931 United States Attn: Olumide Winjobi
Total	0.00 USD

<https://s100.copyright.com/AppDispatchServlet>

1/5

Figure E.4: Copyright clearance for Figure 3.1



RightsLink®

[Home](#)
[Create Account](#)
[Help](#)


ACS Publications
Most Trusted. Most Cited. Most Read.

Title: Production of Hydrocarbon Fuel Using Two-Step Torrefaction and Fast Pyrolysis of Pine. Part 1: Techno-economic Analysis

Author: Olumide Winjobi, David R. Shonnard, Wen Zhou

Publication: ACS Sustainable Chemistry & Engineering

Publisher: American Chemical Society

Date: Jun 1, 2017

Copyright © 2017, American Chemical Society

[LOGIN](#)

If you're a **copyright.com** user, you can login to RightsLink using your **copyright.com** credentials. Already a **RightsLink** user or want to learn more?

PERMISSION/LICENSE IS GRANTED FOR YOUR ORDER AT NO CHARGE

This type of permission/license, instead of the standard Terms & Conditions, is sent to you because no fee is being charged for your order. Please note the following:

- Permission is granted for your request in both print and electronic formats, and translations.
- If figures and/or tables were requested, they may be adapted or used in part.
- Please print this page for your records and send a copy of it to your publisher/graduate school.
- Appropriate credit for the requested material should be given as follows: "Reprinted (adapted) with permission from (COMPLETE REFERENCE CITATION). Copyright (YEAR) American Chemical Society." Insert appropriate information in place of the capitalized words.
- One-time permission is granted only for the use specified in your request. No additional uses are granted (such as derivative works or other editions). For any other uses, please submit a new request.

[BACK](#)
[CLOSE WINDOW](#)

Copyright © 2017 Copyright Clearance Center, Inc. All Rights Reserved. [Privacy statement](#). [Terms and Conditions](#). Comments? We would like to hear from you. E-mail us at customer.care@copyright.com

Figure E.5: Copyright clearance for Chapter 4



RightsLink®

Home

Create Account

Help



ACS Publications
Most Trusted. Most Cited. Most Read.

Title: Production of Hydrocarbon Fuel Using Two-Step Torrefaction and Fast Pyrolysis of Pine. Part 2: Life-Cycle Carbon Footprint
Author: Olumide Winjobi, Wen Zhou, Daniel Kulas, et al
Publication: ACS Sustainable Chemistry & Engineering
Publisher: American Chemical Society
Date: Jun 1, 2017
Copyright © 2017, American Chemical Society

LOGIN

If you're a **copyright.com** user, you can login to RightsLink using your copyright.com credentials. Already a **RightsLink** user or want to [learn more?](#)

PERMISSION/LICENSE IS GRANTED FOR YOUR ORDER AT NO CHARGE

This type of permission/license, instead of the standard Terms & Conditions, is sent to you because no fee is being charged for your order. Please note the following:

- Permission is granted for your request in both print and electronic formats, and translations.
- If figures and/or tables were requested, they may be adapted or used in part.
- Please print this page for your records and send a copy of it to your publisher/graduate school.
- Appropriate credit for the requested material should be given as follows: "Reprinted (adapted) with permission from (COMPLETE REFERENCE CITATION). Copyright (YEAR) American Chemical Society." Insert appropriate information in place of the capitalized words.
- One-time permission is granted only for the use specified in your request. No additional uses are granted (such as derivative works or other editions). For any other uses, please submit a new request.

BACK

CLOSE WINDOW

Copyright © 2017 Copyright Clearance Center, Inc. All Rights Reserved. [Privacy statement](#), [Terms and Conditions](#). Comments? We would like to hear from you. E-mail us at customer.care@copyright.com

Figure E.6: Copyright clearance for Chapter 5